

An investigation into the colorectal cancer  
chemopreventive mechanisms of  
3', 4', 5', 5, 7-pentamethoxyflavone (PMF)

Thesis submitted for the degree of  
Doctor of Philosophy  
At the University of Leicester

By

Isabel Lim Fong MSc (Auckland)

Department of Cancer Studies and Molecular Medicine

University of Leicester

December 2011

## Abstract

### An investigation into the colorectal cancer (CRC) chemopreventive mechanisms of 3', 4', 5', 5, 7-Pentamethoxyflavone (PMF)

Isabel L. Fong

3',4',5',5,7-Pentamethoxyflavone (PMF) is a naturally occurring flavone found in the leaves of *Murraya paniculata* and the fruits of *Neoraputia magnifica*. PMF has been shown to possess potential promise as a colorectal cancer (CRC) chemopreventive agent as it significantly inhibited adenoma development in the *Apc<sup>Min/+</sup>* mouse, a model of gastrointestinal cancer. The chemopreventive activity of PMF was superior to that of two closely related flavone analogues apigenin and tricetin. The aim of the work described in this thesis was to elucidate the mechanisms by which PMF can interfere with carcinogenesis.

PMF was compared to tricetin and apigenin in its abilities to inhibit growth, arrest cell cycle and elicit apoptosis in APC10.1 cells, derived from *Apc<sup>Min/+</sup>* mice. Cells were incubated with these agents (10  $\mu$ M, 24 h) and cDNA microarray analysis was performed to delineate changes in gene expression caused by these flavones. Gene changes were validated using reverse transcriptase-PCR and Western blot. PMF was administered to *Apc<sup>Min/+</sup>* mice to assess its effects on protein expression in adenomas.

PMF was the most growth-inhibitory of the three flavones with an  $IC_{50}$  of 5  $\mu$ M. It arrested the cell cycle at G<sub>1</sub> and G<sub>2</sub> phases and induced a two-fold increase in apoptosis. In the microarray study PMF modulated several key signalling pathways, most notably those involving Wnt, PI3K/Akt/GSK3 $\beta$  and JAK/STAT. In cells *in vitro* PMF significantly altered expression of Wnt8b, Wnt3a, TCF4,  $\beta$ -catenin, GSK3 $\beta$ , survivin, pSTAT3 and MCM7. In mice *in vivo* PMF, at a dietary dose which significantly reduced adenoma development, altered only  $\beta$ -catenin and MCM7 protein levels. These differences were only observed in the adenomas and not the normal mucosa. GSK3 $\beta$ ,  $\beta$ -Catenin and MCM7 may play a role in the CRC chemopreventive activity of PMF.

## Acknowledgement

This thesis would not have been made possible without the guidance and advice of my supervisors Dr. Stewart Sale and Prof. Andreas Gescher. I am grateful to the Ministry of Higher Education, Malaysia and University of Malaysia Sarawak for providing this opportunity for me to further my studies at the University of Leicester, UK. It is an honour for me to thank the Head of Department, Prof. Dr. William Steward, Associate Prof. Karen Brown, Dr. Lynne Howells (proofread), Dr. Hong Cai and postgraduate tutor, Dr. Jacqui Shaw.

I am indebted to my colleagues and friends who guided and supported me throughout my study: Prof. Dr. Peter Greaves (IHC), Dr. Karen Kulbicki (IHC), Dr. Timothy W. Gant (Microarray), Dr. Emma Marczylo (Microarray), Dr. Jin-Li Luo (Microarray), Ms. Kate Phillips (Microarray), Dr. Joan Riley (Microarray), Dr. Shu-Dong Zhang (Microarray), Dr. Mai-Kim Cheng (FACS), Kelsang Dorsem (Dr. Christoph Boes) (FACS, proofread), Dr. Ketan Patel (SPSS), Dr. Shaban Saad (Western blot), Ankur Karmokar (IHC, FACS), Dr. Glen Irving (SPSS), Mr. Mark James (Smurf), Ms. Christina Kurian (chats in between running and transferring of gels), Mdm. Abeer Kholghi (Libyan food!), Mr. Jon Naylor (IT), Mrs. 'Steph' Euden (music and news), and Mdm. Jo Arden (Admin).

I owe my deepest gratitude to my family, especially my mama and my late papa, for their constant love, encouragement and prayers. I would like to show my gratitude to the Dominican friars at Holy Cross Church, Leicester for their friendship, support and pastoral care, more so after papa's demise. Special 'Thank you' to friars Thomas Crean, Duncan Campbell and Gregory Murphy for proofreading my thesis. A melodious 'thank you' to the Holy Cross Church Choir for the joys and challenges of singing in harmony! I would also like to thank my dear former flatmates for their support, encouragement and humour while we embarked on our PhD journey: Dr. Keith Athaide, Dr. Denes Biztray, Dr. Cici Alexander, Ms. Reka Plugor, Ms. Dima Atanasova, and Ms. Amy Furniss. In the short four years, I have gained a huge 'family'. It is indeed a pleasure to thank those who made this thesis possible.

Last but not least, *Deo gratias!*

This thesis is dedicated to my mother, Dr. Julitta Lim Shau-Hua and to the loving memory of my late father, Dr. Frederick Fong Hon-Kah (1936-2010).

*'He shall cure and shall allay their pains, and the apothecary shall make sweet confections and shall make up ointments of health and of his works there shall be no end. For the peace of God is over the face of the earth' (Ecclesiasticus 38:7-9)*

## **Table of Contents**

1	Introduction .....	1
1.1	Carcinogenesis.....	1
1.2	Colorectal cancer (CRC).....	5
1.2.1	Adenomatous polyposis coli (APC).....	7
1.3	Chemoprevention of CRC.....	9
1.4	Preclinical models of CRC.....	12
1.4.1	Cell lines.....	12
1.4.1.1	APC10.1 cells .....	12
1.4.2	Animal models.....	14
1.4.2.1	<i>Apc</i> <sup>Min/+</sup> mouse model.....	17
1.4.3	Studies of gene expression by microarray technology.....	19
1.4.4	Chemopreventive mechanisms .....	21
1.4.4.1	Inhibition of cell proliferation .....	21
1.4.4.2	Cell cycle.....	22
1.4.4.3	Induction of apoptosis .....	27
1.4.4.4	Modulation of Wnt signalling pathway.....	30
1.4.4.5	Modulation of Phosphoinositol-3 kinase (PI3K)/Akt/GSK3 $\beta$ .....	34
1.4.4.6	STAT3 and its pathway.....	36
1.5	Flavonoids .....	37
1.5.1	Methoxyflavones.....	39

1.5.1.1	Apigenin (4', 5, 7-trihydroxyflavone).....	41
1.5.1.2	Tricin (4', 5, 7-trihydroxy-3', 5'-dimethoxyflavone) .....	44
1.5.1.3	Pentamethoxyflavone (3',4',5',5,7-pentamethoxyflavone) (PMF) ...	47
1.6	Aims and objectives.....	49
2	Materials and methods .....	51
2.1	Materials.....	51
2.1.1	APC10.1 cell line .....	51
2.1.2	<i>Apc</i> <sup>Min/+</sup> mouse treatment regime.....	51
2.1.3	Buffers.....	53
2.1.3.1	4-(2-Hydroxyethyl) piperazine-1-ethanesulfonic acid (HEPES).....	53
2.1.3.2	Diethylpyrocarbonate (DEPC)-treated water .....	53
2.1.3.3	Running Buffer (Western blot, WB).....	53
2.1.3.4	Transfer buffer (WB) .....	53
2.1.3.5	10% Ammonium persulfate.....	53
2.1.3.6	Cell lysis buffer (Roche, UK).....	54
2.1.3.7	Phosphate-buffered saline-Tween (PBST) buffer (WB).....	54
2.1.3.8	Blocking buffer (WB) .....	54
2.1.3.9	Antigen retrieval buffer (Immunohistochemistry).....	54
2.1.3.10	Endogenous peroxidase-inhibiting buffer .....	54
2.1.3.11	Primary antibody diluent .....	55

2.1.3.12	3, 3'-diaminobenzidine (DAB) + Substrate buffer (DakoCytomation, UK) (provided by kit) .....	55
2.1.3.13	DAB Chromogen (DakoCytomation, UK).....	55
2.2	Methods.....	55
2.2.1	Maintenance of APC10.1 cells .....	55
2.2.2	Passage of cell lines .....	55
2.2.3	Formulation of stock solution for treatment of cells.....	56
2.2.4	Treatment with flavones .....	56
2.2.4.1	Assessment of cell proliferation .....	56
2.2.4.2	Treatment of cells with flavones for cell cycle assay .....	57
2.2.4.3	Treatment of cells with flavones for apoptosis assay.....	58
2.2.5	mRNA microarray.....	59
2.2.5.1	Treatment of cells with flavones.....	63
2.2.5.2	RNA extraction .....	64
2.2.5.3	Reverse transcription.....	65
2.2.5.4	RNA hydrolysis .....	66
2.2.5.5	Purification of cDNAs.....	66
2.2.5.6	Coupling of labelled cDNAs .....	67
2.2.5.7	Clean up of labelled cDNAs .....	67
2.2.5.8	Preparation of microarray slides .....	68
2.2.5.9	Hybridisation of cDNAs onto microarray slides .....	68

2.2.5.10	Washing of the microarray slides .....	69
2.2.5.11	Analysis of fluorescence and data interpretation .....	69
2.2.6	Validation of gene changes using reverse transcriptase-PCR (RT-PCR) .	71
2.2.7	Western blot (WB) technique .....	75
2.2.7.1	Preparation of cell lysate .....	75
2.2.7.2	Protein assay .....	76
2.2.7.3	Western blot (WB) .....	77
2.2.7.4	Optimisation of antibodies.....	80
2.2.8	<i>In vivo</i> study using <i>Apc</i> <sup>Min/+</sup> mouse model (PPL80/2167).....	83
2.2.8.1	Treatment regime of study.....	83
2.2.8.2	Immunohistochemistry.....	83
2.2.8.3	Assessment of adenoma number and size .....	86
2.2.8.4	Western blot on <i>in vivo</i> samples .....	87
2.2.9	Statistical analysis .....	87
2.2.9.1	Student's t-test and analysis of variance (ANOVA).....	87
2.2.9.2	Mann-Whitney U test.....	88
3	Investigation into the effects of flavones on cell proliferation, cell cycle and apoptosis in APC10.1 murine adenoma cells .....	89
3.1	Introduction .....	89
3.2	Effects of flavones on cell proliferation.....	89
3.3	Effects of flavones on cell cycle.....	92

3.4	Effects of flavones on apoptosis .....	97
3.5	Discussion .....	103
4	Investigation into the effects of flavones on gene expression in APC10.1 cells. .	106
4.1	Introduction .....	106
4.2	Number of genes changed by flavones .....	106
4.2.1	Gene changes with fold change cut-off of 1.5 .....	108
4.2.2	Gene changes with fold change cut-off of 1.3 .....	112
4.2.3	Common gene changes caused by flavones .....	113
4.2.4	Pathway analyses of genes affected by flavones .....	117
4.3	Effects of PMF on molecular functions in APC10.1 cells .....	122
4.4	Effects of PMF on biological processes in APC10.1 cells.....	125
4.5	Effects of PMF on cellular components in APC10.1 cell line. ....	128
4.6	Overall effects of PMF on APC10.1 cells.....	130
4.7	Validation of gene changes using reverse transcriptase-PCR (RT-PCR) .....	144
4.8	Gene validation using WB .....	147
4.8.1	Proteins in Wnt signalling pathway modulated by PMF.....	148
	Figure 4.15 Effects of PMF on levels of proteins closely associated with the Wnt signalling pathway (mean $\pm$ SD). .....	149
4.8.2	Proteins associated with regulation of cell cycle .....	150
4.8.3	Proteins associated with transcription, translation and cell proliferation	152
4.8.4	Proteins associated with apoptosis.....	154

4.9	Discussion .....	155
5	Effects of PMF on <i>Apc</i> <sup>Min/+</sup> mice <i>in vivo</i> .....	161
5.1	Introduction .....	161
5.2	Effects of PMF on adenoma number and burden .....	162
5.3	Effects of PMF on expression of mechanistically important proteins in the small intestine and colon.....	166
5.4	Discussion .....	181
6	General Discussion.....	183
7	Appendices.....	191
8	Articles published.....	192
8.1	Articles: .....	192
	Sale, S., I. L. Fong, et al. (2009). "APC10.1 cells as a model for assessing the efficacy of potential chemopreventive agents in the <i>Apc</i> (Min) mouse model <i>in vivo</i> ." <i>Eur J Cancer</i> 45(16): 2731-5.....	192
8.2	Abstracts and conference proceedings:.....	192
9	References .....	193

## **List of figures**

Figure 1.1 The three basic sequential steps of carcinogenesis. ....	2
Figure 1.2 The hallmarks of cancer: biological capabilities of the cancer cell. Adapted from Hanahan and Weinberg, 2011.....	5
Figure 1.3 Different genetic pathways that are involved in the multi-step carcinogenesis model. Adapted from Fearon and Vogelstein, 1990; Hung and Chung, 2006; Stein et al., 2009.....	8
Figure 1.4 Two major strategies for cancer chemoprevention. Adapted from Greenwald , 2002. ....	10
Figure 1.5 A schematic diagram of the cell cycle. Adapted from DiPaola, 2002 and Schmitt et al, 2007a. ....	22
Figure 1.6 A schematic diagram depicting the extrinsic, intrinsic and p53-mediated apoptotic pathways. Adapted from Chipuk and Green, 2008, Diehl et al., 1998 and Chipuk et al., 2006.....	27
Figure 1.7 The Wnt Signalling Pathway. Adapted from Kawasaki et al., 2001, Takahashi-Yanaga and Sasaguri, 2008 and Takahashi-Yanaga and Sasaguri, 2009. ....	32
Figure 1.8 A schematic diagram of the phosphatidylinositol 3'-kinase-Akt signalling pathway. Adapted from Osaki et al., 2004, Cantley, 2002 and Li et al., 2011. ....	34
Figure 1.9 Benzo- $\gamma$ -pyrone .....	37
Figure 1.10 The basic structure of flavonoids. ....	37
Figure 1.11 The basic chemical structure of flavones.....	39
Figure 1.12 The chemical structure of apigenin (4',5, 7-trihydroxyflavone).....	41

Figure 1.13 The chemical structure of tricetin (4',5,7-trihydroxy-3',5'-dimethoxyflavone). .....	44
Figure 1.14 The chemical structure of 3',4',5',5,7-pentamethoxyflavone (PMF).....	47
Figure 2.1 The feeding regime of <i>Apc<sup>Min/+</sup></i> mouse model for short (A) and long (B) term animal studies.....	52
Figure 2.2 A schematic diagram showing the sequential steps from treatment of cell to the end results of pathway analysis. ....	63
Figure 2.3 A real-time scan of a microarray slide (left) and a magnified grid containing excited probes hybridised to specific genes (dots) (right). ....	70
Figure 2.4 Layout of a 96-well optical reaction plate template for RT-PCR. ....	75
Figure 2.5 A standard BSA calibration curve at absorbance of 595 nm. ....	76
Figure 2.6 Layout of transfer cassette for WB.....	80
Figure 3.1 Dose-dependent inhibition of cell proliferation by apigenin (A), tricetin (B) and PMF (C) in APC10.1 cells on day 3 (open) and day 6 (closed). ....	91
Figure 3.2 A representative cell cycle profile of untreated APC10.1 at 24 h.....	93
Figure 3.3 Effects of apigenin at 5, 10 and 20 $\mu$ M on the cell cycle of APC10.1 cells at 24 h (A), 48 h (B), 72 h (C) and 96 h (D). ....	94
Figure 3.4 Effects of tricetin at 5, 10 and 20 $\mu$ M on the cell cycle of APC10.1 cells at 24 h (A), 48 h (B), 72 h (C) and 96 h (D).....	95
Figure 3.5 Effects of PMF at 5 and 10 $\mu$ M on the cell cycle of APC10.1 cells at 24 h (A), 48 h (B), 72 h (C) and 96 h (D).....	96
Figure 3.6 Representative fluorescence scattergrams of flow cytometric analysis of APC10.1 cells exposed to control (etoposide or medium) and flavone PMF for 96 h. ....	98

Figure 3.7 Representative fluorescence scattergrams of flow cytometric analysis of APC10.1 cells exposed to up to 10 $\mu$ M PMF for up to 96 h.....	99
Figure 3.8 Pro-apoptotic effects of apigenin on APC10.1 cells at 48 h (A), 72 h (B) and 96 h (C). .....	100
Figure 3.9 Pro-apoptotic effects of tricetin on APC10.1 cells at 48 h (A), 72 h (B) and 96 h (C). .....	101
Figure 3.10 Pro-apoptotic effects of PMF on APC10.1 cells at 48 h (A), 72 h (B) and 96 h (C). .....	102
Figure 4.1 Principle component analysis (PCA) of gene change post 24-h incubation of APC10.1 cells with 10 $\mu$ M apigenin (left), tricetin (middle) or PMF (right). .....	109
Figure 4.2 Volcano plots illustrating the position of each gene, p-value and cut-off margins for A (left) and B (right) slides for apigenin (top), tricetin (middle) and PMF (bottom). .....	110
Figure 4.3 Venn diagrams depicting the number of genes altered by apigenin (A), tricetin (T), or PMF (P) in APC10.1 cells using a p-value<0.05. ....	115
Figure 4.4 Venn diagrams depicting the genes altered by apigenin (A), tricetin (T), or PMF (P) in APC10.1 cells using a p-value<0.01. ....	116
Figure 4.5 Gene Ontology (GO) Tree Prune depicting molecular functions in APC10.1 cells exposed to 10 $\mu$ M PMF after 24-h incubation (p<0.05). .....	124
Figure 4.6 Gene Ontology (GO) Tree Prune depicting biological processes in APC10.1 cells exposed to 10 $\mu$ M PMF after 24-h incubation (p<0.05). .....	127
Figure 4.7 Gene Ontology (GO) Tree Prune depicting biological processes in APC10.1 cells exposed to 10 $\mu$ M PMF after 24-h incubation (p<0.05). .....	129

Figure 4.8 Heat map analysis of genes involved in Wnt, TLR and STATs signalling pathways, modulated by apigenin (A), tricetin (T) and PMF (P) relative to control. ....	135
Figure 4.9 Heat map analysis of genes involved in Hedgehog signalling pathway, apoptosis and initiation of transcription, modulated by apigenin (A), tricetin (T) and PMF (P) relative to control. ....	138
Figure 4.10 Heat map analysis of genes involved in cell cycle modulated by apigenin (A), tricetin (T) and PMF (P) relative to control.....	139
Figure 4.11 Effects of apigenin on biochemical pathways based on gene list from the microarray analysis (p-value<0.05) using DAVID/ EASE.....	141
Figure 4.12 The different biochemical pathways modulated by PMF based on the microarray analysis (p-value<0.05) using DAVID/ EASE.....	142
Figure 4.13 Effects of PMF on genes associated with Wnt signalling pathway in APC10.1 cells.....	145
Figure 4.14 Effects of PMF on genes closely associated with Hedgehog signalling pathway (Ptch1, Wnt8b), TLR pathway (Tollip, Rela), apoptosis pathway (Rela, Tnfrsf10b) and cell transformation (Vav3).....	146
Figure 4.15 Effects of PMF on levels of proteins closely associated with the Wnt signalling pathway (mean $\pm$ SD). ....	149
Figure 4.16 Effects of PMF on levels of proteins closely associated with regulation of the cell cycle (mean $\pm$ SD). ....	150
Figure 4.17 Effects of PMF on the levels of proteins closely associated with transcription, translation and cell proliferation (mean $\pm$ SD). ....	152
Figure 4.18 Effects of PMF on the levels of proteins closely associated with apoptosis (mean $\pm$ SD). ....	154

Figure 5.1 Frequency distribution of adenoma burden depicting non-normal distribution of the adenoma burden in this animal study. ....	163
Figure 5.2 Effects of PMF on the total number of adenoma in control (open) or long term PMF-treated (closed) <i>Apc<sup>Min/+</sup></i> mice. ....	164
Figure 5.3 Effects of PMF on the total adenoma burden in control (open) or long term PMF-treated (closed) <i>Apc<sup>Min/+</sup></i> mice.....	165
Figure 5.4 Effects of PMF on Bax (A), p21 (B), Akt1 (C), GSK3 $\beta$ (D), pGSK3 $\alpha$ (E), pGSK3 $\beta$ (F), Survivin (G), MCM7 (H), caspase-3 cleaved (I) and $\beta$ -catenin (J) expressions in control and PMF-treated animal adenoma (A, open) or mucosa (M, closed) lysates. ....	169
Figure 5.5 Effects of PMF on the normal crypts, aberrant crypts foci, normal villi and adenomas in the colons of <i>Apc<sup>Min/+</sup></i> mice that received control or 0.2% w/w PMF, stained for GSK3 $\beta$ mouse antibody at magnifications of 10x and 20x.....	172
Figure 5.6 Effects of PMF on the normal crypts, aberrant crypt foci, normal villi and adenomas in the small intestines of <i>Apc<sup>Min/+</sup></i> mice that received control or 0.2% w/w PMF, stained for GSK3 $\beta$ mouse antibody at magnifications of 10x and 20x. ....	175
Figure 5.7 Effects of PMF on the normal crypts, aberrant crypts foci, normal villi and adenomas in the colons of <i>Apc<sup>Min/+</sup></i> mice that received control or 0.2% w/w PMF, stained for MCM7 mouse antibody at magnifications of 10x and 20x. ....	177
Figure 5.8 Effects of PMF on the normal crypts, aberrant crypts foci, normal villi and adenomas in the small intestines of <i>Apc<sup>Min/+</sup></i> mice that received control or 0.2% w/w PMF, stained for MCM7 mouse antibody at magnifications of 10x and 20x. ....	180

Figure 6.1 Effects of PMF on some of the hallmark chemopreventive mechanisms and pathways implicated in carcinogenesis.....	189
---	-----

Figure 7.1 PageRuler™ Prestained Protein Ladder (left) and Spectra™ Multicolor High Range protein ladder (right) for WB. ....	191
---	-----

### **List of tables**

Table 1.1 Some of the CRC cell lines derived from either human or mouse that are utilised for studies of carcinogenesis <i>in vitro</i> .....	13
Table 1.2 Widely used rodent models for CRC study.....	16
Table 1.3 Kinases, phosphatases, cyclins, stimulators, inhibitors and downstream genes associated with the eukaryotic cell cycle.....	26
Table 2.1 The Labelling mix constituents for reverse transcription. ....	65
Table 2.2 Washing regime performed on the array slides.....	69
Table 2.3 Fifteen genes closely associated with CRC, cell cycle arrest and apoptosis were shortlisted. The forward and reverse primers (mouse origin) of these genes were generated for Reverse Transcriptase- PCR.....	73
Table 2.4 Formulations for Real Time Master Mix (RT-MM) for 200 reactions.....	74
Table 2.5 Formulation of a 10-μL reaction mix for each RNA.....	74
Table 2.6 Formulation for addition of SyBr Green to the RNA reaction mix (n=28). ...	74
Table 2.7 Constituents for preparation of 8%, 10% and 15% resolving gels respectively for WB. ....	79
Table 2.8 Constituents for preparation of stacking gel.....	79
Table 2.9 Dilutions of primary and secondary antibodies were performed in blocking buffer of 5% milk in PBST. ....	81

Table 3.1 IC <sub>50</sub> values for apigenin, tricetin and PMF for inhibition of APC10.1 cell growth (n=3, p<0.05).....	90
Table 4.1 Number of genes changed by apigenin, tricetin or PMF (10 μM) on slides A and B at p-value<0.05 and fold change of 1.5. ....	111
Table 4.2 Number of gene change by the apigenin, tricetin or PMF on slides A and B at p-value<0.05 and fold change of 1.3. ....	113
Table 4.3 A summary of pathways delineated from the gene lists changed by apigenin, tricetin or PMF (p-value<0.05, with direction of gene change). ....	120
Table 4.4 Genes changed exclusively by PMF (p<0.05) with the same direction as tricetin and apigenin. ....	121
Table 4.5 List of molecular functions affected by 10 μM PMF after 24 h incubation in APC10.1 cells.....	123
Table 4.6 Biological processes associated with genes affected by 10 μM PMF after 24 h incubation with APC10.1 cells.....	126
Table 4.7 List of cellular components affected by 10 μM PMF after 24h incubation in APC10.1 cells.....	128
Table 4.8 Pathways generated by gene lists for PMF (p<0.05).....	131
Table 4.9 Summary of different mechanisms of action triggered by 10 μM PMF treatment in APC10.1 cells (p-value<0.05). ....	143

**List of equations:**

Equation 1 Volume of adenoma in colon: .....	86
Equation 2 Volume of adenoma in small intestine: .....	86

## **Table of abbreviations**

### **Abbreviation**

°C	Celsius
ACADM	Acyl-Coenzyme A dehydrogenase
ACF	Aberrant crypt foci
AIN-93G	American Institute of Nutrition growth purified diet-93G
Akt	Protein kinase B
ANOVA	Analysis of variance
AOM	Azoxymethane
APAF-1	Apoptosis-protease-activating factor-1
APC	Adenomatous polyposis coli
Apigenin	4',5, 7-trihydroxyflavone
ATCC	American type culture collection
ATP	Adenosine-5'-triphosphate
Axin	Axis inhibition protein
BAX	BCL-2 associated X protein
BAX	Bcl-2-associated X protein
BCL9L	B-cell CLL/lymphoma 9-like protein
Bcl-xL	B-cell lymphoma-extra large
BDNF	Brain-derived neurotrophic factor
Bid	Bcl-2 interacting domain death agonist
BSA	Bovine serum albumin
Caco-2	Human epithelial colorectal adenocarcinoma cells
caspase	Cysteiny aspartate-specific proteinase
Cdc, Cdk	Cyclin-dependent kinase
Cdc6	Cell division cycle 6
CDH1	E-cadherin
Cdk	Cyclin-dependent kinase
Cdkn	Cyclin-dependent kinase inhibitor
Cdt1	Chromatin licensing and DNA replication factor 1
chrysin	5,7-dihydroxyflavone
CIN	Chromosomal instability
CK1 $\alpha$	Casein kinase 1 $\alpha$
CKI	Cyclin kinase inhibitor
cm	Centimetre
COX2	Cyclooxygenase 2
Coxibs	Inhibitors of cyclooxygenase 2
CRC	Colorectal, colorectum
CrkL	Adapter molecule crk-like protein
Ct	Cycle threshold
CTMP	Carboxyl-terminal modulator protein
Cy, Ccn	Cyclin
Cy3	Cyanine 3
Cy3-dUTP	Cy3-2'-deoxyuridine-5'triphosphate
Cy5	Cyanine 5
DAB	3, 3'-diaminobenzidine
DCC	Deleted in colon cancer

DEPC	Diethylpyrocarbonate
DISC	Death-inducing signalling complex
Diversin	Planar cell polarity protein
DMEM	Dulbecco's minimal essential medium
DMH	1, 2-dimethylhydrazine
DMSO	Dimethyl sulfoxide
DNA	Deoxyribonucleic acid
DPX	Distyrene plasticiser and xylene
DU145	Human prostate cancer cells
Dvl1, Dsh	Dishevelled 1
ECL	Enhanced luminol-based chemiluminescent
EDTA	Ethylenediaminetetraacetic acid
EGCG	Epigallocatechin gallate
ENU	Ethylnitrosourea
ErbB2	Erythroblastic leukaemia B2
ERK	Extracellular-signal regulating kinase
Exp	Expected
FACS	Fluorescence-activated cell sorting
FADD	Fas-associated death domain protein
FAP	Familial adenomatous polyposis
FasL	Fas-binding ligand
FDR	False discovery rate
FITC	Fluorescein-isothiocyanate
Frat1	Frequently rearranged in advanced T-cell lymphomas 1
G <sub>0</sub>	Gap <sub>0</sub> , senescence phase in cell cycle
G <sub>1</sub>	Gap <sub>1</sub> , checkpoint in cell cycle
G <sub>2</sub>	Gap <sub>2</sub> , checkpoint in cell cycle
GADD45	Growth arrest and DNA damage 45
GLUT1	Glucose transporter 1
GO	Gene ontology
GOFFA	Gene ontology for functional analysis
G-protein	Guanine nucleotide-binding protein
GSK3 $\beta$	Glycogen synthase kinase $\beta$
h	Hour
H&E	Haematoxylin and eosin stain
HBL-100	Human-derived non-malignant breast cells
HCEC	Human colon-derived epithelial cells
Hela	Human epithelial cervical cancer cells
HEPES	4-(2-Hydroxyethyl) piperazine-1-ethanesulfonic acid
HIF1 $\alpha$	Hypoxia-inducible factor 1 $\alpha$
HMG-CoA	3-hydroxy-3-methylglutaryl-coenzyme A
hMLH1	Human mutl homolog 1
hMSH2	Human muts homolog 2
hMSH3	Human muts homolog 3
hMSH6	Human muts homolog 6
HNPCC	Hereditary non-polyposis colon cancers
HRP	Horse-radish peroxidase
Hs3st1	Heparan sulfate glucosamine 3-O-sulfotransferase 1
HT-29	Human colon adenocarcinoma grade II cell line

IC <sub>50</sub>	Half maximal inhibitory concentration
IEN	Intraepithelial neoplasia
IFN	Interferon
IGF-1	Insulin-like growth factor-1
ILK	Integrin-linked kin
IMS	Industrial methylated spirit
INK4	Inhibitors of Cdk4
INT6	Integrator complex subunit 6
IQ	2-amino-3-methylimidazo[4,5-f]quinoline
ISRE	Interferon-stimulate response element
KEGG	Kyoto Encyclopaedia of Genes and Genomes
Kip	Cyclin-dependent kinase inhibitor 1B
LEF	Lymphoid enhancer factor
LNCap	Androgen sensitive human prostate adenocarcinoma
LOH	Loss of heterozygosity
Lrp5	Low-density lipoprotein receptor-related protein 5
M	Mitosis phase in cell cycle
MACC	Metastasis associated in CRC
MCL1	Myeloid leukemia cell differentiation protein 1
MCM7	Mini-chromosome maintenance protein 7
MDA-MB-468	Human-derived breast tumour cells
MEEBO	Mouse exonic evidence-based oligonucleotides
MEK	Mitogen-activated protein kinase
mg	Milligram
miRNA	Microribonucleic acid
Min	Multiple intestinal neoplasia
min	Minute
mL	Millilitre
mM	Millimolar
Mol. Wt.	Molecular weight
MOMP	Mitochondrial outer membrane permeabilisation
mRNA	Messenger ribonucleic acid
MSI	Microsatellite instability
NaCl	Sodium chloride
NAG-1	Non-steroidal anti-inflammatory drug-activated gene 1
NaOH	Sodium hydroxide
Nfatc2	Nuclear factor of activated T-cells 2 protein
ng	Nanogram
nM	Nanomolar
NSAIDs	Non-steroidal anti-inflammatory drugs
NTC	Non-template control
obs	Observed
ODC	Ornithine decarboxylase
PAPS	3'-phosphoadenosine-5'-phosphosulfate
PBS	Phosphate-buffered saline
PBST	Phosphate-buffered saline-Tween
PCA	Principle component analysis
PCG1 $\alpha$	Polycomb group 1 $\alpha$
PDKs	Phosphoinositide-dependent kinases

PGE <sub>2</sub>	Prostaglandin E2
P-glycoprotein	Permeability glycoprotein
pGSK3 $\alpha$	Phosphorylated glycogen synthase kinase 3 alpha
pGSK3 $\beta$	Phosphorylated glycogen synthase kinase 3 beta
PH	Plekstrin homology
PI	Propidium iodide
PI2P	Phosphatidylinositol- 4, 5-bisphosphate
PI3K	Phosphatidylinositol 3-kinase
PI3P	Phosphatidylinositol-3,4,5-triphosphate
Pim1	Proto-oncogene serine/threonine-protein kinase
PMF	3',4',5',5,7-pentamethoxyflavone
PMT	Photomultiplier tube
PP1, PP2A, PP2B	Phosphatases serine / threonine
pRb	Retinoblastoma protein
PS	Phosphatidylserine
Ptch1	Patched1, tumour suppressor for sonic hedgehog pathway
PTEN	Phosphatase and tensin homolog
PTP	Tyrosine protein phosphatases
Rela	Transcription factor p65
RGB	Red:green:blue
ROS	Reactive oxygen species
rRNA	Ribosomal ribonucleic acid
RT	Room temperature
RTK	Receptor tyrosine kinase
RT-MM	Real time master mix
RT-PCR	Reverse transcriptase-polymerase chain reaction
S	Synthesis phase in cell cycle
SCID	Severe compromised immunodeficiency
SD	Standard deviation
SDS	Sodium dodecyl sulfate
SH2	Src homology 2
SLC2A1	Solute carrier family 2 (facilitated glucose transporter)
SNP	Single-nucleotide polymorphisms
SNU C4	Human colon cancer cells
SSC	Saline sodium citrate
STAT	Signal transducer and activator of transcription
SULTs	Sulfotransferases
SW480	Human colon adenocarcinoma cell line
SyBr	SYBR Green I cyanine dye
Tb11	Transcriptional co-factor Transducin (beta)-like 1
TCF	Transcription factor
TEMED	N,N,N',N'-tetramethyl-ethylenediamine
TGF $\beta$	Transforming growth factor beta
TGF $\beta$ IIR	Transforming growth factor beta isoform II receptor
TLR	Toll-like receptor
TNF	Tumour necrosis factor
Tnfrsf10b	Tumor necrosis factor receptor superfamily, member 10b
Tollip	Toll-interacting protein

TRAIL/ APOP2L	TNF-related apoptosis-inducing ligand
Tricin	4',5,7-trihydroxy-3',5'-dimethoxyflavone
TrkB	Tyrosine kinase B
tRNA	Transfer ribonucleic acid
Tween®20	Polyoxyethylenesorbitan monolaurate
UDP-UGT	Uridine diphosphate-glucuronosyltransferase
UK	United Kingdom
UP	Ultra-pure
USFDA	United States Food and Drug Administration
V	Voltage
v:v	Volume per volume
Vav3	Guanine nucleotide exchange factor , oncogene
W	Watt
WAF1	P21 wild type p53-activated fragment 1
WB	Western blot
β-TRCP	β-Transducin repeat-containing protein
μg	Microgram
μL	Microlitre
μM	Micromolar

# **1 Introduction**

According to data from the World Health Organisation, cancer contributes to approximately 13% (7.8 million deaths) of mortality worldwide (Ferlay J, 2008). Of these cancer-related mortalities, one third could have been prevented with early detection and treatment. In developed countries, cancer is the most prevalent cause of non-communicable disease death (WHO, 2011). Globally, the five most frequent cancers are those of the lung, stomach, liver, colorectum (CRC) and breast (WHO, 2011).

In 2005, cancer mortality in the United Kingdom (UK) reached 142,000 cases with 55,000 cases accounted for by people aged 70 years old or above. This translates to 21.8% of main causes of death in the United Kingdom (WCRF/AICR, 2007, Ferlay J, 2008).

In 2007, approximately one-third of non-communicable causes of death in the UK were caused by cancer, with CRC being the second most common cancer after breast cancer in women and the third most common cancer in men after prostate and lung cancer (Ferlay J, 2008).

## **1.1 Carcinogenesis**

A cell is a complex entity containing genetic information encoded in DNA with critical stages and checkpoints to ensure that normal growth, development, function and survival are stringently regulated. Any dysregulation can elicit mechanisms to safeguard

cell integrity such as DNA repair (Christmann et al., 2003). If these repair mechanisms are not sufficient in safeguarding the integrity of the genetic information in the cell, then programmed cell death (apoptosis) ensues. When the integrity of the cell and its check-points are compromised, uncontrollable cell replication and proliferation occur (Hanahan and Weinberg, 2000). This is the initiation of carcinogenesis.

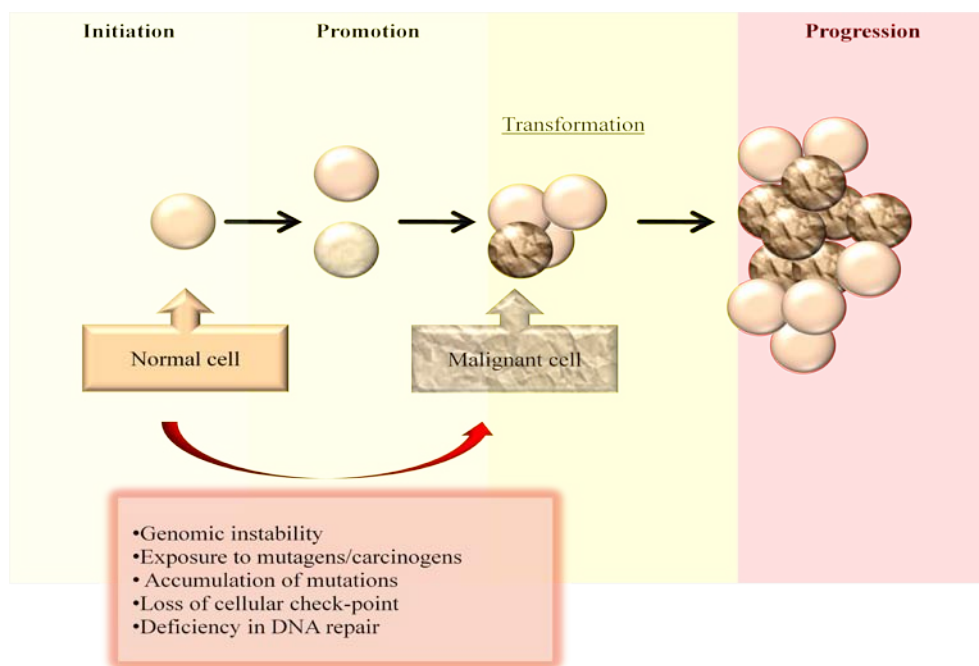


Figure 1.1 The three basic sequential steps of carcinogenesis.

Three major steps that characterize carcinogenesis: initiation, promotion and progression. The inset box shows factors that can trigger irreversible initiation steps in normal cells that cause them to become malignant.

Carcinogenesis can be categorized into three major series of steps that span over 15-30 years: initiation, promotion and progression (Figure 1.1). It is a process characterized by

gradual selective activation and accumulation of carcinogenic oncogenes (Bos, 1988), irreversible dysfunction and/or loss of repair mechanisms, and ultimately loss of function of tumour suppressor genes (Dove et al., 1995) or genes that trigger apoptosis (Gatenby and Vincent, 2003). The newly generated phenotype enables the mutated cells to evade growth control (Gatenby and Vincent, 2003). The distinct sequential steps of carcinogenesis which occur over a prolonged duration provide windows of opportunity for anti-carcinogenic intervention studies.

There are several factors that cause cancer initiation independently or synergistically. These can be categorized into endogenous and exogenous factors (Lutz and Fekete, 1996). Endogenous factors include heritable susceptibility determinants which encompass genomic instability, dysfunction or loss of mitotic checkpoints, deficiency in DNA repair mechanisms, accumulation of these mutations and accumulation of products of metabolism and inflammation (Shen, 2011, Schwartz-Albiez et al., 2009). Exogenous factors include exposure to mutagens/carcinogens encountered in the environment, and lifestyle factors such as smoking and dietary habits (Reynolds et al., 2011). During the initiation event, the mutagen or carcinogen or their metabolites interact with nucleic acids in the cell leading to the activation of oncogenes, dysfunction of repair mechanisms and/or loss of tumour suppressor genes. When steps are not taken to reduce the frequency of, or prevent altogether, exposure to these risk factors, irreversible and uncontrollable DNA damage ensues.

The promotion stage is an early event in tumour development. Factors that influence the promotion stage include the anatomy and physiology of the epithelial surfaces as well as the phenotypical advantage of the mutated cells over normal cells. The early cancerous phenotype has a few barriers to overcome for continual proliferation. Studies have

demonstrated that alterations in the phosphatidylinositol 3-kinase (PI3K) pathway, or mutations of E-cadherin (*CDH1*), *Ras*, adenomatous polyposis coli (*APC*) or  $\beta$ -catenin play vital roles at this stage (Coll et al., 2002, Delcommenne et al., 1998). The downstream effects of autocrine or paracrine induction of growth factor production elevate the expression of membrane receptors or up-regulate genes within signal-transduction pathways (Fenton et al., 2008). This increases the ability of the mutated cells to proliferate. Prolonged exposure to mutagens/carcinogens not only causes genetic mutation, but also influences many factors *in milieu* including growth factors, hormonal balance and cytokine activation. In most cases, these effects can be halted, reversed or repaired (Gatenby and Vincent, 2003).

The progression stage is characterized by karyotypic instability, evolution and development of irreversible, aneuploid malignant neoplasms. When a mutated cell enters the progression stage, it can become resistant to anoikis through evasion of apoptosis via mutation of *Ras* which regulates both proliferation and senescence of cells. As hyperplasia sets in, the hyper-proliferating cell needs stromal support for angiogenesis and formation of the extracellular matrix. Up-regulation of phosphoMYC and/or stabilisation of hypoxia-inducible factor 1 $\alpha$  (HIF1 $\alpha$ ) enable mutated cells to maintain a high level activation of glycolysis, even under aerobic conditions (Giles et al., 2006, Chiacchiera et al., 2009). This elevation increases acid production, thereby induces caspase activities and apoptosis via p53-dependent pathways. The acidic extracellular pH promotes increased motility and invasion, consistent with increased glucose uptake and GLUT1 (or SLC2A1) expression, as seen at the late stages of *in situ* cancer of the oesophagus, breast, prostate or colon (Du et al., 2009, Melstrom et al.,

2011). Thus, the hyper-proliferating cells become invasive with metastatic capability (Giles et al., 2006, Chiacchiera et al., 2009).

## 1.2 Colorectal cancer (CRC)

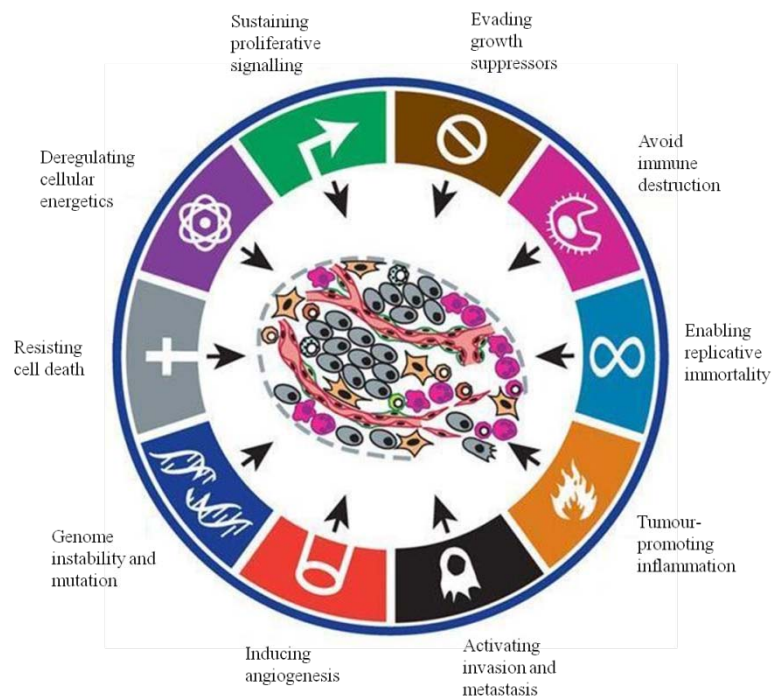


Figure 1.2 The hallmarks of cancer: biological capabilities of the cancer cell. Adapted from Hanahan and Weinberg, 2011.

In normal intestinal epithelium, the events of proliferation, differentiation, migration and cell death are tightly regulated to ensure stringent perpetual cell turnover. When these events are de-regulated due to acquisition of several hallmarks of carcinogenesis (Figure 1.2), hyper-proliferation results at the expense of differentiation. Cells become

hyperplastic and gradually dysplastic, and finally aberrant crypt foci (ACF) are formed (Cheng and Lai, 2003, Cravo et al., 1994). These foci continue to progress to benign adenomas or adenomatous polyps. Eventually, most of these benign adenomas (10%) transform into malignant tumours and become carcinomas (Fearon and Vogelstein, 1990, WHO, 2011).

In general, intestinal cancer cell types can be categorised into adeno-carcinomas, mucinous carcinomas and adeno-squamous carcinomas. Each of these can be further divided according to their hereditary or non-hereditary origin. In CRC, the hereditary class can be further divided into familial adenomatous polyposis (FAP) (Northover and Murday, 1989), Gardner Syndrome (Palmer, 1982) and hereditary non-polyposis CRC (Lynch I and II syndromes) (Lynch et al., 1985), while non-hereditary CRC encompasses adenomas and carcinomas.

It has been estimated that the progression of benign adenomatous lesions to carcinoma takes approximately 5-15 years (Leslie et al., 2002). The genetic profile of the various stages of colorectal tumour progression has been delineated (Fearon and Vogelstein, 1990, Pinto et al., 2003, Yu et al., 2006). Generally, CRC can be divided into two classes, familial (75%) and sporadic (25%) (Cooper et al., 2010). In sporadic CRC, genomic instability, namely chromosomal instability (CIN) and microsatellite instability (MSI) account for 85% and 15%, respectively (Figure 1.3) (Itzkowitz and Yio, 2004). Loss of genomic stability of tumour suppressor genes and induction of oncogenes generate favourable conditions for the progression and development of CRC.

A specific mutation is a prerequisite to each stage of progression along the adenoma-carcinoma event. Mutation of the adenomatous polyposis coli gene (*APC*) is the

decisive initiating event in both FAP-associated cancer as well as sporadic cancer, triggering the activation of the Wnt signalling pathway.

### **1.2.1 Adenomatous polyposis coli (APC)**

The adenomatous polyposis coli (APC) tumour suppressor gene encodes the APC protein. This protein has many functions including control of Wnt signalling pathway, involvement in chromosomal segregation at mitosis, cell adhesion, migration and apoptosis (Fodde, 2003).

In FAP, this autosomal dominant *Apc* gene plays a pivotal role in triggering the initiation and progression of CRC (Powell et al., 1992). In humans, germline inactivation of this gene predisposes individuals to develop hundreds to thousands of adenomatous polyps in the colon and rectum (Kinzler and Vogelstein, 1996). Since any loss of normal *APC* function is likely to lead to tumour formation (Fodde et al., 1994), the restoration of *APC* can prevent it. Ninety percent of CRC cases are due to truncation of the *APC* gene (Fodde et al., 2001). In this instance, the elimination of mutated cells carrying the truncated gene can be done by promoting apoptosis or surgical excision (Morin et al., 1996).

At present, colonoscopic polypectomy, surgical removal of polyps, is the most effective intervention and prevention method. As surgery is costly, time-consuming and comes with several risk factors including complications during and after the operation, it is not always the most plausible and desirable treatment especially for those with hereditary predisposition to CRC.

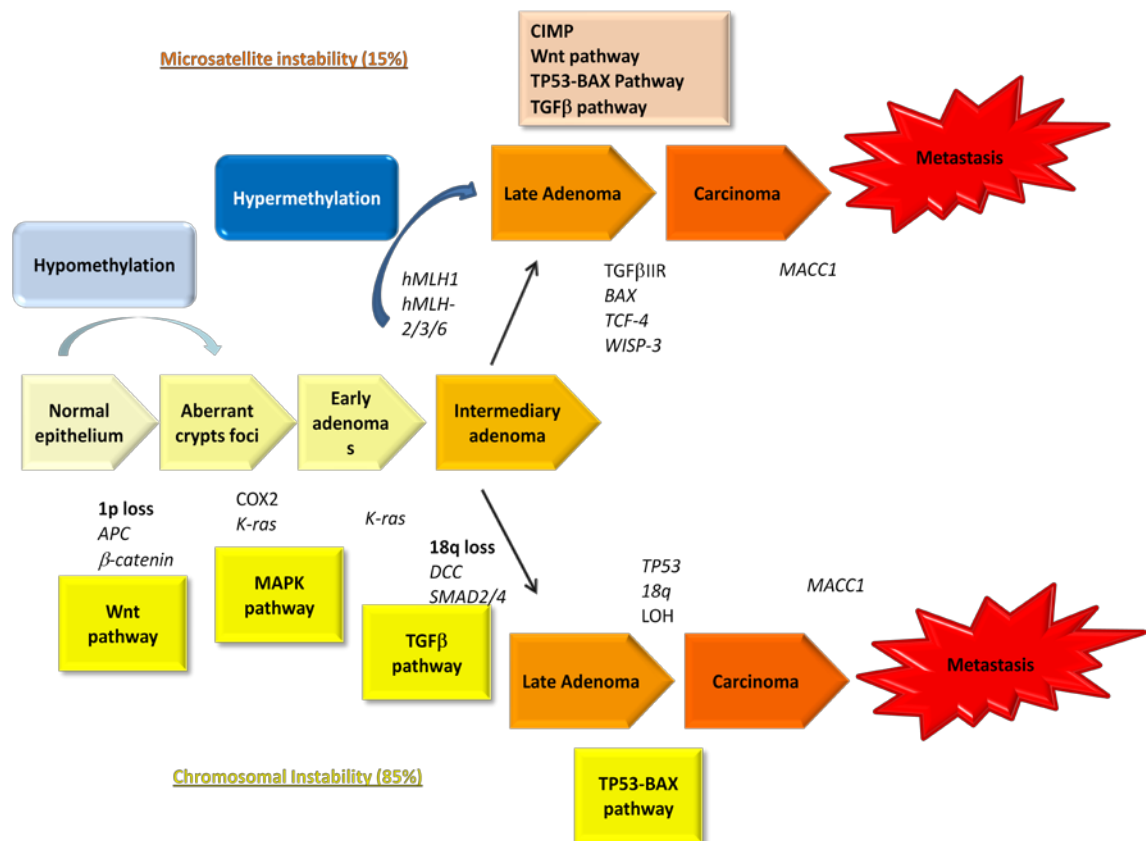


Figure 1.3 Different genetic pathways that are involved in the multi-step carcinogenesis model. Adapted from Fearon and Vogelstein, 1990; Hung and Chung, 2006; Stein et al., 2009.

Hereditary CRC can be divided into two distinct genetic pathways: 1. CIN (85%) and 2. MSI (15%). Different genes implicated in each pathway are included (APC=Adenomatous polyposis coli, BAX=BCL-2 associated X protein, COX2=Cyclooxygenase 2, DCC=Deleted in colon cancer, LOH=Loss of heterozygosity, hMLH1= human mutL homolog 1, hMSH2= human mutS homolog 2, hMSH3=human mutS homolog 3, hMSH6=human mutS homolog 6, MACC=Metastasis associated in CRC, TCF=Transcription Factor, TGFβIIIR=Transforming growth factor beta isoform II receptor).

### 1.3 Chemoprevention of CRC

Chemoprevention is the use of compounds, whether they are natural or synthetic by origin, to impede the progression of disease (Pan et al., 2011). In the field of cancer, chemoprevention is defined as strategies adopted to prevent cancer or treatment of identifiable pre-cancer, also known as intraepithelial neoplasia, IEN (Bonovas et al., 2008). As the different transitional stages of CRC development, initiation, promotion and progression span approximately 15 to 30 years, there is a long term window of opportunity encompassing these stages for effective intervention to be implemented.

There are several strategies for intervention at the initiation stage of carcinogenesis (Figure 1.4) including inhibiting the metabolic carcinogen toxification pathway (heterocyclic amines such as 2-amino-3-methylimidazo[4,5-f]quinoline, IQ), augmenting the efficiency of carcinogen detoxification, mopping up electrophiles and reactive oxygen species (ROS), and enhancing DNA repair (Dibra et al., 2010). Further down the promotion and progression stages, the scavenging of damaging ROS and decreasing the presence of inflammatory molecules (Kahn and Morrison, 1997) help to reduce exposure to harmful endogenous and exogenous factors. Decreasing the rate of cell proliferation, promoting cell differentiation (Knowles and Milner, 2000, Garay and Engstrom, 1999) and stimulating apoptosis reduce the incidence of hyperplasia (Ben-Amotz et al., 2010, Cheung et al., 2009). At the later stage of carcinogenesis, enhancing immunity (Rajamanickam et al., 2010) and halting angiogenesis (Zhou et al., 1999) are means to prevent progression to malignancy. Targeting one or several of the steps may prevent or delay the development of cancer (Greenwald, 2002, Yao et al., 2011).

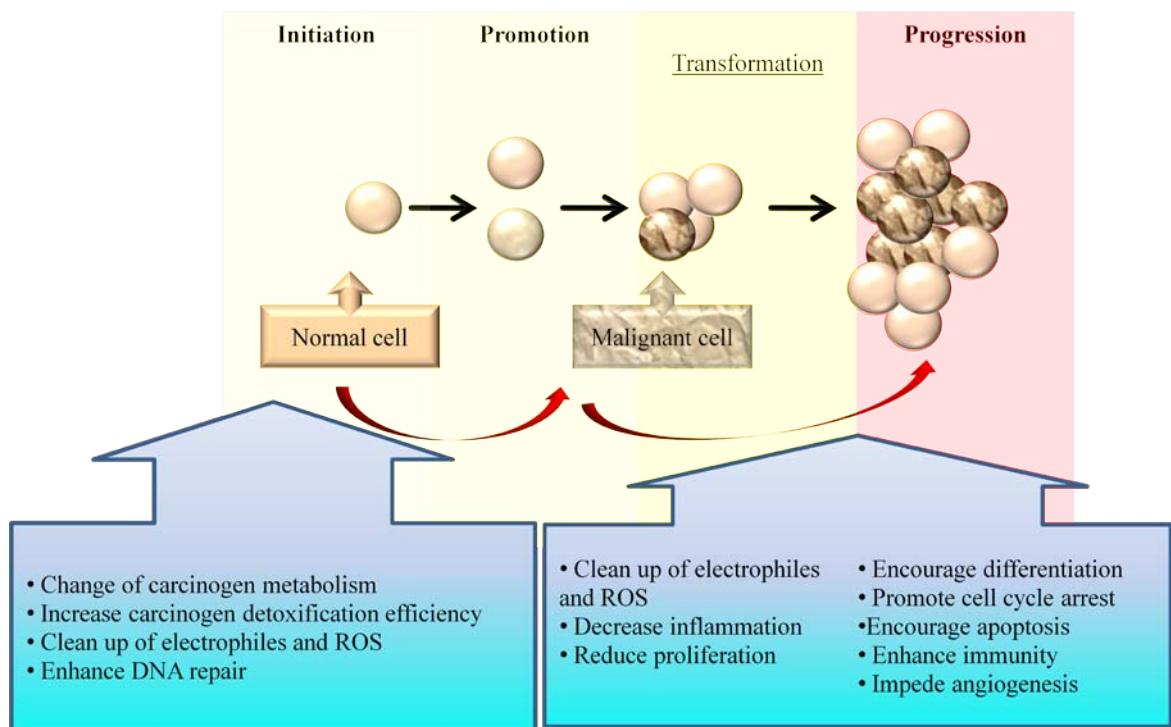


Figure 1.4 Two major strategies for cancer chemoprevention. Adapted from Greenwald , 2002.

There are two general approaches to cancer chemoprevention (see inset boxes): 1) anti-initiation steps, 2) anti-promotion and anti-progression steps. The chemopreventive agents that act on the first step are called blockers while those that act on the subsequent stages are known as suppressors. ROS=reactive oxygen species.

Chemopreventive agents work in two general ways: they are blocking agents or suppressing agents (De Flora and Ferguson, 2005, Ferguson, 1994). Blocking agents prevent carcinogens from reaching, or reacting with, the critical target sites (Santamaria

et al., 1988), chelating and conjugating carcinogens (chlorophyllin, lemon grass extracts) (Suaeyun et al., 1997). Blocking agents inhibit metabolic activation reactions (Walle et al., 2007) and facilitate excretion of the carcinogen (for example, dietary fibre sources) (Ferguson et al., 2005).

Suppressing agents prevent the earliest events of the neoplastic process (Morais et al., 2010, Zhang et al., 2010). The mechanisms of suppressing agents are not well defined, but they have been shown to modulate downstream effects of oncogenic changes (Wattenberg, 1983). Suppressing agents can inhibit enzymes from initiating, and so halt, reverse or neutralise the effects of carcinogens by interacting with nuclear receptors (Zhang et al., 2010). For instance, tocotrienol (vitamin E) suppresses erythroblastic B2 (ErbB2) pathway by inhibiting the HMG-CoA reductase and induces apoptosis (Shirode and Sylvester, 2010, Shin-Kang et al., 2011).

Chemoprevention is particularly useful in the case of malignancies for which the early stages of the disease are well-defined with a window of duration for intervention, for instance, CRC. This is not the case for many other types of cancer. Treatments such as surgical intervention with preventive intent are invasive and costly. There is evidence that non-steroidal anti-inflammatory drugs (NSAIDs) such as aspirin and selective inhibitors of cyclooxygenase (Coxibs) can suppress CRC development (Lynch, 2008, Shirode and Sylvester, 2010). However, these drugs have unwanted side effects, especially the coxibs which can cause cardiovascular damage (Dajani and Islam, 2008). Therefore, the search for novel chemopreventive agents is desirable.

## 1.4 Preclinical models of CRC

Preclinical models of CRC carcinogenesis are cancer cell lines *in vitro* and rodents *in vivo*.

### 1.4.1 Cell lines

Cancer cell line-based screening provides information on effects of compounds more rapidly than animal model-based screening. These cell lines reflect different stages of tumour progression, and *in vitro* assays allow studies of cell proliferation/growth inhibition, cell cycle, differentiation, cell adhesion, and apoptosis. The cell lines which are widely used to study CRC carcinogenesis are summarised in Table 1.1.

#### 1.4.1.1 APC10.1 cells

The APC10.1 cell line has been derived from the small intestine of a female *Apc*<sup>Min/+</sup> mouse and retains its heterozygosity of both *APC* genotype and a non-activated *Wnt*-signalling pathway. Its premalignancy status has been shown to mirror the sequential steps of adenoma formation in humans (De Giovanni et al., 2004). The cell line was obtained in the Leicester laboratory from a research group in Bologna and has been shown to be a reasonable model to elucidate agents which may impede adenoma development (Sale et al., 2009).

Table 1.1 Some of the CRC cell lines derived from either human or mouse that are utilised for studies of carcinogenesis *in vitro*.

Cell line	Malignancy	Literature
APC10.1	Isolated from adenoma in the small intestine of <i>Apc</i> <sup>Min/+</sup> mouse. Heterozygous <i>Apc</i> genotype. A non-activated Wnt signalling pathway. Exhibits early neoplastic phenotype. Xenografting requires high cell dosage and long latency.	(De Giovanni et al., 2004)
HT-29 (ATCC HTB-38)	Derived from human epithelial colorectal carcinoma. Positive for oncogenes <i>myc</i> , <i>ras</i> , <i>myb</i> , <i>fos</i> , <i>sis</i> , <i>p53</i> while negative for <i>abl</i> , <i>ros</i> , and <i>src</i> . These cells are positive for transforming growth factor beta (TGFβ) and mucin expression.	(Chen et al., 2011b, Shelton et al., 2011, Trainer et al., 1988)
HCA7	Derived from a primary human colon adenocarcinoma. Confluent monolayers form "domes" or "hemi-cysts" due to vectorial fluid transport resulting in fluid accumulation in localised areas of the monolayer. Used in nude mice xenograft studies. Cells are structurally polarized with sparse microvilli present at the apical surface but absent from the basolateral surface. Cells are connected by apical tight junctions and frequent desmosomes.	(Abdel-Rahman et al., 2005, Cuthbert et al., 1985, Debucquoy et al., 2009)
HCT116 (ATCC CCL-247)	Derived from human epithelial colorectal carcinoma. Positive for TGFβ1 and TGFβ2 expression. A mutation in the codon 13 of the <i>Ras</i> proto-oncogene. Used in both <i>in vitro</i> and <i>in vivo</i> xenograft studies.	(Brattain et al., 1981, Howells et al., 2010, Shelton et al., 2011)

### 1.4.2 Animal models

Rodent models are an invaluable tool in the study of multi-step carcinogenesis as well as helping to assess the efficacy of putative chemopreventive agents (Fodde and Smits, 2001, Taketo, 2006, Taketo and Edelman, 2009). Rodent models enable investigation into the effects of interventions in terms of rate of occurrence, multiplicity, volume and/or burden of lesions after a relatively short duration (10-16 weeks). Retrospective analyses of results on CRC preventive agents in human and rodents have shown reasonable consistency between these two species. For example, in carcinogen-induced rat studies, protective effects of aspirin, calcium and carotene mirror that of controlled intervention studies of adenoma recurrence in human (Corpet and Pierre, 2003, Corpet and Pierre, 2005). Such experimental models enable investigators to prioritize the advancement of putative chemopreventive agents into clinical settings on the basis of their pharmacodynamics and pharmacokinetics (Hung et al., 2010).

In the field of CRC, there are several rodent models currently available. These include transgenic, carcinogen-induced, mutant and xenograft models (Nandan and Yang, 2010). Transgenic models allow specific genetic information such as that contained in oncogenes to be spliced into the genome of the rodent. They are also used to elucidate genes that may either have a knockdown or knockout effect that is heritable. Carcinogen-induced models develop spontaneous tumours when the rodents are exposed to carcinogens such as 1, 2-dimethylhydrazine (DMH) (Perse and Cerar, 2011), ethylnitrosourea (ENU) (Moser et al., 1995a) or azoxymethane (AOM) (Takahashi and Wakabayashi, 2004). Mutant models such as *Apc*<sup>Min/+</sup> mice carry a heterozygous point mutation while homozygous mutation results in death. These models require routine screening to ensure early detection of genetic drift. Xenograft models using nude mice

and severe compromised immunodeficiency (SCID) mice enable characterisation of human cancer cell lines and solid tumour implantation *in vivo* without rejection by the rodent host immune system (Boivin et al., 2003, McCart et al., 2008, Taketo, 2006).

In this study, assessment on the efficacy of the flavones was performed in the *Apc*<sup>Min/+</sup> mouse model. 3',4',5',5,7-pentamethoxyflavone (PMF) was added to the diet to investigate its effects on adenoma size and burden. Table 1.2 lists animal models for the study of CRC.

Table 1.2 Widely used rodent models for CRC study.

Rodent model	Description	Literatures
Cre Lox model FabplCre;Apc (15lox/+)	Mice exhibited longer survival. Tumours are formed in the large intestine, mimics the progression of human FAP-associated CRC and sporadic CRC. Low number of intestinal tumours, 231 tumours from 36 animals (Hinoi et al., 2007).	(Hinoi et al., 2007, Robanus-Maandag et al., 2010, Sansom et al., 2004)
<i>Apc</i> <sup>Min/+</sup>	ENU-induced point mutation results in <u>m</u> ultiple <u>i</u> ntestinal <u>n</u> eoplasia (MIN) in mouse. This mouse carries a mutant allele <i>Apc</i> that has an invasive, dominant nonsense mutation at codon 850. Truncated Apc protein is stably expressed and it has autosomal dominant phenotype. <i>Apc</i> <sup>Min/+</sup> mouse mimics the canonical multi-step formation of FAP in human. Number of polyps per mouse:~30- >100	(Cai et al., 2009a, Cai et al., 2006, Cai et al., 2005b, Moser et al., 1992)
<i>Apc</i> <sup>1638N/+</sup>	Heterozygous mouse develops invasive multifocal cutaneous follicular cysts, desmoid tumours and polyposis of the upper gastrointestinal tract. This mouse carries a protein truncated at codon 1638 with neomycin inserted in antisense orientation into exon 15 which encodes nearly all the functional <i>Apc</i> domains. Number of polyps per mouse: <10	(Edelmann et al., 1999, Robanus-Maandag et al., 2010)
<i>Apc</i> <sup>Δ716</sup>	This mouse carries a truncated protein at codon 716 with neomycin inserted into exon 15. An out-pocketing of proliferating cells from a single crypt that extends over time into the interior of an adjoining villus. Gradually, the intravillus microadenomas are formed followed by the generation of polyposis. The nuclear β-catenin which accumulates in the adenomas, once stabilised is responsible for triggering the intestinal tumour formation. Number of polyps per mouse:~300	(Fodde et al., 1994, Oshima et al., 1997, Sheng et al., 1998)
DMH/AOM Rat	F344, Wistar or Sprague-Dawely rat is chemically-induced by DMH or its metabolite, AOM. Dose-dependent induction of colorectal tumours. Genotype and phenotype of the tumours developed mimic those in human sporadic colon cancer. Number of polyps per rat: dose-dependent	(Bousserouel et al., 2010, Bousserouel et al., 2011, Perse and Cerar, 2011)

#### 1.4.2.1 *Apc*<sup>Min/+</sup> mouse model

The most commonly used genetically-driven animal model of CRC is the *Apc*<sup>Min/+</sup> mouse. It carries a mutant allele of murine *Apc* that has an invasive, dominant nonsense mutation at codon 850 stably expressing the truncated Apc protein (Luongo et al., 1994, Su et al., 1992). This truncating *Apc* gene mutation genetically activates the transformation of crypt stem cells within days (Barker et al., 2009). This transformation mirrors the start of multi-step formation of FAP as observed in the human condition (Moser et al., 1990).

Homozygous *Apc*<sup>Min/Min</sup> mice die during embryogenesis (Moser et al., 1995b). Linkage analysis and direct sequencing of the *Apc* gene in the heterozygous *Apc*<sup>Min/+</sup> mouse has shown approximately 90% homology to that in humans (Su et al., 1992). Throughout the *Apc*<sup>Min/+</sup> mouse average life-span of 120 days, lesions develop mimicking the sequential progression of FAP in human (Moser et al., 1992, Preston et al., 2008). The mutation of the *Apc* gene manifests itself by the formation of multiple intestinal adenomas from the duodenum through to the colon (Lamlum et al., 2000a, Lamlum et al., 2000b, Preston et al., 2008). Thus, this mouse model allows assessment of the preneoplastic and/or neoplastic lesion formation in untreated mice and of the effect of intervention on the lesions (Dove et al., 1994, Leow et al., 2005, Luongo et al., 1994).

There are a few differences between *Apc*<sup>Min/+</sup> mice and FAP patients. In *Apc*<sup>Min/+</sup> mice, most of the adenomas are found in the small intestine, with a few polyps in the colon. In contrast, in FAP patients most of the adenomas occur in the colon. This observation suggests that the mechanisms of tumorigenesis may differ between small intestine and colon (Yamada and Mori, 2007). To address this, a new tissue-specific, conditional, *Apc* mutant *Fabp1Cre;Apc*<sup>15lox/+</sup> mouse model has been generated (Robanus-Maandag et

al., 2010). Other differences between *Apc*<sup>Min/+</sup> mice and FAP patients include bacterial distribution within the alimentary canal, creating different microenvironments between *Apc*<sup>Min/+</sup> mice and humans. The cell turnover in the intestine of the *Apc*<sup>Min/+</sup> mouse is also faster than that in humans (Bertagnolli, 1999).

### **1.4.3 Studies of gene expression by microarray technology**

Microarray is a tool that allows the high-throughput, global analysis of gene changes in a single experiment (Pollack, 1999). It enables comparative genome analysis and functional genome analysis of thousands of genes in a specific diseased tissue (Murphy, 2002). Microarrays were developed to utilise the new clone resource that came from the development of capillary sequencing and its application to the high throughput screening of mRNA libraries. Since the elucidation of whole genomes, the format has moved largely to oligonucleotides deduced from the sequence, but the method of their utilisation remains the same (Thompson and Pine, 2009, Thompson et al., 2007). Furthermore, the application of microarray technology has evolved to find application not just in mRNA transcriptome analysis, but for the detection of DNA events such as single-nucleotide polymorphisms (SNP) and deletions, microRNAs, DNA sequencing and epigenetic analysis, to name but a few (Pine et al., 2008, Wulfkuhle et al., 2004, Mendrick, 2011).

In the early days of the development of the technology, there were issues with reproducibility between platforms and laboratories (Shi et al., 2008, Shi et al., 2004). As the technology improved, many of these issues have been resolved, and this was tested by a consortium convened by the United States Food and Drug Administration (USFDA) (Shi et al., 2006, Shi et al., 2010). The technology has therefore developed into a robust and versatile platform that finds many applications in genomic science and in particular cancer research (Malinowski, 2007, McConnell et al., 2009).

The microarray method has been developed, improved and used in various cancers to delineate the genes and subsequent pathways associated with the cancer of interest (Khan et al., 1999, Bartels and Tsongalis, 2009, Link et al., 2010). This method was

used to study differential gene expression from primary to advanced stages of cancer (Matsuyama et al., 2010) in cancer of the colorectum (Suzuki et al., 2011, Heijink et al., 2011, Kim et al., 2011), lung (Chen et al., 2011a, Du et al., 2010), breast (van 't Veer et al., 2002, Sun et al., 2011), ovary (Bommer et al., 2009, Espinosa et al., 2011) and prostate (Dhanasekaran et al., 2001, Heemers et al., 2011). Profiles of differentially regulated genes have been used as markers of efficacy in chemoprevention or biomarkers to determine cancer risk in patients (Nambiar et al., 2004, Link et al., 2010).

The stringent specificity of microarrays allows the identification of a differentially expressed gene from the background of a plethora of gene expressions in a disease scenario.

#### **1.4.4 Chemopreventive mechanisms**

In this section, mechanisms and pathways relevant to flavones, the focus of this thesis, are discussed. Particular emphases are placed on inhibition of cell proliferation, modulation of cell cycle and induction of apoptosis. Aspects of the Wnt, PI3K/Akt/GSK3 $\beta$  and STAT signalling pathways closely associated with CRC are also described.

##### **1.4.4.1 Inhibition of cell proliferation**

One of the means of halting the progression of cancer is by halting the proliferation of damaged/mutated cells. A pathway of interest is the signal transducer and activator of transcription (STAT) pathway. Studies have shown that continuous activation of this pathway, especially STAT3, correlates to elevated cell proliferation and tumour growth (Corvinus et al., 2005). Downstream events of STAT3 include gene expression, G<sub>1</sub> to S phase of cell cycle progression and growth. Inhibition of mutated cell proliferation can be induced by interruption and/or arrest of the cell cycle (Meeran and Katiyar, 2008). This process can either be reversible or irreversible. Ultimately, induction of apoptosis ensures a permanent elimination of mutated cells.

### 1.4.4.2 Cell cycle

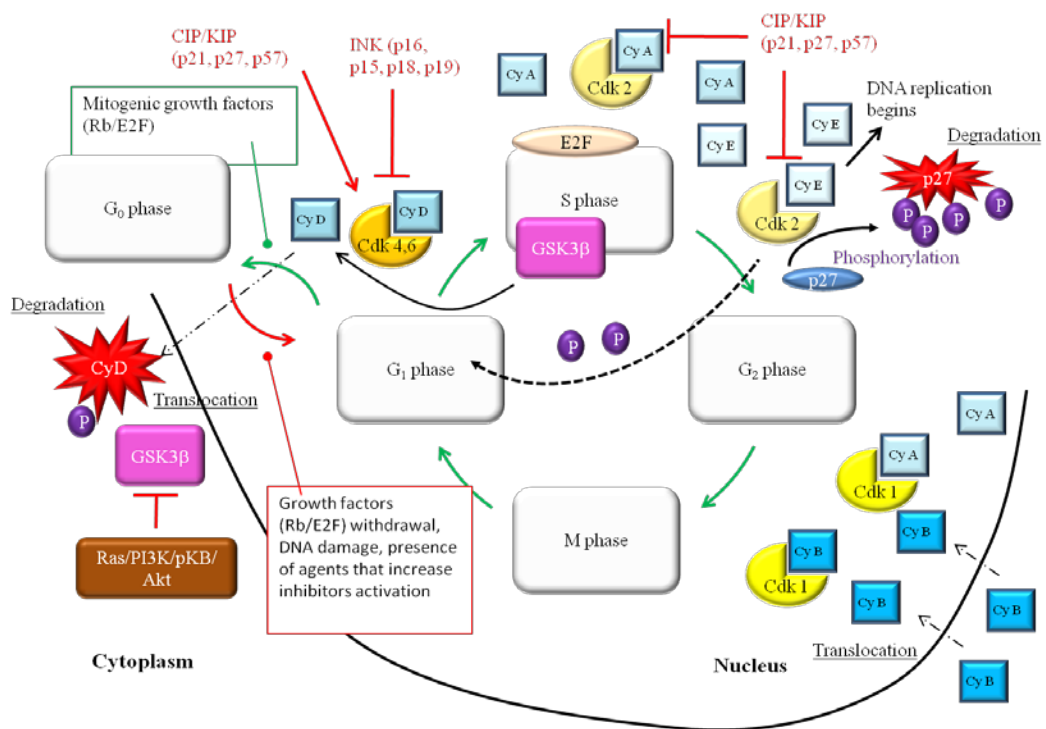


Figure 1.5 A schematic diagram of the cell cycle. Adapted from DiPaola, 2002 and Schmitt et al, 2007a.

In a normal somatic cell, the cell cycle is divided into 4 phases. G<sub>1</sub> = gap 1; S = synthesis; G<sub>2</sub> = gap 2; M = mitosis. Cy= cyclin; Cdk = cyclin-dependent kinase; INK4= inhibitors of Cdk4.

In normal somatic cells, there are four distinctive phases that ensure accurate duplication of the genome (Norbury and Nurse, 1992). Figure 1.5 illustrates that the cell

cycle is characterised by four major phases  $G_1$ , with a sub-phase called  $Gap_0$  ( $G_0$ , resting phase), S,  $G_2$  and M. These phases are regulated by two major checkpoints within the cycle: the  $G_1/S$  and  $G_2/M$  checkpoints. In the  $G_1$  phase, the cell increases in size whilst preparing to synthesize DNA, RNA and proteins for entry into S phase. Before entering S phase, the cell passes through the  $G_1/S$  DNA damage checkpoint. This is to ascertain that everything is ready for DNA synthesis and to prevent premature entry into the next phase of the cycle.

Overall, the progression of the cell cycle is governed by activation and deactivation of complexes between cyclin-dependent kinases (Cdks) and their heterodimeric cyclin partners. The activation of the cyclin/Cdk complexes is achieved through several pathways including phosphorylation and dephosphorylation of proteins such as  $\beta$ -catenin and retinoblastoma protein (pRb) at specific amino acid sites. Hyperphosphorylated Rb dissociates from the E2F/DP1/Rb complex, activating E2F responsive genes. This activation drives transcription and translation (Castedo et al., 2002a, Castedo et al., 2002b). As a safeguard, the formation of cyclin/CDK is regulated by its counterparts, cyclin-dependent kinase inhibitors (CKIs), regulate the assembly and activity of the complexes (Ortega et al., 2002, Besson et al., 2008, Schwartz, 2002). When the cell stops proliferating, it exits the cell cycle and enters into a non-dividing, inactive state denoted as  $G_0$ . Table 1.3 shows a summary of the kinases, phosphatases, cyclins, stimulators, inhibitors and downstream genes associated with the cell cycle.

A cell that enters the cell cycle in the absence of appropriate signals, will normally be programmed to die or senesce (Lowe et al., 2004). In a mutated cell, the integrity of the checkpoints are compromised. Overexpression of cyclins and CDKs, with the loss of function of their inhibitors, CKIs (Ortega et al., 2002) results in the uncontrollable up-

regulation of the cell cycle. Subsequently, uncontrollable growth leads to hyperplasia (Neise et al., 2010, Nevins, 2001).

Genes, such as *MCM7* that encodes mini-chromosome maintenance protein, are also attractive targets for chemoprevention. *MCM7* plays an important role in the initiation of DNA replication. This protein permits one round of DNA replication initiation and elongation in eukaryotic cells (Kearsey and Labib, 1998). It forms a heterohexamer with *MCM2-6*. DNA replication factors, *Cdc6* and *Cdt1*, recruit *MCM2-7* complex to replication origins on the chromatin. This heterohexamer complex binds to chromatin in late mitosis and  $G_1$  and is removed in S- and  $G_2$  phases of cell cycle (Kearsey and Labib, 1998). *Cdt1* destruction and geminin, which stringently regulates *Cdt1* are key elements in suppressing *MCM2-7* chromatin binding in S-phase (Nishihara et al., 2009). Among *MCM7* roles are interactions with cyclin D1-dependent kinase (Gladden and Diehl, 2003) and cyclin A (Chibazakura et al., 2010). During the S phase of the cell cycle, *MCM7* also interacts with tumour suppressor integrator complex subunit 6 (*INT6*) (Buchsbaum et al., 2007) which is a direct target of the *MYCN* transcription factors (Tsai et al., 2004). This transcription factor interacts with *Rad17* in human checkpoint signalling which detects DNA damage during S-phase in cell cycle (Tsao et al., 2004).

Studies have showed *MCM* proteins to be promising markers for tumour prediction (Luo, 2011). *MCM7* and its counterparts are down-regulated in cell cycle exit and this has been used to distinguish differentiated from non-differentiated cells (Gonzalez et al., 2005, Tachibana et al., 2005), particularly in CRC (Nishihara et al., 2008, Pillaire et al., 2010). *MCM7* has been shown to play a critical role in the initiation stage of carcinogenesis, especially in the development of neoplasia. Overexpression of *MCM7*

was only moderately associated with proliferation and has been correlated with negative outcome in CRC patients (Pillaire et al., 2010). In the study described by Pillaire et al., 90% of those patients whose tumours were characterised by low expression of MCM7 survived compared with 40% of patients with over-expressed MCM7.

Table 1.3 Kinases, phosphatases, cyclins, stimulators, inhibitors and downstream genes associated with the eukaryotic cell cycle.

Phases	G <sub>1</sub>	S	G <sub>2</sub> /M
Kinases	CDK4/6	CDK2, Cdc2 (Cdk1)	CDK1
Phosphatase	Cdc25A	Cdc25A	Cdc2 (Cdk1)
Cyclins	Cyclin D1,2,3	Cyclin A1,2,3, cyclin B1,2	Cyclin B1,2
Stimulators	Growth factors, Myc	Myc	
Inhibitor of kinase (INK) / Alternative reading frame (ARF)	GSK3 $\beta$ , p21, p27, p15 INK4B p19INK4D, p18INK4C, p16INK4A,	CDK2 (auto), p21Cip, p27Kip1, p57	Wee1, Myt1, p21Cip, growth arrest and DNA damage 45 (GADD45)
Upstream genes		CDK7, cyclin H	
Downstream genes	$\beta$ -catenin, Rb, E2F, cyclin E1,2, cyclinA1,2,3	E2F, p53, c-myc, APAF-1, pRb, cyclin A1,2,3, cyclin E1,2	Myosin histone H1, p53, p21 wild type p53-activated fragment 1 (WAF1), Bcl-xL

### 1.4.4.3 Induction of apoptosis

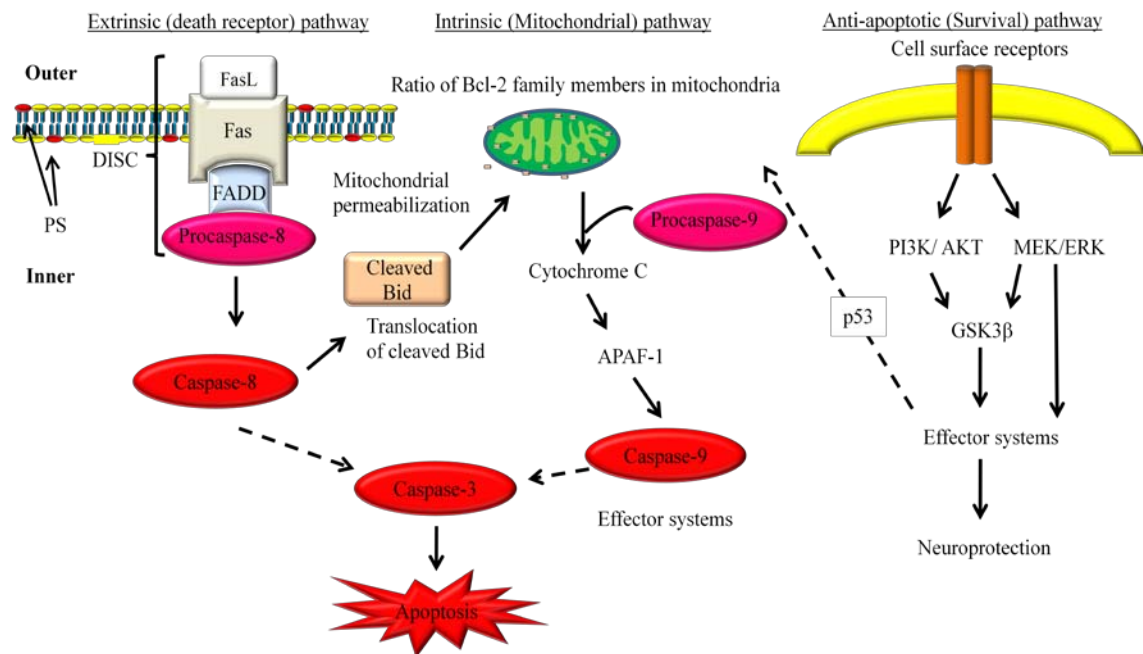


Figure 1.6 A schematic diagram depicting the extrinsic, intrinsic and p53-mediated apoptotic pathways. Adapted from Chipuk and Green, 2008, Diehl et al., 1998 and Chipuk et al., 2006.

PS= Phosphatidylserine; DISC=Death-inducing signalling complex; FasL= Fas-binding ligand; FADD=Fas-associated death domain protein; Bid=Bcl-2 interacting domain death agonist; APAF-1=apoptosis-protease-activating factor-1; ERK=extracellular-signal regulating kinase; MEK=Mitogen-activated protein kinase.

Apoptosis is a form of programmed cell death which does not affect surrounding cells. It is an integral, co-ordinated process characterised by inter-nucleosomal DNA fragmentation, nuclear condensation, cytoskeletal disruption, membrane blebbing,

exposure of phosphatidylserine (PS) on the outer cell surface and eventual cell shrinkage (Elmore, 2007). The increased presence of translocated PS from the inner to the outer leaflet of the cell surface lipid bilayer signals the removal of apoptotic cells and debris by phagocytic cells (Schlegel and Williamson, 2001, Williamson et al., 2001). Apoptosis is essential in maintaining tissue homeostasis, development and differentiation, and elimination of damaged cells (Greenwood and Gautier, 2005, Norbury and Hickson, 2001). Another form of cell death is called necrosis and is characterised by features including rupture of the plasma membrane within the vicinity of inflammatory lesions and damage to surrounding cells and tissues (Kiaris and Schally, 1999, Savill and Fadok, 2000).

There are two major pathways that result in apoptosis: the death receptor pathway and mitochondrial pathways (Figure 1.6). Both of these pathways involve the sequential degradation of cellular components and proteins by activation of cysteinyl aspartate-specific proteinase (caspase) cascades. Both pathways converge to activate apoptosis. The death receptor pathway is activated by the binding of a ligand to its corresponding death receptor. For instance, the binding of Fas ligand (FasL) to the Fas receptor changes the structural conformation of the adaptor molecule which interacts with the receptor. The altered adaptor molecule then binds to the initiator procaspases namely caspase-8, 9, and 10 (Prendergast, 1999). Caspase-8 cleaves Bid (Bcl-2 interacting domain death agonist), a member of the Bcl-2 effector family. This interaction induces mitochondrial outer membrane permeabilisation (MOMP). MOMP creates proteolipid pores allowing the release of cytochrome c from the intermembrane space of mitochondria (Gupta et al., 2009, Chipuk et al., 2006, Chipuk and Green, 2008). Cytochrome c binds to apoptotic protease-activating factor (APAF) and forms an

intracellular apoptosome complex. This complex is an adaptor protein which activates and engages pro-caspase 9 (Garcia-Heredia et al., 2010). Subsequently, effector caspases, namely caspase-3,-6,-7, are activated, and these interact with a wide range of substrates to ensure the destruction of the cell (Tang et al., 2009). One particular protein of interest in the apoptosis pathway is survivin. Survivin is a bi-functional regulator of apoptosis and cell proliferation located in mitochondria. When in the cytoplasm, survivin suppresses apoptosis, but when it has been translocated into the nucleus, it acts as a chromosomal passenger protein at the G<sub>2</sub>/M check point of the cell cycle (Beltrami et al., 2004, Dohi et al., 2004). Survivin has been shown to act via the extrinsic pathway by augmenting the expression of Fas ligand (Asanuma et al., 2004).

Another indirect route to apoptosis is via the cell survival pathway. Following activation of cell surface receptors namely TrkB, a member of the tyrosine kinase family with high affinity for ligands such as brain-derived neurotrophic factor (BDNF), anti-apoptotic pathways via PI3K/Akt and MEK/ERK are initiated. Both these pathways inhibit GSK3 $\beta$  activity (Watson, 2006). Inactivation of GSK3 $\beta$  causes destabilisation of  $\beta$ -catenin, priming  $\beta$ -catenin for ubiquitination and proteolysis degradation instead of nuclear translocation and subsequent binding to the transcription factor TCF/LEF. This inactivation of GSK3 $\beta$  triggers the p53-mediated mitochondrial apoptotic pathway (Vene et al., 2008, Schmitt et al., 2007b). Activation of p53 also drives the expression of certain pro-apoptotic Bcl-2 family members and APAF-1 (Hofseth et al., 2004).

In terms of chemoprevention, induction of apoptosis is a mechanism which can counteract the progression of mutated cells and uncontrollable cell growth as it destroys damaged cells while leaving the normal cells unharmed (Watson, 2006).

#### **1.4.4.4 Modulation of Wnt signalling pathway**

In the initiation stage of CRC progression, APC plays a crucial role in the Wnt (signalling) pathway (Figure 1.7). In a normal epithelial cell, APC is bound to a multi-protein destruction complex in the cytoplasm. This multi-protein complex is made up of a tumour suppressor/scaffold protein Axin, GSK3 $\beta$ , APC and Diversin, which recruits Casein Kinase I to the complex, in the cytoplasm (Schwarz-Romond et al., 2002, van Amerongen et al., 2009, Behrens et al., 1998, Satoh et al., 2000, Choi et al., 2004). Dishevelled 1 (Dvl1, also known as Dsh), a cytoplasmic phosphoprotein inhibits Axin-promoted GSK3 $\beta$ -dependent phosphorylation of  $\beta$ -catenin (Kishida et al., 1999). While  $\beta$ -catenin is constitutively produced in the cell cytoplasm, it is also kept in-check by this multi-protein complex. When  $\beta$ -catenin is bound to this complex, it is destabilised and targeted for destruction via the ubiquitin-proteasome degradation pathway (Morin *et al.*, 1996, Polakis, 1997). In the absence of nuclear  $\beta$ -catenin, the transcription cofactor T-cell factor/lymphoid enhancer factor (TCF/LEF) recruits the co-repressor protein Groucho to the target gene enhancers and represses their transcription (Barker et al., 2000).

When the Wnt signalling pathway is triggered via the binding of Wnt protein to the Frizzled receptor of the cell (Gazit et al., 1999), the coupling of the multi-protein complex is disrupted. Dvl1 binds to the cytoplasmic tail of Frizzled and is activated. Activated Dvl1 inhibits CK1 $\alpha$  and GSK3 $\beta$  (Takahashi-Yanaga and Sasaguri, 2009). As GSK3 $\beta$  is phosphorylated and rendered inactive,  $\beta$ -catenin remains unphosphorylated and is therefore not targeted for degradation (Novak and Dedhar, 1999, Huelsken and Behrens, 2002, van Es et al., 2003). Integrin-linked kinase (ILK) also phosphorylates GSK3 $\beta$  to inhibit GSK3 $\beta$  activity (Novak and Dedhar, 1999). Free  $\beta$ -catenin gradually

accumulates in the cytosol and translocates into the nucleus (Yost et al., 1996). In the nucleus,  $\beta$ -catenin forms a complex with TCF/LEF and initiates the expression of over 500 downstream genes including oncogenes c-myc, survivin and cyclin D1 (Cavallo et al., 1998, Zhang et al., 2001, Kawasaki et al., 2001, Watson, 2006).

Dysregulation of the Wnt signalling pathway interferes with normal regulation of the cell cycle and gene expression and leads to uncontrolled growth and eventually hyperplasia (Ireland et al., 2004, Sansom et al., 2004, Caldwell et al., 2008). Without efficient growth control, in a short time, numerous polyps form in the gastrointestinal tract. Many of these polyps gradually transform and become malignant adenocarcinomas (Del Rio et al., 2010, Inomata et al., 1996).

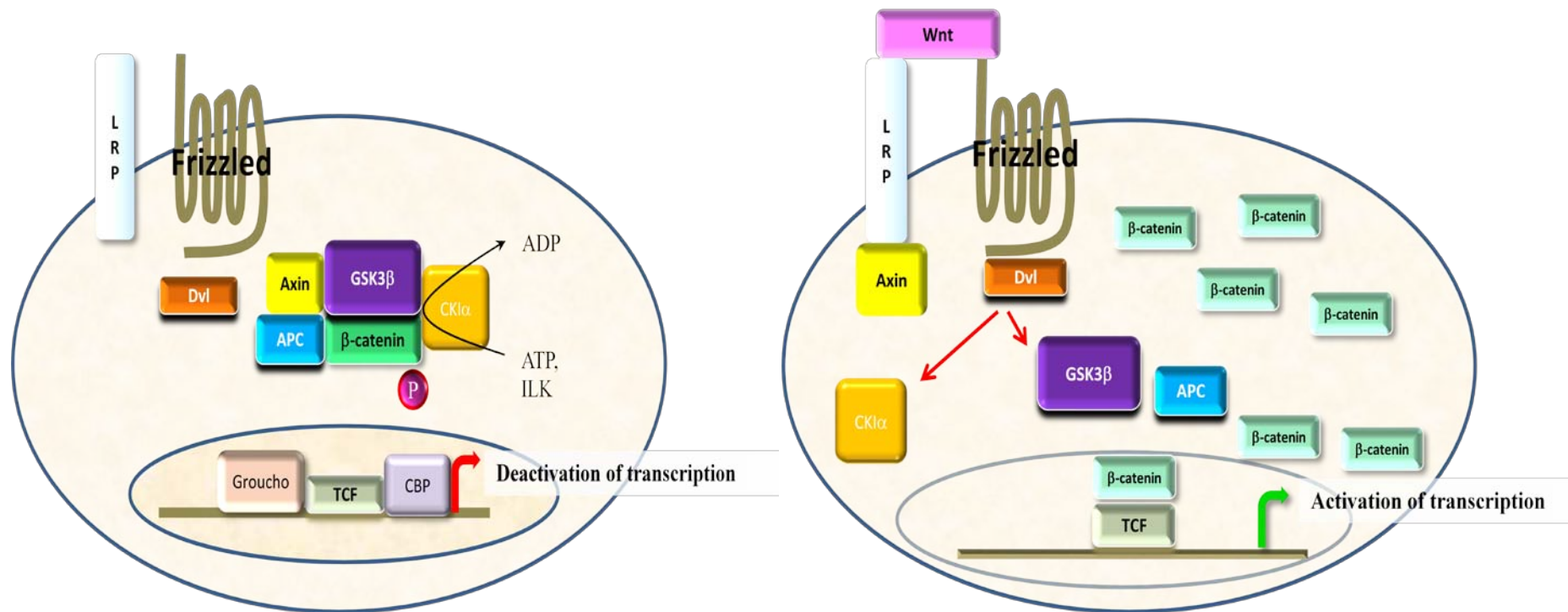


Figure 1.7 The Wnt Signalling Pathway. Adapted from Kawasaki et al., 2001, Takahashi-Yanaga and Sasaguri, 2008 and Takahashi-Yanaga and Sasaguri, 2009.

In the absence of Wnt ligand (left), Dishevelled (Dvl) degrades ubiquitously produced  $\beta$ -catenin in the cytosol. Upon the binding of Wnt ligand to Frizzled (right), Frizzled is activated and Dvl is phosphorylated via Axin. Activated Dvl inhibits (red arrows) CK1 $\alpha$  and GSK3 $\beta$ . This

prevents GSK3 $\beta$  and CK1 $\alpha$  from phosphorylating  $\beta$ -catenin. Unphosphorylated  $\beta$ -catenin escapes recognition by  $\beta$ -transducin repeat-containing protein ( $\beta$ -TRCP) for ubiquitination and proteosomal degradation. Dissociation of the multi-protein destruction complex occurs. Free  $\beta$ -catenin accumulates in the cytosol and is transported into the nucleus, where it binds to transcription factors TCF/LEF. This leads to activation of downstream genes such as c-myc, survivin and cyclin D1 (Kawasaki et al., 2001, Takahashi-Yanaga and Sasaguri, 2008, Takahashi-Yanaga and Sasaguri, 2009).

#### 1.4.4.5 Modulation of Phosphoinositid-3 kinase (PI3K)/Akt/GSK3 $\beta$

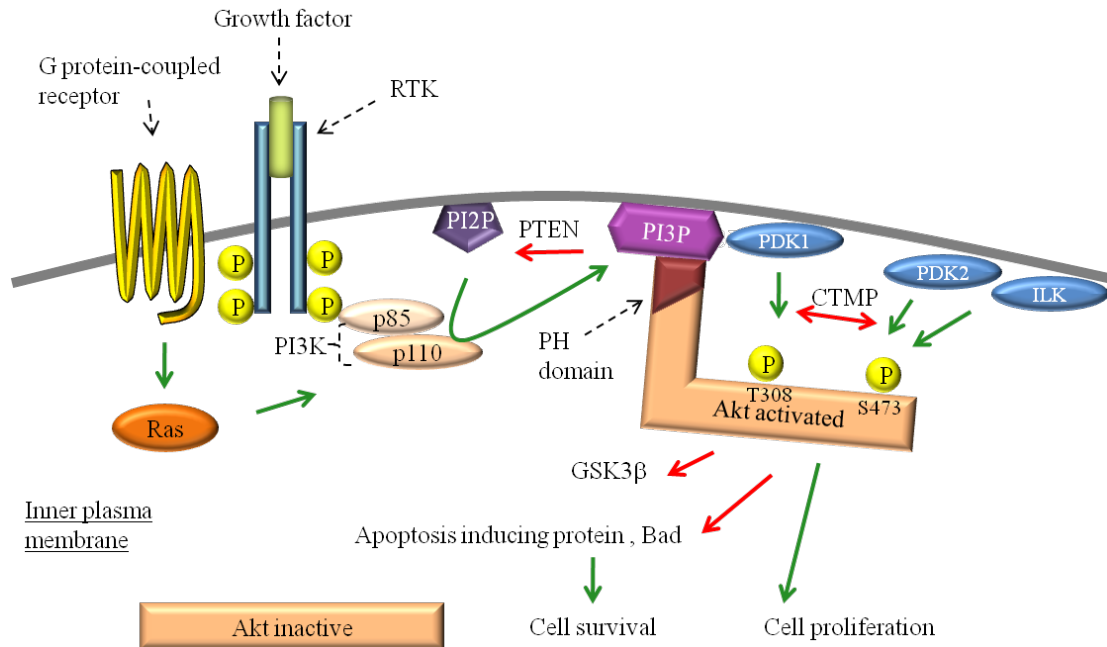


Figure 1.8 A schematic diagram of the phosphatidylinositol 3'-kinase-Akt signalling pathway. Adapted from Osaki et al., 2004, Cantley, 2002 and Li et al., 2011.

The binding of growth factors to their G-protein coupled receptors or receptor tyrosine kinase (RTK) triggers the phosphorylation of phosphatidylinositol-3-kinase (PI3K). One of the subunits of PI3K, p110 subsequently phosphorylates phosphatidylinositol-4,5-bisphosphate to phosphatidylinositol-3,4,5-triphosphate (PI3P). PI3P causes translocation of inactive Akt to plasma membrane. The pleckstrin homology domain (PH) of Akt binds to PI3P, activates Akt and causes conformational change to Akt. 3-Phosphoinositide-dependent kinases (PDKs 1, 2) and integrin-linked kinase (ILK) further phosphorylate Akt to activate and stabilise the new conformation. Carboxyl-terminal modulator protein (CTMP) is an Akt inhibitor that halts phosphorylation of

Akt by PDKs 1 and 2. Activated Akt modulates numerous cellular processes including transcription, translation, cell proliferation and cell survival.

As the Wnt signalling pathway is one of the critical pathways associated with CRC (Clevers, 2006), pathways upstream of Wnt signalling (Sun and Jin, 2008, Li et al., 2011) are pivotal. One of these upstream pathways is the PI3K/Akt/GSK3 $\beta$  pathway (Figure 1.8).

The PI3K/Akt pathway phosphorylates GSK3 $\beta$  and down-regulates GSK3 $\beta$  activity (Ueki et al., 1998, Sutherland et al., 1993). In its active state, GSK3 $\beta$  phosphorylates cyclin D1 and initiates cyclin D1 translocation into the cytoplasm (Takahashi-Yanaga and Sasaguri, 2008). Phosphorylation of cyclin D1 at the Thr 286 site marks it for ubiquitinylation and proteosomal degradation (Diehl et al., 1998, Diehl et al., 1997). Hence, this pathway drives the up-regulation of cyclin D1 translation and suppresses cyclin D1 degradation (Jirmanova et al., 2002).

The PI3K/Akt/GSK3 $\beta$  pathway affects protein synthesis (Johnson et al., 2009), cell survival (Itoh et al., 2002), cell cycle (Wang et al., 2009), proliferation (Lee et al., 2010) and glucose metabolism (Lee et al., 2010).

#### **1.4.4.6 STAT3 and its pathway**

The STAT3 signalling pathway has been associated with CRC progression (Kusaba et al., 2006, Ma et al., 2004, Corvinus et al., 2005). STAT3 is a member of a family of cytoplasmic proteins that contain a Src homology 2 (SH2) – domain. STAT3 is activated via a tyrosine phosphorylation cascade by cytokines and growth factors (Ma et al., 2004). Upon activation, STAT3 dimerizes with other STATs as hetero- or homodimers, which are translocated into the nucleus. In the nucleus, these dimers bind to specific sites including *cis* element interferon (IFN)-stimulate response element (ISRE). They initiate transcription of genes associated with inflammation. Apart from inflammation, STAT3 is also implicated in cell growth via myc, pim-1, cyclin D1 and apoptosis via p21/WAF1 (Barre et al., 2003). To halt downstream activation of transcription, STAT3 binds preferentially to a conserved element in the promoter of inhibitor p21/WAF1 and activates this cell cycle regulatory gene. When STAT3 is constitutively activated, it promotes the early stage of CRC (Corvinus et al., 2005, Baral et al., 2009). In response to oncogenic heterotrimeric guanine nucleotide-binding protein (G-protein), several oncogenic non-receptor tyrosine kinases including src, Abl, and Jak were found to be capable of activating STAT3 (Ram and Iyengar, 2001, Cong et al., 1999, Zou and Calame, 1999). This activation is essential for the malignant transformation of cells and modulates important pathways including PI3K/Akt signalling (Zou and Calame, 1999, Ram and Iyengar, 2001). Recently, a study has shown cross-talk between STAT3 and GSK3 $\beta$  in the nucleus of the embryonic heart (Pedretti and Raddatz, 2011).

## 1.5 Flavonoids

Flavonoids are plant phenols which are ubiquitously found in plants, providing colour and flavour in many fruits and vegetables. It has been estimated that humans consume 1-2 g of flavonoids per day on average (Scalbert and Williamson, 2000).

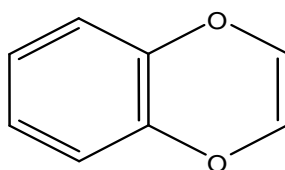


Figure 1.9 Benzo- $\gamma$ -pyrone

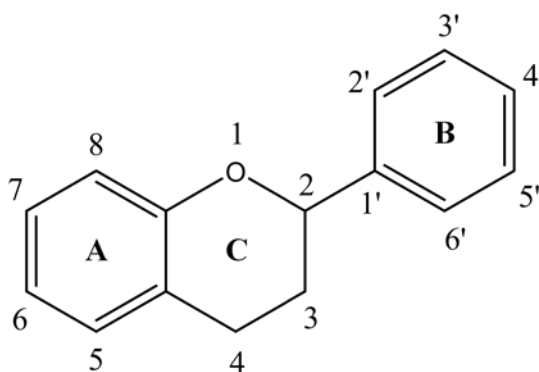


Figure 1.10 The basic structure of flavonoids.

Chemically, flavonoids are predominantly derived from benzo- $\gamma$ -pyrone (Figure 1.9) and consist of 2 aromatic benzene rings connected by a linear 3-carbon chain (Figure 1.10). The A ring stems from acetate pathway synthesis with hydroxylation at the 5 and 7 positions. The B ring can be generated via the Shikimate pathway, and it is commonly

hydroxylated at positions 3', 4', 5'. Substitution in the C-ring gives rise to six major subgroups, namely flavones (e.g. apigenin, tricetin), flavonols (e.g. quercetin, kaempferol), flavanones (e.g. naringenin, hesperidin), catechins or flavanols (epicatechin, gallic catechin), anthocyanidins (malvidin, cyanidin), and isoflavones (genistein, daidzein).

The cancer chemopreventive capacity of flavonoids is dependent on many structural features including the substituents on the C-ring (Beecher, 2003). The pattern and nature of ring substitution, ie hydroxyl or methoxy, influence efficacy (Cai et al., 2009b, Wen and Walle, 2006a). Flavonoids are metabolised in the liver and in the gastrointestinal tract by the gut microflora (Manach et al., 2004, Manach et al., 2005). They can be conjugated to *O*-glucuronide, *O*-sulfonate or *O*-methyl metabolites (Scalbert et al., 2005). Glucuronidation, replacement of the hydrogen atom of the phenolic flavonoid OH by a glucuronyl moiety catalysed by uridine diphosphate (UDP)-glucuronosyltransferase (UGT), renders the molecule more water soluble. This allows fast elimination of flavonoids from the body via the urine or faeces. Fast elimination reduces the bioavailability of the parent compound. Sulfonation, replacement of the hydrogen atom of the phenolic flavonoid OH by a sulfonyl moiety, is mediated by sulfotransferases (SULTs) in the presence of the co-factor 3'-phosphoadenosine-5'-phosphosulfate (PAPS) (Gamage et al., 2006). Generally, metabolic conjugates are pharmacologically less active than their parent compounds. Methoxyflavones can undergo oxidative demethylation catalysed by liver cytochrome P450 monooxygenases. The *O*-demethylated metabolites can undergo secondary metabolism by conjugation as described above. Oxidative demethylation of methoxyflavones tends to be slower than glucuronidation and sulfonation of their

hydroxyl analogues (Otake et al., 2002, Cai et al., 2010). Therefore, methoxyflavones are present much longer in the body to exert chemopreventive activities than hydroxyflavones.

### **1.5.1 Methoxyflavones**

Figure 1.11 The basic chemical structure of flavones.

Figure 1.11 shows the flavone structure. Methoxylated flavones have been suggested to have superior chemopreventive properties when compared with their hydroxylated counterparts (Cai et al., 2009b, Walle, 2007). This is because hydroxylated flavones are susceptible to rapid and efficient glucuronidation which their methoxylated counterparts cannot undergo. This conjugation results in the fast removal of flavones from the body. Oxidative demethylation of a methoxylated flavone results in the removal of the methyl group from the flavone. Overall, the metabolic removal of methoxylated flavones from

the body tends to be slower than that of hydroxylated flavones, thus methoxylated flavones exhibit higher metabolic stability than their hydroxyl analogues (Walle et al., 2007, Cai et al., 2010). Flavones that have both hydroxy and methoxy groups are metabolised slower than hydroxylated flavones, but faster than fully methoxylated flavones. Walle and Walle demonstrated the relationship between the position of methoxy group in flavones and metabolic stability (Walle and Walle, 2007). In that study, 5,7-dimethoxyflavone and 5-methoxyflavone were found to be more resistant to metabolism than 4'-methoxyflavone, 3'-methoxyflavone, 5, 4'-dimethoxyflavone, and 7,3'-dimethoxyflavone. Flavones with a methoxy group in the B-ring were found to be the most susceptible to oxidation (Walle and Walle, 2007). Methoxylated flavones are more rapidly absorbed into cells when compared to their hydroxy analogues. Methoxylated flavones may be promising candidates as chemopreventive agents (Walle and Walle, 2007, Wen and Walle, 2006a, Wen and Walle, 2006b).

The biological potency of the flavonoids is very much dependent on individual flavonoid structure (Kuntz et al., 1999). Flavones have been shown to be particularly interesting from the standpoint of anti-carcinogenic action. Several *in vitro* studies have shown that flavones can inhibit cell transformation and proliferation (Winkelmann et al., 2007, Dihal et al., 2008, Pan et al., 2002).

In *in vivo* studies, flavones such as apigenin (Shukla et al., 2005), tricetin (Cai et al., 2005a, Cai et al., 2009b), 5,7-dimethoxyflavone (Walle et al., 2007) have been shown to be chemopreventive by reducing the number of adenomas in rodent models at doses that can be achieved by a diet rich in fruits and vegetables (Winkelmann et al., 2007).

### 1.5.1.1 Apigenin (4', 5, 7-trihydroxyflavone)

Figure 1.12 The chemical structure of apigenin (4',5, 7-trihydroxyflavone).

Apigenin is a flavone with 3 hydroxyl groups (Figure 1.12). It is predominantly found in herbs, vegetables and fruits such as cloves, barley, parsley, celery, Chinese cabbage and star fruit (Patel et al., 2007, Miean and Mohamed, 2001, Wei et al., 1990).

In *in vitro* studies, a dose response assay in SNU C4 human CRC cells, apigenin inhibited cell growth at 72 h with an  $IC_{50}$  of  $1.8 \pm 0.5 \mu\text{M}$  (Lee et al., 2009). In the human colon carcinoma cell lines SW480, HT-29 and Caco-2, the  $IC_{50}$  for growth inhibition by apigenin at 48 h were  $40 \mu\text{M}$ ,  $50 \mu\text{M}$  and  $70 \mu\text{M}$ , respectively (Wang et al., 2000). Apigenin was found to trigger the caspase cascade in HT29 cells when cells were exposed to  $90 \mu\text{M}$  of apigenin for 72 h (Turktekin et al., 2011). When Caco-2 cells were exposed to apigenin at  $10 \mu\text{M}$  or  $30 \mu\text{M}$ , it significantly reduced ornithine decarboxylase (ODC) activity by 26% and 57% , respectively (Au et al., 2006).

Apigenin induced G<sub>2</sub>/M arrest, inhibited p34 kinase activity (Cdc2), reduced cyclin D1 and cyclin B1 protein production and accumulation in a reversible manner in SW480, Caco-2 and HT29 cells (Wang et al., 2000, Turktekin et al., 2011). Apigenin was also shown to reverse the transformation of HCT116 cells and inhibit Ras and Fas activations, which if left unchecked contribute to tumour cell survival, in a dose-dependent manner (Klampfer et al., 2004, Shukla and Gupta, 2007). Apigenin augmented the kinase activity of ERK with downstream Elk phosphorylation, as well as p38 and its downstream transcription factor-2 (TF-2) thereby modulating the MAPK cascade in HCT116 cells (Van Dross et al., 2003). Apigenin also modulated p21, induced cell cycle arrest and activated pro-apoptotic proteins such as non-steroidal anti-inflammatory drug-activated gene 1 (NAG-1) and p53 (Zhong et al., 2010). Apigenin was demonstrated to exert anti-metastatic effect by up-regulation of CD26, a multi-functional cell surface protein on HT29 and HRT18 cells, which links cells to fibronectin (Lefort and Blay, 2011).

In a study in our laboratory, apigenin exhibited dose-dependent growth inhibition of APC10.1 cells with an IC<sub>50</sub> of 18 µM (Cai et al., 2009b). In *in vivo* studies, apigenin inhibited ODC and the development of aberrant crypt foci in the CF-1 mouse model. In contrast, adenoma formation was not inhibited by apigenin in the *Apc*<sup>Min/+</sup> mouse model (Au et al., 2006, Cai et al., 2009b). In this laboratory, *Apc*<sup>Min/+</sup> mice received apigenin at 0.2% w/w in the diet. In this case, apigenin showed no efficacy in reducing the number of adenomas (Cai et al., 2009b). The concentrations of apigenin found in plasma, liver and small intestinal mucosa were 0.09 ± 0.08 nM, 1.5 ± 1.0 nmol/g and 86 ± 47 nmol/g, respectively (Cai et al., 2006). Using the same animal model, Zhong et al. demonstrated that when mice received a bolus containing a low (25 mg/kg) or high dose (50 mg/kg)

of apigenin every other day for a month, there was significant reduction in polyp number and load in both treatment groups, although there was no difference in adenoma size between control and treatment groups. Serum concentrations in mice were  $13.4 \pm 1.0 \mu\text{M}$  in the low treatment group, much higher than what was observed in our previous study (Zhong et al., 2010).

In the clinical setting, 87 patients made up of 36 patients with resected colon cancer and 51 patients after polypectomy were divided into two groups. In the study, 31 patients received daily standard dosage of a flavonoid mixture containing apigenin (20 mg) and epigallocatechin gallate (EGCG) (20 mg) over a sustained period of 2-5 years. The combined recurrence rate for neoplasia was 7% in the treated patients and 47% (56 patients) in the control patients ( $P=0.027$ ) (Hoensch et al., 2008). The result suggests the chemopreventive efficacies of flavonoids, observed *in vitro* and *in vivo* were translatable into a clinical setting.

### 1.5.1.2 Tricin (4', 5, 7-trihydroxy-3', 5'-dimethoxyflavone)

Figure 1.13 The chemical structure of tricin (4',5,7-trihydroxy-3',5'-dimethoxyflavone).

Tricin is a flavone with 2 methoxy and 3 hydroxy groups (Figure 1.13). This flavone is commonly found in the Poaceae family of grass which includes rice bran (~4.5 µg tricin per 10 g rice bran), bamboo (8 g per 40 000 kg dried leaves), sugar cane, oats, barley and wheat (Hudson et al., 2000, Oyama et al., 2009).

Tricin has been shown to inhibit the growth of APC10.1 and SW480 cells with IC<sub>50</sub> values of 13 and 16 µM, respectively (Cai et al., 2009b, Hudson et al., 2000). Studies in this laboratory showed the inhibitory properties of tricin on COX enzymes with IC<sub>50</sub> values of approximately 1 µM in human colon-derived epithelial cells (HCEC) and

adenocarcinoma HCA7 cells. At 5  $\mu\text{M}$ , tricetin was able markedly to reduce prostaglandin E2 (PGE<sub>2</sub>) level in HCEC and HCA7 cells, by 36% (P<0.01) and 35% (P<0.05), respectively (Cai et al., 2005a).

In human-derived breast tumour cells MDA-MB-468, tricetin exerted an irreversible cell cycle arrest in the G<sub>2</sub>/M phase without inducing apoptosis. In contrast, in HBL-100 human-derived non-malignant breast cells, cell cycle arrest caused by tricetin was reversible, suggesting that tricetin acts selectively against these tumour cells (Cai et al., 2004).

In female FvB mice which received tricetin in the diet at 0.05, 0.2 or 0.5% for 7 days, the steady-state levels in plasma, liver and small intestine were between 0.1-0.3, 0.4-2.2 and 30-460  $\mu\text{M}$ , respectively (Cai et al., 2005b). It is interesting to note that the levels in the small intestine were much higher than the IC<sub>50</sub> levels of 0.6 and 16  $\mu\text{M}$  observed *in vitro* in SW480 and MDA-MB-468 cells respectively (Hudson et al., 2000, Cai et al., 2009b). Tricetin lacks genotoxicity at these concentrations (Verschoyle et al., 2006). In a comparative study of apigenin and tricetin, the levels of tricetin in plasma, liver and mucosa were found to surpass those of apigenin by 350, 33 and 100% (Cai et al., 2007). Thus, studies in our laboratory demonstrated considerable metabolic stability of tricetin in the biophase (Cai et al., 2004, Cai et al., 2005b).

In a study performed in this laboratory, *Apc*<sup>Min/+</sup> mice received American Institute of Nutrition-93G (AIN-93G) diet containing tricetin (0.2% w/w) throughout their post-weaning life span (4-18weeks). Tricetin reduced the formation of adenomas in the small intestine, particularly the proximal small intestine. Tricetin reduced the number of adenomas by 33% (P<0.05) in comparison with mice on the control diet (Cai et al.,

2005a). In the small intestinal mucosa and blood of those mice which received triclin, PGE<sub>2</sub> levels were significantly reduced by 34% (P<0.01) and 40% (P<0.05) respectively, relative to those mice which received the control diet (Cai et al., 2005a). The level of triclin detected in the plasma, liver and small intestinal mucosa were 0.12 ± 0.12 nM, 8.0 ± 3.8 nmol/g and 238 ± 64 nmol/g, respectively (Cai et al., 2009a). Overall, triclin is a promising candidate for CRC chemopreventive activity and thus was included in this study.

### 1.5.1.3 Pentamethoxyflavone (3',4',5',5',7-pentamethoxyflavone) (PMF)

Figure 1.14 The chemical structure of 3',4',5',5',7-pentamethoxyflavone (PMF)

Pentamethoxyflavone, 3',4',5',5',7-pentamethoxyflavone (PMF), is an analogue of apigenin and tricetin with 5 methoxy groups (Figure 1.14). PMF is found in the leaves of *Murraya paniculata*, a member of the Rutaceae plant family, which is contained in traditional Indonesian herbal medicines (Kinoshita and Firman, 1997). It has also been isolated from the fruits of the Brazilian plant, *Neoraputia magnifica* (Tomazela et al., 2000).

PMF displayed dose-dependent anti-proliferative potential with an  $IC_{50}$  of 6  $\mu$ M in APC10.1 cells (Cai et al., 2009b). *Apc*<sup>Min/+</sup> mice that received 0.2% w/w PMF in their

diet had a median concentration of PMF at 1.08 nmol/mL (10<sup>th</sup> and 90<sup>th</sup> percentile: 0.633 and 2.385 nmol/mL) and 108.5 nmol/g (10<sup>th</sup> and 90<sup>th</sup> percentile: 38.9 and 164.4 nmol/g) in the plasma and small intestinal mucosa, respectively (Cai et al., 2009a). When the small intestine of these mice was analysed, the adenoma number in comparison with controls was reduced by 47.5%. When the mice were fed 0.2% w/w flavones in their diet, mice which received PMF had the lowest number of adenomas compared with tricetin or apigenin. Adenoma burden per mouse that received PMF (23.9 mm<sup>3</sup>) was halved in comparison with control (49.9 mm<sup>3</sup>) (Cai et al., 2009b). Overall, PMF was superior to its two analogues in terms of anti-proliferation *in vitro* and reduction of adenoma number and burden in the small intestine *in vivo*. The higher metabolic stability and greater ability of PMF to dock into the cyclooxygenase active site as compared to tricetin and apigenin may explain its superiority (Cai et al., 2009b, Cai et al., 2009a, Cai et al., 2006, Cai et al., 2005b, Cai et al., 2003).

Another polymethoxyflavone that was efficacious for chemoprevention is tangeretin (5,6,7,8,4'-pentamethoxyflavone). Tangeretin elicited properties including anti-oxidation (Ratty and Das, 1988), anti-inflammation (Chen et al., 2007), anti-proliferation (So et al., 1996, Kawaii et al., 1999), apoptosis induction (Hirano et al., 1995), anti-invasiveness (Bracke et al., 1991), anti-metastasis (Bracke et al., 1989) and modulation of cell cycle (Ishii et al., 2009, Pan et al., 2002) and permeability of glycoprotein (P-glycoprotein) (Ishii et al., 2009, Takanaga et al., 2000).

In view of these findings, this study aims to delineate the anti-carcinogenic mechanism of action of PMF further for potential development as a putative cancer chemopreventive agent.

## 1.6 Aims and objectives

There are more than 5000 flavonoids which have been identified in nature, and the number is increasing as the technology in phytochemistry analysis is advancing. In the Leicester laboratory, three flavones, apigenin, tricetin and PMF, have been tested for inhibition of adenoma development in the *Apc*<sup>Min/+</sup> mouse model (see sections 1.5.1.1-1.5.1.3) (Cai et al., 2009a, Cai et al., 2010, Cai et al., 2009b). Chemically, these flavones share the same core structure, but differ in substituents. In this study, the abilities of these flavones to elicit anti-proliferative potential, to promote cell cycle arrest and to stimulate apoptosis in *in vitro* studies have been compared in detail.

PMF has pronounced anti-proliferative potential in the murine-derived adenoma cell line APC10.1. It was more potent in reducing the number of adenomas and adenoma burden in *Apc*<sup>Min/+</sup> mice than tricetin or apigenin (see sections 1.5.1.1-1.5.1.3). There seems to be a relationship between potency and chemical structure, specifically between hydroxy and methoxy moieties (see sections 1.5 and 1.5.1). The underlying mechanisms by which these flavones exert efficacy still remain unclear. There have been very few studies on the effects of tricetin and PMF at the molecular level, so there is a dearth of knowledge of any potential mechanistic markers of efficacy.

The overall aim of this study has been to contribute to the understanding of the mechanisms by which these flavones may exert cancer chemopreventive activity. This may help formulate criteria to optimise the selection of flavones for development as potential CRC chemopreventive agents. The study focussed on PMF. Five different experimental strategies have been adopted to understand the mechanisms exerted by the flavones. The specific objectives of these experiments are as follows:

1. To explore differences between apigenin, tricetin and PMF in terms of their ability to inhibit proliferation of murine APC10.1 cells.
2. To compare the effects of these flavones on the cell cycle and cell survival/apoptosis in APC10.1 cells.
3. To compare the effects of these three flavones on gene expression in APC10.1 cells *in vitro*.
4. To delineate the mechanisms by which PMF may exert its effects on growth, cell cycle and apoptosis, as well as on adenoma development.
5. To establish the robustness of the delineated mechanisms by comparing the effects of PMF on protein expression in APC10.1 cells and adenomatous tissue in the *Apc<sup>Min/+</sup>* mouse model.

## 2 Materials and methods

### 2.1 Materials

#### 2.1.1 APC10.1 cell line

The APC10.1 cell line is derived from the intestinal adenomas of  $Apc^{Min/+}$  mouse and retains its heterozygosity of both  $Apc$  genotype and a non-activated Wnt signalling pathway. The cell line was a kind gift from Dr Carla De Giovanni (Cancer Research Section, Department of Experimental Pathology, University of Bologna) (De Giovanni et al., 2004).

#### 2.1.2 $Apc^{Min/+}$ mouse treatment regime

The animal study was performed using C57BL/6J Min/+ ( $Apc^{Min/+}$ ) mice under animal project license PPL80/2167. These mice were originally obtained from Jackson Laboratory (Bar Harbor, USA). The mice were bred in the Biomedical Services facility of University of Leicester. The genotype of each mouse was confirmed routinely by using polymerase chain reaction (Perkins et al., 2002). The mice were randomly divided into control or treatment group. The control mice received bolus made up of AIN-93G diet *ad libitum* while treatment mice received 0.2% w/w flavone in the diet *ad libitum*. Within these categories, the mice were further grouped into short term and long term (Figure 2.1) studies.

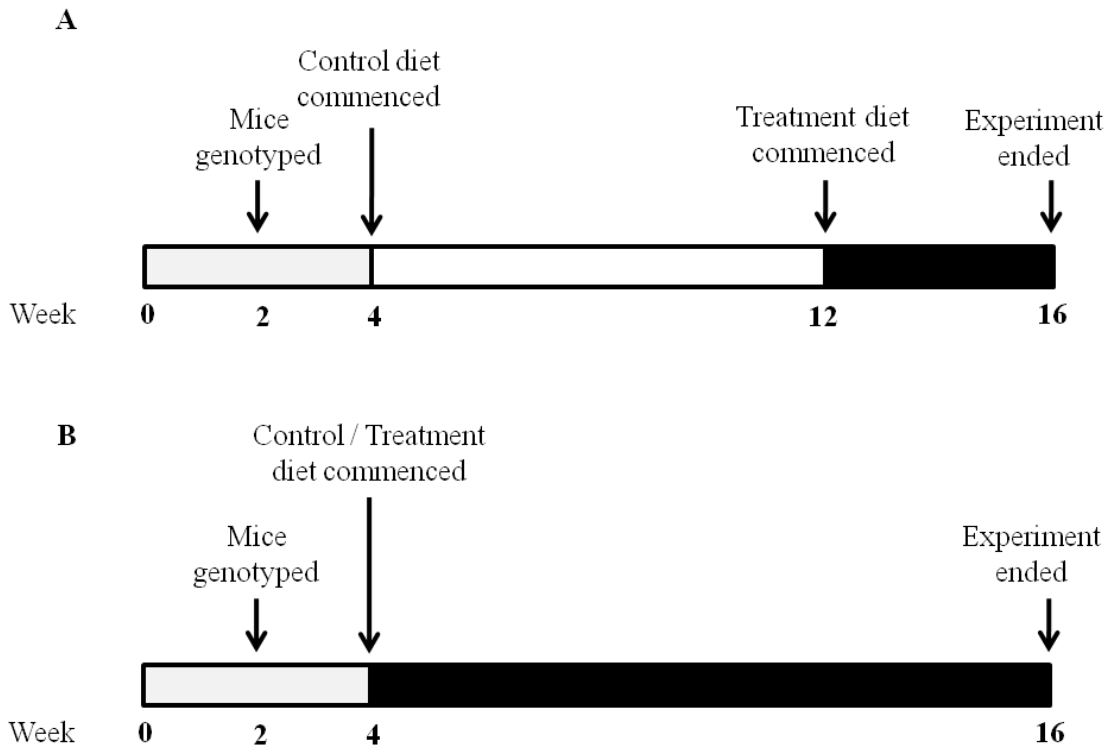


Figure 2.1 The feeding regime of  $Apc^{Min/+}$  mouse model for short (A) and long (B) term animal studies.

In the  $Apc^{Min/+}$  mouse model, mice are genotyped at 2 weeks old. In the short term study (A), the mice were weaned and received AIN-93G control diet from week 4 onwards. At week 12, mice in treatment group received AIN-93G diet containing test agent while the control group continued on with AIN-93G diet. The experiment was terminated at week 16. In the long term study (B), the mice were weaned and received either AIN-93G diet (control) or AIN-93G diet containing test agent (treatment) from week 4 onwards. The experiment was terminated at week 16.

### **2.1.3 Buffers**

#### **2.1.3.1 4-(2-Hydroxyethyl) piperazine-1-ethanesulfonic acid (HEPES)**

1 M HEPES (Sigma, UK) (238.30 g) was prepared in 1000 mL of ultra pure (UP, 18.2 MΩ) (Barnstead Nanopure Diamond UV-UF Laboratory Water Purification System, UK) water, and the pH was adjusted to pH 7.0. The solution was sterile-filtered before use.

#### **2.1.3.2 Diethylpyrocarbonate (DEPC)-treated water**

DEPC-treated water was used throughout the work involving microarray. This buffer was made up of 1000 mL of UP water and 0.1% DEPC (Sigma, UK) (1 mL) and stirred overnight. The solution was autoclaved before use.

#### **2.1.3.3 Running Buffer (Western blot, WB)**

Running buffer was made up by diluting 100 mL of concentrated 0.25 M Tris / 1.92 M GLYCINE / 1% SDS (10X) (Geneflow Ltd., UK) with 900 mL of UP water to achieve 1000 mL of working tank buffer at 0.025 M Tris / 0.192 M Glycine / 0.1% SDS.

#### **2.1.3.4 Transfer buffer (WB)**

Transfer buffer was made up by diluting 100 mL of concentrated 0.25 M Tris / 1.92 M GLYCINE (10X) (Geneflow Ltd., UK) with 200 mL of methanol (Fisher Scientific, UK) and 700 mL of UP water to achieve 1000 mL of working tank buffer at 0.025 M Tris / 0.192 M Glycine / 20% methanol.

#### **2.1.3.5 10% Ammonium persulfate**

1 g of ammonium persulfate (Sigma, UK) was dissolved in 10 mL UP water. This stock solution was stored at 4°C.

#### **2.1.3.6 Cell lysis buffer (Roche, UK)**

One tablet of cOmplete, mini protease inhibitor cocktail and a tablet of PhosSTOP were diluted in 10 mL of Lysis-M Reagent to achieve a cell cycle buffer containing 1 mM ethylenediaminetetraacetic acid (EDTA) and a blend of phosphatase inhibitor (to inhibit a broad spectrum of phosphatases, for example acid and alkaline phosphatases serine / threonine (PP1, PP2A, and PP2B) and tyrosine protein phosphatases (PTP). Lysis-M Reagent contains mild detergent in 25 mM bicine buffer (pH 7.6). Aliquots of cell lysis buffer at 1 mL were stored at -20°C for long term storage.

#### **2.1.3.7 Phosphate-buffered saline-Tween (PBST) buffer (WB)**

Ten tablets of PBS (1 tablet per 100 mL UP water) (Oxoid Ltd., UK) and 1 mL of Tween®20 (polyoxyethylenesorbitan monolaurate) (Sigma, UK) were dissolved in 1000 mL UP water.

#### **2.1.3.8 Blocking buffer (WB)**

10 g of semi-skimmed milk (Marvel, UK) were dissolved in 200 mL PBST. This was stored at 4°C and was used no later than 48 h after preparation.

#### **2.1.3.9 Antigen retrieval buffer (Immunohistochemistry)**

Antigen retrieval buffer was made up by dissolving 2.1 g of monohydrate citric acid (Sigma, UK) in 1000 mL of UP water and pH adjusted to 6.0 with 2 M sodium hydroxide (Sigma, UK).

#### **2.1.3.10 Endogenous peroxidase-inhibiting buffer**

33 mL of 30% Perdrogen® (Sigma, UK) were diluted in 300 mL UP water to give a 3% hydrogen peroxide solution.

### **2.1.3.11 Primary antibody diluent**

50 mg of bovine serum albumin (BSA) (Sigma, UK) was dissolved in 5 mL of PBS to give a 10% BSA solution. Fresh solution was prepared each time and used to dilute primary antibody for immunohistochemistry use.

### **2.1.3.12 3, 3'-diaminobenzidine (DAB) + Substrate buffer (DakoCytomation, UK) (provided by kit)**

This substrate buffer was made up of imidazole-HCL buffer at pH 7.5 containing hydrogen peroxide and an anti-microbial agent.

### **2.1.3.13 DAB Chromogen (DakoCytomation, UK)**

This solution was made up of 3, 3'-diaminobenzidine in chromogen solution.

## **2.2 Methods**

### **2.2.1 Maintenance of APC10.1 cells**

APC10.1 cells were cultured as adherent monolayer cells at 37°C in a humidified incubator supplemented with 5% CO<sub>2</sub>. APC10.1 cells were maintained in Dulbecco's minimal essential medium (DMEM) (Sigma,UK) containing Glutamax I and glucose (1000 mg/L) and 20% foetal calf serum (Invitrogen, UK).

### **2.2.2 Passage of cell lines**

Cells were passaged every 3-4 days at approximately 70-80% confluency following restoration from frozen stocks. The cell line was not sub-cultured more than 30 times. In the routine cell passage, the medium was aspirated and the cells were washed with 10

mL warmed sterile PBS (pH 7.2). Cells were treated with 3 mL of warmed sterile 1x trypsin-EDTA (Gibco, UK) and incubated for 5 minutes (min) at 37°C. The cell detachment was confirmed by microscopy before 7 mL of medium were added to neutralise the trypsin-EDTA. Repeated pipetting was performed to achieve a single-cell suspension. The cell suspension was centrifuged at 400 x g for 5 min and the supernatant was discarded. The cell pellet was resuspended in 10 mL medium and cell count was performed. Cells were seeded at 10<sup>5</sup> cells per T75 flask (Nunc, UK).

### **2.2.3 Formulation of stock solution for treatment of cells.**

Stock solutions of apigenin (APIN Chemicals Ltd., USA), tricetin (decode Genetics, USA) and PMF (APIN Chemicals Ltd., USA) were prepared in dimethyl sulfoxide (DMSO) (Sigma, UK) at a concentration of 20 mM and fresh stocks were prepared for every experiment. Cells were treated so that control and treatment cells all received the same volume of DMSO, and that this volume did not exceed a final concentration of 0.1% DMSO.

### **2.2.4 Treatment with flavones**

#### **2.2.4.1 Assessment of cell proliferation**

APC10.1 cells were seeded at a density of 2,500 cells per well, in a 24-well plate (Nunc, UK), in culture medium. Cells were exposed up to 20 µM apigenin or tricetin, or up to 10 µM PMF for 144 hours (h). To perform cell counts, the treatment medium was removed, the cells were washed in warmed PBS buffer and 0.5 mL trypsin was added to each well (1x). The plates were incubated for 5 min, after which 0.5 mL fresh, warmed

medium was added and the cells gently pipetted. 1 mL of the resultant solution was mixed with 9 mL of Coulter® Isoton® II diluent (Beckman Coulter, UK) and the cells counted using a Z2 Coulter Particle Count and Size Analyser (Beckman Coulter, UK). Growth curve experiments were performed in triplicate. The results are calculated as the mean  $\pm$  SD for each set of triplicate. The IC<sub>50</sub> values were calculated from a plot of cell number as a percentage of control versus drug concentration using the linear phase of the curve.

#### **2.2.4.2 Treatment of cells with flavones for cell cycle assay**

The cells were seeded at  $5 \times 10^5$  cells per T75 flask in normal growth medium overnight to allow for adherence onto the surface of the flask. The cells were exposed up to 20  $\mu$ M of apigenin or tricetin and up to 10  $\mu$ M of PMF, in addition to control. The medium was aspirated and 20 mL of treatment medium per flask were added to each treatment flask. Triplicates of each treatment were performed. The cells were exposed to the treatment medium for up to 96 h. The cells were washed, harvested and counted. The cells were incubated overnight at 4°C in 70% ethanol to disrupt the cell membrane to allow propidium iodide (PI) (Sigma, UK) stain into the cells. The cells were centrifuged at 400 x g, 4°C for 10 min and resuspended in 800  $\mu$ L PBS prior to sequential addition of 100  $\mu$ L RNase A (Sigma, UK) at 1 mg/mL, and 100  $\mu$ L PI at 50  $\mu$ g/mL. The cells were analysed by using a FACScan flow cytometry. The analysis of the raw data was performed using software Modfit LT for Mac V 2.0. The population of cells in different cell cycle phases was calculated using analysis of variance (ANOVA) and Student's t-test.

### **2.2.4.3 Treatment of cells with flavones for apoptosis assay**

This method enables quantitative assessment of live cells and cells which are undergoing apoptosis (Vermees et al., 1995). When cells are undergoing apoptosis, the membrane phospholipid phosphatidylserine (PS) is translocated from the inner leaflet of the plasma membrane to the outer leaflet, exposing PS. Annexin V, a calcium-dependent phospholipid-binding protein, has a high affinity for PS. Annexin V binds to apoptotic and necrotic cells while it is not taken up by live cells. Simultaneous incubation with Annexin V and PI further distinguishes between apoptotic cells and necrotic cells as the necrotic cell membrane is permeable to PI stain. The Annexin V used in this work was conjugated to fluorescein-isothiocyanate (FITC). Thus, concurrent staining of cells with Annexin-FITC and PI resulted in necrotic or late apoptotic cells staining positive for FITC and PI, early apoptotic cells staining positive for FITC, and live cells remaining unstained.

The cells were seeded at  $2 \times 10^5$  cells in 100 mm Petri dishes (Nunc, UK) in normal growth medium overnight to allow for adherence onto the surface of the dish. The cells were exposed up to 20  $\mu\text{M}$  of apigenin or tricetin and up to 10  $\mu\text{M}$  of PMF, in addition to vehicle control and positive control 200 nM etoposide (Sigma, UK). The medium was aspirated and 10 mL of treatment medium per dish were added to each treatment flask. Triplicates of each treatment were performed. The cells were exposed to the treatment medium for up to 96 h. The cells that had detached during the incubation period were pipetted into labelled centrifuge tubes. The adherent cells were washed, harvested by trypsinisation and pooled with the detached cells. The cells were centrifuged at 400 x g and incubated for 30 min in normal growth medium in humidified, 37°C, 5% CO<sub>2</sub> incubator. The cells were centrifuged at 400 x g, 4°C for 5 min. The supernatant was discarded and the cells were passed through a cell strainer at 0.2  $\mu\text{m}$  (Falcon, UK) to

achieve single-cell suspension. The cells were resuspended in 380  $\mu\text{L}$  binding buffer at 10 mM HEPES/ NaOH, pH 7.4, 140 mM NaCl, 2.5 mM  $\text{CaCl}_2$  (Bender MedSystems). The cells were incubated with 10  $\mu\text{L}$  Annexin V-FITC (provided with kit) for 10 min in the dark at 4°C. The cells were washed and 10  $\mu\text{L}$  PI at 20  $\mu\text{g}/\text{mL}$  (Bender MedSystems) was added and analysis was performed using a FACScan flow cytometry with CellQuest software package.

### **2.2.5 mRNA microarray**

Microarray is a tool which allows global analysis of the expression of thousands of genes in a single experiment. It enables comparative genome analysis, functional genome analysis, and pathway analysis to delineate pathways and biomarkers of interest. By resequencing of DNA, further investigation into the change in the gene expression of mRNAs can be validated to depict modulation of physiological and pathological change. Gene regulation based on the assumption that genes regulated in parallel share common control mechanisms subsequently allows identification of patterns of gene change that define disease status and which may be of use as biomarkers or prognostic indicators (Murphy, 2002, van 't Veer et al., 2002).

The basic method for mRNA expression microarrays, which were the predominant types used in this project, involves extraction of RNA from the control and treated cells, amplification and conversion of RNA to cDNAs. During the process of conversion of the mRNA to cDNAs, labelling with a fluorescent tag is achieved. For dual colour microarrays, two different labels are used for the two samples that will be co-hybridised

to the microarray. When one sample is going to be used per microarray, then usually only one fluorescent label is employed.

Where the signal is expected to be low, an amplification step can be incorporated in the labelling procedure. Once labelled, this complex probe is then applied to the microarray where the different cDNA sequences find complimentary sequences on the microarray. After hybridisation and washing, the degree of hybridisation for each sequence on the microarray is achieved by laser excitation of the fluorescent labels and measurement of the emission. Each of the illuminated spots of DNA is measured. The vast quantities of raw data, real-time images and gene identification are then acquired for analysis. The raw data from each test sample is based on the Cyanine (Cy) fluorescence ratio (Cy 3/Cy 5) and these are kept separately as individual data while the pooled RNA is treated as the common reference. In a ubiquitous biological setting, most of the genes remain unchanged.

Owing to the different chemistries of the fluorescent labels, there is some dye bias in the results obtained. This is often dealt with by a dye-swapping technique (Kerr and Churchill, 2001, Sterrenburg et al., 2002). This technique requires the assay to be run twice by swapping the probes between samples and reference. However, when a common reference approach is used such as in this study, the change in gene expression can be compared without the need for dye swaps because the common reference acts to control the dye bias variability.

In a comparison study of common reference and dye-swap technique, the cDNA probes spotted on the array with common reference showed reproducible hybridisation signal in 99.5% of the cDNA probes and no significant difference between the two methods with 95% of the arrays within a difference of  $\pm 0.2$ -fold change (Sterrenburg et al.,

2002, Wei et al., 2004). Thus, common reference cDNA microarray demonstrated reproducibility and consistency within and between each microarray slide, moreover, halving the time and cost of running the assay in relation to the dye-swapping method. This method is recommended when investigating the gene expression levels across multiple samples in a time course experiment (Sterrenburg et al., 2002, Wei et al., 2004).

By pooling samples, biological variance can be masked and false confidence and underestimates may result (Churchill, 2002). Hence, a reliable and consistent statistical formula is needed. In this study, each sample was compared to a common reference sample (Zhang and Gant, 2004, Zhang and Gant, 2005).

Statistical analysis is performed on the raw data and a significant deviation from the arbitrary zero or null is an indication of gene change. The normalised data thus reads either minus (-) indicating down-regulation or plus (+) indicating up-regulation of gene expression relative to the common reference.

One of the advantages of this method is that it allows a high throughput of data and enables the global view of interactions between genes before and after treatment in a single assay. By employing fluorescence detection, competitive hybridisation to the same microarray can be used to compare targets derived from different samples. Cy3-2'-deoxyuridine-5'triphosphate (Cy3-dUTP) and Cy5-dUTP in the complementary DNA (cDNA) are frequently co-labelled because these two dyes have high incorporation efficiencies with reverse transcriptase, good photo-stability and yield, as well as being widely spaced in their excitation and emission spectra, permitting high discriminating optical filtration. In this experiment, the microarrays were designed and prepared in Dr. Tim Gant's laboratory, MRC Toxicology, Leicester.

After each microarray slide had been scanned, the raw data from the study was subjected to several levels of statistical models and analysis. Firstly, global normalisation was performed using statistical software designed by Dr. Shu-Dong Zhang (Zhang and Gant, 2004) by integrating the ANOVA model proposed by Kerr et al. (Kerr and Churchill, 2001, Kerr et al., 2000) to remove the systematic bias that may result from intrinsic variability including variations of concentrations between two mRNAs and possibly the variation of photo-amplifier voltages used between the two fluorescent channels when the images were scanned.

In this study, 2 time points of 24 h and 48 h and 2 concentrations of 5  $\mu\text{M}$  and 10  $\mu\text{M}$  were used for testing biological effects of apigenin, tricetin and PMF. To study the global gene expression of APC10.1 cells when treated with apigenin, tricetin or PMF in addition to control (0  $\mu\text{M}$ ) at time points of 24-h and 48-h, a 2-way ANOVA was implemented. This statistical model normalises the raw data and estimates real changes in gene expression (Kerr et al, 2000). This was to investigate the effects of PMF on these cells and the relationship between treatment concentration and time. In this study, a total of 19975 genes generated a large volume of data and in order to have a manageable number of genes to work with, false discovery rate was used (FDR). FDR was first proposed by Benjamini and Hochberg (Benjamini and Hochberg, 1995, Datta, 2005) as a means to define and control the rate of FDR in order to narrow down a large volume of data to a more manageable and statistically significant size. In this study, lists of genes were categorised based on increase or decrease of gene expression in relation to the interaction between concentration and time of APC10.1 cells.

This was followed by local normalisation with statistical software written by Dr. Zhang, integrating the LOWESS procedure. A two-sample t-test was implemented to further

study the individual effects of concentration and time on the gene expression of APC10.1 cells. A 1.5-fold increase or decrease of a gene was used as the cut-off point with a p-value equal to or less than 0.05. Lists of genes were grouped based on the increase or decrease of gene expression in relation to concentrations or time. A schematic diagram of the microarray analysis used in this study is shown in Figure 2.2.

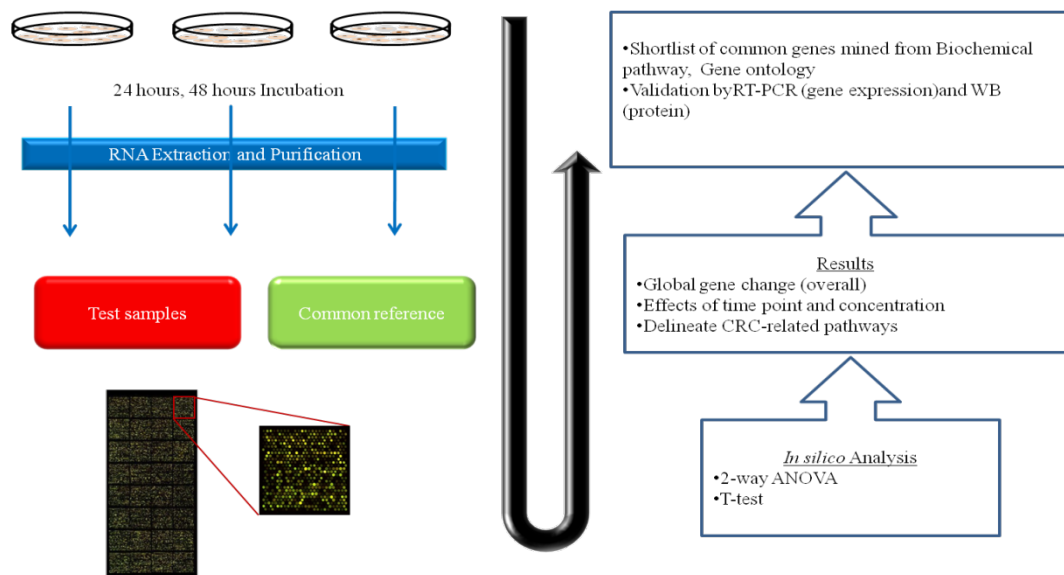


Figure 2.2 A schematic diagram showing the sequential steps from treatment of cell to the end results of pathway analysis.

### 2.2.5.1 Treatment of cells with flavones

Cells were seeded at  $5 \times 10^5$  cells per T75 flask in normal growth medium overnight to allow for adherence onto the surface of the flask. The cells were exposed to  $10 \mu\text{M}$  PMF for up to 48 h. The cells were washed and harvested by trypsinisation. Cell count

was performed to ensure that the cell pellet contained less than  $10^7$  cells to enable optimal RNA yield and purity during RNA extraction. 24 individual samples were obtained and regarded as individual data points for each flavone. The cells were centrifuged and the supernatant was discarded. The cells were stored in *RNAlater*<sup>®</sup> (Qiagen Ltd., UK) in Eppendorf tubes at -20°C for future RNA extraction.

#### **2.2.5.2 RNA extraction**

The cells were retrieved from -20°C storage, centrifuged and the supernatant containing *RNAlater*<sup>®</sup> was discarded. RNA extraction was performed using *RNeasy*<sup>®</sup> Mini Kit (Qiagen, UK) as instructed by the manufacturer. The cell pellet was loosened thoroughly by flicking the tube before 600 µL of Buffer RLT were added to lyse the cells. The lysates were homogenised by continuous, rigorous pipetting motion. The lysates were completely homogenised with the appearance of a transparent, clear solution. Ethanol precipitation was performed by adding 600 µL of 70% ethanol to the lysate. The resulting white precipitate was transferred to an *RNeasy* spin column and centrifuged at 4000 x g for 15 seconds (sec). The lysate was washed once with 700 µL of Buffer RW1 and twice with 500 µL of Buffer RPE. Each time, the eluant was discarded. A new collection tube was used for the collection of extracted RNA by washing the column twice with 50 µL of RNase-free water.

The yield and purity of each RNA sample were obtained using GeneQuart Pro absorbance reader (Amersham Biosciences, UK). The samples were diluted 1:20 with sterile water. Sterile water was used as reference and the absorbance was measured at 260 nm and 280 nm. An  $Abs_{260}:Abs_{280}$  ratio of between 1.6 and 1.9 indicates a protein-free preparation. A ratio reading of less than 1.6 indicates contamination of RNA with

protein. The absorbance of RNA extracted from the samples was between 1.6 and 2.1 for this experiment.

### 2.2.5.3 Reverse transcription

Each sample of extracted RNA was aliquoted at 10 µg. A common reference was reconstituted by pooling aliquots of 10 µg from each sample. The following procedures were performed on the samples of extracted RNA and the common reference.

The extracted RNA at 10 µg was pipetted into a PCR tube containing 13 µL DEPC-treated water (see section 2.1.3.2), 1 µL of the anchored oligo dT<sub>23</sub>N<sub>2</sub> (Sigma Genosys, UK) and 1 µL of pentadecamers (Sigma Genosys, UK). The mixture in the PCR tube was initially heated to 95°C for 5 min before lowering the temperature to 70°C for 10 min in a PCR thermal cycler (MJ Research, Canada). The mixture was then snap-cooled on ice for 1 min.

Table 2.1 The Labelling mix constituents for reverse transcription.

<b>Nucleotide</b>	<b>Stock (mM)</b>	<b>Volume (µL)</b>	<b>Final concentration in reaction (mM)</b>
dATP (Sigma Genosys, UK)	100	15	0.50
dGTP (Sigma Genosys, UK)	100	15	0.50
dCTP (Sigma Genosys, UK)	100	15	0.50
dTTP (Sigma Genosys, UK)	100	6	0.20
aadUTP (Ambion, UK)	50	18	0.30
5X first strand buffer (Invitrogen, UK)		600	1X
0.1 M Dithiothreitol (DTT) (Invitrogen, UK)	100	300	0.01
RNAsin (Invitrogen, UK)		100	
DEPC-treated water		331	
<b>Total Volume</b>		<b>1400</b>	

Labelling mix was reconstituted as shown in Table 2.1 and aliquots were prepared and stored at -80°C. Labelling mix of 14 µL and 1 µL of Superscript™ III Reverse Transcriptase (Invitrogen, UK) were added to the mixture and mixed well by flicking the tube. The mixture was centrifuged and incubated at 50°C for 3 h. The mixture was cooled down to 4°C.

#### **2.2.5.4 RNA hydrolysis**

10 µL of 0.5 M EDTA (Sigma, UK) were added to the cooled mixture prior to addition of 10 µL of 1N NaOH (Sigma, UK). The mixture was incubated at 65°C for 15 min. After the incubation, 25 µL of 1 M HEPES (Sigma, UK) at pH 7.0 were added to the mixture.

#### **2.2.5.5 Purification of cDNAs**

The mixture was filtered using Microcon Ultracel YM-30 filters (Amicon, UK) according to the manufacturer's instruction. DEPC-treated water (375 µL) was pipetted into the filter column before the mixture was transferred onto the filter. The mixture was centrifuged at 4000 x g for 1 min to ensure no leakage or faulty filters were used. The column was centrifuged for another 5 min and the eluant was discarded. The column with the mixture was washed twice more with 450 µL of DEPC-treated water and each time the eluant was discarded. The column was then centrifuged for a shorter period of 2 min at each spin to reduce the volume on the filter until a small part of the filter was visible. The column was then inverted into a new collection tube and centrifuged for 2 min to collect the filtrate of purified cDNA. The concentration of the cDNA was measured using a NanoDrop (Thermo Scientific, UK). The cDNA was further dried down using a SpeedVac until all liquid had evaporated.

### **2.2.5.6 Coupling of labelled cDNAs**

The dried down cDNA was resuspended in 7  $\mu\text{L}$  of DEPC-treated water before 1  $\mu\text{L}$  of 1 M sodium carbonate (Sigma, UK) buffered at pH 9.0 was added to the mixture. Two dyes were used for this assay; Alexa Fluor 555 (Invitrogen, UK) (reference) and Alexa Fluor 647 (Invitrogen, UK) (sample). These dyes were reconstituted at 20  $\mu\text{g}/\mu\text{L}$  stock with DMSO. Aliquots of each dye at 2  $\mu\text{L}$  were added to the designated reference and sample respectively. The dye was incubated with the mixture for 1 h at room temperature (RT) in the dark (wrapped in foil). 4.5  $\mu\text{L}$  of 4 M hydroxylamine (Sigma, UK) were added to each mixture and incubated for 15 min at RT in the dark. The sample and its corresponding reference were combined and 35  $\mu\text{L}$  of 0.1 M sodium acetate (Sigma, UK) at pH 5.2 were added.

### **2.2.5.7 Clean up of labelled cDNAs**

In order to remove the excess dyes, QIAquick® PCR purification kit (Qiagen, UK) was used as instructed by the manufacturer. The combined, labelled cDNA was washed with 250  $\mu\text{L}$  of Buffer PB and centrifuged for 1 min at 4000 x g. The eluant was discarded. The cDNA was washed with 750  $\mu\text{L}$  of Buffer PE and centrifuged for 1 min at 4000 x g. The eluant was again discarded and the column was centrifuged for 1 min at 4000 x g to dry the cDNA. A new collection tube was used and the 30  $\mu\text{L}$  of Buffer EB was added and the column was incubated for 1 min at RT prior to centrifugation of 1 min at 4000x g. The eluate was retained. The concentration of the labelled cDNA was measured using a NanoDrop (Thermo Scientific, UK) to determine the incorporation of the dyes.

### **2.2.5.8 Preparation of microarray slides**

Glass slides (26 mm x 75 mm) (Thermo Scientific, UK) were washed twice in 0.2% sodium dodecyl sulfate (SDS) (Sigma, UK) solution for 2 min before transferring to two washes of deionised water for 2 min respectively. This was performed on a platform rocker at a speed of 25 cycles per min. The slides were dried by centrifugation at 300 x g at 4°C and stored in the dark until further use.

### **2.2.5.9 Hybridisation of cDNAs onto microarray slides**

1 µL of tRNA (4 mg/mL) (Invitrogen, UK), 40 µL of Genisphere Buffer (Genisphere, Spain) and 40 µL of DEPC-treated water were added to each labelled cDNA mix. The combined mixture was denatured at 100°C for 5 min and incubated for 1 h at 42°C. A washed array slide was placed between an array template slide as a guide and a cover slip. A volume of 40 µL of cDNA per slide was pipetted onto the end of the cover slip and allowed capillary action to draw the cDNA into the slide. There were a total of 25,118 individual genes on the in-house gene lists based on the mouse exonic evidence-based oligonucleotides (MEEBO) (Shi et al., 2006). Some of these genes had replicates which made up to a total of 38,690 spots. These were spread over 2 slides with approximately 19,970 genes from the murine genome covering each of two gene chip slides (slides A and B).

5 mL of DEPC-treated water were pipetted into the well at the bottom of the hybridisation chamber (Genetrix, Spain). The microarray slides were placed on the rack of the chamber before the chamber was shut and incubated at 42°C overnight.

#### 2.2.5.10 Washing of the microarray slides

The slides were retrieved from the chamber and washed with different dilutions of saline sodium citrate (SSC) (Sigma, UK) as described in Table 2.2.

Table 2.2 Washing regime performed on the array slides.

Wash		Platform rocker
1	1 x SSC, 0.03% SDS in DEPC-treated water	25 cycles per min for 5 min
2	0.20 x SSC in DEPC-treated water	25 cycles per min for 3 min
3	0.05 x SSC in DEPC-treated water	25 cycles per min for 3 min

The slides were dried by centrifugation at 300 x g for 4 min. The slides were read using 4 laser channels GenePix Pro 6 on Axon 4200 Microarray Scanner (Axon Instruments, UK) at wavelengths of 532 nm for Alexa 555 (reference) and 635 nm for Alexa 647 (sample) and the analysis was performed using GenePix Pro 5 (Axon, UK).

#### 2.2.5.11 Analysis of fluorescence and data interpretation

A preview scan of 100 micron scanning at 5 micron resolution was performed to identify the main array feature and the total area needed to scan. A final high resolution scan at 100 micron at 10 micron resolution was acquired (Figure 2.3). In order to achieve the best signal-to-noise ratio, the automated photomultiplier tube (PMT) adjustment was set at 0.005%, permitting only 5 out of 100,000 data points to be oversaturated or overexposed. As long as the PMT had a signal-to-ratio of between 400 and 900, the integrity of the data was preserved. The scatter plot of the slide acted as a guide to balance the intensity of each wavelength.

Gene Pix Pro 6 displays 4 laser channels. In this experiment, only two single-channels were used. Dye Cy3 is excited by 532 nm green laser light and dye Cy5 is excited by 635 nm red laser light. Thus, the common reference appeared green while the sample appeared red. In the acquired ratio image, a red spot indicated that the sample for this gene was more abundant than the common reference i.e. that there was higher activity in the sample than in the reference. Conversely, a green spot indicated that the sample has a lower activity than the reference. A yellow spot indicated that there is no change in the activity level between the sample and reference.

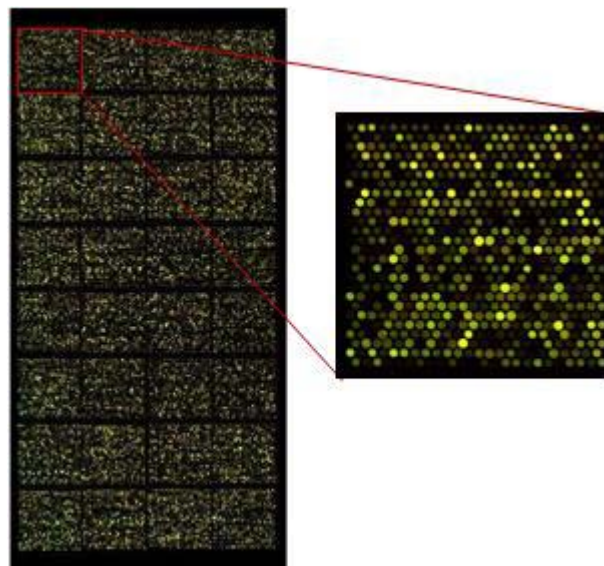


Figure 2.3 A real-time scan of a microarray slide (left) and a magnified grid containing excited probes hybridised to specific genes (dots) (right).

The lists of genes with significant changes at different conditions were compiled. These lists were analysed using ArrayTrack (Version 3.5) and a web-based gene set analysis

tool kit at <http://bioinfo.vanderbilt.edu/webgestalt/> which systematically organises large sets of genes according to their functions, target tissues, and involvement in different pathways. The results were compared between these two analyses. Genes closely associated with CRC, cell cycle arrest and apoptosis, which were obtained from these two methods, were compared. The genes were selected with reference to their p-values. For further confirmation of gene changes, a further software package, Expression Analysis Systemic Explorer (EASE), was used. This software enables the generation of biological themes from a list of genes. It does this by prioritising the genes according to p-values and fold change (Hosack et al., 2003).

#### **2.2.6 Validation of gene changes using reverse transcriptase-PCR (RT-PCR)**

A list of genes of interest was compiled. Genes that are closely associated with cell cycle arrest, apoptosis and colorectal carcinogenesis were selected. Forward and reverse primers of these shortlisted genes were designed using online software packages EMSEMBL, BLAST and licensed Primer Express 2.0 (Table 2.3). The primers were commercially generated for research purpose only.

In a 0.5-mL Eppendorf tube, 100 ng/ $\mu$ L of RNA was reconstituted in autoclaved, UP water to a final volume of 50  $\mu$ L. This was performed for all the samples stated above (see section 2.2.5.1). A non-template control (NTC) (negative control) containing UP water was also included in this validation.

The RNA of 25 samples (24 samples, 1 NTC) was denatured for 3-4 min at 95°C. The tubes were centrifuged and cooled on ice. From each of the RNA samples, 20  $\mu$ L were mixed with 180  $\mu$ L of reaction mix (see Table 2.4 and Table 2.5). The mixture in the

tube was centrifuged down and incubated for 1 h at 50°C, which was followed by 4 min incubation at 17°C in a PCR thermal cycler (MJ Research, Canada). Thereafter, the mixture was cooled down to 4°C.

SyBr Green is a cyanine dye which binds to DNA, absorbs blue light ( $\lambda_{\text{max}} = 488 \text{ nm}$ ) and emits green light ( $\lambda_{\text{max}} = 522 \text{ nm}$ ). As in Figure 2.3, 24  $\mu\text{L}$  of SyBr Green/RNA reaction mix (see Table 2.6) was pipetted into each well of a 96-well MicroAmp® optical reaction plate (Applied Biosystems, UK). 1  $\mu\text{L}$  of cDNA were added to this to make up a final volume of 25  $\mu\text{L}$ . The plate was sealed with MicroAmp® optical adhesive film (Applied Biosystems, UK). The plate was centrifuged at 300 x g, 4°C for 4 min. The plate was placed inside the 96-well block and automated ABI PRISM® 7000 Sequence detection system (Applied Biosystems, UK) was initiated. The plate underwent one cycle of 50°C for 2 min, one cycle of 95°C for 10 min, 40 cycles of 95°C for 15 sec each and the final dissociation stage of one cycle of 60°C for 1 min. A positive reaction is detected by accumulation of SyBr Green fluorescent signal. The cycle threshold (Ct) is the number of cycles required for the fluorescent signal to exceed the background level. Ct levels are inversely proportional to the amount of target nucleic acid in the sample. In a 40-cycle amplification, Ct level of less than 29 is indicative of an abundance of target nucleic acid, a level between 30-37 is indicative of a moderate amount of target nucleic acid, and between 38-40 is indicative of weak amount of target nucleic acid in a sample. The raw data was analysed according to the difference in Ct value between gene of interest and housekeeping gene  $\beta$ -actin. The results represented as the ratio of the difference between control and treatment groups were calculated as the mean  $\pm$  SD using Student's t-test. A ratio above 1 denotes up-regulation while below 1 denotes down-regulation of gene expression.

Table 2.3 Fifteen genes closely associated with CRC, cell cycle arrest and apoptosis were shortlisted. The forward and reverse primers (mouse origin) of these genes were generated for Reverse Transcriptase- PCR.

Gene Name	Forward Primers	Reverse Primers	Length(bp)
Bcl9l	GCTGGATCAGGCCCTAAAG	GTACCTGCTGATGGCGTATTCA	69bp
Dvl3	TCAGCAGCTCCACAGAACAGA	AAAGACGAGGACCGCTCAATC	103bp
Wnt3a	AAGCCACCCGGGAGTCA	CTGCACAGGAGCGTGCTACT	78bp
Nfatc2	ATGAGAGCCACCATCGACTGT	TTCCGCAGCTCGATGTCA	65bp
Rela	GCAGTATTCCTGGCGAGAGAA	TCCTGTGTAGCCATTGATCTTGA	74bp
GSK3b	AGTGGTGAGAAGAAAGATGAGGTCTAC	TGTCTGGCGACTCTGTACACTGT	80bp
Ptch1	ACCCAGCCGACCCAGATT	GGCCACATCAAGAGGTTTGG	68bp
Tollip	GCTGCAGTATGGAGGAACAGTTG	TGCCAATTTTGCCTGTACCA	70bp
Wnt 8b	AGCTAACCGGGAGACAGCATT	TGCAGTTTCTAGTCAGGGTGTACATA	74bp
Dact2	AGACCCAGCTCAGGTTTCTATGA	CGGTCGCTGCAAACAGATG	83bp
Lrp5	GGATCCTGCACATGGGTACAT	TCTACAATGATCTTCCGGGTACTG	99bp
TCF4	TGGATTTTCAGTGCGATGTTTTTC	TGTCCACTCGCCAAAGAAGTT	73bp
Frat1 (PEG12)	CGACCCTGGCGATTGTG	TTAGCTGCCAGGGACAAGAAG	69bp
Tnfrsf10b	CAGGCTGTCTTTGTTCCAGTAACA	TCCTCCGGCCGCTGTAG	71bp
Vav3	GGCCTTCCCGACTTAATAGATGA	CCTCGCCGTACACACAGTCA	73bp

Table 2.4 Formulations for Real Time Master Mix (RT-MM) for 200 reactions.

Nucleotide	Stock	Volume (μL)	Final concentration in reaction
dATP	100 mM	20.0	0.5mM
dGTP	100 mM	20.0	0.5mM
dCTP	100 mM	20.0	0.5mM
dTTP	100 mM	20.0	0.2mM
aadUTP	50 mM	18.0	0.3mM
5X first strand buffer		400.0	1X
0.1 M DTT	100 mM	20.0	0.01M
Magnesium chloride (Sigma, UK)	50 mM	100.0	
Random hexamer (Sigma Genosys, UK)		19.8	
DEPC-treated water		1012.2	
<b>Total Volume</b>		<b>1650.0</b>	

Table 2.5 Formulation of a 10-μL reaction mix for each RNA.

Reagents	Volume (μL)
Real time master mix (Table 2.4)	8.25
RNasin® Plus (Promega, UK)	0.25
Superscript™ III Reverse Transcriptase	0.50
RNA (100 ng /μl)	1.00
<b>Total volume</b>	<b>10.00</b>

Table 2.6 Formulation for addition of SyBr Green to the RNA reaction mix (n=28).

Reagents	Volume (μL)
FastStart Universal SyBr Green Master Mix (ROX)(2X) (Roche, UK)	350.0
Forward primer (Sigma Genosys, UK) (see Table 2.3)	6.3
Reverse primer (Sigma Genosys, UK) (see Table 2.3)	6.3
cDNA (n=28)	28.0
DEPC-treated water	309.4
<b>Total volume</b>	<b>700.0</b>

	1	2	3	4	5	6	7	8	9	10	11	12
A	C1	C2	C3	P1	P2	P3	C4	C5	C6	P5	P6	P7
B	C1	C2	C3	P1	P2	P3	C4	C5	C6	P5	P6	P7
C	C1	C2	C3	P1	P2	P3	C4	C5	C6	P5	P6	P7
D	NTC	NTC	NTC				NTC	NTC	NTC			
E	C7	C8	C9	P9	P10	P11	C10	C11	C12	P13	P14	P15
F	C7	C8	C9	P9	P10	P11	C10	C11	C12	P13	P14	P15
G	C7	C8	C9	P9	P10	P11	C10	C11	C12	P13	P14	P15
H	NTC	NTC	NTC				NTC	NTC	NTC			

Figure 2.4 Layout of a 96-well optical reaction plate template for RT-PCR.

In each 96-well optical reaction plate, 4 different pairs of primers (forward and reverse) were tested. C denotes control, P denotes PMF-treated sample, NTC denotes non-template control, green represents housekeeping gene  $\beta$ -actin, and pink, blue and yellow represent the location of each pair of primers, and shaded wells are empty. Each sample was performed in triplicate. The gene expression level was calculated as the mean and SD relative to  $\beta$ -actin expression.

## 2.2.7 Western blot (WB) technique

### 2.2.7.1 Preparation of cell lysate

The cells treated as described in section 2.2.4.1 were harvested and centrifuged at 4000 x g for 15 min at 4°C. The supernatant was removed and the cell pellets were stored at -80°C overnight. The pellets were thawed on ice, transferred into Eppendorf tubes and

centrifuged at 4000 x g, 15 min at 4°C. The supernatants were removed by pipetting. The cell pellet was resuspended in cell lysis buffer (see section 2.1.3.6). The lysate was homogenised by pipetting for approximately 30 sec before being left to lyse ice for 15 min. The contents were centrifuged at 4000 x g for 15 min at 4°C. The supernatant (cell lysate) from each tube was transferred into a new labelled Eppendorf tube and protein assay was performed.

### 2.2.7.2 Protein assay

A protein standard, BSA at stock concentration of 1 mg/mL was used. 1 mL of each concentration ranging from 0-25 µg/mL was reconstituted. 800 µL of each diluted BSA stock were mixed with 200 µL of Bradford protein assay dye reagent concentrate (5X) (Bio-Rad, UK). The mixture was vortexed and the absorbance of the mixture was measured using a spectrophotometer at 595 nm. A standard curve of absorbance versus protein concentration (µg/mL) was prepared (Figure 2.5).

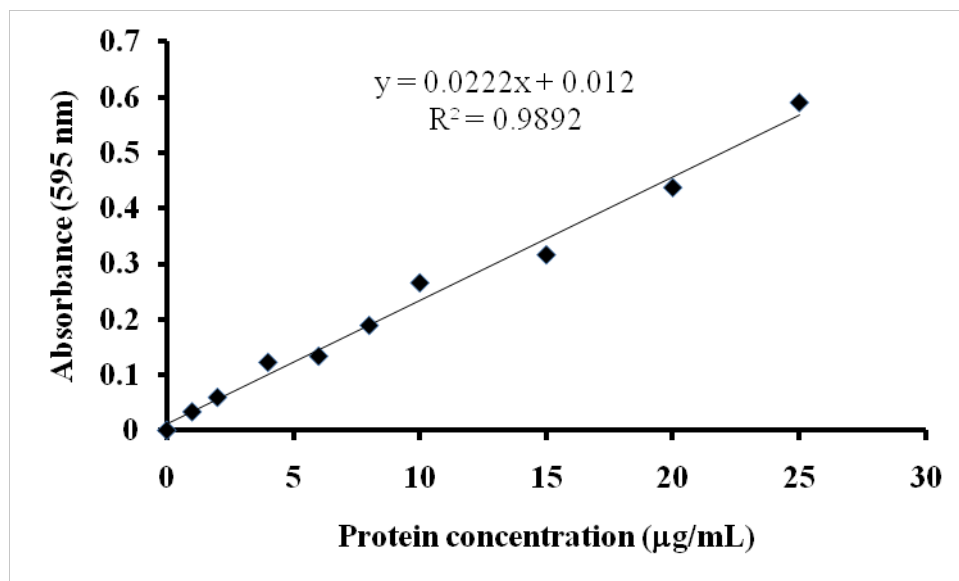


Figure 2.5 A standard BSA calibration curve at absorbance of 595 nm.

Bovine serum albumin (protein standard) was serially-diluted and mixed with Bradford protein assay dye reagent. The mixture was measured using a spectrophotometer at 595 nm. The absorbance of the mixture was measured and plotted. A regression equation ( $R^2$ ) value of close to 1 denotes the linearity fit of the data points.

For each sample replicate, 2  $\mu\text{L}$  of lysate was added to 998  $\mu\text{L}$  of UP water. The tubes were vortexed to mix well. 200  $\mu\text{L}$  of diluted cell lysate were discarded and 200  $\mu\text{L}$  of Bradford protein assay dye reagent concentrate (5X) were added. The mixture was vortexed and the absorbance of the mixture was measured using a spectrophotometer at 595 nm. Protein concentration for each lysate was extrapolated and calculated using the standard curve in Figure 2.5. An equal volume of Laemmli loading buffer (2x) (Sigma, UK) was added to each protein lysate and vortexed to mix well. The resulting mixtures were heated at 100°C for 5 min prior to storage at -80°C.

### **2.2.7.3 Western blot (WB)**

SDS-polyacrylamide gels of 8-15% (w/v) were cast according to the molecular weight of the protein of interest (Table 2.7). Stacking gel was cast and used as the generic stacking gel for all percentages of gels (Table 2.8). PageRuler™ Prestained protein ladder (Fermentas, UK) or Spectra™ Multicolor high range protein ladder (Fermentas, UK) (5  $\mu\text{L}$  per well) (Figure 7.1) was added into both peripheral wells of the gel. Equal amounts of protein (10-50  $\mu\text{g}$ ) were loaded into the designated wells on the gel. The gels were placed inside a tank filled with running buffer (see section 2.1.3.3). The proteins were resolved through the gel initially at 50 V for 1 h before the voltage was

increased to 100 V for the next subsequent 30 min or until the lowest band of the coloured protein ladder was approximately 0.5 cm from the edge of the gel.

The resolved proteins were transferred to a nitrocellulose membrane (Geneflow Ltd., UK) (Figure 2.6) at 100 V for 2 h on ice to prevent overheating of the membrane in the tank filled with transferring buffer (see section 2.1.3.4). The membrane (blot) was blocked in blocking buffer (see section 2.1.3.8) at 4°C overnight.

The blots were probed with designated, optimised primary antibodies in blocking buffer for 2 h at RT. The strips were washed with PBST (see section 2.1.3.7) for 5 min each time for a total of 5 washes. The strips were probed with corresponding optimised horse-radish peroxidase (HRP) conjugated secondary antibodies for 1 h at RT. These strips were washed with PBST for 5 min each time for a total of 5 washes. Enhanced luminol-based chemiluminescent (ECL) reagent set (Geneflow Ltd., UK) (1:1 ratio of reagent A and reagent B) was reconstituted as described by the manufacturer and pipetted onto the strips. Excess ECL was removed. The membrane strips were wrapped in Saran wrap (SC Johnson & Son, UK) and placed in a Hypercassette™ (Amersham, UK). The ECL hyperfilm (GE Healthcare, UK) was exposed to the membrane strips in the dark room for 5 sec to 30 min. The films were developed using an automated table top developer AGFA Curix 60, type 9462/106 (AGFA, UK) to visualise the presence of the proteins of interest. In order to confirm equal loading of protein, a house-keeping protein  $\beta$ -actin was probed in each membrane. To quantify the amount of protein present on the film, densitometry was performed using GeneSnap version 6.01 (SynGene, UK) on Bioimaging System (SynGene, UK). A software package GeneTools version 3.03.03 (SynGene, UK) was used to quantify the intensity of bands prior to statistical analysis.

Table 2.7 Constituents for preparation of 8%, 10% and 15% resolving gels respectively for WB.

Reagents	Volume per 8% gel ( $\mu\text{L}$ )	Volume per 10% gel ( $\mu\text{L}$ )	Volume per 15% gel ( $\mu\text{L}$ )
Distilled, deionised water	4600.0	4000.0	1300.0
ProtoGel® 30% (w/v) Acrylamide:0.8% (w/v) Bis-Acrylamide Stock Solution (37.5:1) (Geneflow Ltd., UK)	2700.0	3400.0	5000.0
ProtoGel® Resolving Buffer (4X) (1.5M Tris-HCL, 0.4% SDS, pH8.8) (Geneflow Ltd., UK)	2500.0	2500.0	2500.0
10% Ammonium persulfate (see 2.1.3.5)	100.0	100.0	100.0
N,N,N',N'-tetramethyl-ethylenediamine (TEMED) (Geneflow Ltd., UK)	7.5	7.5	7.5

Table 2.8 Constituents for preparation of stacking gel.

Reagents	Volume per gel ( $\mu\text{L}$ )
Distilled, deionised water	3400.0
ProtoGel® 30% (w/v) Acrylamide:0.8% (w/v) Bis-Acrylamide Stock Solution (37.5:1)	850.0
ProtoGel® Stacking Buffer (0.5M Tris-HCL, 0.4% SDS, pH6.8) (Geneflow Ltd., UK)	625.0
10% Ammonium persulfate (see 2.1.3.5)	50.0
TEMED	7.5

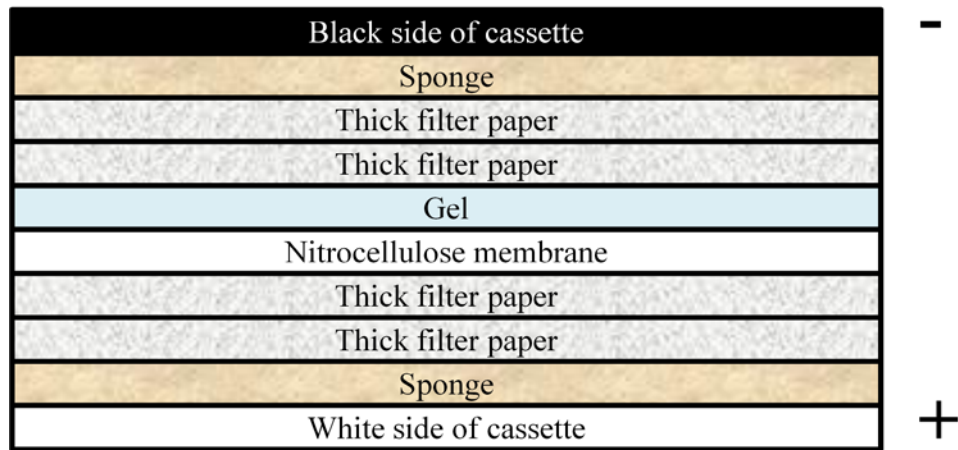


Figure 2.6 Layout of transfer cassette for WB.

The transfer cassette is loaded with sponges, thick filter papers, nitrocellulose membrane and polyacrylamide gel to facilitate the transfer of protein from polyacrylamide gel onto the nitrocellulose membrane.

#### 2.2.7.4 Optimisation of antibodies

All primary antibodies were optimised (Table 2.9) in blocking buffer with the loading of 10-50  $\mu\text{g}$  cell lysate per well.

Table 2.9 Dilutions of primary and secondary antibodies were performed in blocking buffer of 5% milk in PBST.

Columns 1 and 2 show the name of the protein and its corresponding expected (exp) and observed (obs) molecular weight on WBs. Columns 3 and 4 show the different optimised dilutions for primary and secondary antibodies respectively. Column 5 lists the manufacturers of the primary antibodies. The secondary anti-goat IgG HRP-linked antibody was sourced from Santa Cruz, USA, and the secondary anti-rabbit and anti-mouse IgG HRP-linked antibodies were from Cell Signalling, New England Biolabs., UK.

<b>Protein</b>	<b>Mol. Wt (kDa)</b>	<b>Primary antibody (v:v)</b>	<b>Secondary antibody (v:v)</b>	<b>Manufacturer</b>
ACADM	47	1:1000	1:2000 anti-rabbit	Abcam
Akt1	62	1:1000	1:2000, anti-goat	Cell Signalling
BAX	20	1:1000	1:2000 anti-rabbit	Cell Signalling
Bcl9l	157	1:500	1:2000, anti-goat	Santa Cruz
BCL-xl	30	1:1000	1:2000, anti-rabbit	Cell Signalling
Caspase-3 cleaved	17-19	1:1000	1:2000 anti-rabbit	Cell Signalling
Cdc2	34	1:1000	1:2000, anti-rabbit	Cell Signalling
Cdc2-P	34	1:1000	1:2000,anti-rabbit	Cell Signalling
CDK4	30	1:1000	1:2000, anti-mouse	Cell Signalling
CrkL	34	1:1000	1:2000,anti-rabbit	Abcam
Cyclin B1	48	1:1000	1:2000, anti-rabbit	Cell Signalling
Cyclin D1	36	1:1000	1:2000, anti-mouse	Cell Signalling
Dvl3	exp 78, obs 95	1:1000	1:2000, anti-rabbit	Abcam
Frat1	exp 30-35, obs 55	1:1000	1:2000, anti-goat	Abcam
GSK3 $\beta$	46	1:1000	1:2000, anti-rabbit	Cell Signalling
GSK3 $\beta$ -P	46, 51	1:1000	1:2000, anti-rabbit	Cell Signalling
Lrp5	56	1:1000	1:2000, anti-goat	Abcam
MCL1	40	1:1000	1:2000,anti-rabbit	Cell Signalling
MCM7	80	1:1000	1:2000, anti-mouse	Abcam
Nfatc2	135	1:500	1:1000, ant-goat	Santa Cruz

<b>Protein</b>	<b>Mol. Wt (kDa)</b>	<b>Primary antibody (v:v)</b>	<b>Secondary antibody (v:v)</b>	<b>Manufacturer</b>
p21 waf1/Cip1	21	1:1000	1:2000, anti-mouse	Cell Signalling
p27 Kip1	27	1:1000	1:2000, anti-rabbit	Cell Signalling
PTEN	54	1:1000	1:2000, anti-rabbit	Cell Signalling
PTEN-P	54	1:1000	1:2000, anti-rabbit	Cell Signalling
Ptch1	161	1:1000	1:2000 anti-rabbit	Abcam
STAT3	86	1:1000	1:2000 anti-rabbit	Cell Signalling
STAT3-p	79, 86	1:1000	1:2000 anti-rabbit	Cell Signalling
STAT5	90	1:1000	1:2000 anti-rabbit	Cell Signalling
STAT5-p	90	1:1000	1:2000 anti-rabbit	Cell Signalling
STAT6	110	1:1000	1:2000, anti-rabbit	Cell Signalling
STAT6-P	110	1:1000	1:2000, anti-rabbit	Cell Signalling
Survivin	16	1:1000	1:2000 anti-rabbit	Cell Signalling
Tbl1	exp 58, obs 65	1:1000	1:2000, anti-goat	Abcam
TCF4	exp 79, 66	1:1000	1:2000, anti-mouse	Millipore
Vav3	95	1:1000	1:2000, anti-rabbit	Abcam
Wnt3a	exp 39, obs 68	1:1000	1:2000, anti-rabbit	Abcam
Wnt8b	exp 39, obs 32	1:1000	1:2000, anti-rabbit	Abcam
$\beta$ -actin	43	1:2000	1:5000, anti-goat	Abcam
$\beta$ -catenin	92	1:50 000	1:2000 anti-mouse	Cell Signalling

### **2.2.8 *In vivo* study using *Apc*<sup>Min/+</sup> mouse model (PPL80/2167)**

A breeding colony was established and maintained by mating male C57BL/6J *Apc*<sup>Min/+</sup> mice purchased from the Jackson Laboratory (Bar Harbor, USA) with female C57BL/6J (wild-type) also purchased from the Jackson Laboratory. The mice received standard AIN-93G diet and water *ad libitum*. Ear punching of offspring were performed at week 3 to enable identification of genotype by allele specific PCR. The general maintenance of the mice was carried out by Biomedical Services, University of Leicester, UK.

#### **2.2.8.1 Treatment regime of study**

The animals were from the study conducted by Dr. Hong Cai under animal project license PPL80/2167 granted by the UK Home Office, and the experimental design was vetted and approved by the Ethical Committee for Animal Experimentation, University of Leicester. Mice (n=14-25 per treatment group) received standard AIN-93G diet or AIN-93G diet supplemented with 0.2% w/w apigenin, tricetin or PMF commencing from week 12 to week 16 (short term, Figure 2.1) or week 4 to week 16 (long term, see Figure 2.1). At the end of the study, the animals were culled. From each animal, the small intestine and colon were separately rolled into a 'swiss-roll' from distal to proximal end and embedded into paraffin as described by Moolenaar and Ruitenberg (Moolenaar and Ruitenberg, 1981).

#### **2.2.8.2 Immunohistochemistry**

##### **2.2.8.2.1 Serial rehydration of sections**

Paraffin-embedded, 'swiss-rolled' small intestines from the *in vivo* study were cut into sections of 4 µm thickness and placed on polysine slides (Thermo Scientific, UK). The paraffin was removed by heating the slides at 65°C for 1 h. The slides immediately

underwent a serial rehydration by sequential immersion in neat xylene (GENTA Environmental Ltd., UK) twice for 3 min each time, in 99% Industrial Methylated Spirit (IMS) (GENTA Medical, UK) twice for 3 min each time, and in 95% IMS twice for 3 min each time before immersion in water.

#### **2.2.8.2.2 Preparation of sections for primary antibody binding**

The slides were transferred and microwaved on full power (800 W) for 20 min in antigen retrieval buffer (see section 2.1.3.9) before cooling down in PBS for 10 min. The slides were washed twice at 5-min intervals with PBS and dried. To halt the endogenous peroxidase activity, the slides were incubated in endogenous peroxidase inhibiting buffer (see section 2.1.3.10) for 30 min at RT. The slides were washed twice for 5 min in PBS, dried and placed face up in a humidified slide chamber. The slides were treated with Novocastra™ Protein Block (Leica, UK) and incubated in the dark for 5 min at RT. The protein block was gently rinsed off. The slides were washed twice for 5 min in PBS. Primary antibody diluent (see section 2.1.3.11) was used to dilute the primary antibody of interest. In this study, the optimised dilutions for GSK3 $\beta$  (Cell Signalling, UK) and MCM7 (Abcam, UK) were 1:100 and 1:200, respectively. A hydrophobic barrier pen (Dako, UK) was used to draw around the tissues before diluted primary antibody of interest was pipetted onto the sections. The slides were incubated overnight in the closed (dark), humidified slide chamber at 4°C.

#### **2.2.8.2.3 Preparation for secondary antibody binding**

The slides were retrieved from 4°C and incubated for 4 h at RT in the dark before the primary antibody was rinsed off from the sections. The slides were washed twice for 5 min before Novocastra™ Post Primary Block (Leica, UK) was pipetted onto the sections. The slides were returned to the chamber and incubated for 30 min in the dark

at RT. After the slides were washed twice for 5 min, a mixture of 2 mL Rabbit on Rodent HRP-Polymer Detection (MenaPath, A. Menarini Diagnostic, UK) and 2 drops (approximately 40  $\mu$ L) of Mouse Super Background Blocker (MenaPath, A. Menarini Diagnostic, UK) was pipetted onto the sections. The slides were incubated in the chamber for 30 min in the dark at RT. After the mixture had been removed, the slides were washed twice for 5 min and dried. A mixture of 1:20 (v:v) 3, 3'-diaminobenzidine (DAB) chromogen (see section 2.1.3.13) to DAB substrate buffer (see section 2.1.3.12) (Dako, UK) was pipetted onto the sections. The slides were incubated for 5 min in the dark at RT. The mixture was rinsed off and the slides were immersed for 30 sec in Mayer's Haematoxylin solution (Sigma, UK) before being placed in a staining trough with running water to rinse off the excess stain.

#### **2.2.8.2.4 Serial dehydration of sections**

The slides were dehydrated by the reversal sequence of immersion in 95% IMS twice for 3 min, in 99% IMS twice for 3 min and finally twice in neat xylene for 3 min. Cover slips were placed on the sections with the aid of distyrene plasticiser and xylene (DPX) Mountant (Fluka, UK). The slides were left to air dry prior to microscopy analysis.

#### **2.2.8.2.5 Haematoxylin and eosin (H&E) staining of tissue sections**

Paraffin-embedded, human breast tumour sections were cut into sections of 4  $\mu$ m thickness and placed on polysine slides (Thermo Scientific, UK). The animal tissue (see section 2.2.8.1) and human tissue slides were placed into a rack before being put through automated Leica ST4040 H&E linear stainer (Leica, UK).

#### **2.2.8.2.6 Microscopy analysis**

Microscopy analysis was performed using Leica DM2500 photomicroscope (Leica, UK) at magnifications of x4, x10 and x20. The microphotographs were formatted using Photoshop Element 7 as described by Dr. Gary Marty to achieve a uniform white background (Marty, 2007). A scoring system was devised with the assistance of pathologist Dr. Peter Greaves. For each slide, adenomas and aberrant crypt foci were scored. The results were also scored independently by Dr. Greaves.

#### **2.2.8.3 Assessment of adenoma number and size**

This animal study was repeated to obtain data on the size and burden of adenomas in the animal. In this study, at week 16, the animals were euthanised. The small intestine and colon were removed and flushed with saline. The intestines were cut open longitudinally. The number of adenomas was counted under a light magnifying glass. The tumour size was measured using digital calliper (Vernier, UK). Adenoma volume ( $\text{mm}^3$ ) was calculated using the appropriate equations below (Tomayko and Reynolds, 1989):

Equation 1 Volume of adenoma in colon:

Volume of sphere ( $\text{mm}^3$ ) =  $\frac{4}{3} \times \pi \times r^3$ , where  $\pi$  is 3.142, r is the radius of the adenoma

Equation 2 Volume of adenoma in small intestine:

Volume of hemisphere ( $\text{mm}^3$ ) =  $\frac{2}{3} \times \pi \times r^3$ , where  $\pi$  is 3.142, r is the radius of the adenoma

#### **2.2.8.4 Western blot on *in vivo* samples**

Adenomas from the colon and small intestine were excised and kept in separate tubes. The mucosa scrapings from each mouse were kept in separate tubes. The content of each tube was centrifuged and weighed. Lysis buffer (see section 2.1.3.6) at 3x v/w was added to each tube. The tissue was homogenised using a bench top homogeniser type X-1020 (Ystral, Germany). The tubes were incubated on ice for 15 min before the contents were centrifuged at 4000 x g for 15 min at 4°C. The supernatant (tissue lysate) from each tube was transferred into a new labelled Eppendorf tube. Protein assay was performed and the protein concentration of each sample was obtained from the calibration curve in Figure 2.5. WB was performed on the samples (see section 2.2.7.3). Densitometry was performed and the content of the protein of interest was quantified.

#### **2.2.9 Statistical analysis**

##### **2.2.9.1 Student's t-test and analysis of variance (ANOVA)**

The ANOVA (SPSS version 18.0) was performed on raw data obtained from cell proliferation, cell cycle, and apoptosis assays, and global analysis on microarray data respectively. As there are more than two parameters involved, this test was selected over t-test. The student t-test was performed on raw data from RT-PCR and WB as it involves only 1 parameter (treatment). T-test was also performed to assess the change in gene expression between control and treatment. For all these statistical analyses, the p-value <0.05 was established by *post hoc* Bonferroni or Dunnett test.

The statistical analysis for microarray assay was performed using a software programme called Normalise and t-test Gene expression data 1.1.0 designed by Dr.

Shu-Dong Zhang of MRC Toxicology Unit, University of Leicester, UK. The red:green:blue (RGB) ratio from each slide was individually normalised by treating the background fluorescence as zero and incorporated a gene ID to each designated dot. The 4 replicates of each treatment were further normalised using Lowess-normalised  $\log_2$  ratio from the Statistical Analysis on Rowwise data, another software package designed by Dr. Shu-Dong Zhang. A data matrix was generated and 2-way ANOVA were performed to compare global change of different treatments and time points on the cells. The  $\log_2$  ratios were used as indication of the significance of up-regulation or down-regulation of gene expression. FDR was calculated for each gene in the 2-way ANOVA and the threshold for FDR was set at 0.25.

#### **2.2.9.2 Mann-Whitney U test**

This statistical test was used for our animal study as the sample size is small and it is not normally distributed according to the F-test. These two animal groups are independent of each other and the measurements for the size of adenomas were rank ordered.

### **3 Investigation into the effects of flavones on cell proliferation, cell cycle and apoptosis in APC10.1 murine adenoma cells**

#### **3.1 Introduction**

Inhibition of the growth of mutated or pre-cancerous cells is one of the mechanisms by which agents can exert chemopreventive activity. This can be achieved by interrupting the cell cycle and / or promoting apoptosis (see chapter 1.4.4). The work described in this chapter aims to compare the three flavones apigenin, tricetin and PMF for their abilities to cause growth inhibition, cell cycle arrest and induce apoptosis in murine APC10.1 cells. The APC10.1 cell line is derived from the adenomas of *Apc*<sup>Min/+</sup> mouse model. By using this cell line, the study may be indicative of the effects observed in *Apc*<sup>Min/+</sup> mice *in vivo*.

#### **3.2 Effects of flavones on cell proliferation**

APC10.1 cells were exposed to apigenin, tricetin or PMF for 6 days. DMSO was the vehicle control. The cells were exposed to apigenin and tricetin at concentrations up to 20 µM, or to PMF at up to 10 µM (at higher concentrations, PMF precipitated out of solution). At days 3 and 6, cells were counted.

All three flavones demonstrated dose-dependent growth inhibition (Figure 3.1). Overall, PMF exhibited the strongest growth inhibition followed by tricetin and apigenin.

In APC10.1 cells (Table 3.1), the IC<sub>50</sub> for growth inhibition by PMF was 5.26 ± 2.1 μM and 4.99 ± 2.0 μM on days 3 and 6, respectively. The IC<sub>50</sub> of triclin was 9.42 ± 1.9 μM on day 3 and 8.36 ± 1.2 μM on day 6. The IC<sub>50</sub> of apigenin was 13.0 ± 2.5 μM on day 3 and 22.3 ± 14.0 μM on day 6.

Table 3.1 IC<sub>50</sub> values for apigenin, triclin and PMF for inhibition of APC10.1 cell growth (n=3, p<0.05).

Time point	Treatment		
	Apigenin (μM)	Tricin (μM)	PMF (μM)
Day3	13.0 ± 2.5	9.42± 1.9	5.26 ± 2.1
Day 6	22.3 ± 14.0	8.36 ± 1.2	4.99 ± 2.0

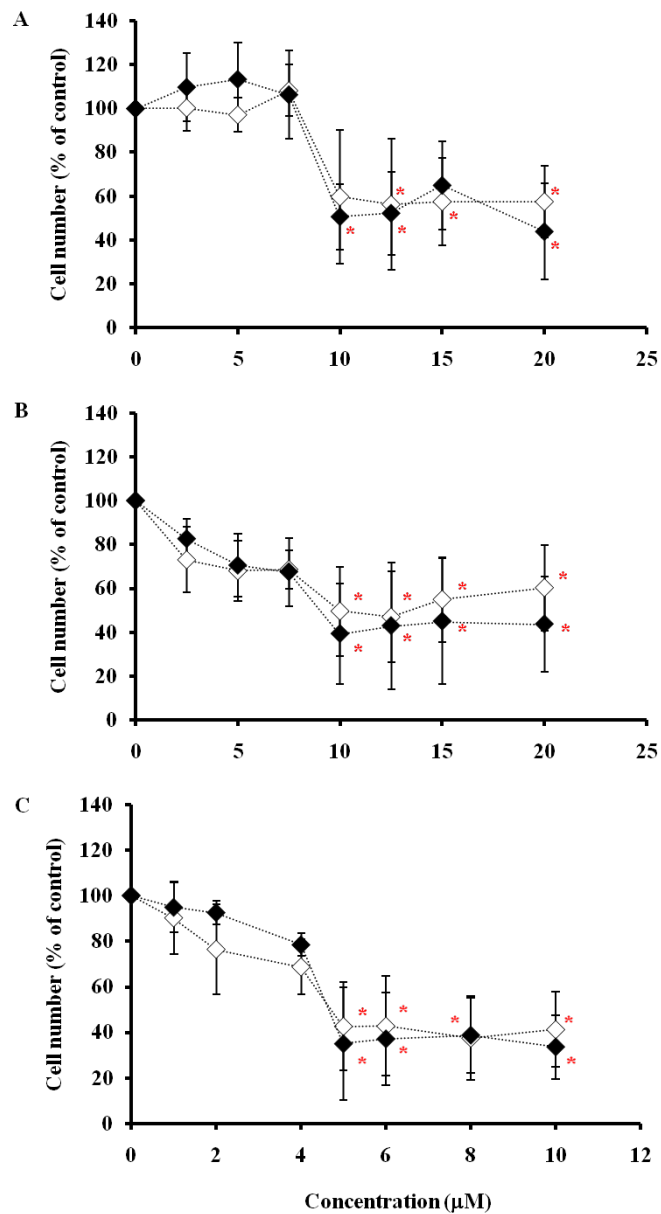


Figure 3.1 Dose-dependent inhibition of cell proliferation by apigenin (A), triclin (B) and PMF (C) in APC10.1 cells on day 3 (open) and day 6 (closed).

The cell number is expressed as a percentage of control cells. Values are the mean and SD of three replicates, n=3. ANOVA with Bonferroni test, and Dunnett t-test were performed. The red asterisk \* denotes that the difference between values is statistically significant (p<0.05).

### 3.3 Effects of flavones on cell cycle

Cell cycle assay was performed and all three flavones were investigated in APC10.1 cells. The inclusion of the time points at 24 h and 48 h was governed by the consideration that at later time points these flavones may have been metabolised or degraded. The time points were chosen on the basis of the results for growth inhibition. Concentrations were chosen to be below and above the IC<sub>50</sub> values. The cells were exposed to the flavones up to 96 h and then stained with PI before data was acquired (Figure 3.2).

In APC10.1 cells, apigenin at 20 µM induced cell cycle arrest in G<sub>1</sub> and G<sub>2</sub>/M at 48 h (Figure 3.3) while at 72 h, G<sub>1</sub> arrest. When APC10.1 cells were exposed to tricetin, cell cycle arrest was observed at 24 h, 48 h and 72 h but not at 96 h (Figure 3.4). At the 24 h time point, tricetin at 5 µM induced G<sub>2</sub>/M arrest. At 48 h and 72 h, tricetin induced G<sub>2</sub>/M arrest at 5, 10 and 20 µM. When APC10.1 cells were exposed to 10 µM PMF, G<sub>1</sub> cell cycle arrest was observed at all time points (Figure 3.5). At 48 h, G<sub>2</sub>/M arrest was observed at 5 and 10 µM. At 72 h and 96 h, 10 µM of PMF induced G<sub>2</sub>/M arrest. Arguably, PMF demonstrated more sustained effects on cell cycle than apigenin or tricetin.

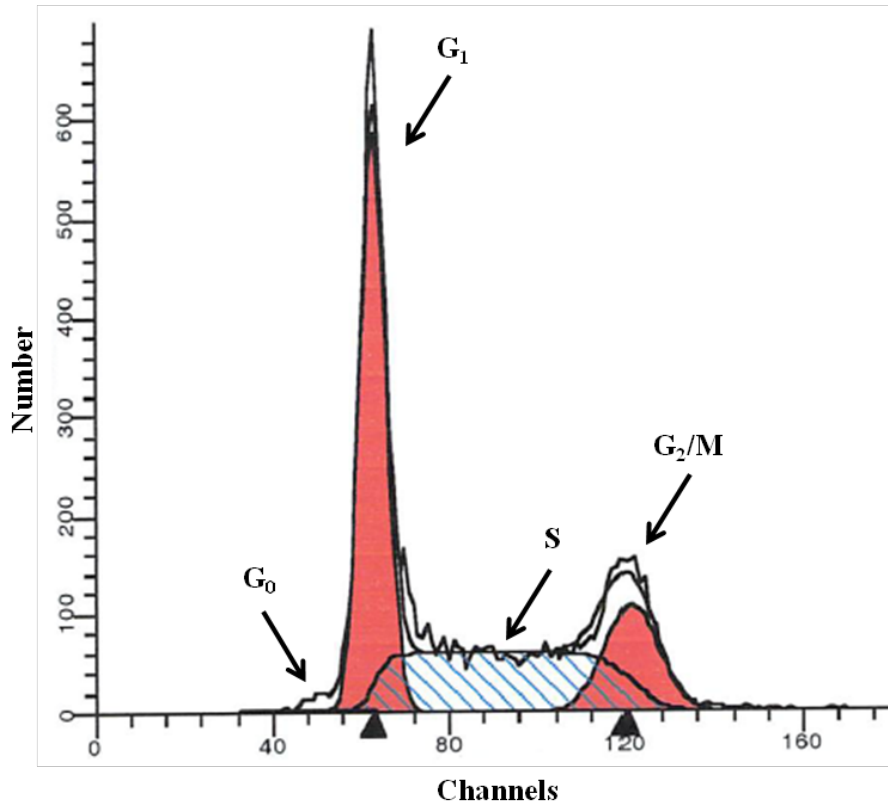


Figure 3.2 A representative cell cycle profile of untreated APC10.1 at 24 h.

In a normal somatic cell, there are 4 distinctive phases of cell cycle. These are Gap<sub>1</sub> (G<sub>1</sub>) with a sub-phase called G<sub>0</sub>, S, G<sub>2</sub> and M. In G<sub>0</sub> phase, the cell is in senescence. In G<sub>1</sub> phase, the cell increases in size, preparing to synthesize DNA, RNA and proteins for entry into S phase. In S phase, synthesis of DNA, RNA and proteins occur. In G<sub>2</sub>/M phase, nuclear and cytoplasmic division occur.

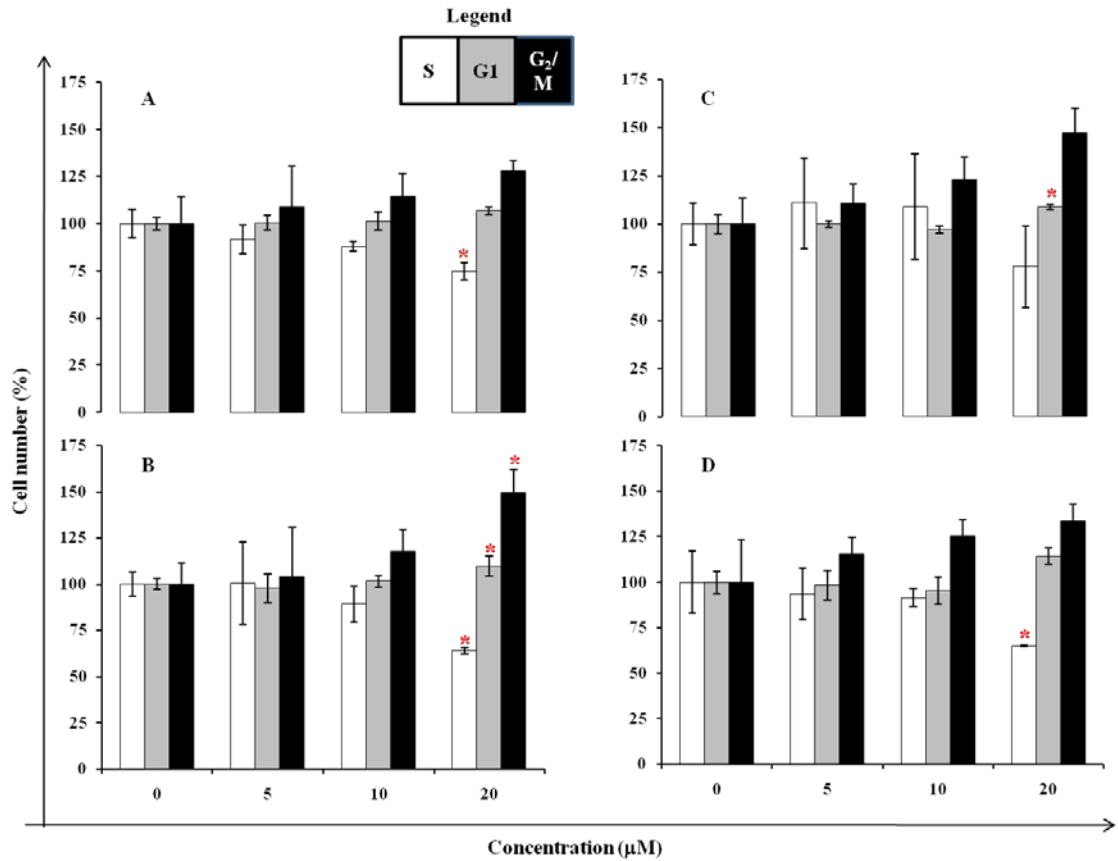


Figure 3.3 Effects of apigenin at 5, 10 and 20  $\mu\text{M}$  on the cell cycle of APC10.1 cells at 24 h (A), 48 h (B), 72 h (C) and 96 h (D).

APC10.1 cells were exposed to up to 20  $\mu\text{M}$  apigenin with DMSO as vehicle. The cell cycle phases are denoted as follows: S phase (white), G<sub>1</sub> phase (grey) and G<sub>2</sub>/M (black). Results are the mean  $\pm$  SD of triplicate experiments. Statistical significance of  $p < 0.05$  is denoted by a red asterisk \*.

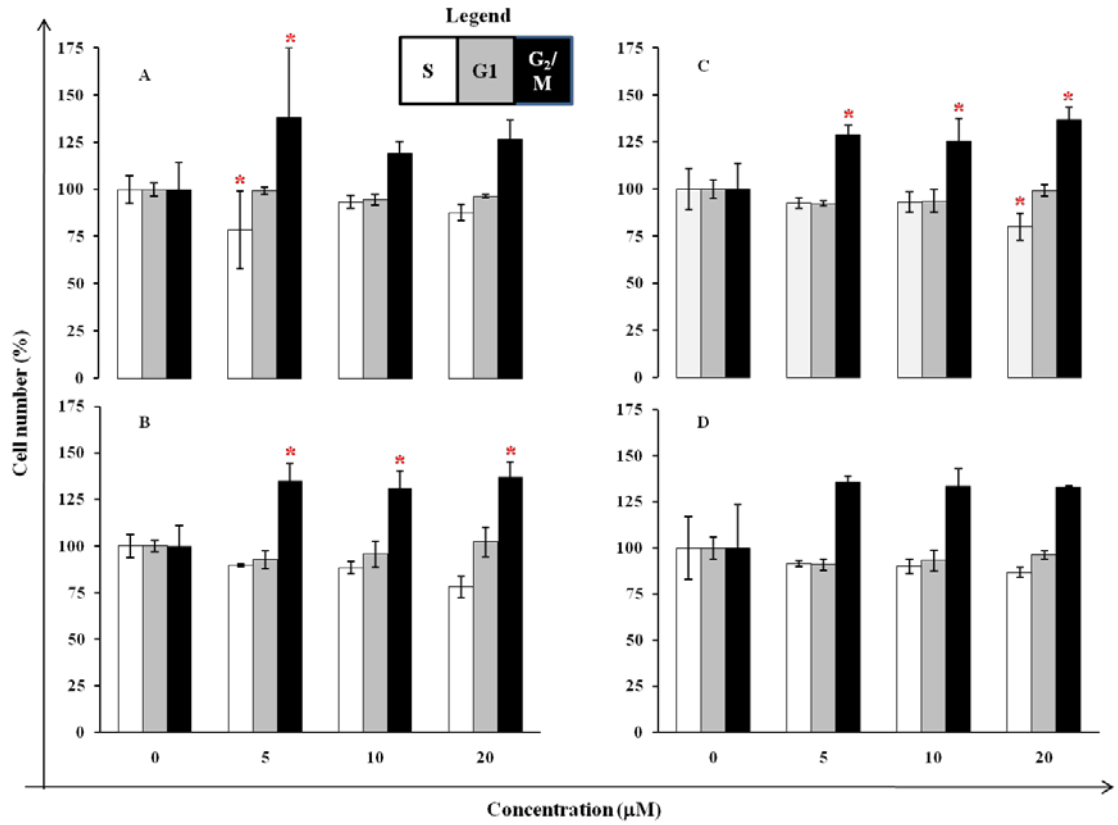


Figure 3.4 Effects of triclin at 5, 10 and 20  $\mu\text{M}$  on the cell cycle of APC10.1 cells at 24 h (A), 48 h (B), 72 h (C) and 96 h (D).

APC10.1 cells were exposed to up to 20  $\mu\text{M}$  triclin with DMSO as vehicle. The cell cycle phases are denoted as follows: S phase (white), G<sub>1</sub> phase (grey) and G<sub>2</sub>/M (black). Results are the mean  $\pm$  SD of triplicate experiments. Statistical significance of  $p < 0.05$  is denoted by a red asterisk \*.

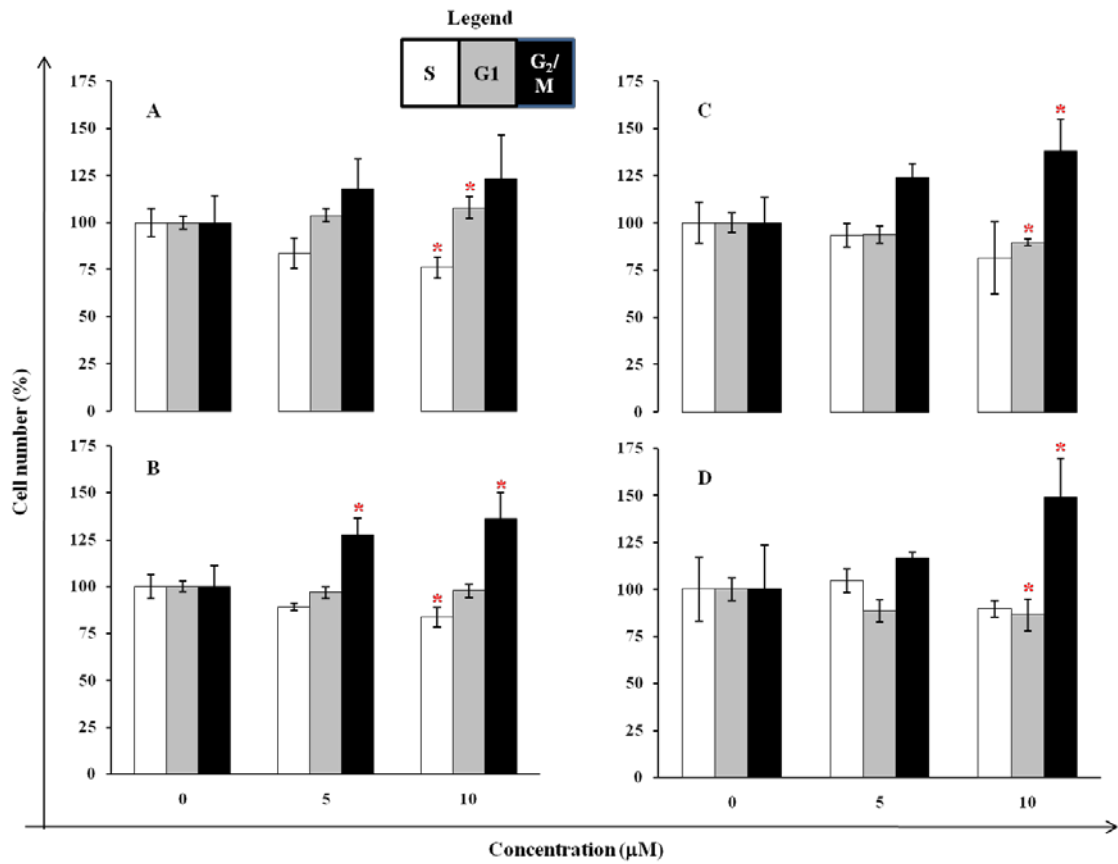


Figure 3.5 Effects of PMF at 5 and 10  $\mu\text{M}$  on the cell cycle of APC10.1 cells at 24 h (A), 48 h (B), 72 h (C) and 96 h (D).

APC10.1 cells were exposed to up to 10  $\mu\text{M}$  PMF with DMSO as vehicle. The cell cycle phases are denoted as follows: S phase (white), G<sub>1</sub> phase (grey) and G<sub>2</sub>/M (black). Results are the mean  $\pm$  SD of triplicate experiments. Statistical significance of  $p < 0.05$  is denoted by a red asterisk \*.

### 3.4 Effects of flavones on apoptosis

Cells were exposed to flavones for 96 h and then stained with Annexin-V-FITC before data was acquired (Figure 3.6). The three flavones exhibited pro-apoptotic properties that were dose- and time-dependent in APC10.1 cells (Figure 3.7).

When APC10.1 cells were exposed to apigenin at concentrations of 5  $\mu\text{M}$  to 20  $\mu\text{M}$  for 48 h, the percentage of apoptosis in APC10.1 cells doubled from 6.4% to 13.0% (Figure 3.8). At 72 h at concentrations of 5  $\mu\text{M}$  to 20  $\mu\text{M}$ , the percentage of apoptosis in these cells increased from 11.1% to 13.7%. At 96 h at concentrations of 5  $\mu\text{M}$  to 20  $\mu\text{M}$ , the percentage of apoptosis in these cells increased slightly from 9.4% to 10.8%.

When the APC10.1 cells were exposed to tricetin up to 20  $\mu\text{M}$ , the percentage of apoptosis was also increased, particularly at 72 h (Figure 3.9). At 48 h, no significant apoptosis was observed between untreated and treated cells. A significant drop in live cells at 72 h was observed at 5  $\mu\text{M}$  with 12.6% accounted for cells underwent apoptosis. At 72 h and 20  $\mu\text{M}$ , tricetin exhibited potency in triggering apoptosis in 12.4% of cells as compared to 7.3% of unexposed cells. At 96 h at concentrations of 5  $\mu\text{M}$  to 20  $\mu\text{M}$ , the percentage of apoptosis in these cells increased slightly from 11.0% to 11.9%.

When the APC10.1 cells were exposed to increasing concentrations of PMF up to 10  $\mu\text{M}$ , the percentage of apoptosis was also elevated (Figure 3.10). At 48 h, PMF increased apoptosis from 1.5- to 1.7-fold as compared to control. At 72 h, this trend was also observed from 1.2- to 1.9-fold. As with apigenin and tricetin, at 96 h, the potential of PMF to induce apoptosis in APC10.1 cells dropped as compared to control.

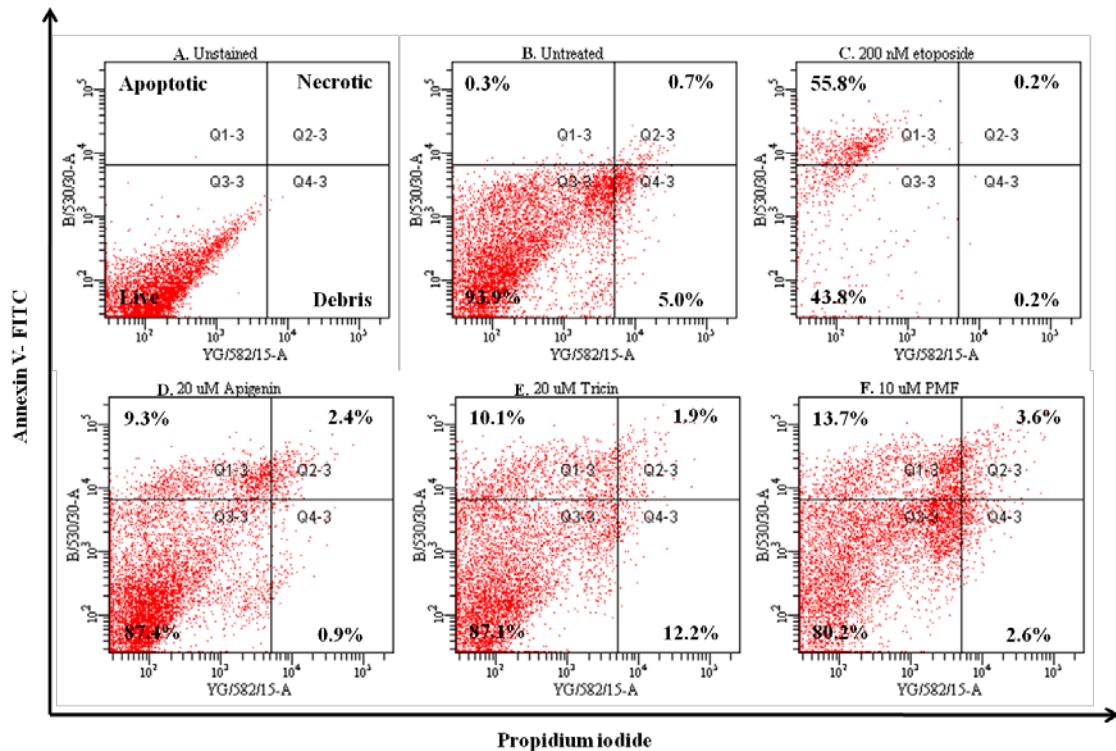


Figure 3.6 Representative fluorescence scattergrams of flow cytometric analysis of APC10.1 cells exposed to control (etoposide or medium) and flavone PMF for 96 h.

APC10.1 cells were exposed to up to 20  $\mu\text{M}$  apigenin or tricetin and 10  $\mu\text{M}$  PMF for 96 h. Cells were stained with Annexin V-FITC and PI as detailed in section 2.2.4.3. Live cells take up neither Annexin V nor PI and appear in the lower left quadrant (Q3-3). Apoptotic cells take up Annexin V and appear in the top left quadrant (Q1-3). Necrotic cells take up both Annexin V and PI and appear in the top right quadrant (Q2-3). Debris appears in the lower right quadrant (Q4-3). **A.** Unstained control APC10.1 cells. **B.** Cells exposed to 0  $\mu\text{M}$  PMF. **C.** Cells exposed to 200 nM etoposide (positive control). Cells were exposed to 20  $\mu\text{M}$  apigenin (**D**), 20  $\mu\text{M}$  tricetin (**E**) or 10  $\mu\text{M}$  PMF (**F**), respectively. A shift of cells from live to apoptotic and necrotic was observed in the presence of flavones. Triplicates were performed and the cell number was calculated based on 10,000 events.

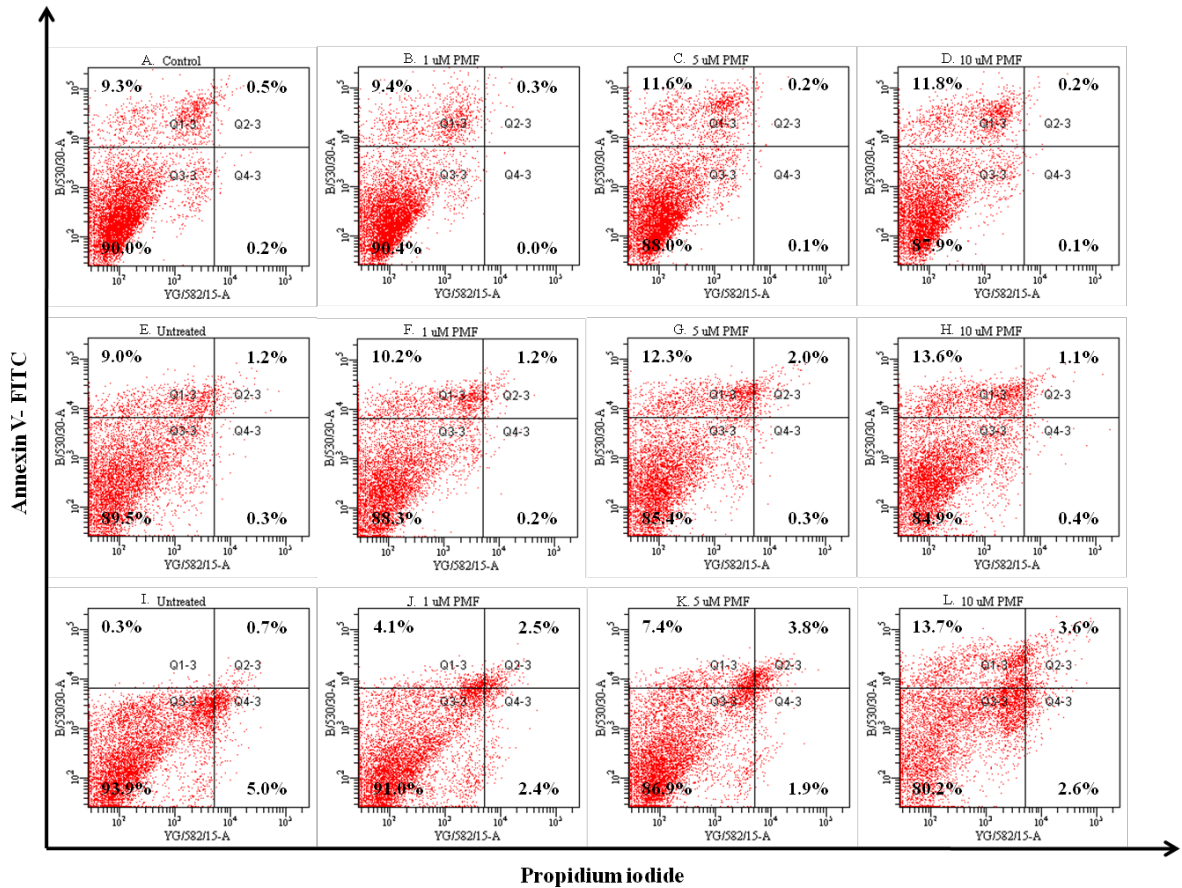


Figure 3.7 Representative fluorescence scattergrams of flow cytometric analysis of APC10.1 cells exposed to up to 10  $\mu$ M PMF for up to 96 h.

APC10.1 cells were exposed to 0 (A,E,I), 1 (B,F,J), 5 (C, G, K), 10 (D, H, L)  $\mu$ M of PMF for 48 (A, B, C, D), 72 (E, F, G, H), and 96 h (I, J, K, L). Cells were stained with Annexin V-FITC and PI as detailed in section 2.2.4.3. Live cells take up neither Annexin V nor PI and appear in the lower left quadrant (Q3-3). Apoptotic cells take up Annexin V and appear in the top left quadrant (Q1-3). Necrotic cells take up both Annexin V and PI and appear in the top right quadrant (Q2-3). Debris appears in the lower right quadrant (Q4-3). A significant shift of cells from live to apoptotic and necrotic was observed. Triplicates were performed and the cell number was calculated based on 10,000 events.

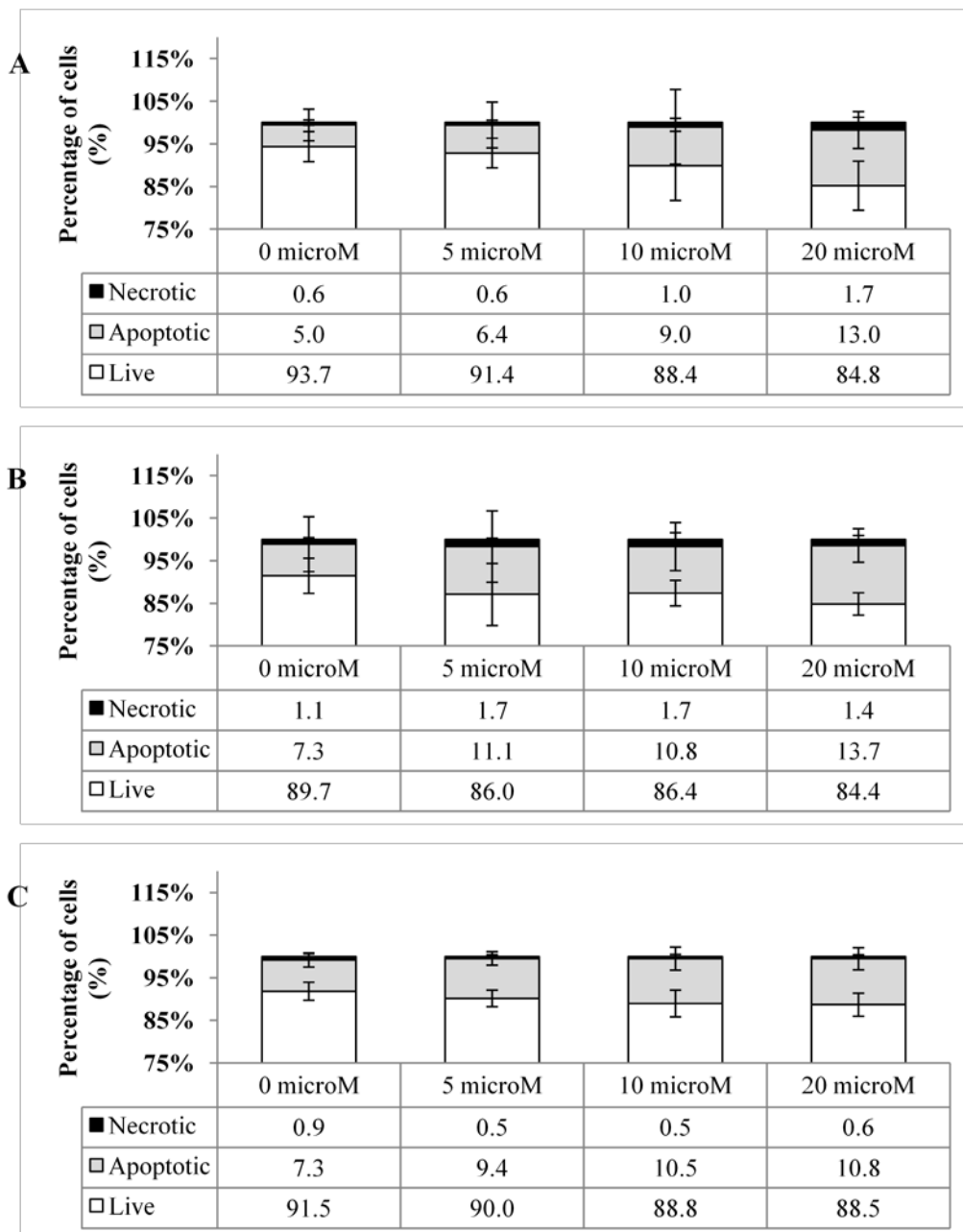


Figure 3.8 Pro-apoptotic effects of apigenin on APC10.1 cells at 48 h (A), 72 h (B) and 96 h (C).

APC10.1 cells were exposed to apigenin at up to 20  $\mu$ M. FACS analysis was performed. Cells were categorised as live (white), apoptotic (grey) and necrotic (black). Debris was omitted from the plots. Results are the mean  $\pm$  SD of triplicate experiments, red asterisks \* denote statistical significance ( $p < 0.05$ ) between apigenin and control.

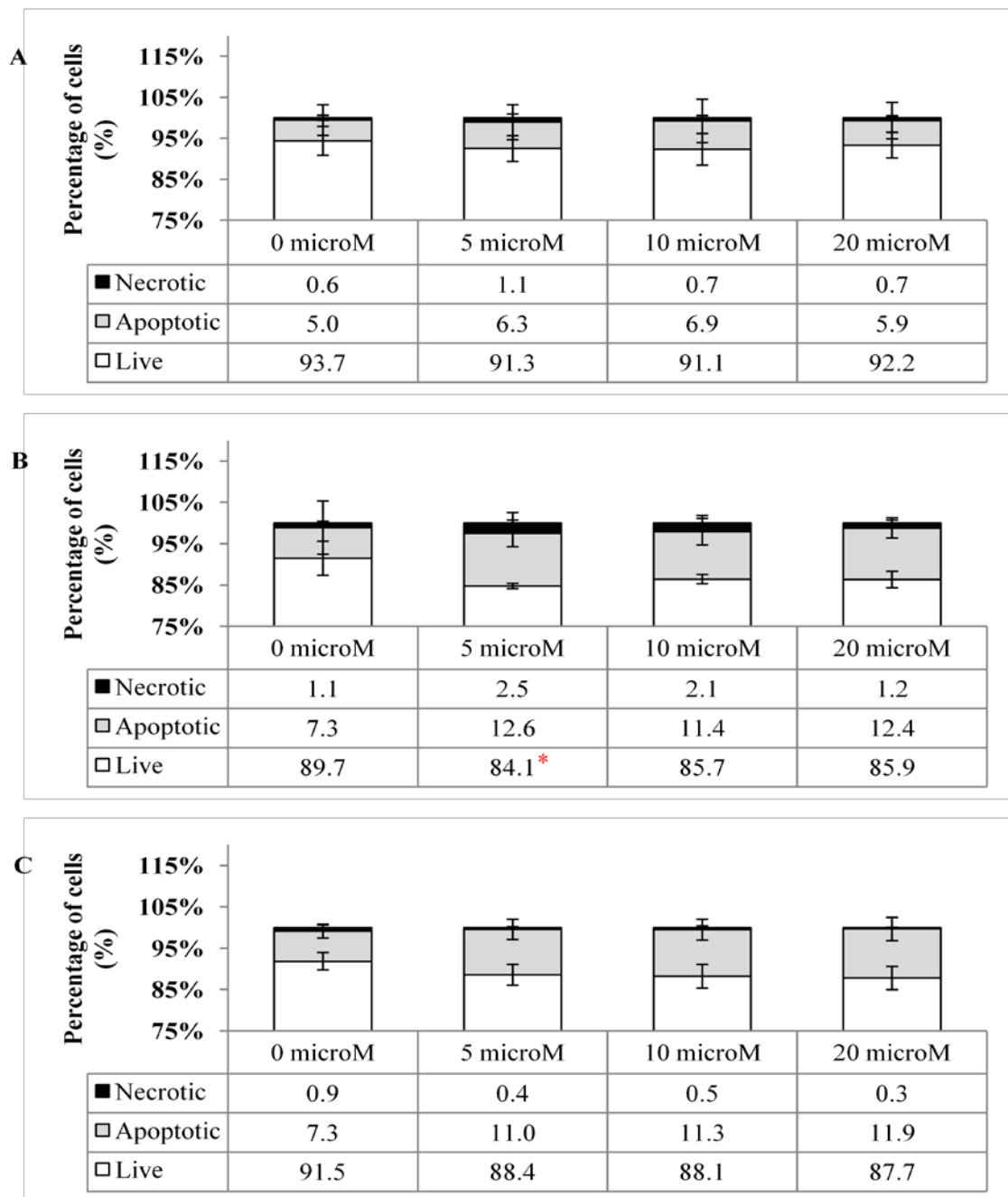


Figure 3.9 Pro-apoptotic effects of triclin on APC10.1 cells at 48 h (A), 72 h (B) and 96 h (C).

Cells were exposed to triclin at up to 20  $\mu$ M. FACS analysis was performed. Cells were categorised as live (white), apoptotic (grey) and necrotic (black). Debris was omitted from the plots. Results are the mean  $\pm$  SD of triplicate experiments, red asterisks \* denote statistical significance ( $p < 0.05$ ) between triclin and control.

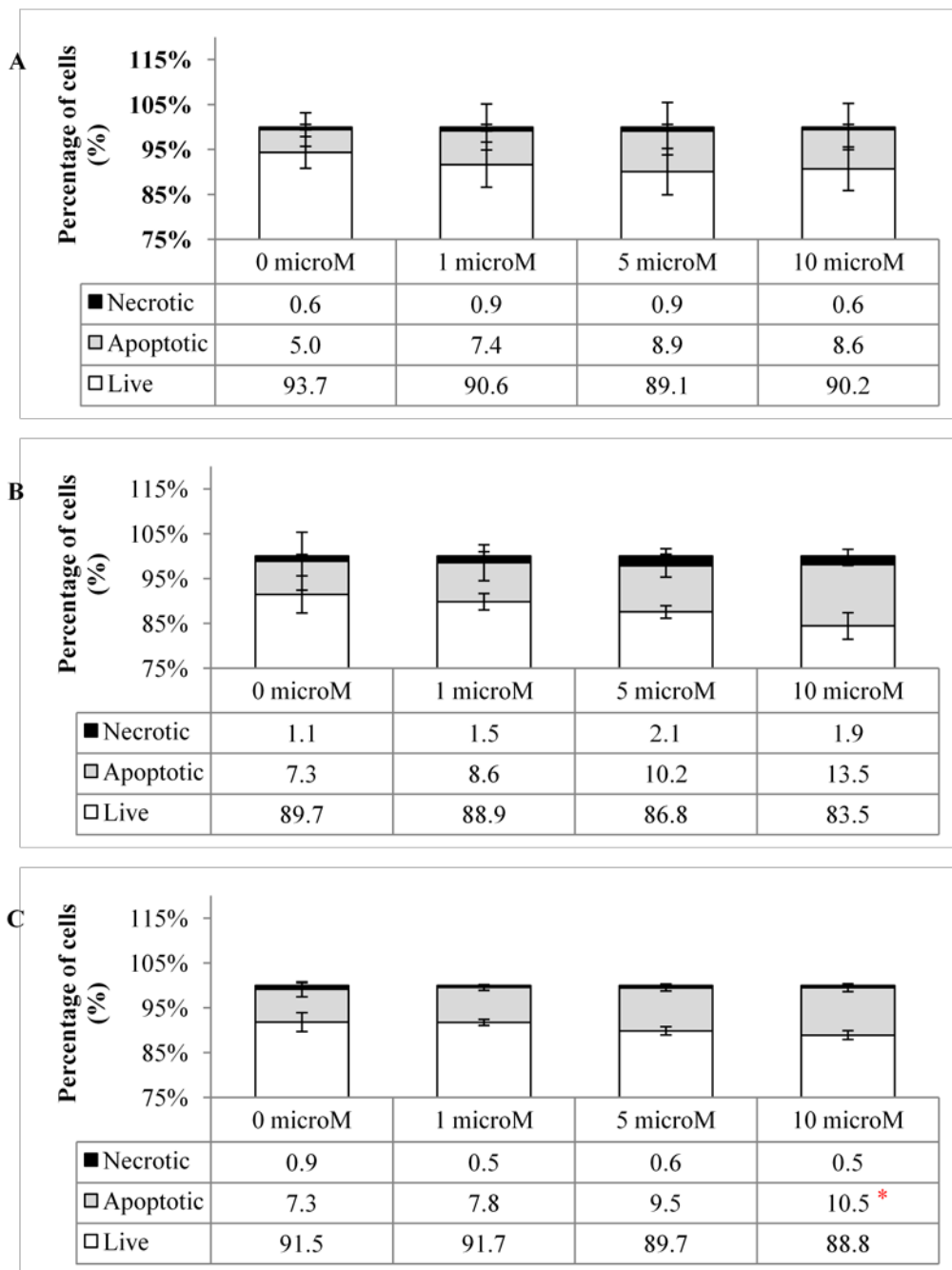


Figure 3.10 Pro-apoptotic effects of PMF on APC10.1 cells at 48 h (A), 72 h (B) and 96 h (C).

Cells were exposed to PMF at up to 10  $\mu$ M. FACS analysis was performed. Cells were categorised as live (white), apoptotic (grey) and necrotic (black). Debris was omitted from the plots. Results are the mean  $\pm$  SD of triplicate experiments, red asterisks \* denote statistical significance ( $p < 0.05$ ) between PMF and control.

### 3.5 Discussion

The results described demonstrate the differential potencies of the flavones in terms of growth inhibition, cell cycle arrest and pro-apoptotic properties. The growth inhibition properties of the flavones were dose-dependent while the effects of the compounds on cell cycle arrest and apoptosis induction were dose-dependent and time-dependent.

The inhibition of cell proliferation, cell cycle arrest and apoptosis induction by apigenin and tricetin has been well-studied. In contrast, little information is available on PMF. In the human colon carcinoma cell lines SW480, HT-29 and Caco-2, apigenin has been demonstrated to inhibit growth and induce G<sub>2</sub>/M arrest (Wang et al., 2000). The IC<sub>50</sub> values of apigenin in these cells at 48 h were 40 µM, 50 µM and 70 µM, respectively. At 48 h at the concentration of 80 µM, apigenin induced maximal G<sub>2</sub>/M arrest in these cells. Apigenin has also been shown to induce apoptosis in human adenocarcinoma SNU-C4 and human breast adenoma MDA-MB-231 cells (Barber et al., 2008). Apigenin has also been shown to be a strong growth inhibitor and inducer of tumour necrosis factor-related apoptosis (TRAIL/APOP2L) in HeLa, LNCap and DU145 cells (Szliszka et al., 2009, Szliszka et al., 2008).

In the study described here, APC10.1 cells were used. The IC<sub>50</sub> values for apigenin were 13.0 ± 2.5 µM on day 3 and 22.3 ± 14.0 µM on day 6. Apigenin has obviously different inhibitory effects on different cell lines. The results also show loss of efficacy with prolonged exposure, hinting at a biphasic property profile, as suggested before with reference to quercetin and apigenin (Dihal et al., 2006, Walle et al., 2007). This may explain the different potencies of apigenin in several studies performed (Wang et al., 2000). Moreover, it is likely that the hydroxy moieties on apigenin facilitate its rapid metabolism and rendering its metabolites less active than the parent compound. On day 3, both PMF and tricetin were superior to

apigenin in their abilities to inhibit growth in these cell lines. Both PMF and tricetin have methoxy groups, whilst apigenin is a phenol, supporting the notion that methoxylated flavones are more potent in inhibiting cell proliferation than their phenolic unmethoxylated analogues.

The cell cycle assay suggests a different mechanism of action for the methoxylated and the hydroxylated analogues. Arrest at G<sub>1</sub> phase of the cell cycle leads to slowing down of growth and induction of cell death, while G<sub>2</sub>/M arrest drives the cells towards apoptosis (DiPaola, 2002). At the early time point of 48 h, apigenin exhibited both G<sub>1</sub> and G<sub>2</sub>/M arrest. At 72 h, apigenin showed mainly cell cycle arrest in the G<sub>1</sub> phase (see section Figure 3.2). This is in contrast to some studies which detected only G<sub>2</sub>/M arrest for apigenin (McVean et al., 2002, Trochon et al., 2000). Tricetin and PMF arrested the cell cycle mainly at G<sub>2</sub>/M after 96-h. This reflects the effects of PMF and tricetin on cell proliferation. As apigenin induced mainly G<sub>1</sub> arrest at later time points, this may explain the loss of efficacy of apigenin on day 6 in inhibiting cell proliferation.

In this study, PMF was efficacious in suppressing proliferation of APC10.1 cells on days 3 and 6. At early time points, PMF caused cell cycle arrest at G<sub>2</sub>/M and induced apoptosis in APC10.1 cells. Tangeretin (5, 6, 7, 8, 4'-pentamethoxyflavone), an isomer of PMF, exerted cellular effects similar to those described here for PMF. Tangeretin was shown to induce growth inhibition, promoting G<sub>2</sub>/M arrest and apoptosis in HL-60 human leukaemic cells (Hirano et al., 1995, Pan et al., 2002). In healthy human peripheral blood mononuclear cells (PBMCs), tangeretin did not exhibit any cytotoxicity.

Overall, PMF was superior to tricetin and apigenin in its effects on the inhibition of cell growth. PMF also exerts significant cell cycle arrest and induction of apoptosis. However, these anti-carcinogenic properties of PMF, particularly its pro-apoptotic effects, may not

explain the pronounced reduction in the number of adenomas observed *in vivo*. Therefore, genetic profiling was utilised to delineate potential mechanisms of action triggered by PMF in APC10.1 cells.

## **4 Investigation into the effects of flavones on gene expression in APC10.1 cells.**

### **4.1 Introduction**

The results described in chapter 3 suggest that PMF has time- and dose-dependent effects on growth, cell cycle and apoptosis *in vitro*. PMF exhibited stronger growth inhibition than tricetin or apigenin in APC10.1 cells. PMF also exerted significant cell cycle arrest and apoptosis induction in comparison with control. These are some of the key characteristics of a chemopreventive agent.

At present, little is known about the mechanisms of action of flavones and of PMF especially (see section 1.5.1.3). In this part of the work, APC10.1 cells were exposed to PMF, tricetin or apigenin (10  $\mu$ M) for 24 h. The cells were harvested, lysed and the RNA was extracted. All the RNA extracts exhibited absorbances between 1.6-1.9 ( $Abs_{260}:Abs_{280}$ ), indicating high purity and the absence of protein. Microarray analysis was performed to obtain information on the mechanisms associated with anti-carcinogenesis. The aim of the work described here was to understand changes in gene expression of adenoma cell caused by PMF in comparison to those elicited by its two congeners.

### **4.2 Number of genes changed by flavones**

In order to obtain an overview of the spread of genes changed by these flavones, principle component analysis was performed (Figure 4.1). When these plots were centralised on the centre-axis, the spread of gene change by each flavone for each replicate was illustrated.

When the majority of the red (control) and blue (treatment) dots are close together at the centre axis, as observed for 'apigenin' treatment, the result suggest apigenin has minimal or no effect on gene expression in comparison with 'control'. When the red and blue dots are distinct groups, as observed for 'tricin' and 'PMF', the results show that these two flavones have significant effects on gene expression change in comparison with control. The further the dots are from the origin of the plot, the greater the gene change is between the control and 'tricin' and 'PMF'.

Owing to the vast volume of data accrued, it was necessary to assign arbitrary cut-off points to generate manageable gene lists. An arbitrary fold change of 1.5 and p-values of 0.05 were used to generate gene lists for comparison. Volcano plots from ArrayTrack depict the changes of individual genes (dot) caused by each flavone in relation to the control group for both A and B gene chip slides (Figure 4.2). Two gene chip slides were used, as there were too many genes to fit onto one slide (see section 2.2.5.9). Comparisons made between the 3 flavones for both gene chip slides show that the greatest number of gene changes occurred with PMF, when both p-value and fold change were considered. PMF also caused changes to the largest number of genes, with significance in terms of p-value (pink dots) and fold change (yellow dots). On both A and B slides, tricin exhibited the least number of non-significant (black dots) gene changes among these three flavones.

Two fold change cut-offs of 1.5 and 1.3 with different permutations of significant p-values 0.05 or 0.01 were tested. In the case of fold change of 1.5 and p-value of less than 0.01, the gene list was too small to perform pathway analysis. Tables 4.1 and 4.2 summarise the permutation of p-value and fold change to generate optimal gene lists.

#### **4.2.1 Gene changes with fold change cut-off of 1.5**

At a p-value<0.05 and a fold change cut-off of 1.5 (Table 4.1, rows 1 and 2), the number of significant gene changes caused by apigenin on slides A and B was 165 and 99, respectively. Of those significant genes on slide A, 73 were up-regulated and 92 were down-regulated. On slide B, 53 were up-regulated and 46 were down-regulated. The number of genes with significant p-values only on slides A and B was 28 and 55, respectively, while the number of genes with significant fold changes only on slides A and B was 1524 and 954, respectively.

At p-value<0.05 and fold change cut-off of 1.5 (Table 4.1, rows 3 and 4), the number of significant genes changed by triclin was higher than that seen with apigenin. On slides A and B, the numbers of genes changed significantly was 211 and 456, respectively. Of the significant genes on slide A, 111 were up-regulated and 100 were down-regulated. On slide B, 171 genes were up-regulated and 285 genes were down-regulated. The number of genes with only significant p-values on slides A and B was 17 and 36, respectively, while the number of genes with significant fold changes only on slides A and B was 1375 and 1171, respectively.

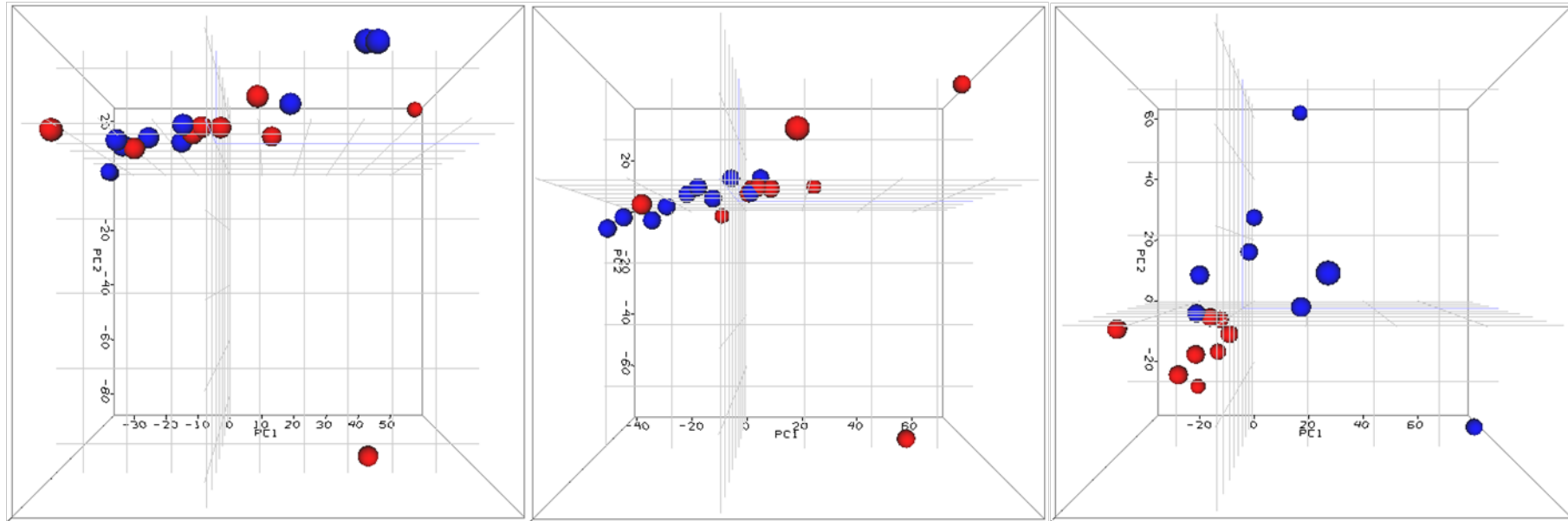


Figure 4.1 Principle component analysis (PCA) of gene change post 24-h incubation of APC10.1 cells with 10  $\mu$ M apigenin (left), tricetin (middle) or PMF (right).

The spread of the red (control) and blue (treatment) dots from the central axis depicts the similarities or differences in gene changes between each replicate of control and treatment groups. Five replicates were performed for apigenin and tricetin while four replicates were performed for PMF.

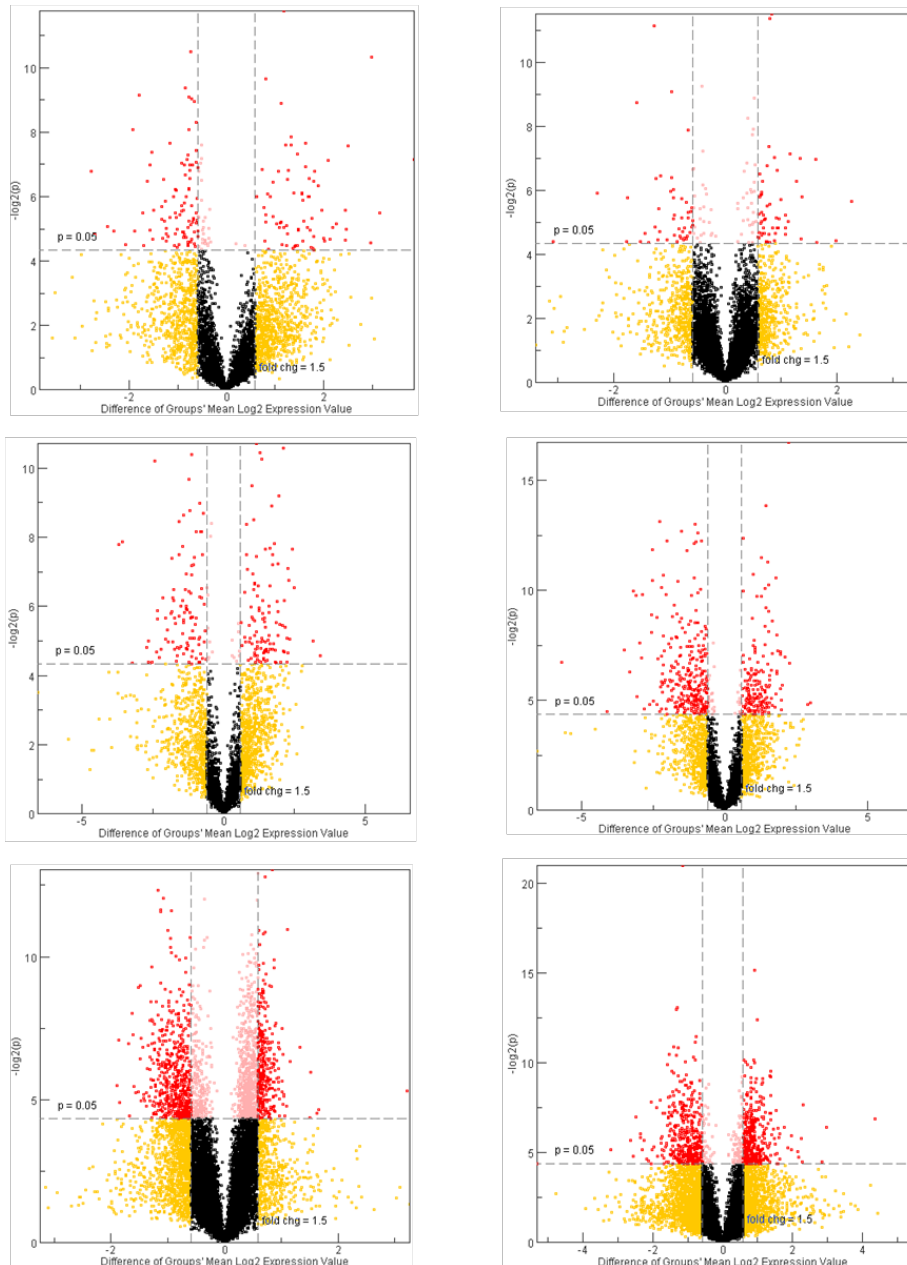


Figure 4.2 Volcano plots illustrating the position of each gene, p-value and cut-off margins for A (left) and B (right) slides for apigenin (top), tricrin (middle) and PMF (bottom).

The different colours mark the significance of each gene on the slide. The slides contained genes from the MEEBO list. The red denotes a significant gene, pink denotes a gene with a significant p-value but not achieving the desired fold change, yellow denotes a gene with a significant fold change and black denote a non-significant gene.

Table 4.1 Number of genes changed by apigenin, tricetin or PMF (10  $\mu$ M) on slides A and B at p-value<0.05 and fold change of 1.5.

The table is divided into 4 categories; genes that were significantly up-regulated or down-regulated in terms of p-value and fold change, genes that were significant in terms of p-value only, genes that were significant in terms of fold change only and genes that were not significant in either p-value or fold change. Five replicates were performed for apigenin and tricetin while four replicates were performed for PMF.

Slide (A/B)	Significant p-value and fold change		Significant p-value	Significant fold change	Non-significant
	up	down			
Apigenin (A)	73	92	28	1524	2678
Apigenin (B)	53	46	55	954	5753
Tricetin (A)	111	100	17	1375	1673
Tricetin (B)	171	285	36	1171	2060
PMF (A)	315	548	892	1765	9735
PMF (B)	373	380	133	2840	5712

When the cells were exposed to PMF, on slide A there was an approximately 5-fold increase in the number of significant genes in comparison to apigenin and a 4-fold increase compared to tricetin. The same trend was observed on slide B with PMF having approximately 7.6-fold more significant gene changes than apigenin and 1.7-fold more than tricetin. With the p-value<0.05 and fold change cut-off of 1.5 (Table 4.1), the numbers of significant gene changes were 863 (~6.5% of total genes on slide A) and 753 (~8.0% of total genes on slide B) on slides A and B, respectively. Of the significant genes on slide A, 315 were up-regulated

and 548 were down-regulated. On slide B, 373 genes were up-regulated and 380 genes were down-regulated. The number of genes with only significant p-value on both slides A and B were 892 and 133, respectively, while the number of genes with significant fold changes only on slides A and B were 1765 and 2840, respectively. Overall, the number of gene changes caused by PMF increased several fold in comparison to apigenin and triclin.

#### **4.2.2 Gene changes with fold change cut-off of 1.3**

A new set of parameters using a p-value<0.05 and a fold change cut-off of 1.3 was determined (Table 4.2). There are several considerations that need to be taken into account when analysing these data. A large sample size of genes would be more likely to generate pathways with a significant p-value than a smaller sample size. The more genes that are located along a particular pathway, the more likely it is that this pathway is integral to the development of a disease. Some genes may be responsible for a significant change in downstream protein expression, even though their fold change may be quite low.

With this new cut-off, the number of significant genes in terms of both p-value and fold change in slides A and B increased by 0.5-0.6% for apigenin, by 0.5-0.8% for triclin and by 1.1-4.8% for PMF. Despite the lowering of the cut-off point, there was little change in the number of significant genes for the apigenin and triclin groups. The most marked increase was observed in the PMF group on the A slide (4.8%). Lowering the fold change was likely to increase the false discovery rate. Therefore, a combination of further analyses was used to eliminate as many false positives as possible.

Table 4.2 Number of gene change by the apigenin, tricetin or PMF on slides A and B at p-value<0.05 and fold change of 1.3.

The table is divided into 4 categories; genes that were significantly up-regulated or down-regulated in terms of p-value and fold, genes that were significant in terms of p-value only, genes that were significant in terms of fold change only and genes that were not significant in either p-value or fold change. Five replicates were performed for apigenin and tricetin while four replicates were performed for PMF.

Slide (A/B)	Significant p-value and fold change		Significant p-value	Significant fold change	Non-significant
	up	down			
Apigenin (A)	74	113	6	2290	1912
Apigenin (B)	77	63	14	2040	4667
Tricetin (A)	116	109	3	1915	1133
Tricetin (B)	183	304	5	1794	1437
PMF (A)	770	724	261	3801	7699
PMF (B)	441	418	27	4535	4017

### 4.2.3 Common gene changes caused by flavones

The lists of genes changed by apigenin, tricetin and PMF were plotted on Venn diagrams to depict their relationship to each other using a p-value<0.05 (Figure 4.3). Overall, PMF significantly modulated the highest number of genes in APC10.1 cells. The results show that the number of gene changes caused by apigenin, tricetin and PMF without taking into account the direction of change were 311, 640 and 2111, respectively (Figure 4.3, I). Regardless of the gene change direction, the results illustrate that apigenin and PMF changed 57 genes in

common, PMF and tricetin changed 120 genes in common while tricetin and apigenin changed 30 genes in common. Of these genes, there were 3 genes common to all three flavones.

In the *Apc<sup>Min/+</sup>* mouse study (see Chapter 2, section 2.2.8), apigenin had no effect on adenoma development while tricetin and PMF reduced the number of adenomas by approximately 30% and 50%, respectively. In the light of these differences, one may tentatively argue that the gene changes common to tricetin and PMF are more likely to be important in contributing to the anti-carcinogenesis pathways triggered by these flavones. The direction of gene change by all three flavones in terms of up-regulation or down-regulation was taken into account for further analysis (Figure 4.3, II). The total number of gene changes in the same direction caused by apigenin, tricetin and PMF was 395, 787 and 2285, respectively. There were 25 genes common to apigenin and PMF, 61 genes common to PMF and tricetin, and 19 genes common to tricetin and apigenin.

At an arbitrary cut-off  $p\text{-value} < 0.05$  taking into account the direction of gene change, the overall numbers of genes changed particularly by PMF were very high. Another arbitrary cut-off  $p\text{-value} < 0.01$  was set. The results obtained are shown in Figure 4.4. The numbers of gene changes were reduced compared to those at a cut-off  $p\text{-value} < 0.05$ . The number of genes was not large enough to generate gene clusters that would highlight significant pathways. Therefore, the gene lists generated by the three flavones using a cut-off  $p\text{-value} < 0.05$  were retained and used. The results obtained for the three flavones are shown in Table 4.3.

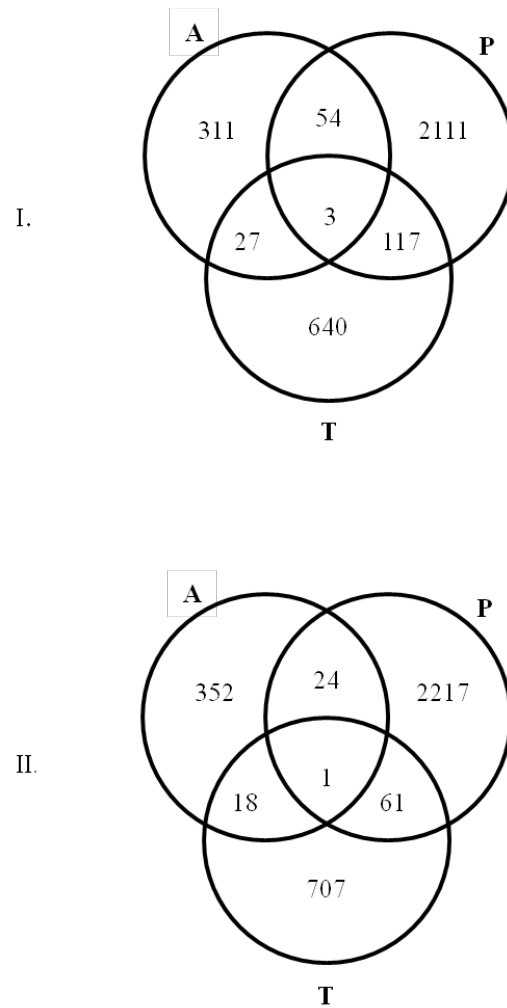


Figure 4.3 Venn diagrams depicting the number of genes altered by apigenin (A), tricetin (T), or PMF (P) in APC10.1 cells using a p-value<0.05.

These cells were exposed to 10  $\mu$ M flavones for 24 h. The direction of gene change (up-regulation or down-regulation) was either omitted (I) or included (II). The significant total genes changed by apigenin were 395 genes (I) and 395 genes (II), by tricetin were 787 genes (I) and 787 genes (II), and by PMF were 2285 genes (I) and 2303 genes (II), respectively.

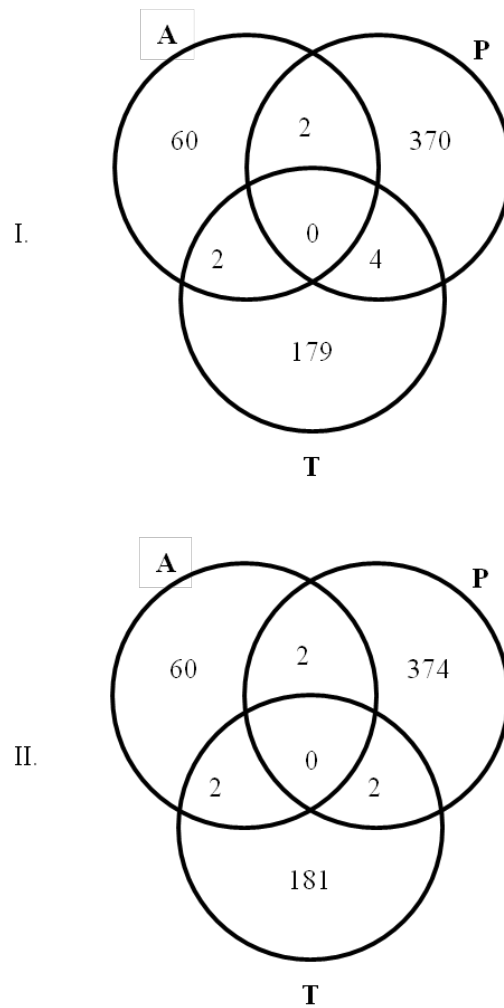


Figure 4.4 Venn diagrams depicting the genes altered by apigenin (A), tricetin (T), or PMF (P) in APC10.1 cells using a p-value<0.01.

These cells were exposed to 10  $\mu$ M flavones for 24 h. The direction of gene change (up-regulation or down-regulation) was either omitted (I) or included (II). The significant total genes changed by apigenin were 64 genes (I) and 64 genes (II), by tricetin were 185 genes (I) and 185 genes (II), and by PMF were 376 genes (I) and 378 genes (II), respectively.

#### 4.2.4 Pathway analyses of genes affected by flavones

Of all the genes in the lists generated, the majority were hypothetical genes or gene fragments (RIKEN genes), and as such were omitted. Some genes were not recognised in the database by the software while the remaining genes were recognised and their functions elucidated. Pathways that had clusters of genes are highlighted. Two software packages, ArrayTrack (Version 3.5) and “webgestalt”, generated similar pathways, thus validating the data. Subsequently, ArrayTrack was selected and used to further analyse the pathways.

From the genes shown in Figure 4.3, II, 352 genes significantly changed ( $p < 0.05$ ) by apigenin were subjected to pathway analyses. A total of 60 genes were recognised and 53 genes were located on pathways. For these 53 genes, 12 pathways were highlighted. Among these pathways, 3 are closely associated with CRC pathways: pentose phosphate, MAPK signalling, and apoptosis. Likewise, for tricetin, a total of 707 genes were subjected to pathway analyses. A total of 72 genes were recognised and 61 genes were located on pathways. There are 20 pathways with gene clusters highlighted for tricetin. Of these pathways, 4 are closely associated with CRC: p53 signalling, cell cycle, Wnt signalling, and MAPK signalling. In the case of PMF, 718 genes out of a total of 2217 genes were subjected to the pathway analyses. Of these 718 genes, 317 genes were located on 88 pathways. Out of these pathways, 7 are closely associated with CRC: T-cell receptor signalling, Hedgehog signalling, Wnt signalling, B-cell receptor signalling, cytokine-cytokine receptor interaction, apoptosis, and Toll-like receptor (TLR) signalling.

The results show that both tricetin and PMF affected genes associated with the Wnt signalling pathway, suggesting that there may be a link to efficacy, as both flavones induced significant adenoma reduction in the *Apc<sup>Min/+</sup>* mouse. The increase in pathways of PMF in comparison with tricetin could be due to the fact that more genes were inserted into the pathway analysis. It

fits the trend observed for cell growth inhibitory potency *in vitro* in APC10.1 cells, PMF>tricin>apigenin.

The list of genes significantly changed by PMF (Figure 4.3, II) was used to highlight different molecular functions, biological processes and cellular components that these genes were responsible for, using an analysis in ArrayTrack called Gene ontology for functional analysis (GOFFA) (Table 4.4).

In terms of molecular function, PMF modulated genes that were responsible for molecular binding, structural molecule activity and transcriptional regulator activity. PMF significantly activated approximately 18% of genes known to modulate structural molecule activity with the likelihood of 2.28-fold higher than under untreated conditions. Structural molecules are proteins which contribute to the integrity of a protein complex, scaffold or which are responsible for the assembly of proteins outside or inside a cell (Pichot et al., 2010). They include mitotic spindle protein, proteins responsible for cell cycle-specific actin rearrangement to protein complexes, membrane transporters, subunits that form ion channels, and protein kinases (Kang et al., 2011). For instance, disruption to the Arp2/3 protein has been associated with disorderly cell cycle-specific actin rearrangement which halts cell motility (Pichot et al., 2010, Winter et al., 1999). Other proteins include mitotic spindle proteins which ensure appropriate separation of chromosomes into two daughter cells during mitosis prior to the subsequent progression of cell cycle. Others are nuclear pore complexes and nucleocytoplasmic transport molecules which enable RNA and ribosomes to move from the nucleus to the cytoplasm while allowing lipids, DNA polymerase, carbohydrates, lamins, or signal molecules to move into the nucleus (Faustino et al., 2010, Jamali et al., 2011). In a recent study, the nuclear pore complex was found to contain a 30 kDa nucleoporin (Nup30) that directly interacts with MAP kinases. This study showed that apigenin inhibits cell

proliferation via MAP kinase pathway by inhibition of phosphomodification of Nup30 (Faustino et al., 2010).

PMF regulated genes responsible for key biological processes including cellular component organisation, cellular developmental and growth. PMF significantly regulated ~ 15% of the genes responsible for growth, with a likelihood of 1.9-fold higher than untreated condition. The results indicate that PMF modulated genes associated with cellular components, namely macromolecular complexes, membrane enclosed lumen (e.g. mitochondria, endoplasmic reticulum), and organelles. On average, PMF affected ~ 10% of the genes associated with cellular components. The effects of PMF on the structural molecular activity, growth and membrane-enclosed lumen, for instance, mitochondria which contain many pro-apoptotic proteins, may directly or indirectly trigger the apoptosis pathway. This activation may result in the retardation and/or reduction of neoplastic growth, adenoma numbers and burden in the intestine of *Apc<sup>Min/+</sup>* mouse model. Therefore, it is possible that the 15% of the genes pertinent to growth changed by PMF are responsible for the effects observed in cells *in vitro* and in mice *in vivo*.

Table 4.3 A summary of pathways delineated from the gene lists changed by apigenin, triclin or PMF (p-value<0.05, with direction of gene change).

The gene list generated from Venn diagrams for each flavone was subjected to ArrayTrack and ‘webgestalt’ analyses. The table shows each flavone with the number of genes entered into the pathway analyses, the number of genes found on pathways and the number of pathways generated. The last column lists the pathways closely associated with CRC.

Flavone	Input gene	Genes found	Genes not found	No. of pathway	Combined results from ArrayTrack ‘webgestalt’
Apigenin	60	53	7	12	<ul style="list-style-type: none"> <li>• Pentose phosphate pathway</li> <li>• MAPK signalling pathway</li> <li>• Apoptosis</li> </ul>
Tricin	72	61	11	20	<ul style="list-style-type: none"> <li>• p53 signalling pathway</li> <li>• Cell cycle</li> <li>• Wnt signalling pathway</li> <li>• MAPK signalling pathway</li> </ul>
PMF	718	317	101	88	<ul style="list-style-type: none"> <li>• T-cell receptor signalling pathway</li> <li>• Hedgehog signalling pathway</li> <li>• Wnt signalling pathway</li> <li>• B-cell receptor signalling pathway</li> <li>• Cytokine-cytokine receptor interaction</li> <li>• Apoptosis</li> <li>• TLR signalling pathway</li> </ul>

Table 4.4 Genes changed exclusively by PMF ( $p < 0.05$ ) with the same direction as tricetin and apigenin.

This table categorises the effects of PMF into three; molecular function, biological function and cellular function components using an analysis of ArrayTrack called GOFFA. The second column shows the number of genes triggered from a total of known genes in that particular function, process or component. P-values and E-values indicate the likelihood that a particular gene is triggered relative to the total genes on the microarray.

<b>Molecular function</b>	<b>Proportion of genes</b>	<b>p-value</b>	<b>E-values</b>
binding	460/5295	0.000	1.47
Structural molecule activity	41/225	0.000	2.28
transcriptional regulator activity	57/556	0.028	1.28
<b>Biological process</b>	<b>Proportion of genes</b>	<b>p-value</b>	<b>E-values</b>
cellular component organisation	97/995	0.019	1.22
Cellular process	479/5550	0.000	1.08
Developmental process	136/1404	0.007	1.21
Establishment of localisation	110/1160	0.027	1.19
Growth	29/191	0.000	1.9
Localisation	126/1330	0.018	1.19
Metabolic process	333/3656	0.000	1.14
Positive regulation of biological process	68/673	0.023	1.26
Reproduction	35/262	0.002	1.67
Reproductive process	34/261	0.003	1.63
<b>Cellular component</b>	<b>Proportion of genes</b>	<b>p-value</b>	<b>E-values</b>
Macromolecular complex	134/1224	0.000	1.37
Membrane-enclosed lumen	38/344	0.025	1.38
Organelle	366/4103	0.001	1.12
Organelle part	130/1317	0.004	1.24

In order to obtain a deeper understanding of the different genes and their corresponding pathways, Gene Ontology (GO) TreePrune analysis was performed on the genes changed by

PMF. As the name suggested, the plot is in the form of a tree, with the highest parent node containing genes that are least specific, while the lowest child node denotes the most specific genes. The results describe the number of genes regulated or deregulated with the corresponding p- and E-values (Table 4.5 - Table 4.7). Each node is a pie-chart that depicts the ratio of the number of genes modulated with the number of genes in the whole set associated with particular molecular functions (Figure 4.5), biological processes (Figure 4.6) or cellular components (Figure 4.7). Hence, this analysis allows results to be further broken down to show the roles of individual genes.

### **4.3 Effects of PMF on molecular functions in APC10.1 cells**

In terms of molecular functions (Table 4.5, denoted by 1), the results indicate that PMF significantly modulated a total of 591 genes with an E-value of 1.07. Of these genes, 460 are responsible for molecular binding, (Table 4.5, denoted by 2) with an E-value of 1.09. This number corresponds to 77.8% (i.e.  $460 \text{ genes} / 591 \text{ genes} \times 100\%$ ) of the pie (Figure 4.5). Among the interesting molecular functions modulated by PMF include rRNA binding, ATP-dependent helicase activity, transferase activities particularly transfer of alkyl or aryl (other than methyl) groups, DNA-directed polymerase activity, protein phosphatase regulator activity, steroid hormone receptor activity, and voltage-gated calcium channel activity. The last-mentioned plays a pertinent role in the up-regulation of gene expression and modulates cell proliferation and apoptosis of colonic cancer (Kang et al., 2004).

Table 4.5 List of molecular functions affected by 10  $\mu$ M PMF after 24 h incubation in APC10.1 cells.

Column 1 contains the assigned gene number to each molecular function affected. Column 2 gives a description of the function while Column 3 gives an indication of the number of genes affected in the associated pathway. Column 4 and 5 give the p-values and E-values.

No.	Function	Number of genes	p-value	E value
1	molecular functions	591	0.000	1.07
2	Binding	460	0.000	1.09
3	Nucleic acid binding	128	0.009	1.21
4	RNA binding	37	0.031	1.37
5	rRNA binding	5	0.007	3.91
6	ATPase activity	16	0.019	1.76
7	ATPase activity, coupled	14	0.014	1.90
8	ATP-dependent helicase activity	7	0.025	2.37
9	Purine NTP-dependent helicase activity	7	0.025	2.37
10	Transferase activity, transferring alkyl or aryl (other than methyl) groups	5	0.032	2.72
11	RNA polymerase activity	5	0.030	2.72
12	DNA-directed polymerase activity	5	0.032	2.72
13	Phosphatase regulator activity	5	0.022	2.98
14	Protein phosphatase regulator activity	5	0.014	3.29
15	Ligand-dependent nuclear receptor activity	8	0.001	3.71
16	Steroid hormone receptor activity	8	0.001	3.71
17	Structural molecule activity	41	0.000	2.28
18	Structural constituent of ribosome	27	0.000	3.34
19	Cation transmembrane transporter activity	27	0.012	1.56
20	Metal ion transmembrane transporter activity	21	0.002	1.98
21	Cation channel activity	16	0.016	1.79
22	Calcium channel activity	7	0.010	2.83
<b>23</b>	<b>Voltage-gated calcium channel activity</b>	<b>5</b>	<b>0.002</b>	<b>5.21</b>
24	Voltage-gated cation channel activity	11	0.003	2.60
25	Cation channel activity	16	0.016	1.79
26	Voltage-gated ion channel activity	13	0.017	1.91
27	Substrate-specific channel activity	20	0.040	1.52
28	Passive transmembrane transporter activity	20	0.042	1.51
29	Channel activity	20	0.042	1.51

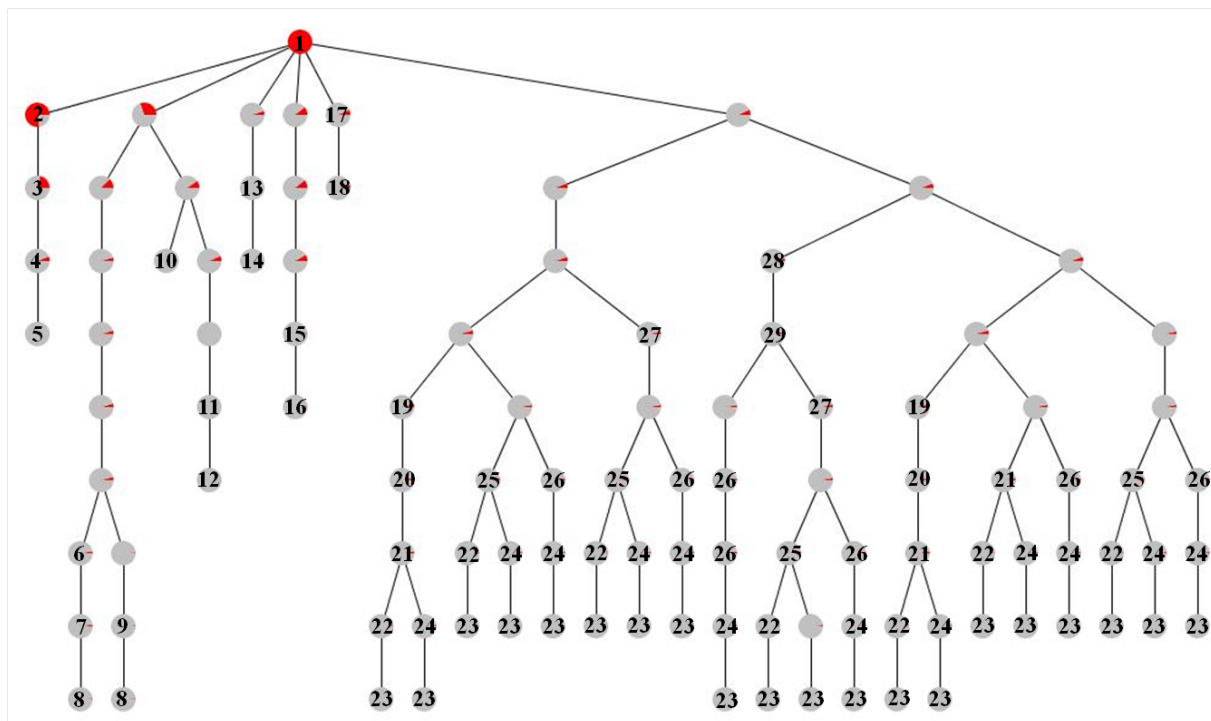


Figure 4.5 Gene Ontology (GO) Tree Prune depicting molecular functions in APC10.1 cells exposed to 10  $\mu$ M PMF after 24-h incubation ( $p < 0.05$ ).

The arbitrary cut-off parameters for this analysis were set at  $p < 0.05$ , Node number  $> 5$  and E-value  $> 2$ . The specific function of each representative node with its corresponding number of genes involved ( $n$ ),  $p$ -value and E-value can be found in Table 4.5. The numbering on each node corresponds to its molecular function on Table 4.5.

#### **4.4 Effects of PMF on biological processes in APC10.1 cells**

The gene list for PMF ( $p\text{-value} < 0.05$ ) was subjected to GOTreePrune to assess the effects of PMF on biological process in APC10.1 cells. The results are shown in Table 4.6. PMF significantly modulated a total of 575 genes responsible for biological processes, with an E-value of 1.13 (Table 4.6, denoted by 1). The child node germane to translation (42 genes,  $p\text{-value} = 0.000$ ,  $E\text{-value} = 2.28$ ) occurred in nearly all the branches of the tree (Figure 4.6). The results suggest that PMF plays a key role in modulating genes responsible for translation processes. Apart from translation, PMF was also implicated in biological processes including regulation of growth, extracellular structure organisation, steroid metabolic process and multi-cellular organism growth.

Table 4.6 Biological processes associated with genes affected by 10  $\mu$ M PMF after 24 h incubation with APC10.1 cells.

Column 1 contains the number assigned to each biological processes affected. Column 2 gives a description of the function while Column 3 gives an indication of the number of genes affected in the associated pathway. Columns 4 and 5 give the p-value and E-value of the associated pathway modulated by the related genes, respectively.

No.	Function	Number of genes	p-value	E value
1	Biological process	575	0.000	1.13
2	Regulation of growth	20	0.000	2.27
3	Cellular component organisation	97	0.019	1.22
4	Extracellular structure organisation	14	0.004	2.19
5	Cellular process	479	0.001	1.08
6	Cellular metabolic process	300	0.000	1.19
7	Cellular biosynthetic process	190	0.000	1.31
8	Cellular macromolecule biosynthetic process	155	0.000	1.32
<b>9</b>	<b>Translation</b>	<b>42</b>	<b>0.000</b>	<b>2.28</b>
10	Steroid metabolic process	14	0.006	2.09
11	Cellular macromolecule metabolic process	246	0.000	1.21
12	Cellular macromolecule biosynthetic process	155	0.000	1.32
13	Cellular protein metabolic process	116	0.004	1.26
14	Growth	29	0.000	1.90
15	Multi-cellular organism growth	13	0.000	2.27
16	Metabolic process	333	0.000	1.14
17	Biosynthetic process	193	0.000	1.31
18	Macromolecule biosynthetic process	156	0.000	1.32
19	Macromolecule metabolic process	263	0.000	1.18
20	Gene expression	163	0.000	1.28
21	Primary metabolic process	301	0.000	1.17
22	Protein metabolic process	132	0.007	1.21

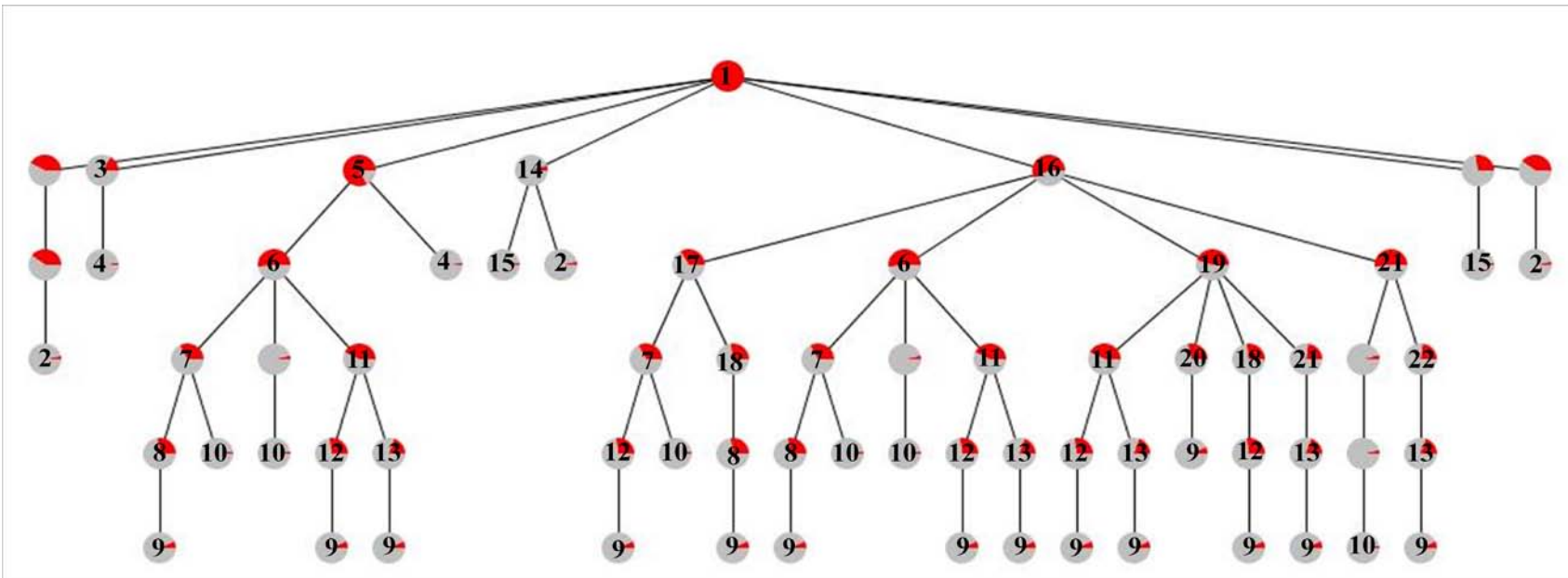


Figure 4.6 Gene Ontology (GO) Tree Prune depicting biological processes in APC10.1 cells exposed to 10  $\mu$ M PMF after 24-h incubation ( $p < 0.05$ ).

The arbitrary cut-off parameters for this analysis were set at  $p < 0.01$ , Node number  $> 12$  and E value  $> 2$ . The specific function of each representative node with its corresponding number of genes involved (n),  $p < \text{value}$  and E-value can be found in Table 4.6. The numbering on each node corresponds to its biological process in Table 4.6.

#### 4.5 Effects of PMF on cellular components in APC10.1 cell line.

When APC10.1 cells were treated with PMF, PMF significantly modulated 603 genes responsible for cellular components (Table 4.7). When GOTreePrune analysis was performed, there was only one common child node, ribosome. This suggests that PMF is capable of modulating translation by exerting its effects on the ribosome component of a cell. This could be a generalised stress response in the cell, leading to the down-regulation of translation, as protein synthesis is a very energy-consuming process (Bolster et al., 2002).

Table 4.7 List of cellular components affected by 10  $\mu$ M PMF after 24h incubation in APC10.1 cells.

Column 1 contains the number assigned to each cellular component affected. Column 2 gives a description of the function while Column 3 gives an indication of the number of genes affected in the associated pathway.

No.	Function	Number of genes	p-value	E value
1	Cellular component	603	0.000	1.05
2	Intracellular	435	0.000	1.10
3	Intracellular part	427	0.000	1.11
4	Cytoplasm	309	0.000	1.19
5	Cytoplasmic part	190	0.000	1.25
6	Ribosome	31	0.000	3.21
7	Intracellular organelle	366	0.000	1.12
8	Intracellular non-membrane-bounded organelle	105	0.000	1.45
9	Ribonucleoprotein complex	45	0.000	2.14
10	Macromolecular complex	134	0.000	1.37
11	Organelle	366	0.001	1.12



#### **4.6 Overall effects of PMF on APC10.1 cells**

From the lists of gene changes generated by GOFFA, PMF significantly regulated molecular function, biological process and cellular components (Table 4.5 - Table 4.7). Several pathways closely associated with the development of CRC were further assessed. These include STATs, cell cycle, apoptosis, Wnt and PI3K/Akt/GSK3 $\beta$  signalling pathways. The data analysis in Table 4.6 shows PMF significantly modulated 575 genes responsible for biological process, particularly transcription, cell cycle and regulation of growth. The results in Table 4.7 show PMF significantly modulated translation by exerting its effects on the intracellular organelles such as the ribosomal component and macromolecular complex of a cell. The Wnt signalling pathway was highlighted by genes common to triclin and PMF, while the PI3K/Akt/GSK3 $\beta$  signalling pathway was selected as it involves one of the key genes of interest, GSK3 $\beta$ .

A further analysis was performed using the Kyoto Encyclopaedia of Genes and Genomes (KEGG). The aim was to obtain information on individual genes that may be of interest or play some role along the pathway of interest. The results show that PMF up- or down-regulated several key genes and their corresponding pathways (Table 4.8). Two main pathways were targeted by PMF: metabolism and regulation of pathways. In the metabolism pathway, 3 branches were highlighted, carbohydrate metabolism, glycan biosynthesis and metabolism, and lipid metabolism. In the regulatory pathway, many branches were highlighted including Hedgehog signalling, Wnt signalling, apoptosis, Toll-like signalling pathway, cell cycle and CRC.

Table 4.8 Pathways generated by gene lists for PMF (p<0.05).

The left column describes different categories of pathways. The second column describes the more specific pathways/maps. The third and fourth columns list the genes found in a specific pathway with its corresponding expression level and its p-value.

Category	Map title	Gene name	Level	
Carbohydrate Metabolism/ Metabolic pathway	Pentose phosphate pathway	Pfkm	↑	
Glycan Biosynthesis and Metabolism/ Metabolic pathway	Chondroitin sulfate biosynthesis	Chst3	↑	
		Xylt2	↓	
Lipid Metabolism/ Metabolic pathway	Biosynthesis of steroids	Mvk	↓	
		Tm7sf2	↓	
Regulatory pathway	<b>Ribosome</b>	<b>Rpl13a</b>	↑	
		<b>Rpl15</b>	↑	
		<b>Rpl18a</b>	↑	
		<b>Rpl26</b>	↑	
		<b>Rpl27a</b>	↑	
		<b>Rpl36</b>	↑	
		<b>Rpl9</b>	↑	
		<b>Rplp1</b>	↑	
		<b>Rps9</b>	↑	
		<b>Uba52</b>	↑	
	Polyunsaturated fatty acid biosynthesis	Elovl2	↓	
		Elovl5	↑	
	Adipocytokine signalling pathway	Ppara	↓	
		Rela	↑	
		Rxb	↑	
		Slc2a4	↑	
	RNA polymerase	Polr2a	↓	
		Polr2e	↑	
	T cell receptor signalling pathway	Cd3d	↓	
		Il2	↑	
		Nfatc2	↑	
		Vav3	↑	
	<b>Hedgehog signalling pathway</b>	<b>Ptch1</b>	↑	
		<b>Wnt8b</b>	↓	
	Regulatory pathway	Basal cell carcinoma	Ptch1	↑
		PPAR signalling pathway	Ppara	↓

Category	Map title	Gene name	Level
Regulatory pathway		Rxrb	↑
	p53 signalling pathway	Wnt8b	↓
		Rrm2	↓
		Trp73	↓
	<b>Wnt signalling pathway</b>	<b>Frat1</b>	↓
		<b>Lrp5</b>	↓
		<b>Nfatc2</b>	↑
		<b>Wnt8b</b>	↓
	Basal transcription factors	Tbp	↓
	Cytokine-cytokine receptor interaction	Cxcl13	↓
		Il15	↓
		Il2	↑
		Il2rg	↑
		Tnfrsf10b	↓
		Xcr1	↓
	<b>Apoptosis</b>	<b>Rela</b>	↑
		<b>Tnfrsf10b</b>	↓
	Natural killer cell mediated cytotoxicity	Nfatc2	↑
		Tnfrsf10b	↓
		Vav3	↑
	Ubiquitin mediated proteolysis	Birc6	↑
		Cdc34	↑
		Herc1	↑
	<b>TLR signalling pathway</b>	<b>Rela</b>	↑
		<b>Tollip</b>	↓
	Jak-STAT signalling pathway	Il15	↓
		Il2	↑
		Il2rg	↑
	MAPK signalling pathway	Cacna1g	↑
		Fgf13	↓
		Map2k5	↑
		Nfatc2	↑
	<b>Cell cycle</b>	<b>Cdc6</b>	↑
		<b>Ywhaz</b>	↑
	DNA polymerase	Pold1	↓
	<b>CRC</b>	<b>Msh3</b>	↓
	Fc epsilon RI signalling pathway	Vav3	↑

Category	Map title	Gene name	Level
	Hematopoietic cell lineage	Cd3d	↓
	mTOR signalling pathway	Eif4b	↓
	VEGF signalling pathway	Nfatc2	↑
		Input genes	418
		Genes not found	317
		Genes found	99
		Pathway	88

The effects of the three flavones were subsequently compared within these specific pathways. The genes obtained from this analysis may provide a starting point to assess the mechanisms of action of these flavones. Heat maps were generated. These maps allow an overview of individual genes changed by apigenin, tricetin and PMF. The heat map plot of the stated genes, as well as those genes mined due to their close proximity and relatedness to the stated genes, were constructed. The list of genes closely associated with CRC includes genes associated with the Wnt signalling pathway (Figure 4.8, A), TLR signalling pathway (Figure 4.8, B), STATs signalling pathway (Figure 4.8, C), Hedgehog signalling pathway (Figure 4.9, A), apoptosis (Figure 4.9, B) and cell cycle signalling pathway (Figure 4.9, C).

In the Wnt signalling pathway (Figure 4.8, A), the heat map shows that *GSK3 $\beta$*  was up-regulated, and that *Frat1* and *Wnt8b* were down-regulated by PMF. *Lrp5* and *TCF4* were down-regulated more by PMF and tricetin than by apigenin. Gene changes in *Dvl3*, *Lrp5*, *Nfatc2* and *Tbllx* were inconclusive, while *Bcl9l* and *Wnt3a* were found to be down-regulated by PMF and apigenin.

In the TLR signalling pathway (Figure 4.8, B), *Rela* was up-regulated by PMF while a change in the *Tollip* gene shows a slight up-regulation by tricetin and apigenin in comparison to PMF.

In the STATs signalling pathway (Figure 4.8, C), the gene changes of *Stat1*, *Stat3*, *Stat4* and *Stat6* were inconclusive, while *Stat2* remained unchanged by all three flavones. *Stat5b* showed a slight down-regulation by PMF, while *Stat5a* was down-regulated by PMF and apigenin.

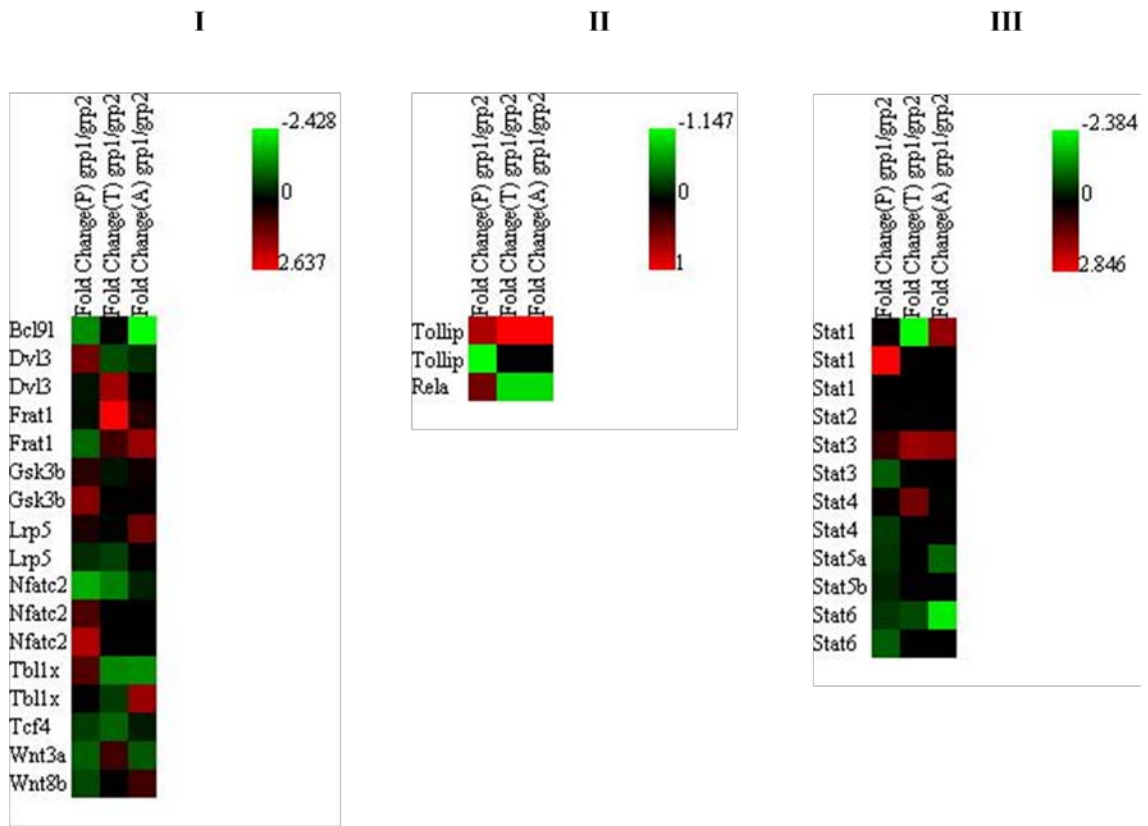


Figure 4.8 Heat map analysis of genes involved in Wnt, TLR and STATs signalling pathways, modulated by apigenin (A), triclin (T) and PMF (P) relative to control.

Fold change was measured by the ratio of grp1:grp2, where grp denotes group, grp1 is the treatment (P, T, or A) group and grp2 is the control group. These genes were closely associated with Wnt signalling pathway (I), TLR signalling pathway (II) and STATs signalling pathway (III).

In the Hedgehog signalling pathway (Figure 4.9, A), the change in the *Ptch1* gene was inconclusive. *Wnt8b* was down-regulated by PMF, remained unchanged by tricetin and up-regulated by apigenin. Heparan sulfate glucosamine 3-O-sulfotransferase 1(Hs3st1) was up-regulated by PMF, remained unchanged by tricetin and down-regulated by apigenin.

In the apoptosis induction pathway (Figure 4.9, B), *Akt1* and *caspase 3* were up-regulated by PMF while *Bax* was down-regulated. Gene changes in *Vav3* and *Tnfrsf10b* were inconclusive. *Rela* remained unchanged by PMF, while it was down-regulated by tricetin and apigenin. The findings of down-regulation of Bax, a pro-apoptotic protein and the up-regulation of caspase-3 by PMF were interesting. When APC10.1 cells were exposed to PMF, significant growth inhibition and apoptosis were observed. However, the degree of apoptosis *in vitro* probably does not solely explain the marked reduction in adenoma numbers, suggesting that there may be pathways other than apoptosis involved.

When APC10.1 cells were exposed to PMF, a pronounced G<sub>2</sub>/M cell cycle arrest was detected, indicative of a reduction in transcription. The down-regulation of a key component of cell transcription, MCM7 by PMF was detected (Figure 4.9, C).

When APC10.1 cells were exposed to PMF, many genes closely associated with cell cycle were modulated, as shown in Figure 4.10. *Cyclin (Ccn) B3* was down-regulated, while *cyclin A2* was up-regulated. The gene regulation of *cyclins B1, D1, D3, G1, I* and *T1* were inconclusive. *Cyclins F* and *H* were down-regulated by PMF and apigenin. *Cyclins E1* and *T2* were down-regulated by PMF, tricetin and apigenin. There is a hint of down-regulation of *cyclin D2* though the result is inconclusive. *Cyclin L1* was down-regulated by both PMF and tricetin. *Cyclins B2, C, and J* remained unchanged by PMF.

PMF was found to down-regulate the gene expression of *cyclin-dependent kinase (Cdk)* 8, up-regulate the gene expressions of *Cdks* 5 and 9, while changes in expressions of *Cdks* 2, 4, 6, 7 and 10 are inconclusive. Concurrently, PMF was found to down-regulate *cyclin-dependent kinase inhibitor (Cdkn)* 1c, 2a\_p16\_Ink4a\_136, 2d while it up-regulated the gene expressions of *phosphorylated 2b (2b\_P)*, 2c\_P and 2d\_P. There were hints of down-regulation of *Cdkn 1b* by PMF, tricetin and apigenin and down-regulation of *Cdkn 2a* by PMF and apigenin while the changes in expressions of *Cdkn 1a* were inconclusive.

PMF also modulated cell division cycle (Cdc) genes in APC10.1 cells. PMF caused down-regulation of *Cdcs* 14a, 16, 20, 23, 27 and 37 while PMF and apigenin caused the down-regulation of *Cdcs* 2a and 40. The results remained inconclusive for *Cdcs* 6, 7, 14b, 25c, 34 and 42 while *Cdcs* 25a, 25b, and 26 gene expression remained unchanged by PMF.

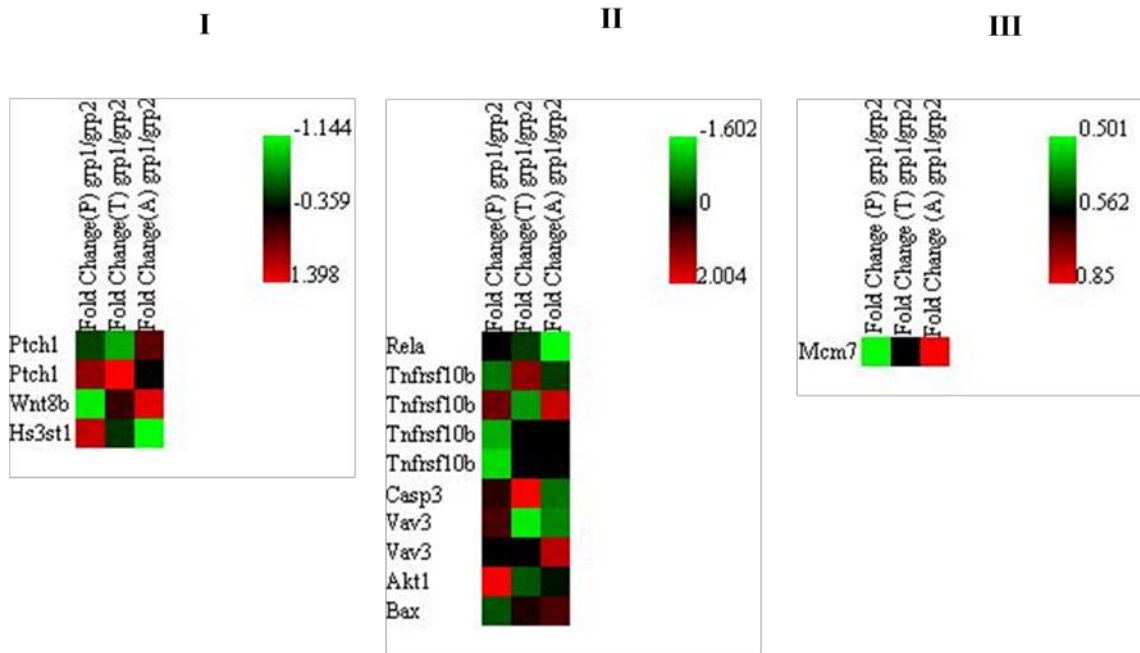


Figure 4.9 Heat map analysis of genes involved in Hedgehog signalling pathway, apoptosis and initiation of transcription, modulated by apigenin (A), tricicn (T) and PMF (P) relative to control.

Fold change was measured by the ratio of grp1:grp2, where grp denotes group, grp1 is the treatment (P, T, or A) group and grp2 is the control group. These genes were closely associated with Hedgehog signalling pathway (I), apoptosis (II) and initiation of transcription (III).



The list of significant genes (see Figure 4.3, Table 4.1) generated for these three flavones was also analysed using 'Expression Analysis Systematic Explorer and Database for Annotation, Visualisation and Integrated Discovery' (EASE/DAVID version 6.7). Interestingly, the analysis came up with only pathways for apigenin (Figure 4.11) and PMF (Figure 4.12). In the case of tricetin, there were many genes up-regulated but without the specificity observed for apigenin or PMF. In this analysis, apigenin triggered the insulin signalling pathway, and the p38 MAPK pathway, which is responsible for glucose metabolism and cell differentiation (Figure 4.11). PMF triggered several other pathways including the Hedgehog signalling pathway and the protein kinase A-related pathway (Figure 4.12). The sub-branches of these pathways include Wnt signalling, tumour growth factor signalling, and Hedgehog regulation of PCG1 $\alpha$ . The latter pathway in turn triggers fatty acid oxidation, mitochondrial metabolism and modulates glucose uptake of the cell. PMF was also shown to play an important role in translation of mRNA to protein by acting on ribosomal RNA. PMF also acted on histone deacetylases in fatty acid oxidation. Three of these pathways of interest are highlighted: Wnt signalling, apoptosis, and cell cycle. Genes from these pathways that are highlighted as well as those that are upstream or downstream from them are grouped in Table 4.9.

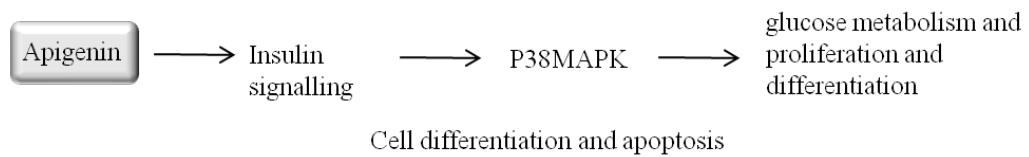


Figure 4.11 Effects of apigenin on biochemical pathways based on gene list from the microarray analysis (p-value<0.05) using DAVID/ EASE.

Another biochemical pathway analysis based on the gene list generated with cut-off p-value<0.05 was performed using DAVID/ EASE. Apigenin was shown to modulate the insulin signaling pathway, particularly the p38 MAPK signaling pathway which is responsible for glucose metabolism, cell proliferation and differentiation.

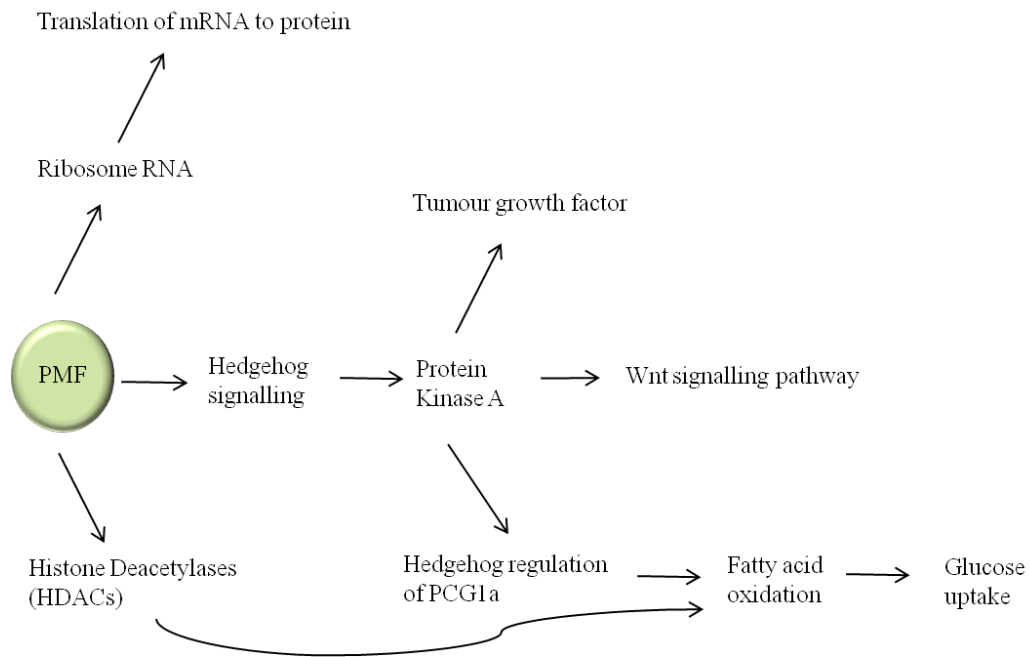


Figure 4.12 The different biochemical pathways modulated by PMF based on the microarray analysis (p-value<0.05) using DAVID/ EASE.

Another biochemical pathway analysis based on the gene list generated with cut-off p-value<0.05 was performed using DAVID/ EASE. PMF was shown to modulate several pathways associated with the translation of mRNA to protein, Wnt signaling via the Hedgehog signaling pathway, and glucose uptake via the activities of histone deacetylases and Hedgehog signaling pathway.

Table 4.9 Summary of different mechanisms of action triggered by 10  $\mu$ M PMF treatment in APC10.1 cells (p-value<0.05).

Overall, four different pathways closely associated with CRC are highlighted and selected for by the gene changes; Wnt signalling, Hedgehog signalling, TLR signalling and apoptosis. The summary is tabulated into three columns, gene name, signalling pathway of interest and either down-regulation (↓) or up-regulation (↑) of genes of interest.

No.	Gene Name	Pathway	Level
1	Bcl9l	Wnt signalling pathway	↓
2	Dact2	Wnt signalling pathway	↓
3	Dvl3	Wnt signalling pathway	↓
4	Frat1	Wnt signalling pathway	↓
5	GSK3b	Wnt signalling pathway	↑
6	Lrp5	Wnt signalling pathway	↓
7	Nfatc2	Wnt signalling pathway	↑
8	TCF4	Wnt signalling pathway	↓
9	Wnt3a	Wnt signalling pathway	↓
10	Wnt8b	Wnt signalling pathway/Hedgehog signalling pathway	↓
11	Ptch1	Hedgehog signalling pathway	↑
12	Rela	Apoptosis	↑
13	Tnfrsf10b	Apoptosis	↓
14	Vav3	Apoptosis	↑
15	Tollip	TLR signalling pathway	↓

#### 4.7 Validation of gene changes using reverse transcriptase-PCR (RT-PCR)

The forward and reverse primers for the shortlisted fifteen genes significantly changed by PMF (see Chapter 2, section 2.2.6, Table 2.3) were designed and commercially obtained. The results obtained by RT-PCR analysis were plotted as genes involved in the Wnt signalling pathway (Figure 4.13) and genes associated with the Hedgehog signalling pathway, TLR signalling pathway, apoptosis pathway and cell transformation (Figure 4.14).

Only six out of fifteen genes of interest were found to exhibit the same gene expression trend (Table 4.9) as observed in the RT-PCR analysis (Figure 4.13-Figure 4.14). In both, mRNA microarray analysis and RT-PCR gene analysis of genes, *Frat1* and *Tollip* were shown to be down-regulated, while *GSK3 $\beta$* , *Nfatc2*, *Ptch1* and *Vav3* were up-regulated by PMF relative to the house-keeping gene  *$\beta$ -actin*. Other genes of interest (*Bcl9l*, *Dact2*, *Dvl3*, *Lrp5*, *TCF4*, *Wnt3a*, *Wnt8b*, *Rela*, *Tnfrsf10b*) were shown to demonstrate the opposite trend as shown in the mRNA microarray analysis.

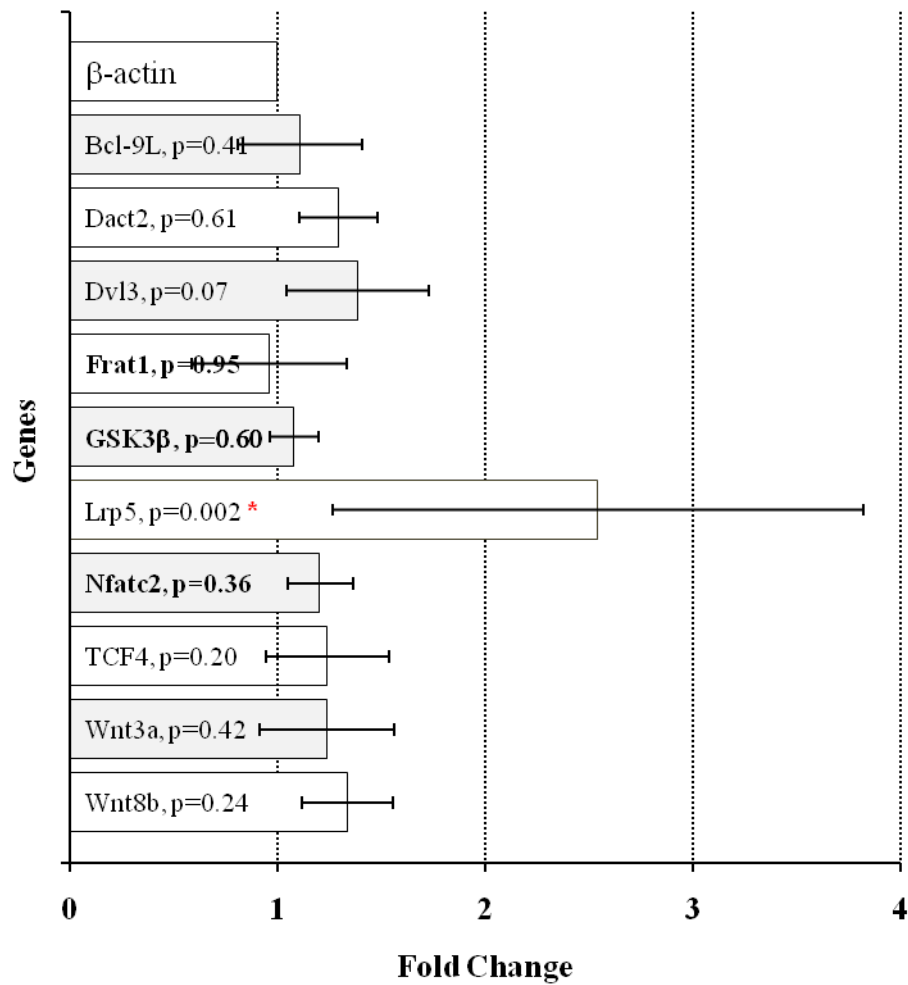


Figure 4.13 Effects of PMF on genes associated with Wnt signalling pathway in APC10.1 cells.

The plot showed the fold change modulated by PMF (10  $\mu$ M, 24 h) based on RT-PCR (mean  $\pm$  SD). Bold font denotes the result of RT-PCR showing the same trend as mRNA result for a protein.  $\beta$ -actin was the house-keeping gene used. The gene expression level of all the other genes was calculated relative to  $\beta$ -actin expression (mean  $\pm$  SD). Asterisk (\*) denotes significant fold change of a protein.

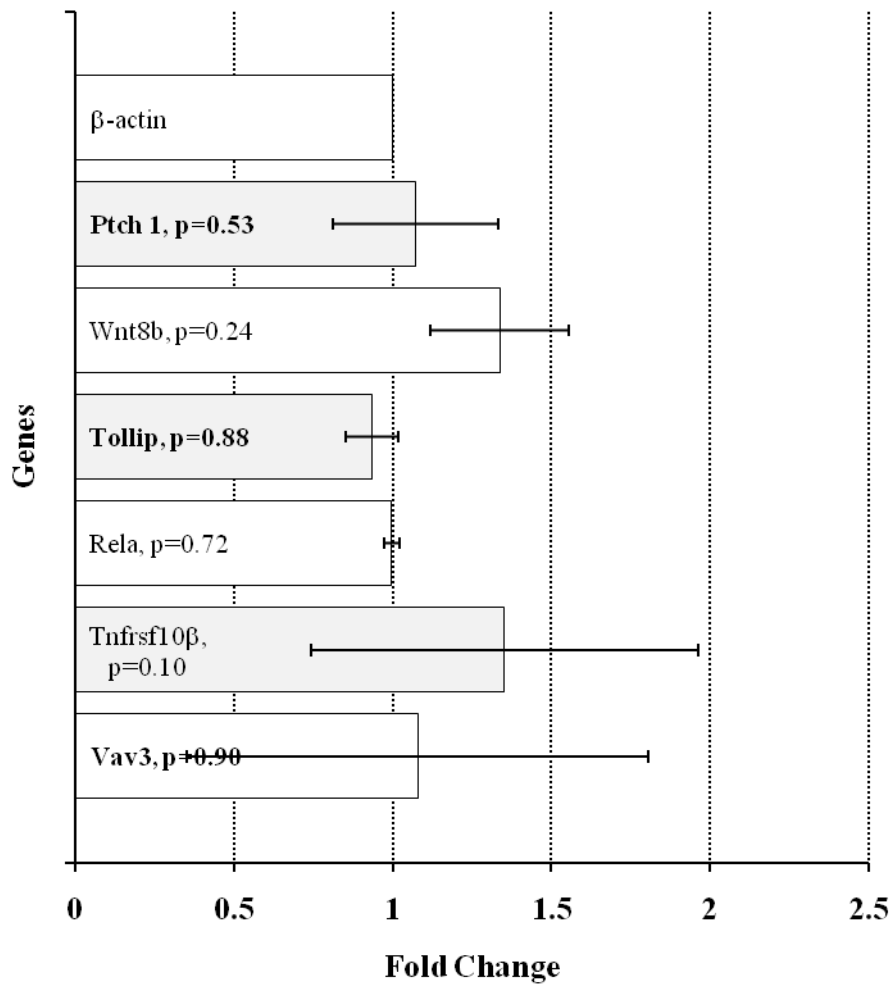


Figure 4.14 Effects of PMF on genes closely associated with Hedgehog signalling pathway (Ptch1, Wnt8b), TLR pathway (Tollip, Rela), apoptosis pathway (Rela, Tnfrsf10b) and cell transformation (Vav3).

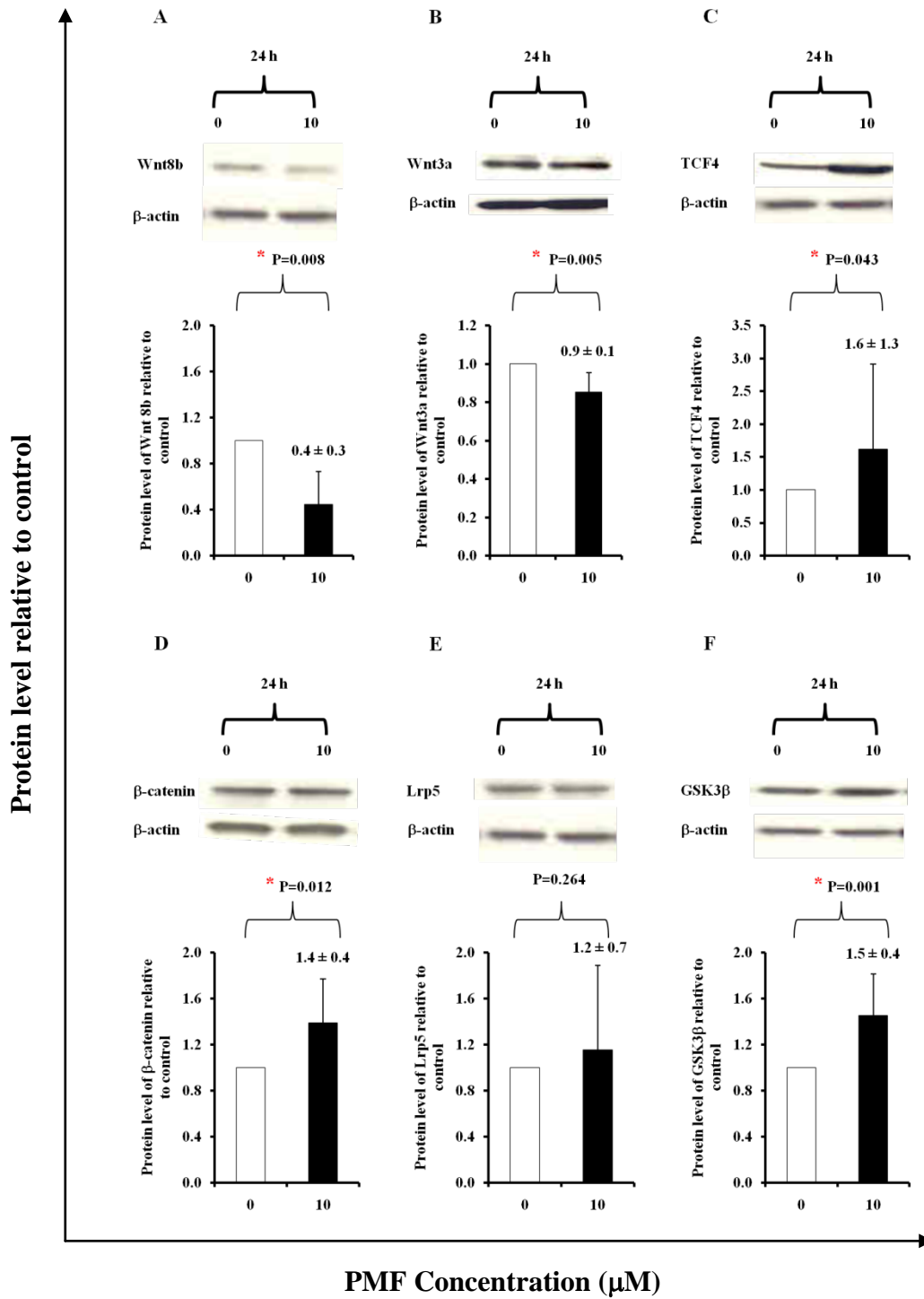
The plot showed the fold change modulated by PMF (10  $\mu$ M, 24 h) based on RT-PCR (mean  $\pm$  SD). Bold font denotes the result of RT-PCR showing the same trend as mRNA result for a protein.  $\beta$ -actin was the house-keeping gene used. The gene expression level of all the other genes was calculated relative to  $\beta$ -actin expression (mean  $\pm$  SD). Asterisk (\*) denotes significant fold change of a protein.

#### 4.8 Gene validation using WB

The genes affected by PMF were also validated independently by Western blotting assessment of proteins encoded by them. Cells were treated with PMF, harvested, lysed and proteins were analysed. In comparison to RT-PCR, WB allows screening of proteins encoded by the genes of interest as well as proteins that are closely associated with the pathways of interest. The 15 genes selected on the basis of the PCR results were used as starting points to study the different pathways of interests. A total of 40 antibodies to proteins related to these pathways were used to assess the effects of PMF on APC10.1 cells.

PMF significantly decreased protein levels of Wnt8b and Wnt3a, while increasing protein levels of TCF4,  $\beta$ -catenin and GSK3 $\beta$  (Figure 4.15), suggesting that PMF is capable of exerting significant effects on the Wnt signalling pathway. It is interesting to note that PMF significantly decreased the protein levels of MCM7 and pSTAT3 (Figure 4.17). These two proteins are pertinent to the initiation of transcription. One may argue that this may cause the observed reduction in cell proliferation *in vitro* and reduction in adenoma number and burden *in vivo*. The survivin levels in APC10.1 cells exposed to PMF were lower than in control cells (Figure 4.18), consistent with the effects of PMF on cell apoptosis (see in chapter 3). There were no significant changes elicited by PMF to levels of proteins closely linked to the regulation of cell cycle (Figure 4.16).

#### 4.8.1 Proteins in Wnt signalling pathway modulated by PMF



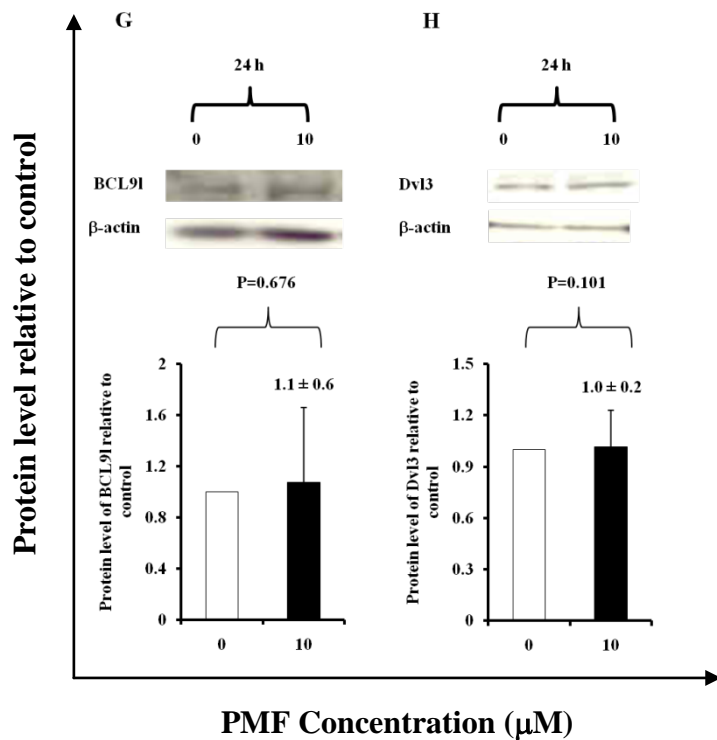


Figure 4.15 Effects of PMF on levels of proteins closely associated with the Wnt signalling pathway (mean  $\pm$  SD).

Lysates of APC10.1 cells exposed to 0 or 10  $\mu$ M PMF were analysed for different proteins associated with Wnt signalling: Wnt8b (A), Wnt3a (B), TCF4(C),  $\beta$ -catenin (D), Lrp5 (E), GSK3 $\beta$  (F), BCL91 (G) and Dvl3 (H). The results are the mean  $\pm$  SD of triplicates. Student's t-test was applied. Asterisk (\*) denotes significant protein changes relative to the housekeeping protein,  $\beta$ -actin.

#### 4.8.2 Proteins associated with regulation of cell cycle

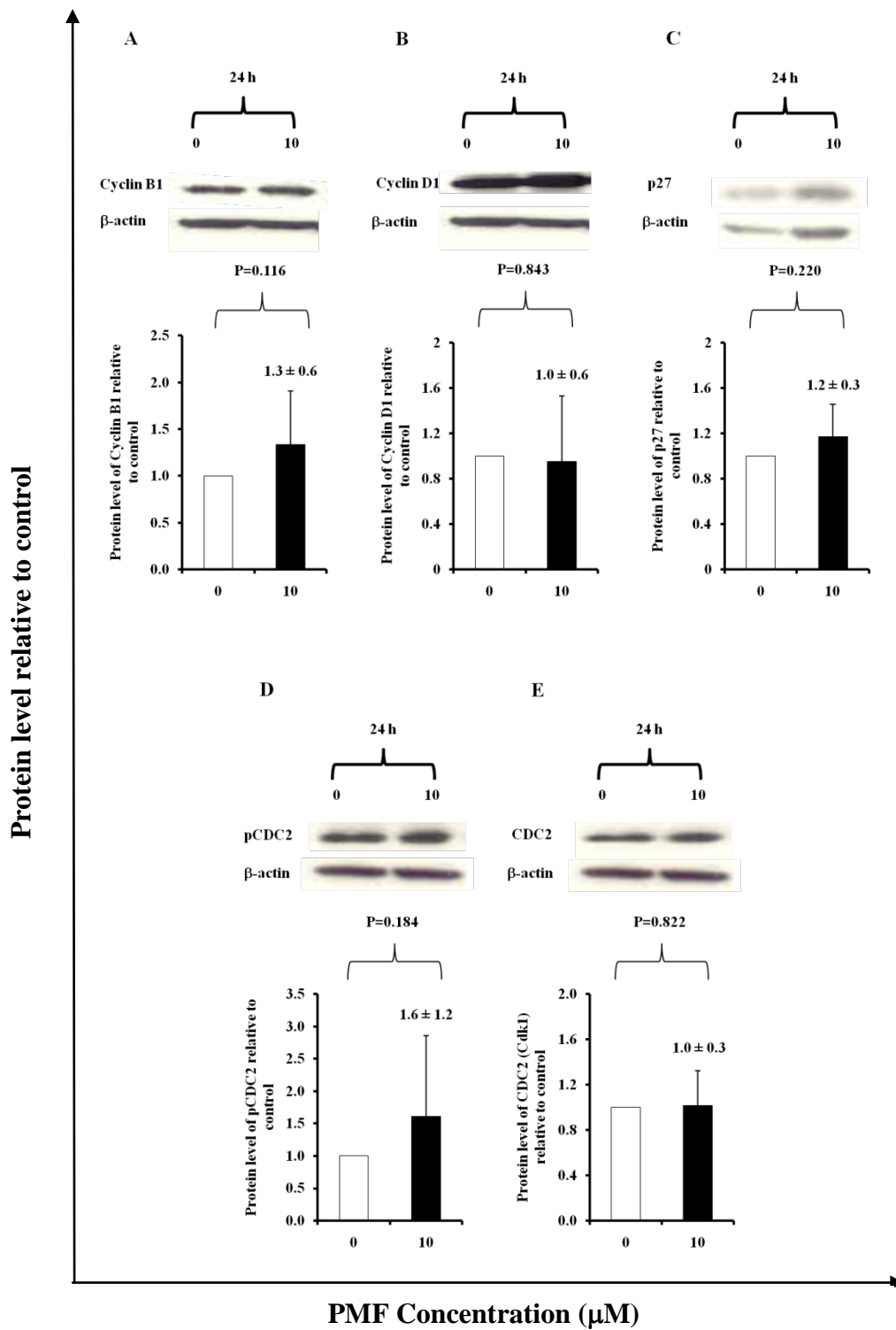


Figure 4.16 Effects of PMF on levels of proteins closely associated with regulation of the cell cycle (mean ± SD).

Lysates of APC10.1 cells exposed to 0 or 10  $\mu$ M PMF were analysed for different proteins closely associated with regulation of cell cycle: Cyclin B1 (A), Cyclin D1 (B), p27 (C), pCDC2 (D) and CDC2 (E). The results are the mean  $\pm$  SD of triplicates. Student's t-test was applied. Asterisk (\*) denotes significant protein changes relative to the housekeeping protein,  $\beta$ -actin.

### 4.8.3 Proteins associated with transcription, translation and cell proliferation

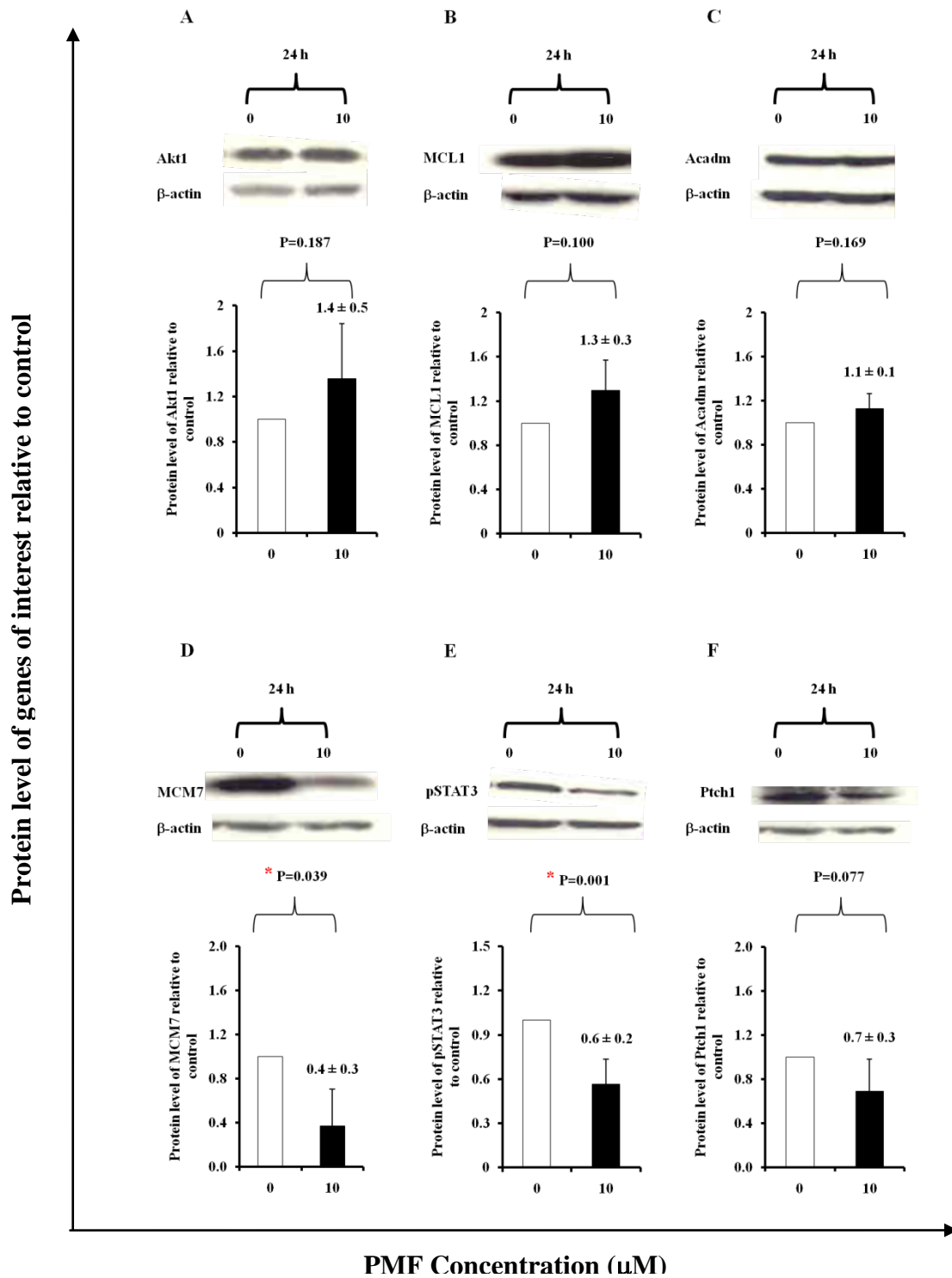


Figure 4.17 Effects of PMF on the levels of proteins closely associated with transcription, translation and cell proliferation (mean  $\pm$  SD).

Lysates of APC10.1 cells exposed to 0 or 10  $\mu$ M PMF were analysed for different proteins closely associated with transcription, translation and cell proliferation: Akt1 (A), MCL1 (B), Acadm (C), MCM7 (D), pSTAT3 (E) and Ptch1 (F). The results are the mean  $\pm$  SD of triplicates. Student's t-test was applied. Asterisk (\*) denotes significant protein changes relative to the housekeeping protein,  $\beta$ -actin.

#### 4.8.4 Proteins associated with apoptosis

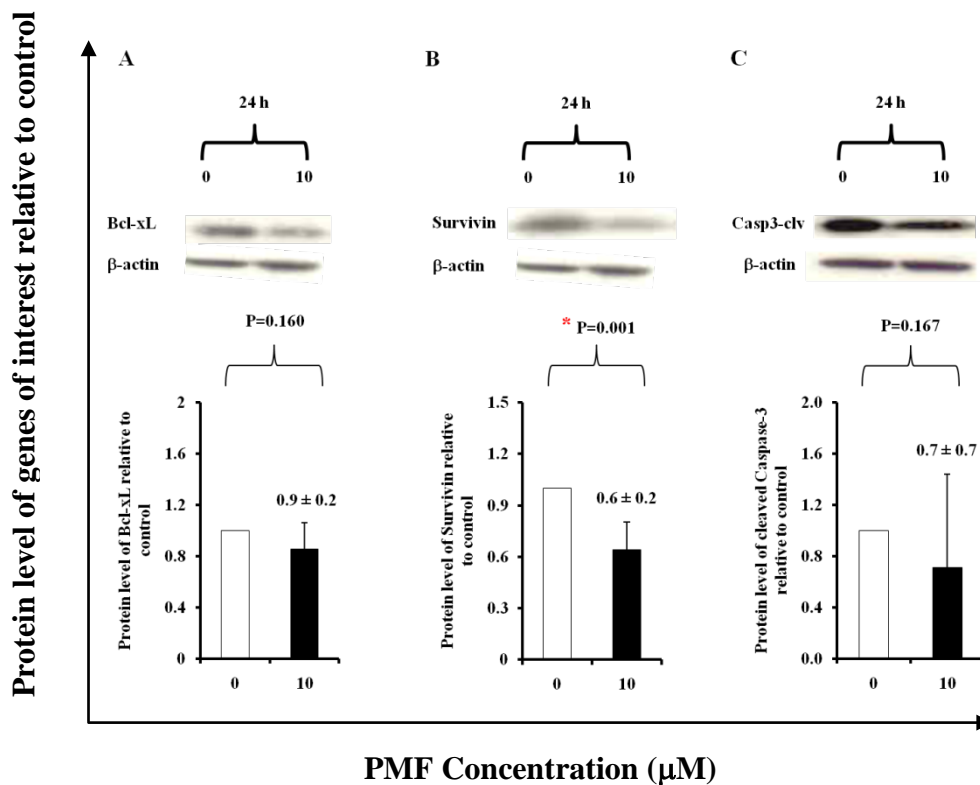


Figure 4.18 Effects of PMF on the levels of proteins closely associated with apoptosis (mean  $\pm$  SD).

Lysates of APC10.1 cells exposed to 0 or 10  $\mu\text{M}$  PMF were analysed for different proteins closely associated with apoptosis: Bcl-xL (A), Survivin (B) and Cleaved caspase-3 (C). The results are the mean  $\pm$  SD of triplicates. Student's t-test was applied. Asterisks (\*) denotes significant protein changes relative to the housekeeping protein,  $\beta$ -actin.

## 4.9 Discussion

With the advancement in molecular biological tools, investigation into the effects of phytochemicals on genes, proteins and metabolites is now possible (Mortensen et al., 2008, Scalbert et al., 2011). In this section, mRNA microarray analysis was performed to identify genes affected by the three flavones in murine adenoma cells. Through the identification of genes, a preliminary elucidation of key signalling pathways modulated by these flavones was achieved. Potential molecular targets of these flavones, could then be delineated.

In the light of the different effects of PMF, tricetin and apigenin on cell growth and adenoma development, it was interesting to compare the gene changes between these flavones. The ranking of flavones based on number of gene changes corresponded with the growth inhibitory potency of the flavones in cells: PMF>tricetin>apigenin. Both tricetin and PMF, which exhibited reduction in adenoma formation *in vivo*, also shared effects on common key signalling pathways in CRC. Therefore, the results suggest a link between molecular pathways and the efficacy of these flavones in terms of reduction of adenoma.

PMF exhibited more distinct gene changes in cells than apigenin (Figure 4.1). There was some crossover between the control and tricetin-treated groups. Such crossover was more pronounced between the apigenin-treated and control groups. Therefore, principle component analysis spells out the ranking of these flavones based on the distinct spread and magnitude in gene change, with PMF being the flavone that elicited most distinct gene changes. This trend was observed in terms of number of genes, with both significant p-value and fold change (Table 4.1 and Table 4.2). It should be noted that some gene changes may be too subtle to elicit a significant downstream effect. There

may also be moderate gene changes upstream and downstream of a particular pathway, while the changes are subtle in the middle of the pathway. However, to simplify this study, emphasis was placed primarily on genes with significant p-values (Figure 4.2).

The Venn diagrams (Figure 4.3-Figure 4.4) show the number of genes overlapping or distinct between the three flavones. As apigenin had no effect on adenoma number or burden (Cai et al., 2007, Cai et al., 2005a), gene changes triggered by apigenin were excluded. Tricin and PMF both showed significant protective effects in this model and therefore the direction of gene change of these genes have been taken into account.

By altering the different fold changes and p-values, different gene lists were obtained. In this study, a cut-off of p-value<0.05 with direction of gene change was used. Lists containing genes significantly changed by PMF, tricetin and apigenin were generated. As expected by the indication of the number of genes for each flavone, the pathway analysis showed apigenin affected fewer pathways than PMF. These pathways were narrowed down to those pathways closely related to CRC. It was interesting to note that PMF triggered significant gene changes in pathways that crosstalk with other downstream pathways including inflammation, initiation of carcinogenesis and apoptosis. A more in-depth investigation into these pathways showed PMF to have effects on molecular functions, biological processes and cellular components of APC10.1 cells. In terms of molecular functions, the analysis indicates that PMF significantly modulated binding, particularly rRNA binding, structural molecule activity, and transcriptional regulatory activity in the cell. These molecular functions could be further broken down to ATP-dependent helicase activity, transferase activity, DNA-directed polymerase activity, protein phosphatase regulator activity, steroid hormone receptor activity and voltage-gated calcium channel implicated in signal

transduction and cancer (Cuddapah and Sontheimer, 2010, Mayer et al., 2011). These activities are essential in pathways such as the cell cycle, Wnt signalling, PI3K/Akt/GSK3 $\beta$  and apoptosis (see chapter 1, section 1.4.4.2-1.4.4.5).

Among many biological processes (Table 4.6, Figure 4.6), the analysis showed that the gene changes by PMF markedly regulated the translation process and growth of cells. At the cellular component level (Table 4.7, Figure 4.7), gene changes caused by PMF suggest a significant influence of PMF on the macromolecular complex, particularly the ribosome component of a cell. Taken together, gene changes caused by PMF affect the translation and growth of cells. All these functions, processes and cellular components are consistent with the protective effects of PMF observed in cells *in vitro* and mice *in vivo*.

An independent analysis using DAVID/EASE was performed with the gene lists generated for each flavone (Figure 4.3, II). A similar outcome was obtained showing gene changes caused by apigenin significantly modulated insulin signalling (Figure 4.11). Insulin may crosstalk with the Wnt signalling pathway in a multi-level manner, involving insulin regulation of the expression of Wnt target genes, a Wnt receptor, as well as mediators of the Wnt signalling pathway (Sun et al., 2010). This finding confirms that apigenin stimulates insulin secretion and glycogen synthesis (Cazarolli et al., 2009). Modulation of the insulin pathway has effects on p38 MAPK, which is responsible for cell differentiation and apoptosis. Studies have shown apigenin to decrease insulin-like growth factor-1(IGF-1)-stimulated cell proliferation and induce apoptosis *in vivo* (Shukla et al., 2005). Down-regulation of IGF-1 causes the inactivation of Akt and its auto-phosphorylation, eventually leading to induction of caspase-9 (Kaur et al., 2008). Apigenin also increases p27/Kip1 expression, a cyclin-

dependent kinase inhibitor 1b, which competes for cyclin D1 binding and contributes to G1 arrest (Shukla and Gupta, 2009). This downstream pathway modulates glucose metabolism, proliferation and differentiation in cells. The microarray results from this study show the different pathways that apigenin may engage in promoting differentiation and apoptosis. However, anti-carcinogenic activities were not observed for apigenin *in vitro* and *in vivo*, indicative that this pathway may not necessarily be critical for activity. The lack of activities of apigenin may also be due to non-efficacious doses. Apigenin at 10  $\mu\text{M}$  is not likely to exhibit any growth inhibition activity as it is below its  $\text{IC}_{50}$  values of 13.0 and 22.3  $\mu\text{M}$  on days 3 and 6, respectively. This may explain why the overall number of genes changed by apigenin is lower than those changed by tricetin and PMF (Figure 4.3). For PMF and tricetin, 10  $\mu\text{M}$  is above or near the  $\text{IC}_{50}$  values. In addition, the cells were treated for 24 h, while *in vivo* studies were performed over several weeks. As for tricetin, there were many up-regulated genes, but in terms of pathways closely associated with CRC, none stood out when analysed using DAVID/EASE.

By using DAVID/EASE analysis, PMF affected three major branches of pathways (Figure 4.12). Firstly, PMF was able to exert effects on ribosomal RNA (rRNA) and thus modulated the translation of mRNA to protein. This confirmed the effects of PMF on cellular components analysed by ArrayTrack and 'webgestalt'. PMF modulated the Hedgehog signalling pathway which would trigger its sub-branch, protein kinase A. This protein is essential in modulating several key pathways namely tumour growth factor-related, Wnt signalling and Hedgehog regulation of Polycomb group 1 $\alpha$  (PCG) pathways. PCG proteins are known to maintain the memory of silent (repressed) transcriptional states of homeotic genes throughout the events of development (Negre et

al., 2006). Regulation of the PCG1 $\alpha$  pathway involves a sub-branch that leads to modulation of fatty oxidation and glucose uptake, both events implicated in cell growth. PMF was also found to act on histone deacetylases, which modulated fatty acid oxidation further downstream.

Fifteen common genes from these three analyses are highlighted in Table 4.9. These genes were subjected to RT-PCR validation. A total of six genes exhibited the same trend as observed in the cDNA microarray analysis. Three of these genes namely *Frat1*, *GSK3 $\beta$*  and *Nfatc2* are involved in Wnt signalling. The other genes were *Ptch1*, *Tollip* and *Vav3*. *Ptch1* is a downstream target gene of sonic Hedgehog-GLI1 pathway (Shahi et al., 2010), *Tollip* is a TLR antagonist (Pimentel-Nunes et al., 2012) and *Vav3* proto-oncogene is linked to aryl hydrocarbon receptor and associated with adhesion and migration of cells (Fernandez-Salguero, 2010).

As the pathway analyses (molecular, biological and cellular) point tentatively to effects of PMF on the initiation and translation of *MCM7*, which is responsible for initiation of genome replication, this protein was also selected as a potential marker. When this gene was mined through the gene lists of flavones, an interesting trend was observed (Figure 4.9, III). All three flavones were able to reduce the expression of the *MCM7* gene, with a potency which mimics growth-inhibitory activity. Therefore, *MCM7* could be an interesting gene to include in further investigations.

WB was used to validate some of the gene changes caused by PMF. Investigation of proteins included those upstream and downstream of a pathway implicated in CRC based on the literature.

PMF modulated transcription directly by targeting molecular binding, particularly rRNA binding, structural molecule activity and transcriptional regulator activity. PMF also affected ribosomes and ribosomal RNA, which are crucial for translation of mRNA to protein. This was evidenced by WB when APC10.1 cells were exposed to PMF at 10  $\mu$ M for 24 h. Some gene changes are subtle but might have critical effects on downstream pathways. Therefore, RT-PCR and WB might not be sensitive enough to detect these changes.

## 5 Effects of PMF on *Apc*<sup>Min/+</sup> mice *in vivo*

### 5.1 Introduction

The studies in cells *in vitro* (Sale et al., 2009) described in sections 1.5.1.1 - 1.5.1.3 suggest that PMF exerts effects on cell proliferation, cell cycle and apoptosis consistent with cancer chemoprevention. These mechanisms may mediate retardation of adenoma formation in the small intestine of mice (Cai et al., 2009b). Results obtained from the microarray study (Chapter 4) highlight gene changes associated with exposure of adenoma cells to PMF, particularly for *GSK3 $\beta$*  and *MCM7*. A recent paper showed that *GSK3 $\beta$*  can suppress tumour progression by down-regulating Wnt-signalling and activating cyclin D1 (Al-Mulla et al., 2011). In Chapter 4.6, PMF at 10  $\mu$ M was shown to increase the expression of the *GSK3 $\beta$*  gene in APC10.1 cells. This up-regulation was also seen by RT-PCR and WB. PMF also reduced the expression of the *MCM7* gene. In terms of Wnt-signalling induced transcription, an increase in *GSK3 $\beta$*  may increase the formation of the destructive complex. This complex binds free  $\beta$ -catenin and marks it for proteolytic degradation, thus preventing translocation of free  $\beta$ -catenin into the nucleus to bind to TCF4 for initiation of transcription. *MCM7* is directly regulated by transcription factor E2F (Shohet et al., 2002), which represses  $\beta$ -catenin/TCF4 transcription (Xie et al., 2009). In the cellular incubations described in Chapter 4.8, PMF caused an increase in *GSK3 $\beta$* ,  $\beta$ -catenin and TCF4, which did not reflect the reduction in *MCM7* expression, suggesting that PMF causes events more complicated than merely triggering Wnt signalling.

In order to find out whether or not the changes observed for GSK3 $\beta$  and MCM7 in adenoma cells *in vitro* are pertinent to adenomas exposed to PMF in intact mice *in vivo*, WB and immunohistochemistry analyses of expression of GSK3 $\beta$  and MCM7 were performed in tissues of *Apc*<sup>Min/+</sup> mice which had received PMF under conditions under which PMF has been shown to inhibit adenoma development *in vivo* (Cai et al., 2009b). *Apc*<sup>Min/+</sup> mice were randomly divided into two groups, control or intervention. Mice in the control group received standard AIN-93G diet *ad libitum*, while mice in the intervention group received AIN-93G diet supplemented with 0.2% w/w PMF for 12 weeks prior to termination of the experiment (weeks 4-16) (section 2.2.8.1).

## 5.2 Effects of PMF on adenoma number and burden

After exposure of *Apc*<sup>Min/+</sup> mice to PMF, the number and burden of adenomas were reduced in comparison with those in the control group. Due to the small sample size and its non-normal distribution, the Mann-Whitney U test was used to establish significance (Figure 5.1).

Most of the adenomas in the *Apc*<sup>Min/+</sup> mice are located in the small intestine. The total number of adenomas in the PMF-treated group was significantly lower than that in the control group. The average number of adenomas per mouse was 28 in the control group and 15 in the PMF group (Figure 5.2). PMF significantly reduced the number of adenomas per mouse in the proximal and distal sections of the small intestine. Adenoma burden per mouse was 59.13 mm<sup>3</sup> in the control group and 32.60 mm<sup>3</sup> in the PMF group (Figure 5.3). This reduction was significant in the medial and distal sections. These results are consistent with the effects seen in the previous *Apc*<sup>Min/+</sup> mouse study (Cai et al., 2009b).

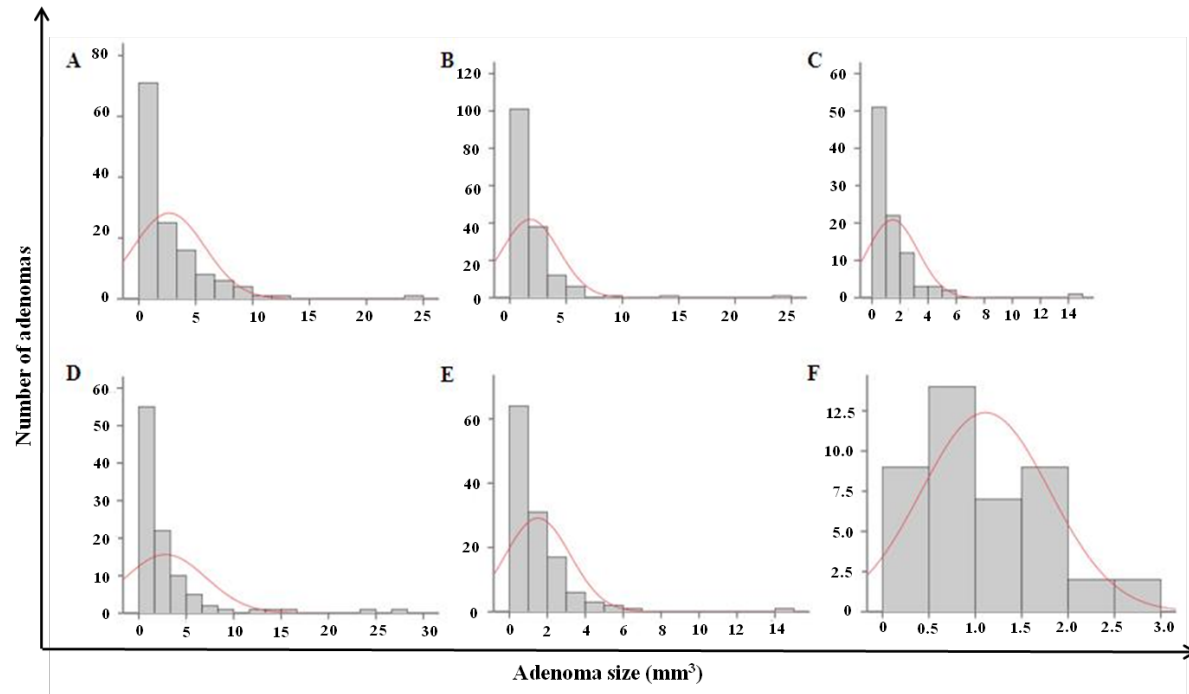


Figure 5.1 Frequency distribution of adenoma burden depicting non-normal distribution of the adenoma burden in this animal study.

A=Adenoma burden in proximal section of control group; B=Adenoma burden in medial section of control group; C= Adenoma burden in distal section of control group; D= Adenoma burden in proximal section of PMF-treated group; E= Adenoma burden in medial section of PMF-treated group; F= Adenoma burden in distal section of PMF-treated group.

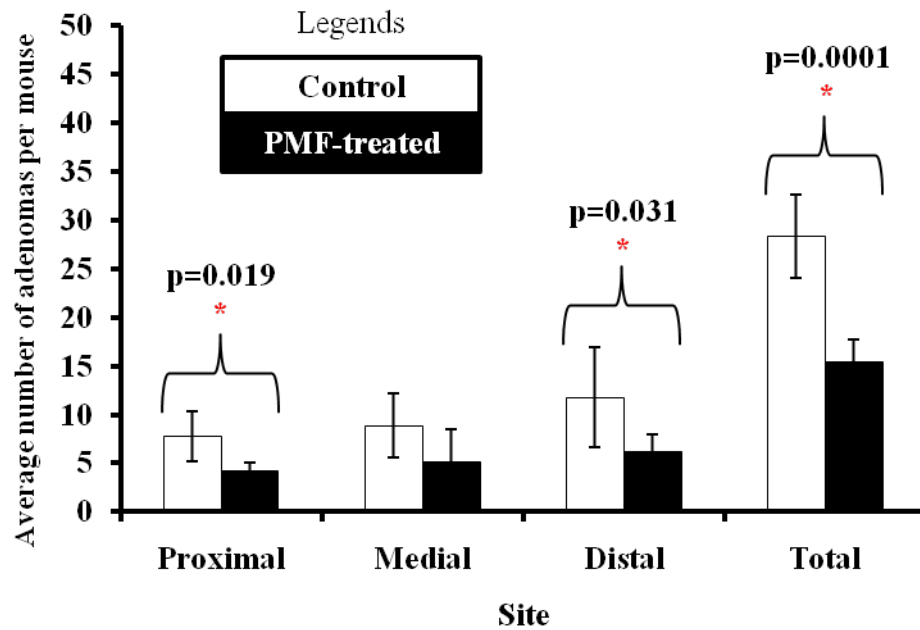


Figure 5.2 Effects of PMF on the total number of adenoma in control (open) or long term PMF-treated (closed) *Ap<sup>c</sup><sup>Min/+</sup>* mice.

*Ap<sup>c</sup><sup>Min/+</sup>* mice received standard AIN-93G diet or 0.2% (w/w) PMF in the diet from week 4 to week 16 prior to termination of the experiment. Adenomas were counted and the data was categorised according to the different sites in the small intestine and the overall total between the control and PMF-treated groups. The error bars denoted standard deviation (white = control group, black = PMF-treated group). Statistical significance is denoted by red asterisks \* ( $n_{\text{control}}=8$ ,  $n_{\text{PMF}}=7$ ,  $p<0.05$ , Mann-Whitney U test).

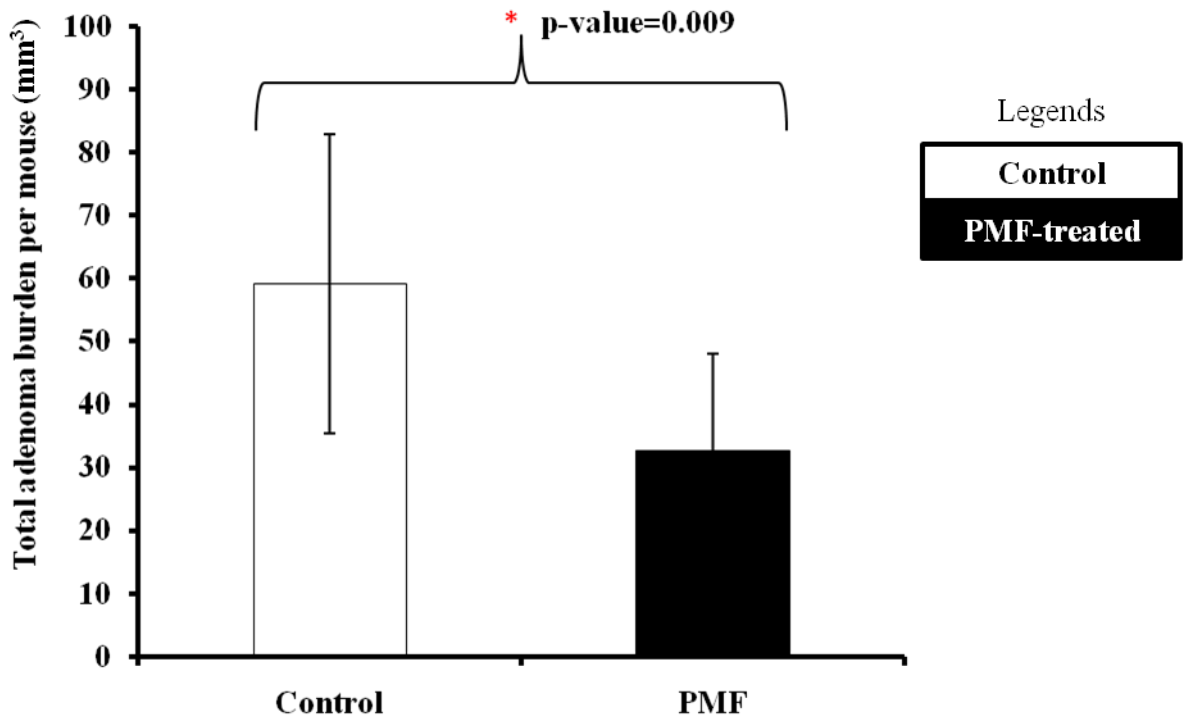


Figure 5.3 Effects of PMF on the total adenoma burden in control (open) or long term PMF-treated (closed) *Apc<sup>Min/+</sup>* mice.

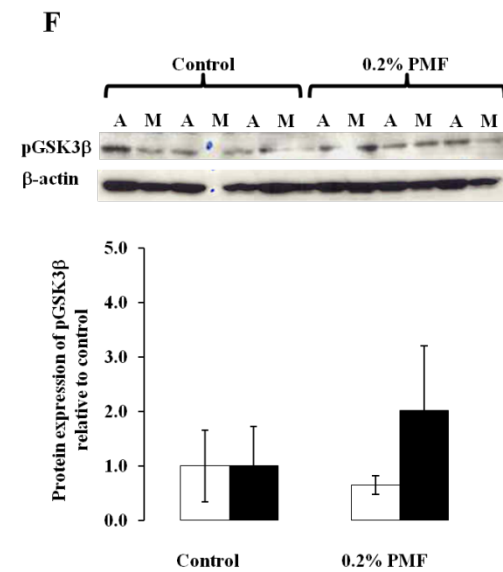
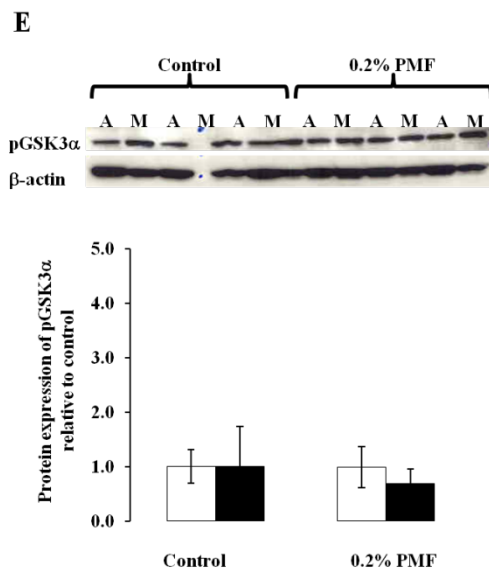
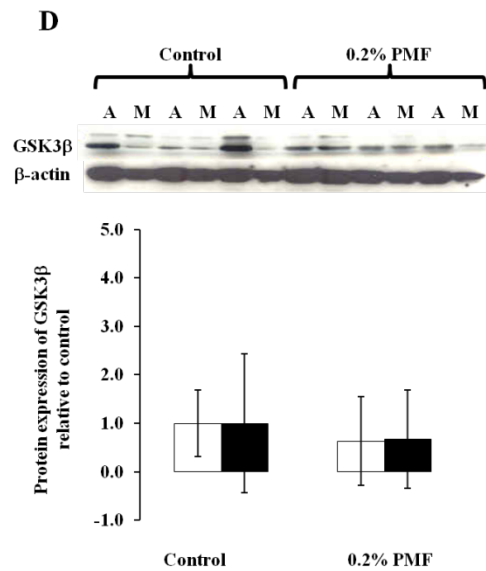
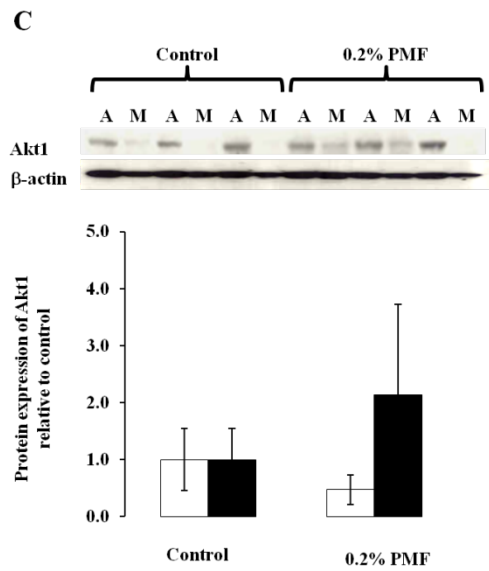
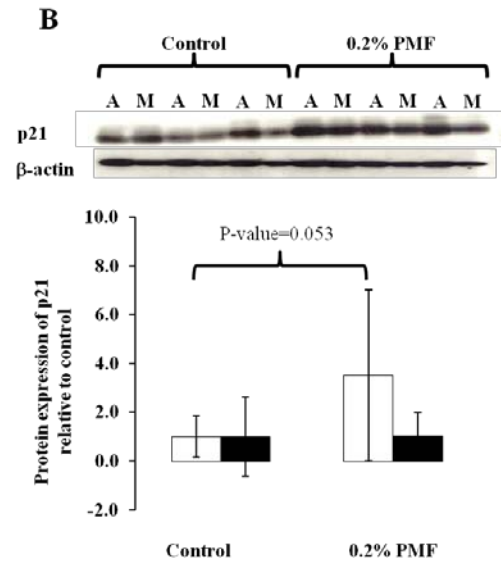
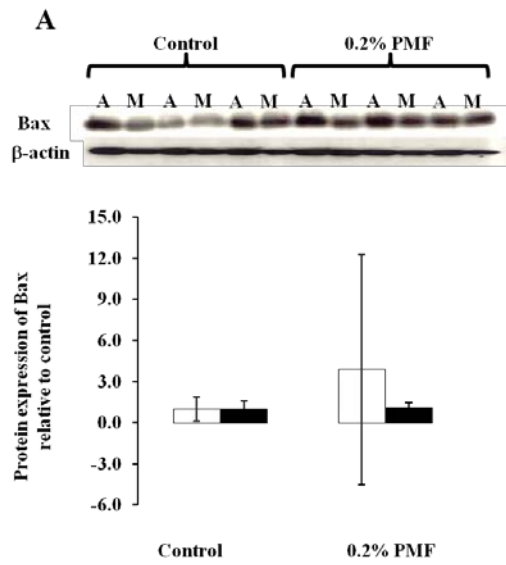
*Apc<sup>Min/+</sup>* mice received standard AIN-93G diet or 0.2% (w/w) PMF in the diet from week 4 to week 16 prior to termination of the experiment. Adenomas were measured and the adenoma volumes were calculated. The results were calculated as means of group and error bars denote standard deviation (open = control group=8, closed = treatment group=7). Statistical significance is denoted by red asterisks \* ( $n_{\text{control}}=8$ ,  $n_{\text{PMF}}=7$ ,  $p<0.05$ , Mann-Whitney U test.).

### **5.3 Effects of PMF on expression of mechanistically important proteins in the small intestine and colon**

Selective proteins were analysed in the adenomas and surrounding mucosa of control and PMF-treated mice. Analysis was by WB (Figure 5.4) and immunohistochemistry (Figure 5.5-Figure 5.7). The choice of proteins studied may be briefly justified as follows: Proteins p21 is linked with cell cycle arrest (section 1.4.4.2), while survivin, cleaved caspase-3 and BAX are key proteins in cell survival and apoptosis (section 1.4.4.3). MCM7, Akt1 and GSK3 $\beta$  are involved in PI3K/Akt/GSK3 $\beta$  signalling and transcription (section 1.4.4.5). GSK3 $\beta$  and its inactive forms, pGSK3 $\alpha$ , pGSK3 $\beta$  together with  $\beta$ -catenin are major proteins in Wnt-signalling (section 1.4.4.4). WB analysis (Figure 5.4) suggests that PMF significantly reduced MCM7 and  $\beta$ -catenin in the adenomas relative to control animals. PMF increased p21 in the adenomas of PMF-treated animal relative to control animals though the results were not significant. PMF failed to affect expression of Bax, Akt1, GSK3 $\beta$ , pGSK3 $\alpha$  and pGSK3 $\beta$ , survivin, and cleaved caspase-3. The tissues of the animals were also assessed by immunohistochemistry. The overall staining for GSK3 $\beta$  (Figures 5.5, 5.6) and MCM7 (Figures 5.7, 5.8) was consistent, suggesting that the antibodies did react in the expected fashion. However, the results showed no significant differences between control mice and mice from the intervention groups.

In a separate experiment, mice received AIN-93G diet supplemented with 0.2% w/w apigenin, tricetin or PMF for only 4 weeks prior to termination of the experiment (weeks 12-16). The objective was to explore differential short-term effects of flavones on the above putative chemoprevention biomarkers as measured by immunohistochemistry. As

in the long-term intervention study with PMF, there were no differences in antibody staining between tissues from control animals and those on either apigenin, tricetin or PMF (results not shown).



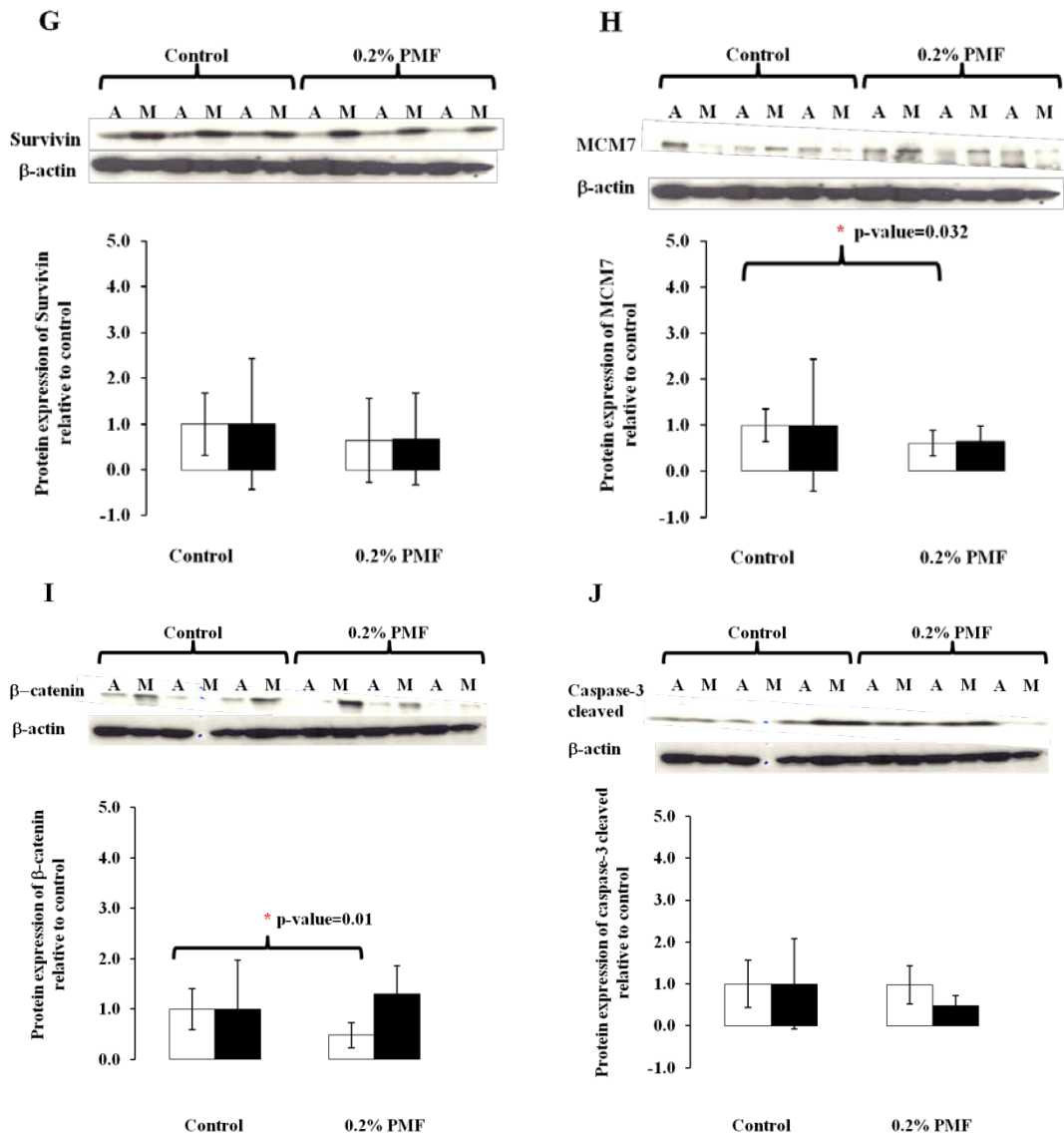
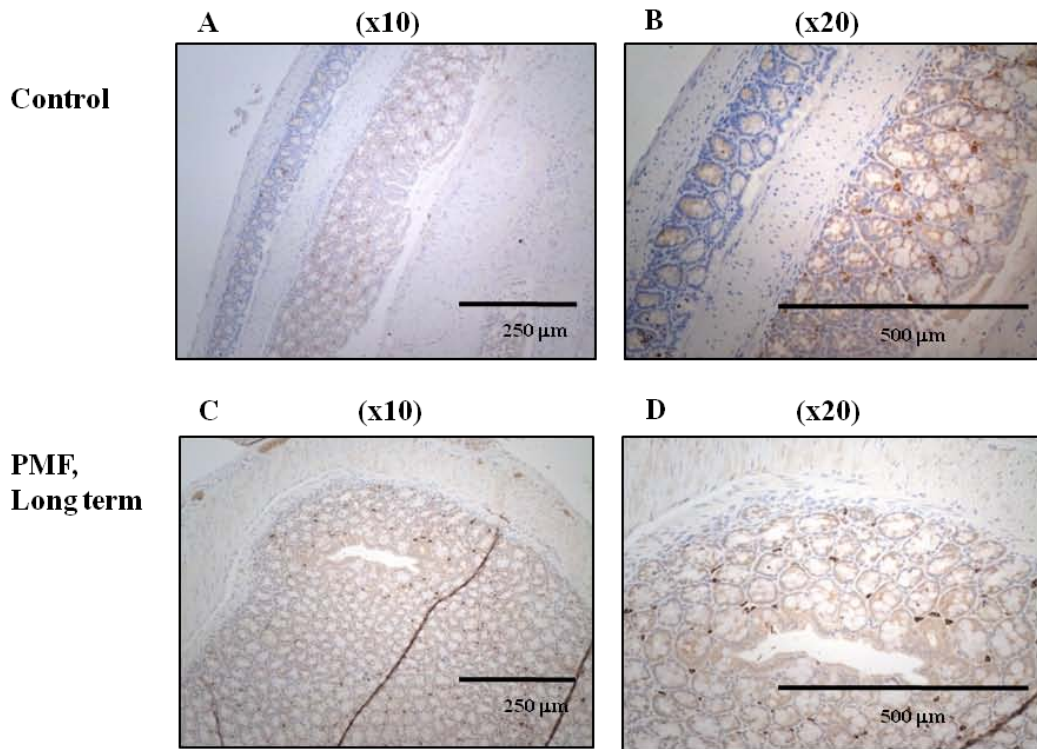


Figure 5.4 Effects of PMF on Bax (A), p21 (B), Akt1 (C), GSK3 $\beta$  (D), pGSK3 $\alpha$  (E), pGSK3 $\beta$  (F), Survivin (G), MCM7 (H), caspase-3 cleaved (I) and  $\beta$ -catenin (J) expressions in control and PMF-treated animal adenoma (A, open) or mucosa (M, closed) lysates.

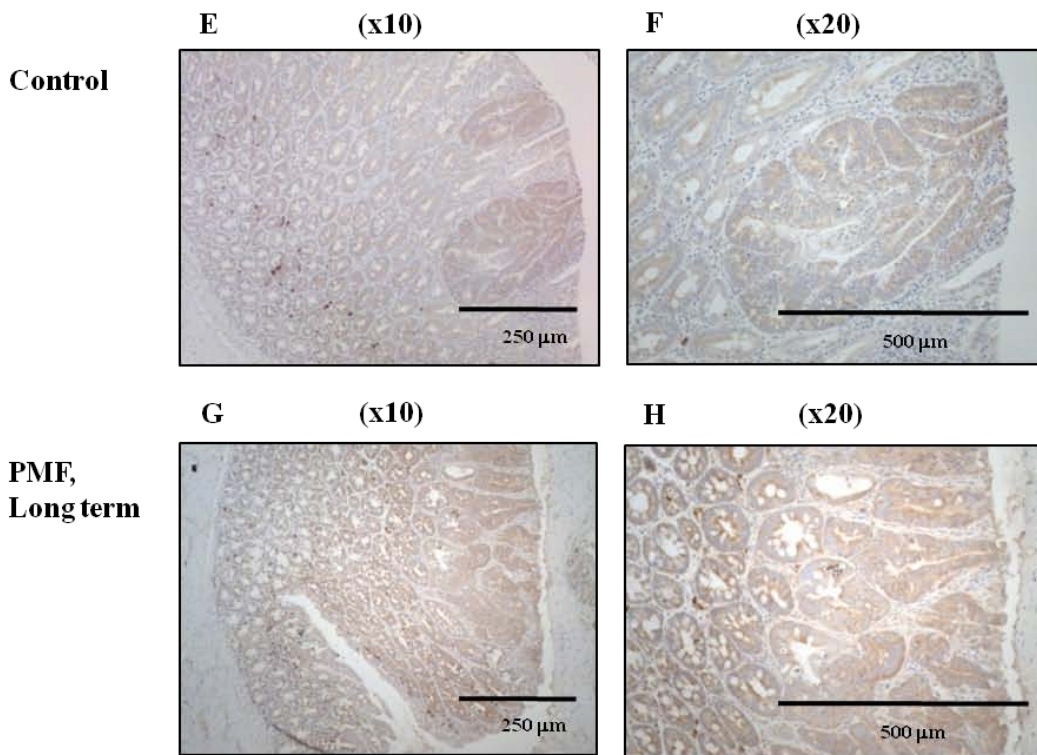
Representative blots depict the individual animals from the long term intervention study. Densitometric ratios of Bax (A), p21 (B), Akt1 (C), GSK3 $\beta$  (D), pGSK3 $\alpha$  (E), pGSK3 $\beta$  (F), Survivin (G), MCM7 (H), caspase-3 cleaved (I) and  $\beta$ -catenin (J) levels

are expressed relative to control (=1) and corrected for protein loading using the housekeeping  $\beta$ -actin. Values are the mean  $\pm$  SD. Triplicates were performed with n=8 for control and n=7 for PMF-treated mice. Student's t-test was employed.

**Normal crypt in colon**



**Aberrant crypts in colon**



### Normal villi in colon

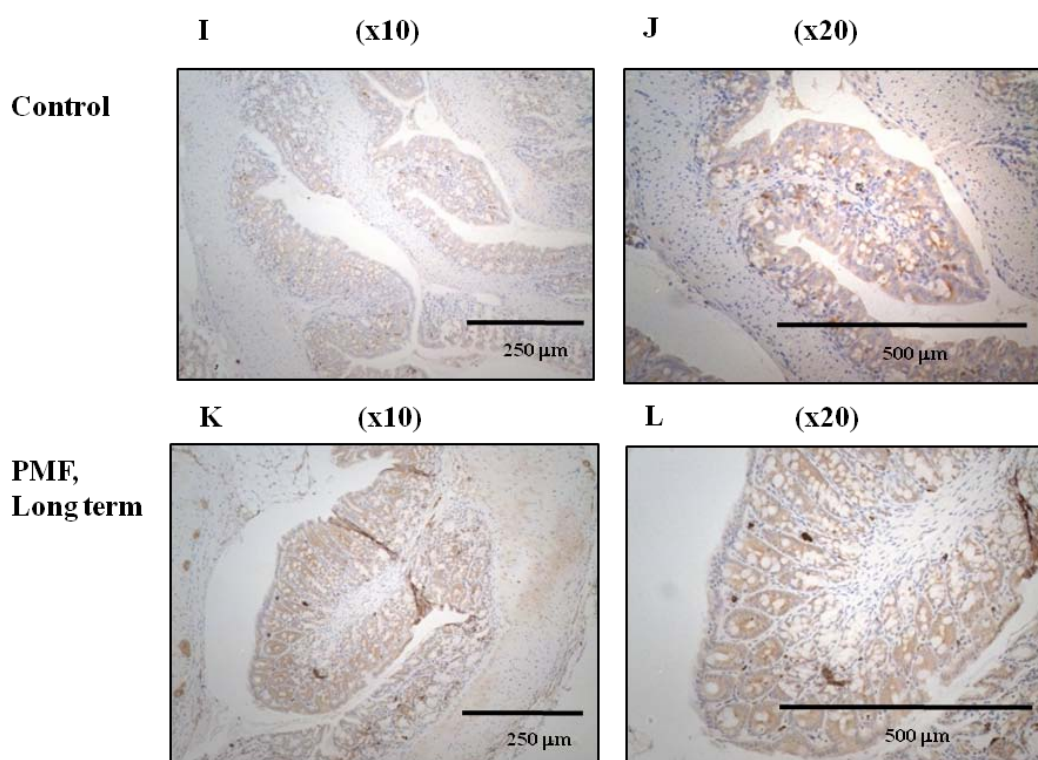
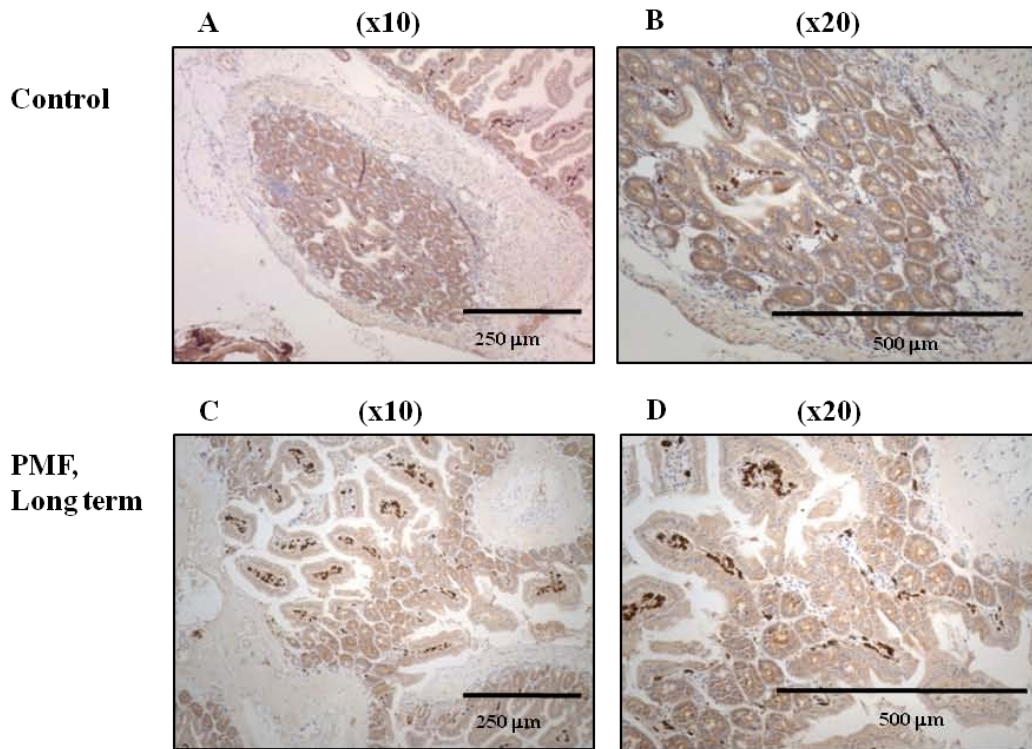


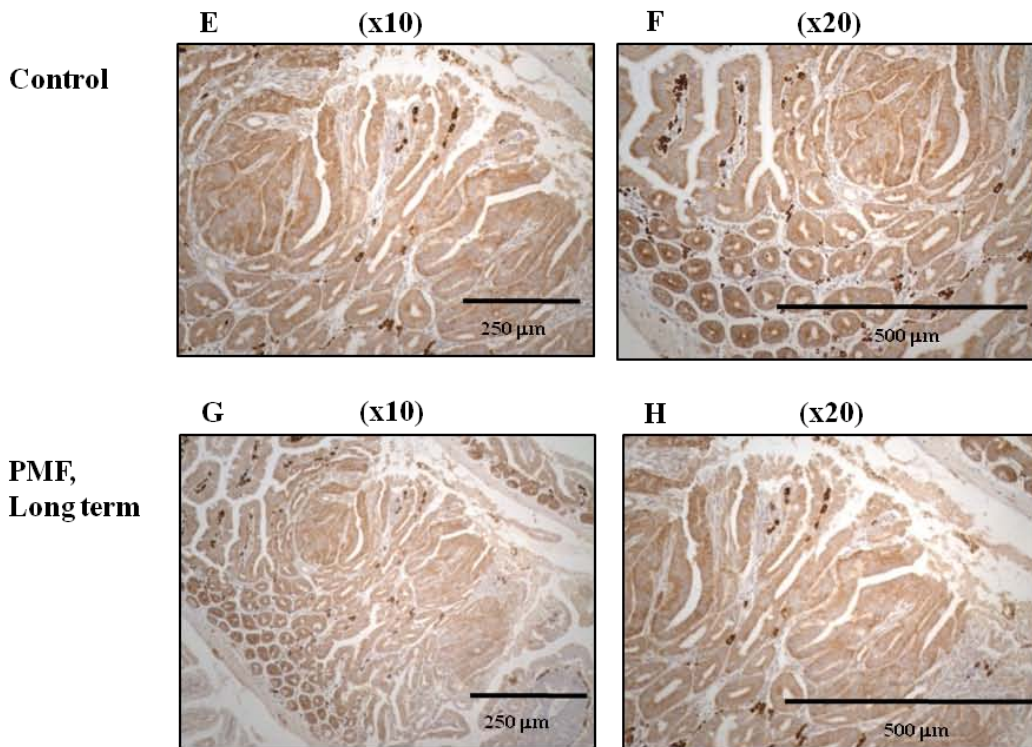
Figure 5.5 Effects of PMF on the normal crypts, aberrant crypts foci, normal villi and adenomas in the colons of *Apc*<sup>Min/+</sup> mice that received control or 0.2% w/w PMF, stained for GSK3β mouse antibody at magnifications of 10x and 20x.

Representative microphotographs depict the tissue sections of control mice or mice receiving 0.2% w/w of PMF from week 4 to week 16. At the end of the duration, mice were culled and intestinal tissues were rolled, fixed and sectioned. The cytoplasm and nuclei in these sections were positively stained with anti-GSK3β antibody. These microphotographs showed the differences between normal (A-D) and aberrant crypts (E-H), and normal villi (I-L) in the colon at x10 or x20 magnification. No villous adenoma was detected in the colon of PMF-treated mice.

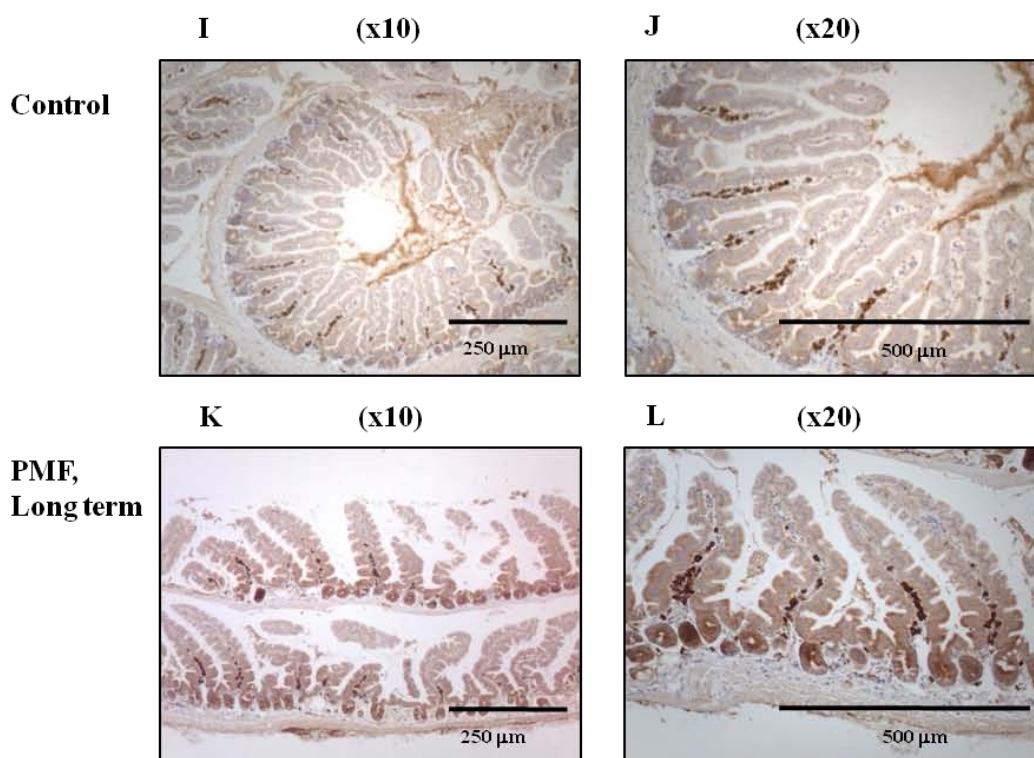
**Normal crypts in small intestine**



**Aberrant crypt foci in small intestine**



**Normal villi in small intestine**



**Abnormal villi in small intestine**

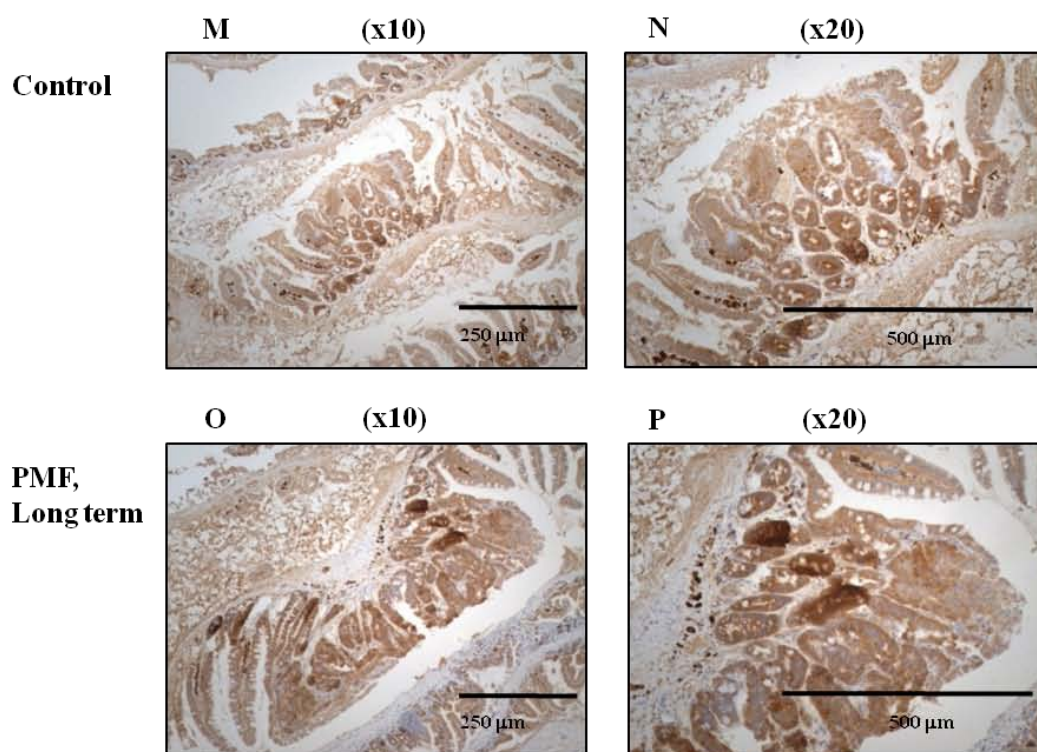
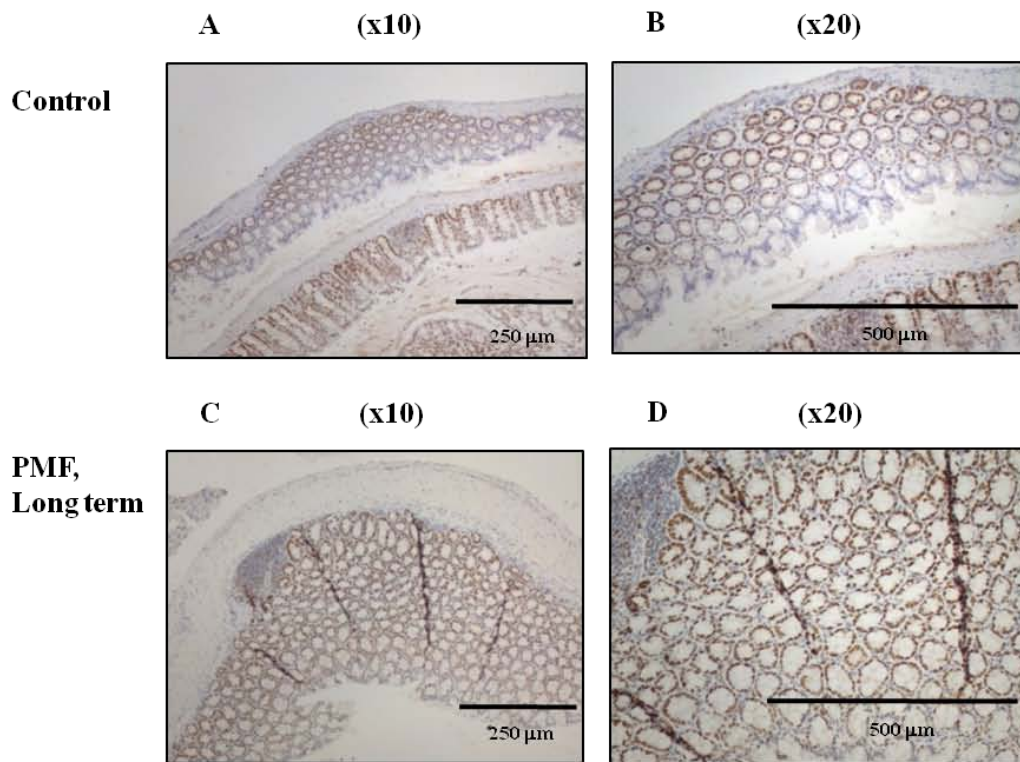


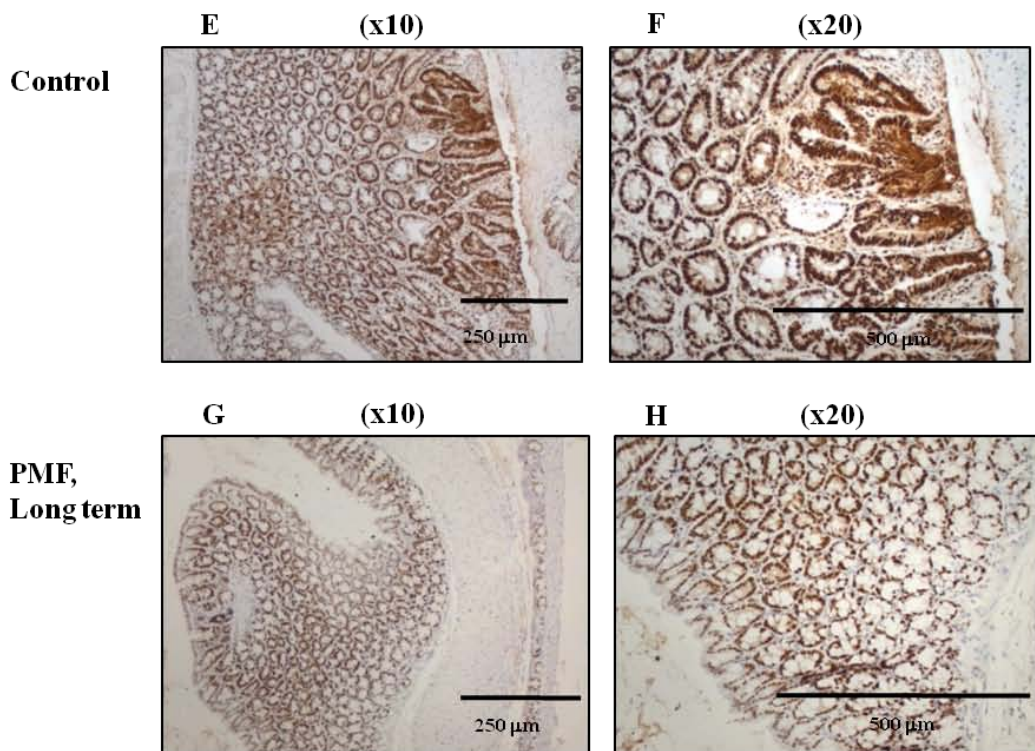
Figure 5.6 Effects of PMF on the normal crypts, aberrant crypt foci, normal villi and adenomas in the small intestines of *Apc<sup>Min/+</sup>* mice that received control or 0.2% w/w PMF, stained for GSK3 $\beta$  mouse antibody at magnifications of 10x and 20x.

Representative microphotographs depict the tissue sections of control mice or mice receiving 0.2% w/w of PMF from week 4 to week 16. At the end of the duration, mice were culled and intestinal tissues were rolled, fixed and sectioned. The cytoplasm and nuclei in these sections were positively stained with anti-GSK3 $\beta$  antibody. These microphotographs showed the differences between normal (A-D) and aberrant crypts (E-H) as well as normal villi (I-L) and villous adenomas (M-P) in the small intestines of these mice at x10 or x20 magnification.

**Normal crypt in colon**



**Aberrant crypts in colon**



**Normal villi in colon**

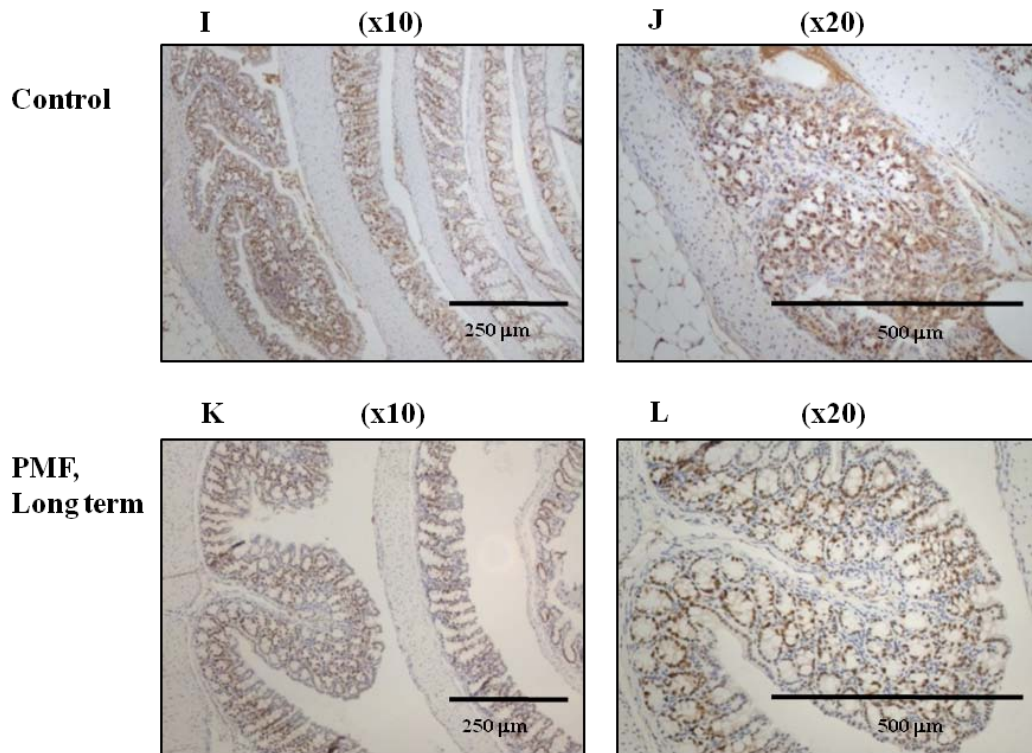
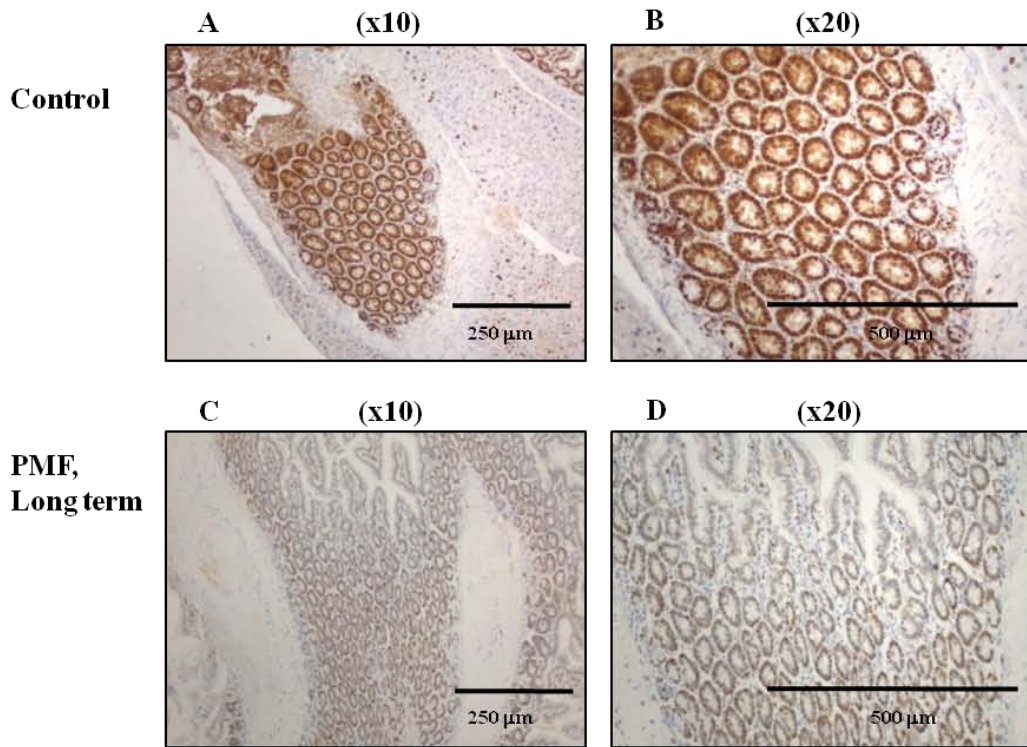


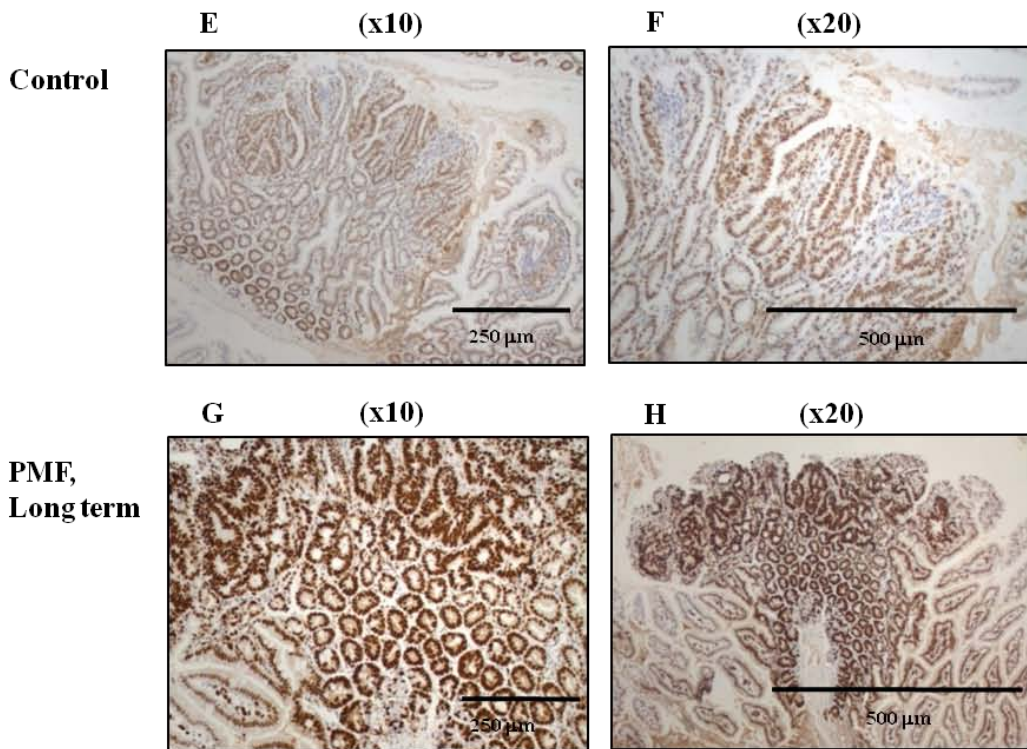
Figure 5.7 Effects of PMF on the normal crypts, aberrant crypts foci, normal villi and adenomas in the colons of *Apc<sup>Min/+</sup>* mice that received control or 0.2% w/w PMF, stained for MCM7 mouse antibody at magnifications of 10x and 20x.

Representative microphotographs depict the tissue sections of control mice or mice receiving 0.2% w/w of PMF from week 4 to week 16. At the end of the duration, mice were culled and intestinal tissues were rolled, fixed and sectioned. The nuclei in these sections were positively stained with anti-MCM7 antibody. These microphotographs showed the differences between normal (A-D) and aberrant crypts (E-H), and normal villi (I-L) in the colon at x10 or x20 magnification. No villous adenoma was detected in the colon of PMF-treated mice.

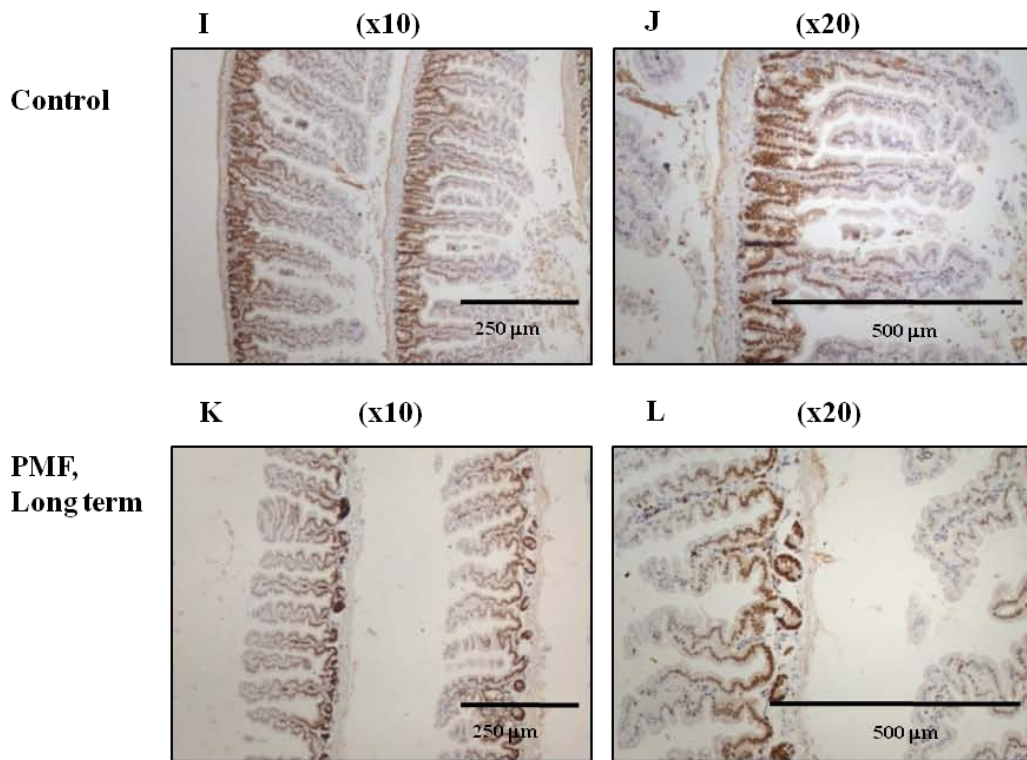
**Normal crypt in small intestine**



**Aberrant crypts in small intestine**



**Normal villi in small intestine**



**Abnormal villi in small intestine**

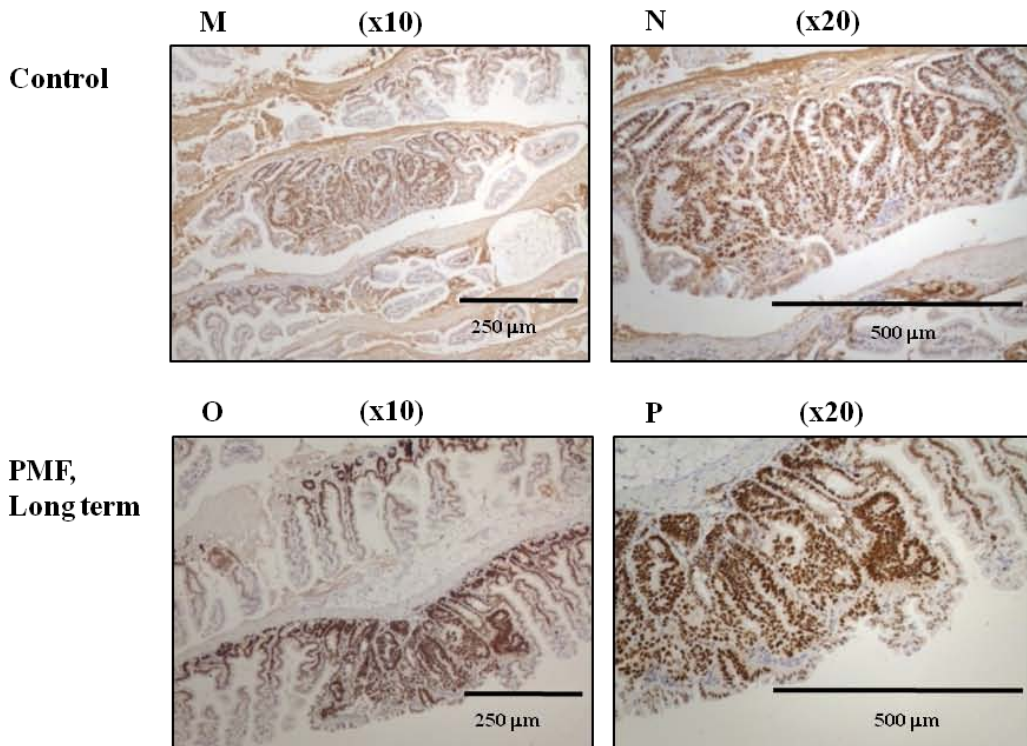


Figure 5.8 Effects of PMF on the normal crypts, aberrant crypts foci, normal villi and adenomas in the small intestines of *Apc<sup>Min/+</sup>* mice that received control or 0.2% w/w PMF, stained for MCM7 mouse antibody at magnifications of 10x and 20x.

Representative microphotographs depict the tissue sections of control mice or mice receiving 0.2% w/w of PMF from week 4 to week 16. At the end of the duration, mice were culled and intestinal tissues were rolled, fixed and sectioned. The cytoplasm and nuclei in these sections were positively stained with anti-MCM7 antibody. These microphotographs showed the differences between normal (A-D) and aberrant crypts (E-H) as well as normal villi (I-L) and villous adenomas (M-P) in the small intestines of these mice at x10 or x20 magnification.

## 5.4 Discussion

In this study, *Apc*<sup>Min/+</sup> mice received PMF for their life-time. The results show that PMF significantly reduced adenoma numbers and adenoma burden after life-time intervention, which is consistent with the results obtained by Cai et al. (Cai et al., 2009b). Mechanistic correlations of the adenoma-retarding effect of PMF were sought using WB. Results show that PMF decreased the levels of MCM7 and  $\beta$ -catenin significantly in the adenomas in comparison with controls. PMF augmented p21 levels although not significantly. These findings are consistent with the reduction in transcription and arrest in cell cycle in cells *in vitro* as described in chapters 3 and 4. The effect on  $\beta$ -catenin supports the suspicion that Wnt signalling is a target pathway for PMF (chapter 4). The results concerning the effect of PMF on the expression of GSK3 $\beta$  and MCM7 in the adenomas could not be confirmed using immunohistochemistry.

An increase in level of  $\beta$ -catenin correlates with an increase in Wnt-signalling-induced transcription. PMF reduced levels of  $\beta$ -catenin in the adenomas in the long term intervention study, suggesting that prolonged exposure of adenomas to PMF halts Wnt-induced transcription. This may correlate with the retardation of adenoma formation observed in *Apc*<sup>Min/+</sup> mice which received PMF for their life-time. Changes in  $\beta$ -catenin were not observed in the *in vitro* study (chapter 4) that mirrors short term intervention. PMF seems to affect the Wnt pathway in these two experimental paradigms in different ways.

In this chapter, an attempt has been made to explain whether or not changes in gene expression observed in adenoma cells *in vitro* after exposure to PMF may predict

changes of expression of the appropriate proteins in adenomas of *Apc<sup>Min/+</sup>* mice which received PMF in their diet. This type of experiment is important in order to delineate the elusive mechanisms by which cancer chemopreventive agents may exert their beneficial activity. The staining results show that the correlation between changes observed in cells *in vitro* and adenoma tissue *in vivo* is minimal. In order to interpret this observation, one has to realise that the gene changes observed *in vitro* were, on the whole, subtle. It is thus possible that they simply did not result in concomitant changes in protein expression. It is necessary for the results obtained using IHC to be supported by results from other assays such as WB and fluorescence *in situ* hybridisation. This is because there are several factors that may affect the outcomes of staining, making it necessary to interpret the results with caution. These factors include thickness of the 'swiss-roll', duration of tissue fixation, rehydration process, pH of antigen retrieval buffer and background staining of primary antibody. Nevertheless, it seems that this approach in which changes exerted by a chemopreventive agent in cells *in vitro* are correlated with changes in the intact animal could be very useful in helping to elucidate chemopreventive mechanisms.

## 6 General Discussion

CRC places a huge toll on healthcare systems world-wide. Chemoprevention is an attractive approach to cancer management as it would reduce cost, morbidity and mortality in a considerable at-risk population. This study was designed to add to the knowledge of novel experimental CRC chemopreventive agents. The aim was to elucidate the CRC chemopreventive mechanisms of flavones, particularly of PMF, and to help develop PMF towards clinical evaluation.

Flavonoids are polyphenols found in abundance in fruits and vegetables, in traditional medicines and some plant-derived beverages (Havsteen, 2002, Potter and Steinmetz, 1996). It is not feasible to assess every known flavonoid for its putative cancer chemopreventive properties in animal models of carcinogenesis. Knowledge of molecular structural features that contribute to their anti-carcinogenicity would help prioritise some of them for preclinical development, but such data are scarce. Methoxy moieties have shown to be important constituents, contributing respect to the anti-carcinogenicity of flavones. For example, 5, 7-dimethoxyflavone and 5,7,4'-trimethoxyflavone were found to exhibit superior anti-carcinogenic properties compared to their hydroxyl analogues chrysin (5,7-dihydroxyflavone) and apigenin (5,7,4'-trihydroxyflavone) in terms of metabolic stability and bioavailability (Walle, 2007, Wen and Walle, 2006a).

In our laboratory, the three flavones apigenin, tricetin and PMF have been compared for their ability to interfere with adenoma development in the *Apc<sup>Min/+</sup>* mouse (Cai et al., 2009b). Apigenin was without efficacy, while tricetin and PMF reduced adenoma formation in the small intestine significantly. The results presented in Chapter 5.2 for PMF are fully consistent with the adenoma development reducing activity reported

before (Cai et al., 2009b). It is likely that PMF, like many other naturally occurring cancer chemopreventive agents, exerts its adenoma-reducing activity via several, perhaps many, mechanisms. Microarray analysis was performed to elucidate the effects of PMF on gene expression in APC10.1 cells, effects which may account for its growth-inhibitory potential *in vitro* and its adenoma-retarding efficacy *in vivo*.

Flavones affected the *in vitro* behaviour of murine adenoma APC10.1 in terms of growth inhibition, cell cycle effects and induction of apoptosis. The rank order of potency *in vitro* mirrors that in the *in vivo* studies: PMF > tricetin > apigenin. Consistently with these *in vitro* and *in vivo* results, the three agents elicited differential gene expression changes.

Apigenin influenced genes associated with pathways related to signalling via insulin, pentose phosphate, MAPK and those involving apoptosis. Apigenin has been shown to promote apoptosis via insulin-signalling in benign leiomyoma smooth muscle cells, which are located mainly in the oesophagus, small intestine and uterus (Kim et al., 2005). The concentration employed in the microarray studies described in chapter 4 (10  $\mu\text{M}$ ) was lower than the  $\text{IC}_{50}$  values for growth inhibition in APC10.1 cells, which were 13 - 22  $\mu\text{M}$ , depending on incubation time. The steady-state concentration of apigenin in the small intestinal mucosa of mice which received apigenin in their diet at 0.2% w/w was  $86 \pm 47 \mu\text{M}$  (Cai et al., 2006), approximately eight-fold more than the concentration employed in the microarray analysis, or four times more than the  $\text{IC}_{50}$  value for growth inhibition. Apigenin has been tested in a clinical trial, and tentatively found to reduce the recurrence rate of colon neoplasia when given in combination with EGCG (Hoensch et al., 2008).

In the case of tricetin, which significantly interfered with murine adenoma development (Cai et al., 2005a), the concentration in the small intestinal mucosa was  $238 \pm 64 \mu\text{M}$ , somewhat higher than the value for apigenin. The concentration of tricetin in the small intestinal mucosa of mice which had received tricetin in their diet at 0.2% w/w was approximately twenty times higher than the concentration employed in the microarray analysis described here. In the microarray study, tricetin at  $10 \mu\text{M}$  modulated the expression of many genes responsible for signalling pathways related to p53, cell cycle, Wnt and MAPK. These pathways are associated with CRC development, suggesting that tricetin may engage anti-carcinogenesis via these pathways.

The effects of PMF on growth, cell cycle and apoptosis, as described in this study, suggest that PMF inhibits growth by arresting cells at the  $G_1$  and  $G_2/M$  phases (see Figure 3.9). Arrest in  $G_1$  causes slowing down of growth, while  $G_2/M$  cell cycle arrest leads eventually to cell death (DiPaola, 2002). An arrest in  $G_1$  is consistent with down-regulation of cyclin D1. This arrest is also associated with inhibition of the activities of Cdc2 (p34) and cyclins B1 and D (see Figure 4.16).  $G_2/M$  arrest is correlated with an increase in pCdc2, which in turn leads to an increase in cyclin B1 (Liu et al., 2007) (Figure 4.16). Active GSK3 $\beta$  phosphorylates cyclin D1 (Diehl et al., 1998), which enables cyclin D1 to translocate into the cytoplasm. Subsequently, cyclin D1 is ubiquitinated and eventually degraded (Diehl et al., 1997). Apart from  $G_2/M$  arrest-induced apoptosis, GSK3 $\beta$  has been reported to modulate cell death in prostate cancer cells via the apoptosis pathway (Vene et al., 2008). The microarray analyses, RT-PCR and WB shown in chapter 4 suggest that PMF may elicit such effects through modulation of signalling pathways linked to Wnt, PI3K/Akt/GSK3 $\beta$  and Stat3. Pathway analyses highlighted several genes that may contribute to the protective effects of PMF.

*GSK3 $\beta$*  and *Nfatc2* were up-regulated while *TCF4* and *Wnt8b* were down-regulated. GSK3 $\beta$  is a key protein that allows crosstalk between Wnt and PI3K/Akt/GSK3 $\beta$ , both closely associated with CRC (Katoh, 2006). Active GSK3 $\beta$  destabilises  $\beta$ -catenin and marks it for degradation. GSK3 $\beta$  also phosphorylates Nfat and promotes nuclear export (Murphy and Hughes, 2002). Nfatc2 is a transcription factor known to trigger cell differentiation in intestinal cells (Wang et al., 2011), and it was elevated by PMF. Wnt8b has been shown to be one of the most potent Wnt signalling molecules stimulating Wnt- $\beta$ -catenin-TCF signalling (Saitoh et al., 2002a). Up-regulation of Wnt8b has been implicated in cells derived from human gastric cancer and murine CRC (Saitoh et al., 2002b). In this study, PMF significantly down-regulated the expression of Wnt8b. PI3K/Akt phosphorylates GSK3 $\beta$  to generate its inactive form, pGSK3 $\beta$  (Sutherland et al., 1993). This inactive form does not bind to  $\beta$ -catenin, and  $\beta$ -catenin accumulates and translocates into the nucleus. By forming a complex with the transcription factor TCF4, transcription is activated. The WB results reported in Chapter 4 suggest that the level of inactive pGSK3 $\beta$  remained unchanged by PMF, and that TCF4 was down-regulated, despite an increase in the active form. Taken together, PMF was shown to target several key genes implicated in CRC. Because of the critical role of GSK3 $\beta$  in Wnt signalling and in CRC, it is conceivable that this pathway plays a major role in the preventive action of PMF. PMF elevated the expression of Akt1, indicative of some effect on the PI3K/Akt/GSK3 $\beta$  pathway, while reducing the expression of Wnt3a, which is known to activate Akt1. Obviously, PMF exerts differential and subtle effects on different components of the PI3K/Akt/GSK3 $\beta$  pathway, which are perhaps, involved in eliciting chemopreventive activity.

PMF significantly reduced the expressions of survivin ( $p < 0.001$ ) (Figure 4.18) and pStat3 ( $p < 0.001$ ) (Figure 4.17). Survivin is a bi-functional regulator of apoptosis and cell proliferation located in mitochondria. When present in the cytoplasm, survivin suppresses apoptosis, but after translocation into the nucleus it acts as a chromosomal passenger protein at the G<sub>2</sub>/M check point of the cell cycle (Beltrami et al., 2004). Survivin has been shown to augment the expression of Fas ligand and trigger apoptosis via the extrinsic pathway (Asanuma et al., 2004). PMF might have induced apoptosis by reduction of survivin in the cytoplasm.

PMF was also shown to reduce the expression of *Tollip*, which encodes an inhibitory adaptor protein in the TLR signalling pathway (Zhang and Ghosh, 2002). A decrease in *Tollip* is consistent with a reduction in pro-inflammatory mediators during inflammation. PMF up-regulated RelA/p65, one of the five constituents of NF- $\kappa$ B, which is implicated in inflammation, cell growth, development and apoptosis, acting via the Toll-like signalling pathway (Chen et al., 1998, Jeon et al., 2011). In order for RelA to elicit an effect, it has to be translocated into the nucleus to stimulate the production of tumour necrosis factor.

PMF-induced elevation of GSK3 $\beta$  may also be implicated in its effects on cell cycle progression from G<sub>1</sub> to S (Jirmanova et al., 2002) (Figure 3.4). Cdc6 is present in the nucleus of a cell during the G<sub>1</sub> phase of the cell cycle. At the start of the S phase, Cdc6 translocates to the cytoplasm and interacts with MCM proteins, including MCM7 (Fujita et al., 1999). Up-regulation of Cdc6 and MCM7 has been implicated in precancerous lesions and formation of oral squamous cell carcinoma (Feng et al., 2008). Cdc6 was shown here to be up-regulated by PMF, while MCM7 was down-regulated (see Figure 4.9). Down-regulation of MCM7 correlates with the up-regulation of p21

and cyclin-dependent kinase inhibitor1. This has been implicated in reduction of transcription and initiation of cancer (Luo, 2011). MCM7 has been suggested as a marker for CRC (Pillaire et al., 2010) and as a diagnostic and prognostic tumour marker in the clinical setting (Giaginis et al., 2010). Down-regulation of MCM7 by PMF was observed not only in the gene analysis in cells but also by WB in adenomas from *Apc<sup>Min/+</sup>* mice, which had received 0.2% w/w PMF, indicative of PMF exerting putative chemoprotective effects consistently in *in vitro* and *in vivo*. Consistent with an effect of PMF on adenoma MCM7 *in vivo*, PMF concentration in the small intestinal mucosa of PMF-treated mice was 108.5  $\mu\text{M}$  (Cai et al., 2009a), about ten-fold higher than the concentration at which PMF affected MCM7 in cells *in vitro*.

Overall, the project described here has shown that PMF can initiate anti-carcinogenic mechanisms counteracting those characterised by Hanahan and Weinberg (Hanahan and Weinberg, 2011) as hallmarks of carcinogenesis (Figure 6.1). Several pathways affected by PMF are closely associated with CRC development. The discovery of chemopreventive mechanisms of PMF may help devise testing strategies for new agents. Knowledge of mechanisms may also help with the development of novel markers of the anti-carcinogenic efficacy of PMF. Gene and protein changes observed here which are relevant to anti-carcinogenesis may help screen for putative functional analogues of PMF. Nevertheless, it has to be emphasised that this notion needs further validation, as the changes observed in the gene analyses were very subtle, and some of the results were not consistent between gene analysis, RT-PCR and WB.

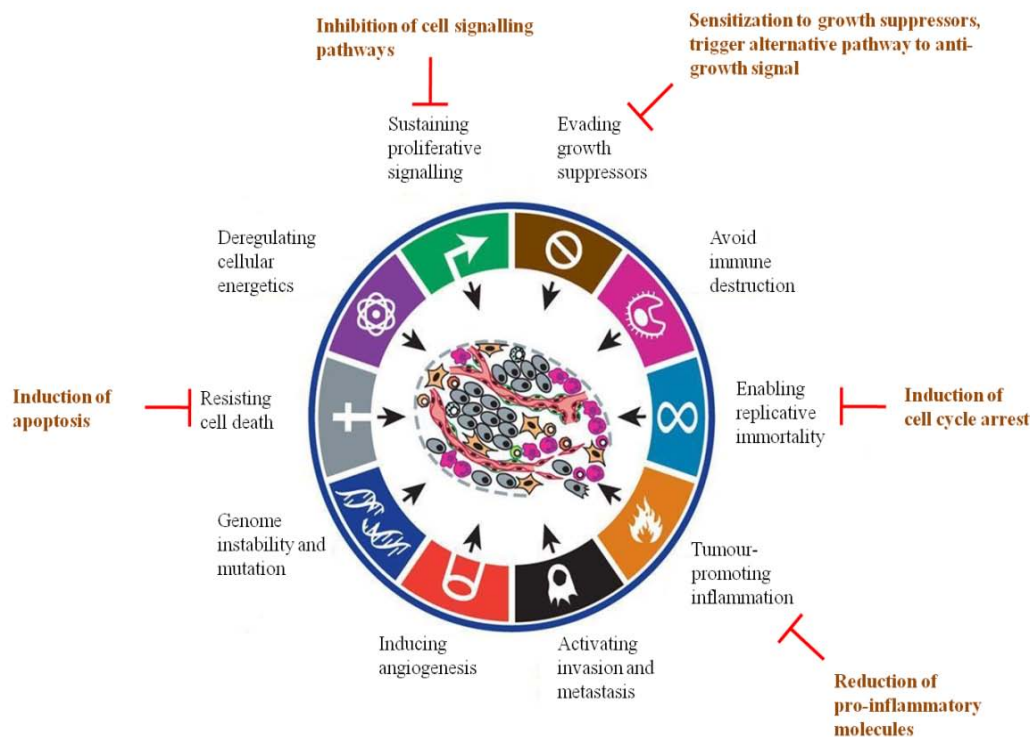


Figure 6.1 Effects of PMF on some of the hallmark chemopreventive mechanisms and pathways implicated in carcinogenesis.

PMF has shown to inhibit cell proliferation, induce cell cycle arrest, and stimulate apoptosis via several signalling pathways linked to Wnt, apoptosis, Stat3, PI3K/Akt./GSK3 $\beta$  and inflammation. These mechanistic pathways affected by PMF are marked by (T-bar). Adapted from (Hanahan and Weinberg, 2011).

Although care must be taken not to over-interpret the differences in gene expression observed between the three flavones, this study supports the tentative pharmacological corollary of the presence of hydroxy (apigenin), methoxy (PMF) or hydroxy and

methoxy (tricin) moieties in flavones. Overall, the findings suggest that tricetin and PMF are more efficacious than apigenin in eliciting anti-carcinogenic mechanisms.

The microarray analyses in this study generated a vast amount of data, particularly in terms of pathways and probable gene targets. These pathways and targets can be pursued further using kinase and phosphoprotein assays. For instance, a study could be undertaken to explore the putative tyrosine kinase inhibitory activity of flavones on the STAT pathway. An investigation on the effects of a combination of flavones such as PMF and apigenin, in the diet of an animal model *in vivo* may also yield interesting results, as shown by Hoensch et al (Hoensch et al., 2008). Recently, there is an emerging awareness of the relevance of intron microRNA contributing to carcinogenesis. A study on the effects of flavones such as PMF on the oncogenic activities of the introns in MCM7 would provide valuable information on gene targets such as MCM7 in cancer chemoprevention.

With a better understanding of the mechanisms of action of PMF, it might be possible in the future to optimise drug design to target genes of importance for CRC carcinogenesis with the aim of preventing the promotion and progression of the disease.

## 7 Appendices

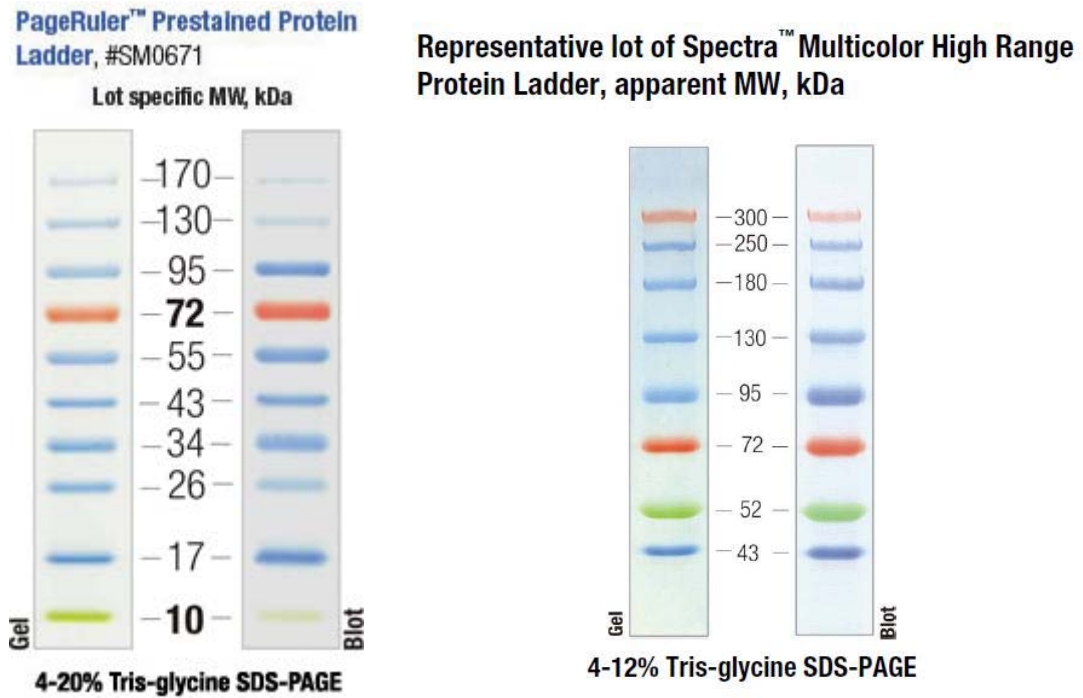


Figure 7.1 PageRuler™ Prestained Protein Ladder (left) and Spectra™ Multicolor High Range protein ladder (right) for WB.

## **8 Articles published**

### **8.1 Articles:**

Sale, S., I. L. Fong, et al. (2009). "APC10.1 cells as a model for assessing the efficacy of potential chemopreventive agents in the Apc(Min) mouse model in vivo." Eur J Cancer 45(16): 2731-5.

### **8.2 Abstracts and conference proceedings:**

Isabel Lim Fong, Jin-Li Luo, Kate M. Phillips, Timothy W. Gant, Andreas Gescher, Stewart Sale (2010) CRC chemopreventive mechanisms of 3', 4', 5', 5, 7-pentamethoxyflavone (PMF) 50th Anniversary meeting: Hallmarks of Cancer – from mechanisms to therapies.

## 9 References

- ABDEL-RAHMAN, W. M., LOHI, H., KNUUTILA, S. & PELTOMAKI, P. 2005. Restoring mismatch repair does not stop the formation of reciprocal translocations in the colon cancer cell line HCA7 but further destabilizes chromosome number. *Oncogene*, 24, 706-13.
- AL-MULLA, F., BITAR, M. S., AL-MAGHREBI, M., BEHBEHANI, A. I., AL-ALI, W., RATH, O., DOYLE, B., TAN, K. Y., PITT, A. & KOLCH, W. 2011. Raf kinase inhibitor protein RKIP enhances signaling by glycogen synthase kinase-3beta. *Cancer Res*, 71, 1334-43.
- ASANUMA, K., TSUJI, N., ENDOH, T., YAGIHASHI, A. & WATANABE, N. 2004. Survivin enhances Fas ligand expression via up-regulation of specificity protein 1-mediated gene transcription in colon cancer cells. *J Immunol*, 172, 3922-9.
- AU, A., LI, B., WANG, W., ROY, H., KOEHLER, K. & BIRT, D. 2006. Effect of dietary apigenin on colonic ornithine decarboxylase activity, aberrant crypt foci formation, and tumorigenesis in different experimental models. *Nutr Cancer*, 54, 243-51.
- BARAL, R., BOSE, A., RAY, C., PAUL, S., PAL, S., HAQUE, E., MISHRA, B., PAL, D., NAGPAL, J. K., PANDA, C. K. & DAS, B. R. 2009. Association of early phase of colorectal carcinogenesis with STAT3 activation and its relevance in apoptosis regulation. *Exp Mol Pathol*, 87, 36-41.
- BARBER, T. D., MCMANUS, K., YUEN, K. W., REIS, M., PARMIGIANI, G., SHEN, D., BARRETT, I., NOUHI, Y., SPENCER, F., MARKOWITZ, S., VELCULESCU, V. E., KINZLER, K. W., VOGELSTEIN, B., LENGAUER, C. & HIETER, P. 2008. Chromatid cohesion defects may underlie chromosome instability in human colorectal cancers. *Proc Natl Acad Sci U S A*, 105, 3443-8.
- BARKER, N., MORIN, P. J. & CLEVERS, H. 2000. The Yin-Yang of TCF/beta-catenin signaling. *Adv Cancer Res*, 77, 1-24.
- BARKER, N., RIDGWAY, R. A., VAN ES, J. H., VAN DE WETERING, M., BEGTHEL, H., VAN DEN BORN, M., DANENBERG, E., CLARKE, A. R., SANSOM, O. J. & CLEVERS, H. 2009. Crypt stem cells as the cells-of-origin of intestinal cancer. *Nature*, 457, 608-11.
- BARRE, B., AVRIL, S. & COQUERET, O. 2003. Opposite regulation of myc and p21waf1 transcription by STAT3 proteins. *J Biol Chem*, 278, 2990-6.
- BARTELS, C. L. & TSONGALIS, G. J. 2009. MicroRNAs: novel biomarkers for human cancer. *Clin Chem*, 55, 623-31.
- BEECHER, G. R. 2003. Overview of dietary flavonoids: nomenclature, occurrence and intake. *J Nutr*, 133, 3248S-3254S.
- BEHRENS, J., JERCHOW, B. A., WURTELE, M., GRIMM, J., ASBRAND, C., WIRTZ, R., KUHL, M., WEDLICH, D. & BIRCHMEIER, W. 1998. Functional interaction of an axin homolog, conductin, with beta-catenin, APC, and GSK3beta. *Science*, 280, 596-9.
- BELTRAMI, E., PLESCIA, J., WILKINSON, J. C., DUCKETT, C. S. & ALTIERI, D. C. 2004. Acute ablation of survivin uncovers p53-dependent mitotic checkpoint functions and control of mitochondrial apoptosis. *J Biol Chem*, 279, 2077-84.

- BEN-AMOTZ, O., ARBER, N. & KRAUS, S. 2010. Colorectal cancer chemoprevention: the potential of a selective approach. *Expert Rev Anticancer Ther*, 10, 1559-62.
- BENJAMINI, Y. & HOCHBERG, Y. 1995. Controlling the false discovery rate: a practical and powerful approach to multiple testing. *Journal of the Royal Statistical Society, Series B*, 57, 289-300.
- BERTAGNOLLI, M. M. 1999. APC and intestinal carcinogenesis. Insights from animal models. *Ann NY Acad Sci*, 889, 32-44.
- BESSON, A., DOWDY, S. F. & ROBERTS, J. M. 2008. CDK inhibitors: cell cycle regulators and beyond. *Dev Cell*, 14, 159-69.
- BOIVIN, G. P., WASHINGTON, K., YANG, K., WARD, J. M., PRETLOW, T. P., RUSSELL, R., BESSELS, D. G., GODFREY, V. L., DOETSCHMAN, T., DOVE, W. F., PITOT, H. C., HALBERG, R. B., ITZKOWITZ, S. H., GRODEN, J. & COFFEY, R. J. 2003. Pathology of mouse models of intestinal cancer: consensus report and recommendations. *Gastroenterology*, 124, 762-77.
- BOLSTER, D. R., CROZIER, S. J., KIMBALL, S. R. & JEFFERSON, L. S. 2002. AMP-activated protein kinase suppresses protein synthesis in rat skeletal muscle through down-regulated mammalian target of rapamycin (mTOR) signaling. *J Biol Chem*, 277, 23977-80.
- BOMMER, G. T., FENG, Y., IURA, A., GIORDANO, T. J., KUICK, R., KADIKOY, H., SIKORSKI, D., WU, R., CHO, K. R. & FEARON, E. R. 2009. IRS1 regulation by Wnt/beta-catenin signaling and varied contribution of IRS1 to the neoplastic phenotype. *J Biol Chem*, 285, 1928-38.
- BONOVAS, S., TSANTES, A., DROSOS, T. & SITARAS, N. M. 2008. Cancer chemoprevention: a summary of the current evidence. *Anticancer Res*, 28, 1857-66.
- BOS, J. L. 1988. The ras gene family and human carcinogenesis. *Mutat Res*, 195, 255-71.
- BOUSSEROUEL, S., KAUNTZ, H., GOSSE, F., BOUHADJAR, M., SOLER, L., MARESCAUX, J. & RAUL, F. 2010. Identification of gene expression profiles correlated to tumor progression in a preclinical model of colon carcinogenesis. *Int J Oncol*, 36, 1485-90.
- BOUSSEROUEL, S., LAMY, V., GOSSE, F., LOBSTEIN, A., MARESCAUX, J. & RAUL, F. 2011. Early modulation of gene expression used as a biomarker for chemoprevention in a preclinical model of colon carcinogenesis. *Pathol Int*, 61, 80-7.
- BRACKE, M., VYNCKE, B., OPDENAKKER, G., FOIDART, J. M., DE PESTEL, G. & MAREEL, M. 1991. Effect of catechins and citrus flavonoids on invasion in vitro. *Clin Exp Metastasis*, 9, 13-25.
- BRACKE, M. E., VYNCKE, B. M., VAN LAREBEKE, N. A., BRUYNEEL, E. A., DE BRUYNE, G. K., DE PESTEL, G. H., DE COSTER, W. J., ESPEEL, M. F. & MAREEL, M. M. 1989. The flavonoid tangeretin inhibits invasion of MO4 mouse cells into embryonic chick heart in vitro. *Clin Exp Metastasis*, 7, 283-300.
- BRATTAIN, M. G., FINE, W. D., KHALED, F. M., THOMPSON, J. & BRATTAIN, D. E. 1981. Heterogeneity of malignant cells from a human colonic carcinoma. *Cancer Res*, 41, 1751-6.

- BUCHSBAUM, S., MORRIS, C., BOCHARD, V. & JALINOT, P. 2007. Human INT6 interacts with MCM7 and regulates its stability during S phase of the cell cycle. *Oncogene*, 26, 5132-44.
- CAI, H., AL-FAYEZ, M., TUNSTALL, R. G., PLATTON, S., GREAVES, P., STEWARD, W. P. & GESCHER, A. J. 2005a. The rice bran constituent tricetin potently inhibits cyclooxygenase enzymes and interferes with intestinal carcinogenesis in ApcMin mice. *Mol Cancer Ther*, 4, 1287-92.
- CAI, H., BOOCOOCK, D. J., STEWARD, W. P. & GESCHER, A. J. 2007. Tissue distribution in mice and metabolism in murine and human liver of apigenin and tricetin, flavones with putative cancer chemopreventive properties. *Cancer Chemother Pharmacol*, 60, 257-66.
- CAI, H., BROWN, K., STEWARD, W. P. & GESCHER, A. J. 2009a. Determination of 3',4',5',5,7-pentamethoxyflavone in the plasma and intestinal mucosa of mice by HPLC with UV detection. *Biomed Chromatogr*.
- CAI, H., HUDSON, E. A., MANN, P., VERSCHOYLE, R. D., GREAVES, P., MANSON, M. M., STEWARD, W. P. & GESCHER, A. J. 2004. Growth-inhibitory and cell cycle-arresting properties of the rice bran constituent tricetin in human-derived breast cancer cells in vitro and in nude mice in vivo. *Br J Cancer*, 91, 1364-71.
- CAI, H., RAYNAUD, D., STEWARD, W. P. & GESCHER, A. J. 2006. A simple HPLC method for the determination of apigenin in mouse tissues. *Biomed Chromatogr*, 20, 1038-42.
- CAI, H., SALE, S., BRITTON, R. G., BROWN, K., STEWARD, W. P. & GESCHER, A. J. 2010. Pharmacokinetics in mice and metabolism in murine and human liver fractions of the putative cancer chemopreventive agents 3',4',5',5,7-pentamethoxyflavone and tricetin (4',5,7-trihydroxy-3',5'-dimethoxyflavone). *Cancer Chemother Pharmacol*, 67, 255-63.
- CAI, H., SALE, S., SCHMID, R., BRITTON, R. G., BROWN, K., STEWARD, W. P. & GESCHER, A. J. 2009b. Flavones as colorectal cancer chemopreventive agents--phenol-o-methylation enhances efficacy. *Cancer Prev Res (Phila Pa)*, 2, 743-50.
- CAI, H., STEWARD, W. P. & GESCHER, A. J. 2005b. Determination of the putative cancer chemopreventive flavone tricetin in plasma and tissues of mice by HPLC with UV--visible detection. *Biomed Chromatogr*, 19, 518-22.
- CAI, H., VERSCHOYLE, R. D., STEWARD, W. P. & GESCHER, A. J. 2003. Determination of the flavone tricetin in human plasma by high-performance liquid chromatography. *Biomed Chromatogr*, 17, 435-9.
- CALDWELL, G. M., JONES, C. E., SOON, Y., WARRACK, R., MORTON, D. G. & MATTHEWS, G. M. 2008. Reorganisation of Wnt-response pathways in colorectal tumorigenesis. *Br J Cancer*, 98, 1437-42.
- CANTLEY, L. C. 2002. The phosphoinositide 3-kinase pathway. *Science*, 296, 1655-7.
- CASTEDO, M., PERFETTINI, J. L., ROUMIER, T. & KROEMER, G. 2002a. Cyclin-dependent kinase-1: linking apoptosis to cell cycle and mitotic catastrophe. *Cell Death Differ*, 9, 1287-93.
- CASTEDO, M., ROUMIER, T., BLANCO, J., FERRI, K. F., BARRETINA, J., TINTIGNAC, L. A., ANDREAU, K., PERFETTINI, J. L., AMENDOLA, A., NARDACCI, R., LEDUC, P., INGBER, D. E., DRUILLENNEC, S., ROQUES, B., LEIBOVITCH, S. A., VILELLA-BACH, M., CHEN, J., ESTE, J. A., MODJTAHEDI, N., PIACENTINI, M. & KROEMER, G. 2002b. Sequential

- involvement of Cdk1, mTOR and p53 in apoptosis induced by the HIV-1 envelope. *EMBO J*, 21, 4070-80.
- CAVALLO, R. A., COX, R. T., MOLINE, M. M., ROOSE, J., POLEVOY, G. A., CLEVERS, H., PEIFER, M. & BEJSOVEC, A. 1998. Drosophila Tcf and Groucho interact to repress Wingless signalling activity. *Nature*, 395, 604-8.
- CAZAROLLI, L. H., FOLADOR, P., MORESCO, H. H., BRIGHENTE, I. M., PIZZOLATTI, M. G. & SILVA, F. R. 2009. Stimulatory effect of apigenin-6-C-beta-L-fucopyranoside on insulin secretion and glycogen synthesis. *Eur J Med Chem*, 44, 4668-73.
- CHEN, C., FU, X., ZHANG, D., LI, Y., XIE, Y. & HUANG, Y. 2011a. Varied Pathways of Stage IA Lung Adenocarcinomas Discovered by Integrated Gene Expression Analysis. *Int J Biol Sci*, 7, 551-66.
- CHEN, F. E., HUANG, D. B., CHEN, Y. Q. & GHOSH, G. 1998. Crystal structure of p50/p65 heterodimer of transcription factor NF-kappaB bound to DNA. *Nature*, 391, 410-3.
- CHEN, J., KATSIFIS, A., HU, C. & HUANG, X. F. 2011b. Insulin Decreases Therapeutic Efficacy in Colon Cancer Cell Line HT29 via the Activation of the PI3K/Akt Pathway. *Curr Drug Discov Technol*.
- CHEN, K. H., WENG, M. S. & LIN, J. K. 2007. Tangeretin suppresses IL-1beta-induced cyclooxygenase (COX)-2 expression through inhibition of p38 MAPK, JNK, and AKT activation in human lung carcinoma cells. *Biochem Pharmacol*, 73, 215-27.
- CHENG, L. & LAI, M. D. 2003. Aberrant crypt foci as microscopic precursors of colorectal cancer. *World J Gastroenterol*, 9, 2642-9.
- CHEUNG, K. L., KHOR, T. O., HUANG, M. T. & KONG, A. N. 2009. Differential in vivo mechanism of chemoprevention of tumor formation in azoxymethane/dextran sodium sulfate mice by PEITC and DBM. *Carcinogenesis*, 31, 880-5.
- CHIACCHIERA, F., MATRONE, A., FERRARI, E., INGRAVALLO, G., LO SASSO, G., MURZILLI, S., PETRUZZELLI, M., SALVATORE, L., MOSCHETTA, A. & SIMONE, C. 2009. p38alpha blockade inhibits colorectal cancer growth in vivo by inducing a switch from HIF1alpha- to FoxO-dependent transcription. *Cell Death Differ*, 16, 1203-14.
- CHIBAZAKURA, T., KAMACHI, K., OHARA, M., TANE, S., YOSHIKAWA, H. & ROBERTS, J. M. 2010. Cyclin A promotes S-phase entry via interaction with the replication licensing factor Mcm7. *Mol Cell Biol*, 31, 248-55.
- CHIPUK, J. E., BOUCHIER-HAYES, L. & GREEN, D. R. 2006. Mitochondrial outer membrane permeabilization during apoptosis: the innocent bystander scenario. *Cell Death Differ*, 13, 1396-402.
- CHIPUK, J. E. & GREEN, D. R. 2008. How do BCL-2 proteins induce mitochondrial outer membrane permeabilization? *Trends Cell Biol*, 18, 157-64.
- CHOI, J., PARK, S. Y., COSTANTINI, F., JHO, E. H. & JOO, C. K. 2004. Adenomatous polyposis coli is down-regulated by the ubiquitin-proteasome pathway in a process facilitated by Axin. *J Biol Chem*, 279, 49188-98.
- CHRISTMANN, M., TOMICIC, M. T., ROOS, W. P. & KAINA, B. 2003. Mechanisms of human DNA repair: an update. *Toxicology*, 193, 3-34.
- CHURCHILL, G. A. 2002. Fundamentals of experimental design for cDNA microarrays. *Nat Genet*, 32 Suppl, 490-5.

- CLEVERS, H. 2006. Wnt/beta-catenin signaling in development and disease. *Cell*, 127, 469-80.
- COLL, M. L., ROSEN, K., LADEDA, V. & FILMUS, J. 2002. Increased Bcl-xL expression mediates v-Src-induced resistance to anoikis in intestinal epithelial cells. *Oncogene*, 21, 2908-13.
- CONG, F., ZOU, X., HINRICHS, K., CALAME, K. & GOFF, S. P. 1999. Inhibition of v-Abl transformation by p53 and p19ARF. *Oncogene*, 18, 7731-9.
- COOPER, K., SQUIRES, H., CARROLL, C., PAPAIOANNOU, D., BOOTH, A., LOGAN, R. F., MAGUIRE, C., HIND, D. & TAPPENDEN, P. 2010. Chemoprevention of colorectal cancer: systematic review and economic evaluation. *Health Technol Assess*, 14, 1-206.
- CORPET, D. E. & PIERRE, F. 2003. Point: From animal models to prevention of colon cancer. Systematic review of chemoprevention in min mice and choice of the model system. *Cancer Epidemiol Biomarkers Prev*, 12, 391-400.
- CORPET, D. E. & PIERRE, F. 2005. How good are rodent models of carcinogenesis in predicting efficacy in humans? A systematic review and meta-analysis of colon chemoprevention in rats, mice and men. *Eur J Cancer*, 41, 1911-22.
- CORVINUS, F. M., ORTH, C., MORIGGL, R., TSAREVA, S. A., WAGNER, S., PFITZNER, E. B., BAUS, D., KAUFMANN, R., HUBER, L. A., ZATLOUKAL, K., BEUG, H., OHLSCHLAGER, P., SCHUTZ, A., HALBHUBER, K. J. & FRIEDRICH, K. 2005. Persistent STAT3 activation in colon cancer is associated with enhanced cell proliferation and tumor growth. *Neoplasia*, 7, 545-55.
- CRAVO, M., FIDALGO, P., PEREIRA, A. D., GOUVEIA-OLIVEIRA, A., CHAVES, P., SELHUB, J., MASON, J. B., MIRA, F. C. & LEITAO, C. N. 1994. DNA methylation as an intermediate biomarker in colorectal cancer: modulation by folic acid supplementation. *Eur J Cancer Prev*, 3, 473-9.
- CUDDAPAH, V. A. & SONTHEIMER, H. 2010. Molecular interaction and functional regulation of CIC-3 by Ca<sup>2+</sup>/calmodulin-dependent protein kinase II (CaMKII) in human malignant glioma. *J Biol Chem*, 285, 11188-96.
- CUTHBERT, A. W., KIRKLAND, S. C. & MACVINISH, L. J. 1985. Kinin effects on ion transport in monolayers of HCA-7 cells, a line from a human colonic adenocarcinoma. *Br J Pharmacol*, 86, 3-5.
- DAJANI, E. Z. & ISLAM, K. 2008. Cardiovascular and gastrointestinal toxicity of selective cyclo-oxygenase-2 inhibitors in man. *J Physiol Pharmacol*, 59 Suppl 2, 117-33.
- DATTA, S. 2005. Empirical Bayes screening of many p-values with applications to microarray studies. *Bioinformatics*, 21, 1987-94.
- DE FLORA, S. & FERGUSON, L. R. 2005. Overview of mechanisms of cancer chemopreventive agents. *Mutat Res*, 591, 8-15.
- DE GIOVANNI, C., LANDUZZI, L., NICOLETTI, G., ASTOLFI, A., CROCI, S., MICARONI, M., NANNI, P. & LOLLINI, P. L. 2004. Apc10.1: an ApcMin/+ intestinal cell line with retention of heterozygosity. *Int J Cancer*, 109, 200-6.
- DEBUCQUOY, A., DEVOS, E., VERMAELEN, P., LANDUYT, W., DE WEER, S., VAN DEN HEUVEL, F. & HAUSTERMANS, K. 2009. 18F-FLT and 18F-FDG PET to measure response to radiotherapy combined with celecoxib in two colorectal xenograft models. *Int J Radiat Biol*, 85, 763-71.
- DEL RIO, P., CRAFA, P., PAPADIA, C., DELL'ABATE, P., FRANZE, A., FRANZINI, G., CAMPANINI, N. & SIANESI, M. 2010. Evaluation of CD10

- positivity in colorectal polyps in neoplastic transformation. *Ann Ital Chir*, 81, 121-7.
- DELCOMMENNE, M., TAN, C., GRAY, V., RUE, L., WOODGETT, J. & DEDHAR, S. 1998. Phosphoinositide-3-OH kinase-dependent regulation of glycogen synthase kinase 3 and protein kinase B/AKT by the integrin-linked kinase. *Proc Natl Acad Sci U S A*, 95, 11211-6.
- DHANASEKARAN, S. M., BARRETTE, T. R., GHOSH, D., SHAH, R., VARAMBALLY, S., KURACHI, K., PIANTA, K. J., RUBIN, M. A. & CHINNAIYAN, A. M. 2001. Delineation of prognostic biomarkers in prostate cancer. *Nature*, 412, 822-6.
- DIBRA, H. K., BROWN, J. E., HOOLEY, P. & NICHOLL, I. D. 2010. Aspirin and alterations in DNA repair proteins in the SW480 colorectal cancer cell line. *Oncol Rep*, 24, 37-46.
- DIEHL, J. A., CHENG, M., ROUSSEL, M. F. & SHERR, C. J. 1998. Glycogen synthase kinase-3beta regulates cyclin D1 proteolysis and subcellular localization. *Genes Dev*, 12, 3499-511.
- DIEHL, J. A., ZINDY, F. & SHERR, C. J. 1997. Inhibition of cyclin D1 phosphorylation on threonine-286 prevents its rapid degradation via the ubiquitin-proteasome pathway. *Genes Dev*, 11, 957-72.
- DIHAL, A. A., VAN DER WOUDE, H., HENDRIKSEN, P. J., CHARIF, H., DEKKER, L. J., IJSSELSTIJN, L., DE BOER, V. C., ALINK, G. M., BURGERS, P. C., RIETJENS, I. M., WOUTERSEN, R. A. & STIERUM, R. H. 2008. Transcriptome and proteome profiling of colon mucosa from quercetin fed F344 rats point to tumor preventive mechanisms, increased mitochondrial fatty acid degradation and decreased glycolysis. *Proteomics*, 8, 45-61.
- DIHAL, A. A., WOUTERSEN, R. A., VAN OMMEN, B., RIETJENS, I. M. & STIERUM, R. H. 2006. Modulatory effects of quercetin on proliferation and differentiation of the human colorectal cell line Caco-2. *Cancer Lett*, 238, 248-59.
- DIPAOLA, R. S. 2002. To arrest or not to G(2)-M Cell-cycle arrest : commentary re: A. K. Tyagi et al., Silibinin strongly synergizes human prostate carcinoma DU145 cells to doxorubicin-induced growth inhibition, G(2)-M arrest, and apoptosis. *Clin. cancer res.*, 8: 3512-3519, 2002. *Clin Cancer Res*, 8, 3311-4.
- DOHI, T., BELTRAMI, E., WALL, N. R., PLESCIA, J. & ALTIERI, D. C. 2004. Mitochondrial survivin inhibits apoptosis and promotes tumorigenesis. *J Clin Invest*, 114, 1117-27.
- DOVE, W. F., GOULD, K. A., LUONGO, C., MOSER, A. R. & SHOEMAKER, A. R. 1995. Emergent issues in the genetics of intestinal neoplasia. *Cancer Surv*, 25, 335-55.
- DOVE, W. F., LUONGO, C., CONNELLY, C. S., GOULD, K. A., SHOEMAKER, A. R., MOSER, A. R. & GARDNER, R. L. 1994. The adenomatous polyposis coli gene of the mouse in development and neoplasia. *Cold Spring Harb Symp Quant Biol*, 59, 501-8.
- DU, L., SCHAGEMAN, J. J., IRNOV, GIRARD, L., HAMMOND, S. M., MINNA, J. D., GAZDAR, A. F. & PERTSEMLIDIS, A. 2010. MicroRNA expression distinguishes SCLC from NSCLC lung tumor cells and suggests a possible pathological relationship between SCLCs and NSCLCs. *J Exp Clin Cancer Res*, 29, 75.

- DU, X. L., YANG, H., LIU, S. G., LUO, M. L., HAO, J. J., ZHANG, Y., LIN, D. C., XU, X., CAI, Y., ZHAN, Q. M. & WANG, M. R. 2009. Calreticulin promotes cell motility and enhances resistance to anoikis through STAT3-CTTN-Akt pathway in esophageal squamous cell carcinoma. *Oncogene*, 28, 3714-22.
- EDELMANN, W., YANG, K., KURAGUCHI, M., HEYER, J., LIA, M., KNEITZ, B., FAN, K., BROWN, A. M., LIPKIN, M. & KUCHERLAPATI, R. 1999. Tumorigenesis in Mlh1 and Mlh1/Apc1638N mutant mice. *Cancer Res*, 59, 1301-7.
- ELMORE, S. 2007. Apoptosis: a review of programmed cell death. *Toxicol Pathol*, 35, 495-516.
- ESPINOSA, I., CATASUS, L., CANET, B., D'ANGELO, E., MUNOZ, J. & PRAT, J. 2011. Gene expression analysis identifies two groups of ovarian high-grade serous carcinomas with different prognosis. *Mod Pathol*.
- FAUSTINO, R. S., MADDAFORD, T. G. & PIERCE, G. N. 2010. Mitogen activated protein kinase at the nuclear pore complex. *J Cell Mol Med*, 15, 928-37.
- FEARON, E. R. & VOGELSTEIN, B. 1990. A genetic model for colorectal tumorigenesis. *Cell*, 61, 759-67.
- FENG, C. J., LI, H. J., LI, J. N., LU, Y. J. & LIAO, G. Q. 2008. Expression of Mcm7 and Cdc6 in oral squamous cell carcinoma and precancerous lesions. *Anticancer Res*, 28, 3763-9.
- FENTON, J. I., LAVIGNE, J. A., PERKINS, S. N., LIU, H., CHANDRAMOULI, G. V., SHIH, J. H., HORD, N. G. & HURSTING, S. D. 2008. Microarray analysis reveals that leptin induces autocrine/paracrine cascades to promote survival and proliferation of colon epithelial cells in an Apc genotype-dependent fashion. *Mol Carcinog*, 47, 9-21.
- FERGUSON, L. R. 1994. Antimutagens as cancer chemopreventive agents in the diet. *Mutat Res*, 307, 395-410.
- FERGUSON, L. R., BRONZETTI, G. & DE FLORA, S. 2005. Mechanistic approaches to chemoprevention of mutation and cancer. *Mutat Res*, 591, 3-7.
- FERLAY J, S. H., BRAY F, FORMAN D, MATHERS C AND PARKIN DM. 2008. GLOBOCAN 2008 Cancer Incidence and Mortality Worldwide in 2008. *IARC CancerBase No. 10* International Agency for Research on Cancer (World Health Organization).
- FERNANDEZ-SALGUERO, P. M. 2010. A remarkable new target gene for the dioxin receptor: The Vav3 proto-oncogene links AhR to adhesion and migration. *Cell Adh Migr*, 4, 172-5.
- FODDE, R. 2003. The multiple functions of tumour suppressors: it's all in APC. *Nat Cell Biol*, 5, 190-2.
- FODDE, R., EDELMANN, W., YANG, K., VAN LEEUWEN, C., CARLSON, C., RENAULT, B., BREUKEL, C., ALT, E., LIPKIN, M., KHAN, P. M. & ET AL. 1994. A targeted chain-termination mutation in the mouse Apc gene results in multiple intestinal tumors. *Proc Natl Acad Sci U S A*, 91, 8969-73.
- FODDE, R., KUIPERS, J., ROSENBERG, C., SMITS, R., KIELMAN, M., GASPAR, C., VAN ES, J. H., BREUKEL, C., WIEGANT, J., GILES, R. H. & CLEVERS, H. 2001. Mutations in the APC tumour suppressor gene cause chromosomal instability. *Nat Cell Biol*, 3, 433-8.
- FODDE, R. & SMITS, R. 2001. Disease model: familial adenomatous polyposis. *Trends Mol Med*, 7, 369-73.

- FUJITA, M., YAMADA, C., GOTO, H., YOKOYAMA, N., KUZUSHIMA, K., INAGAKI, M. & TSURUMI, T. 1999. Cell cycle regulation of human CDC6 protein. Intracellular localization, interaction with the human mcm complex, and CDC2 kinase-mediated hyperphosphorylation. *J Biol Chem*, 274, 25927-32.
- GAMAGE, N., BARNETT, A., HEMPEL, N., DUGGLEBY, R. G., WINDMILL, K. F., MARTIN, J. L. & MCMANUS, M. E. 2006. Human sulfotransferases and their role in chemical metabolism. *Toxicol Sci*, 90, 5-22.
- GARAY, C. A. & ENGSTROM, P. F. 1999. Chemoprevention of colorectal cancer: dietary and pharmacologic approaches. *Oncology (Williston Park)*, 13, 89-97; discussion 97-100, 105.
- GARCIA-HEREDIA, J. M., DIAZ-MORENO, I., NIETO, P. M., ORZAEZ, M., KOCANIS, S., TEIXEIRA, M., PEREZ-PAYA, E., DIAZ-QUINTANA, A. & DE LA ROSA, M. A. 2010. Nitration of tyrosine 74 prevents human cytochrome c to play a key role in apoptosis signaling by blocking caspase-9 activation. *Biochim Biophys Acta*, 1797, 981-93.
- GATENBY, R. A. & VINCENT, T. L. 2003. An evolutionary model of carcinogenesis. *Cancer Res*, 63, 6212-20.
- GAZIT, A., YANIV, A., BAFICO, A., PRAMILA, T., IGARASHI, M., KITAJEWSKI, J. & AARONSON, S. A. 1999. Human frizzled 1 interacts with transforming Wnts to transduce a TCF dependent transcriptional response. *Oncogene*, 18, 5959-66.
- GIAGINIS, C., VGENOPOULOU, S., VIELH, P. & THEOCHARIS, S. 2010. MCM proteins as diagnostic and prognostic tumor markers in the clinical setting. *Histol Histopathol*, 25, 351-70.
- GILES, R. H., LOLKEMA, M. P., SNIJCKERS, C. M., BELDERBOS, M., VAN DER GROEP, P., MANS, D. A., VAN BEEST, M., VAN NOORT, M., GOLDSCHMEDING, R., VAN DIEST, P. J., CLEVERS, H. & VOEST, E. E. 2006. Interplay between VHL/HIF1alpha and Wnt/beta-catenin pathways during colorectal tumorigenesis. *Oncogene*, 25, 3065-70.
- GLADDEN, A. B. & DIEHL, J. A. 2003. The cyclin D1-dependent kinase associates with the pre-replication complex and modulates RB.MCM7 binding. *J Biol Chem*, 278, 9754-60.
- GONZALEZ, M. A., TACHIBANA, K. E., LASKEY, R. A. & COLEMAN, N. 2005. Control of DNA replication and its potential clinical exploitation. *Nat Rev Cancer*, 5, 135-41.
- GREENWALD, P. 2002. Cancer chemoprevention. *BMJ*, 324, 714-8.
- GREENWOOD, J. & GAUTIER, J. 2005. From oogenesis through gastrulation: developmental regulation of apoptosis. *Semin Cell Dev Biol*, 16, 215-24.
- GUPTA, S., KASS, G. E., SZEGEZDI, E. & JOSEPH, B. 2009. The mitochondrial death pathway: a promising therapeutic target in diseases. *J Cell Mol Med*, 13, 1004-33.
- HANAHAHAN, D. & WEINBERG, R. A. 2000. The hallmarks of cancer. *Cell*, 100, 57-70.
- HANAHAHAN, D. & WEINBERG, R. A. 2011. Hallmarks of cancer: the next generation. *Cell*, 144, 646-74.
- HAVSTEEN, B. H. 2002. The biochemistry and medical significance of the flavonoids. *Pharmacol Ther*, 96, 67-202.
- HEEMERS, H. V., SCHMIDT, L. J., SUN, Z., REGAN, K. M., ANDERSON, S. K., DUNCAN, K., WANG, D., LIU, S., BALLMAN, K. V. & TINDALL, D. J.

2011. Identification of a clinically relevant androgen-dependent gene signature in prostate cancer. *Cancer Res*, 71, 1978-88.
- HEIJINK, D. M., FEHRMANN, R. S., DE VRIES, E. G., KOORNSTRA, J. J., OOSTERHUIS, D., VAN DER ZEE, A. G., KLEIBEUKER, J. H. & DE JONG, S. 2011. A bioinformatical and functional approach to identify novel strategies for chemoprevention of colorectal cancer. *Oncogene*, 30, 2026-36.
- HINOI, T., AKYOL, A., THEISEN, B. K., FERGUSON, D. O., GREENSON, J. K., WILLIAMS, B. O., CHO, K. R. & FEARON, E. R. 2007. Mouse model of colonic adenoma-carcinoma progression based on somatic Apc inactivation. *Cancer Res*, 67, 9721-30.
- HIRANO, T., ABE, K., GOTOH, M. & OKA, K. 1995. Citrus flavone tangeretin inhibits leukaemic HL-60 cell growth partially through induction of apoptosis with less cytotoxicity on normal lymphocytes. *Br J Cancer*, 72, 1380-8.
- HOENSCH, H., GROH, B., EDLER, L. & KIRCH, W. 2008. Prospective cohort comparison of flavonoid treatment in patients with resected colorectal cancer to prevent recurrence. *World J Gastroenterol*, 14, 2187-93.
- HOFSETH, L. J., HUSSAIN, S. P. & HARRIS, C. C. 2004. p53: 25 years after its discovery. *Trends Pharmacol Sci*, 25, 177-81.
- HOSACK, D. A., DENNIS, G., JR., SHERMAN, B. T., LANE, H. C. & LEMPICKI, R. A. 2003. Identifying biological themes within lists of genes with EASE. *Genome Biol*, 4, R70.
- HOWELLS, L. M., SALE, S., SRIRAMAREDDY, S. N., IRVING, G. R., JONES, D. J., OTTLEY, C. J., PEARSON, D. G., MANN, C. D., MANSON, M. M., BERRY, D. P., GESCHER, A., STEWARD, W. P. & BROWN, K. 2010. Curcumin ameliorates oxaliplatin-induced chemo-resistance in HCT116 colorectal cancer cells in vitro and in vivo. *Int J Cancer*.
- HUDSON, E. A., DINH, P. A., KOKUBUN, T., SIMMONDS, M. S. & GESCHER, A. 2000. Characterization of potentially chemopreventive phenols in extracts of brown rice that inhibit the growth of human breast and colon cancer cells. *Cancer Epidemiol Biomarkers Prev*, 9, 1163-70.
- HUELSKEN, J. & BEHRENS, J. 2002. The Wnt signalling pathway. *J Cell Sci*, 115, 3977-8.
- HUNG, K. E., MARICEVICH, M. A., RICHARD, L. G., CHEN, W. Y., RICHARDSON, M. P., KUNIN, A., BRONSON, R. T., MAHMOOD, U. & KUCHERLAPATI, R. 2010. Development of a mouse model for sporadic and metastatic colon tumors and its use in assessing drug treatment. *Proc Natl Acad Sci U S A*, 107, 1565-70.
- INOMATA, M., OCHIAI, A., AKIMOTO, S., KITANO, S. & HIROHASHI, S. 1996. Alteration of beta-catenin expression in colonic epithelial cells of familial adenomatous polyposis patients. *Cancer Res*, 56, 2213-7.
- IRELAND, H., KEMP, R., HOUGHTON, C., HOWARD, L., CLARKE, A. R., SANSOM, O. J. & WINTON, D. J. 2004. Inducible Cre-mediated control of gene expression in the murine gastrointestinal tract: effect of loss of beta-catenin. *Gastroenterology*, 126, 1236-46.
- ISHII, K., TANAKA, S., KAGAMI, K., HENMI, K., TOYODA, H., KAISE, T. & HIRANO, T. 2009. Effects of naturally occurring polymethoxyflavonoids on cell growth, p-glycoprotein function, cell cycle, and apoptosis of daunorubicin-resistant T lymphoblastoid leukemia cells. *Cancer Invest*, 28, 220-9.

- ITOH, N., SEMBA, S., ITO, M., TAKEDA, H., KAWATA, S. & YAMAKAWA, M. 2002. Phosphorylation of Akt/PKB is required for suppression of cancer cell apoptosis and tumor progression in human colorectal carcinoma. *Cancer*, 94, 3127-34.
- ITZKOWITZ, S. H. & YIO, X. 2004. Inflammation and cancer IV. Colorectal cancer in inflammatory bowel disease: the role of inflammation. *Am J Physiol Gastrointest Liver Physiol*, 287, G7-17.
- JAMALI, T., JAMALI, Y., MEHRBOD, M. & MOFRAD, M. R. 2011. Nuclear pore complex: biochemistry and biophysics of nucleocytoplasmic transport in health and disease. *Int Rev Cell Mol Biol*, 287, 233-86.
- JEON, J., PARK, K. A., LEE, H., SHIN, S., ZHANG, T., WON, M., YOON, H. K., CHOI, M. K., KIM, H. G., SON, C. G., HONG, J. H. & HUR, G. M. 2011. Water extract of *Cynanchi atrati Radix* regulates inflammation and apoptotic cell death through suppression of IKK-mediated NF-kappaB signaling. *J Ethnopharmacol*, 137, 626-34.
- JIRMANOVA, L., AFANASSIEFF, M., GOBERT-GOSSE, S., MARKOSSIAN, S. & SAVATIER, P. 2002. Differential contributions of ERK and PI3-kinase to the regulation of cyclin D1 expression and to the control of the G1/S transition in mouse embryonic stem cells. *Oncogene*, 21, 5515-28.
- JOHNSON, S. M., GULHATI, P., ARRIETA, I., WANG, X., UCHIDA, T., GAO, T. & EVERS, B. M. 2009. Curcumin inhibits proliferation of colorectal carcinoma by modulating Akt/mTOR signaling. *Anticancer Res*, 29, 3185-90.
- KAHN, M. J. & MORRISON, D. G. 1997. Chemoprevention for colorectal carcinoma. *Hematol Oncol Clin North Am*, 11, 779-94.
- KANG, M., MORSY, N., JIN, X., LUPU, F. & AKBARALI, H. I. 2004. Protein and gene expression of Ca<sup>2+</sup> channel isoforms in murine colon: effect of inflammation. *Pflugers Arch*, 449, 288-97.
- KANG, N. J., SHIN, S. H., LEE, H. J. & LEE, K. W. 2011. Polyphenols as small molecular inhibitors of signaling cascades in carcinogenesis. *Pharmacol Ther*, 130, 310-24.
- KATOH, M. 2006. Cross-talk of WNT and FGF signaling pathways at GSK3beta to regulate beta-catenin and SNAIL signaling cascades. *Cancer Biol Ther*, 5, 1059-64.
- KAUR, P., SHUKLA, S. & GUPTA, S. 2008. Plant flavonoid apigenin inactivates Akt to trigger apoptosis in human prostate cancer: an in vitro and in vivo study. *Carcinogenesis*, 29, 2210-7.
- KAWAII, S., TOMONO, Y., KATASE, E., OGAWA, K. & YANO, M. 1999. Antiproliferative activity of flavonoids on several cancer cell lines. *Biosci Biotechnol Biochem*, 63, 896-9.
- KAWASAKI, H., TOYODA, M., SHINOHARA, H., OKUDA, J., WATANABE, I., YAMAMOTO, T., TANAKA, K., TENJO, T. & TANIGAWA, N. 2001. Expression of survivin correlates with apoptosis, proliferation, and angiogenesis during human colorectal tumorigenesis. *Cancer*, 91, 2026-32.
- KEARSEY, S. E. & LABIB, K. 1998. MCM proteins: evolution, properties, and role in DNA replication. *Biochim Biophys Acta*, 1398, 113-36.
- KERR, M. K. & CHURCHILL, G. A. 2001. Statistical design and the analysis of gene expression microarray data. *Genet Res*, 77, 123-8.
- KERR, M. K., MARTIN, M. & CHURCHILL, G. A. 2000. Analysis of variance for gene expression microarray data. *J Comput Biol*, 7, 819-37.

- KHAN, J., SAAL, L. H., BITTNER, M. L., CHEN, Y., TRENT, J. M. & MELTZER, P. S. 1999. Expression profiling in cancer using cDNA microarrays. *Electrophoresis*, 20, 223-9.
- KIARIS, H. & SCHALLY, A. V. 1999. Apoptosis versus necrosis: which should be the aim of cancer therapy? *Proc Soc Exp Biol Med*, 221, 87-8.
- KIM, D. I., LEE, T. K., LIM, I. S., KIM, H., LEE, Y. C. & KIM, C. H. 2005. Regulation of IGF-I production and proliferation of human leiomyomal smooth muscle cells by *Scutellaria barbata* D. Don in vitro: isolation of flavonoids of apigenin and luteolin as acting compounds. *Toxicol Appl Pharmacol*, 205, 213-24.
- KIM, H. S., KANG, S. H., PARK, C. H., YANG, W. I., JEUNG, H. C., CHUNG, H. C., ROH, J. K., AHN, J. B., KIM, N. K., MIN, B. S. & RHA, S. Y. 2011. Genome-wide molecular characterization of mucinous colorectal adenocarcinoma using cDNA microarray analysis. *Oncol Rep*, 25, 717-27.
- KINOSHITA, T. & FIRMAN, K. 1997. Myricetin 5,7,3',4',5'-pentamethyl ether and other methylated flavonoids from *Murraya paniculata*. *Phytochemistry*, 45, 179-181.
- KINZLER, K. W. & VOGELSTEIN, B. 1996. Lessons from hereditary colorectal cancer. *Cell*, 87, 159-70.
- KISHIDA, S., YAMAMOTO, H., HINO, S., IKEDA, S., KISHIDA, M. & KIKUCHI, A. 1999. DIX domains of Dvl and axin are necessary for protein interactions and their ability to regulate beta-catenin stability. *Mol Cell Biol*, 19, 4414-22.
- KLAMPFER, L., HUANG, J., SASAZUKI, T., SHIRASAWA, S. & AUGENLICHT, L. 2004. Oncogenic Ras promotes butyrate-induced apoptosis through inhibition of gelsolin expression. *J Biol Chem*, 279, 36680-8.
- KNOWLES, L. M. & MILNER, J. A. 2000. Diallyl disulfide inhibits p34(cdc2) kinase activity through changes in complex formation and phosphorylation. *Carcinogenesis*, 21, 1129-34.
- KUNTZ, S., WENZEL, U. & DANIEL, H. 1999. Comparative analysis of the effects of flavonoids on proliferation, cytotoxicity, and apoptosis in human colon cancer cell lines. *Eur J Nutr*, 38, 133-42.
- KUSABA, T., NAKAYAMA, T., YAMAZUMI, K., YAKATA, Y., YOSHIZAKI, A., INOUE, K., NAGAYASU, T. & SEKINE, I. 2006. Activation of STAT3 is a marker of poor prognosis in human colorectal cancer. *Oncol Rep*, 15, 1445-51.
- LAMLUM, H., AL TASSAN, N., JAEGER, E., FRAYLING, I., SIEBER, O., REZA, F. B., ECKERT, M., ROWAN, A., BARCLAY, E., ATKIN, W., WILLIAMS, C., GILBERT, J., CHEADLE, J., BELL, J., HOULSTON, R., BODMER, W., SAMPSON, J. & TOMLINSON, I. 2000a. Germline APC variants in patients with multiple colorectal adenomas, with evidence for the particular importance of E1317Q. *Hum Mol Genet*, 9, 2215-21.
- LAMLUM, H., PAPADOPOULOU, A., ILYAS, M., ROWAN, A., GILLET, C., HANBY, A., TALBOT, I., BODMER, W. & TOMLINSON, I. 2000b. APC mutations are sufficient for the growth of early colorectal adenomas. *Proc Natl Acad Sci U S A*, 97, 2225-8.
- LEE, G., GORETSKY, T., MANAGLIA, E., DIRISINA, R., SINGH, A. P., BROWN, J. B., MAY, R., YANG, G. Y., RAGHEB, J. W., EVERS, B. M., WEBER, C. R., TURNER, J. R., HE, X. C., KATZMAN, R. B., LI, L. & BARRETT, T. A. 2010. Phosphoinositide 3-kinase signaling mediates beta-catenin activation in

- intestinal epithelial stem and progenitor cells in colitis. *Gastroenterology*, 139, 869-81, 881 e1-9.
- LEE, S. W., LEE, J. T., LEE, M. G., LEE, H. W., AHN, S. J., LEE, Y. J., LEE, Y. L., YOO, J., AHN, B. C. & HA, J. H. 2009. In vitro antiproliferative characteristics of flavonoids and diazepam on SNU-C4 colorectal adenocarcinoma cells. *Nat Med (Tokyo)*, 63, 124-9.
- LEFORT, E. C. & BLAY, J. 2011. The dietary flavonoid apigenin enhances the activities of the anti-metastatic protein CD26 on human colon carcinoma cells. *Clin Exp Metastasis*, 28, 337-49.
- LEOW, C. C., POLAKIS, P. & GAO, W. Q. 2005. A role for Hath1, a bHLH transcription factor, in colon adenocarcinoma. *Ann N Y Acad Sci*, 1059, 174-83.
- LESLIE, A., CAREY, F. A., PRATT, N. R. & STEELE, R. J. 2002. The colorectal adenoma-carcinoma sequence. *Br J Surg*, 89, 845-60.
- LI, Y., YANG, K. J. & PARK, J. 2011. Multiple implications of 3-phosphoinositide-dependent protein kinase 1 in human cancer. *World J Biol Chem*, 1, 239-47.
- LINK, A., BALAGUER, F., SHEN, Y., NAGASAKA, T., LOZANO, J. J., BOLAND, C. R. & GOEL, A. 2010. Fecal MicroRNAs as novel biomarkers for colon cancer screening. *Cancer Epidemiol Biomarkers Prev*, 19, 1766-74.
- LIU, X., WANG, J., SUN, B., ZHANG, Y., ZHU, J. & LI, C. 2007. Cell growth inhibition, G2M cell cycle arrest, and apoptosis induced by the novel compound Alternol in human gastric carcinoma cell line MGC803. *Invest New Drugs*, 25, 505-17.
- LOWE, S. W., CEPERO, E. & EVAN, G. 2004. Intrinsic tumour suppression. *Nature*, 432, 307-15.
- LUO, J. H. 2011. Oncogenic activity of MCM7 transforming cluster. *World J Clin Oncol*, 2, 120-4.
- LUONGO, C., MOSER, A. R., GLEDHILL, S. & DOVE, W. F. 1994. Loss of Apc<sup>+</sup> in intestinal adenomas from Min mice. *Cancer Res*, 54, 5947-52.
- LUTZ, W. K. & FEKETE, T. 1996. Endogenous and exogenous factors in carcinogenesis: limits to cancer prevention. *Int Arch Occup Environ Health*, 68, 120-5.
- LYNCH, H. T., KIMBERLING, W., ALBANO, W. A., LYNCH, J. F., BISCONE, K., SCHUELKE, G. S., SANDBERG, A. A., LIPKIN, M., DESCHNER, E. E., MIKOL, Y. B. & ET AL. 1985. Hereditary nonpolyposis colorectal cancer (Lynch syndromes I and II). I. Clinical description of resource. *Cancer*, 56, 934-8.
- LYNCH, P. M. 2008. Chemoprevention with special reference to inherited colorectal cancer. *Fam Cancer*, 7, 59-64.
- MA, X. T., WANG, S., YE, Y. J., DU, R. Y., CUI, Z. R. & SOMSOUK, M. 2004. Constitutive activation of Stat3 signaling pathway in human colorectal carcinoma. *World J Gastroenterol*, 10, 1569-73.
- MALINOWSKI, D. P. 2007. Multiple biomarkers in molecular oncology. II. Molecular diagnostics applications in breast cancer management. *Expert Rev Mol Diagn*, 7, 269-80.
- MANACH, C., SCALBERT, A., MORAND, C., REMESY, C. & JIMENEZ, L. 2004. Polyphenols: food sources and bioavailability. *Am J Clin Nutr*, 79, 727-47.
- MANACH, C., WILLIAMSON, G., MORAND, C., SCALBERT, A. & REMESY, C. 2005. Bioavailability and bioefficacy of polyphenols in humans. I. Review of 97 bioavailability studies. *Am J Clin Nutr*, 81, 230S-242S.

- MARTY, G. D. 2007. Blank-field correction for achieving a uniform white background in brightfield digital photomicrographs. *Biotechniques*, 42, 716, 718, 720.
- MATSUYAMA, T., ISHIKAWA, T., MOGUSHI, K., YOSHIDA, T., IIDA, S., UETAKE, H., MIZUSHIMA, H., TANAKA, H. & SUGIHARA, K. 2010. MUC12 mRNA expression is an independent marker of prognosis in stage II and stage III colorectal cancer. *Int J Cancer*, 127, 2292-9.
- MAYER, S. I., MULLER, I., MANNEBACH, S., ENDO, T. & THIEL, G. 2011. Signal transduction of pregnenolone sulfate in insulinoma cells: activation of Egr-1 expression involving TRPM3, voltage-gated calcium channels, ERK, and ternary complex factors. *J Biol Chem*, 286, 10084-96.
- MCCART, A. E., VICKARYOUS, N. K. & SILVER, A. 2008. Apc mice: models, modifiers and mutants. *Pathol Res Pract*, 204, 479-90.
- MCCONNELL, B. B., BIALKOWSKA, A. B., NANDAN, M. O., GHALEB, A. M., GORDON, F. J. & YANG, V. W. 2009. Haploinsufficiency of Kruppel-like factor 5 rescues the tumor-initiating effect of the Apc(Min) mutation in the intestine. *Cancer Res*, 69, 4125-33.
- MCVEAN, M., WEINBERG, W. C. & PELLING, J. C. 2002. A p21(waf1)-independent pathway for inhibitory phosphorylation of cyclin-dependent kinase p34(cdc2) and concomitant G(2)/M arrest by the chemopreventive flavonoid apigenin. *Mol Carcinog*, 33, 36-43.
- MEERAN, S. M. & KATIYAR, S. K. 2008. Cell cycle control as a basis for cancer chemoprevention through dietary agents. *Front Biosci*, 13, 2191-202.
- MELSTROM, L. G., SALABAT, M. R., DING, X. Z., STROUCH, M. J., GRIPPO, P. J., MIRZOEVA, S., PELLING, J. C. & BENTREM, D. J. 2011. Apigenin down-regulates the hypoxia response genes: HIF-1alpha, GLUT-1, and VEGF in human pancreatic cancer cells. *J Surg Res*, 167, 173-81.
- MENDRICK, D. L. 2011. Transcriptional profiling to identify biomarkers of disease and drug response. *Pharmacogenomics*, 12, 235-49.
- MIEAN, K. H. & MOHAMED, S. 2001. Flavonoid (myricetin, quercetin, kaempferol, luteolin, and apigenin) content of edible tropical plants. *J Agric Food Chem*, 49, 3106-12.
- MOOLENBEEK, C. & RUITENBERG, E. J. 1981. The "Swiss roll": a simple technique for histological studies of the rodent intestine. *Lab Anim*, 15, 57-9.
- MORAIS, M. C., LUQMAN, S., KONDRATYUK, T. P., PETRONIO, M. S., REGASINI, L. O., SILVA, D. H., BOLZANI, V. S., SOARES, C. P. & PEZZUTO, J. M. 2010. Suppression of TNF-alpha induced NFkappaB activity by gallic acid and its semi-synthetic esters: possible role in cancer chemoprevention. *Nat Prod Res*, 24, 1758-65.
- MORIN, P. J., VOGELSTEIN, B. & KINZLER, K. W. 1996. Apoptosis and APC in colorectal tumorigenesis. *Proc Natl Acad Sci U S A*, 93, 7950-4.
- MORTENSEN, A., SORENSEN, I. K., WILDE, C., DRAGONI, S., MULLEROVA, D., TOUSSAINT, O., ZLOCH, Z., SGARAGLI, G. & OVESNA, J. 2008. Biological models for phytochemical research: from cell to human organism. *Br J Nutr*, 99 E Suppl 1, ES118-26.
- MOSER, A. R., DOVE, W. F., ROTH, K. A. & GORDON, J. I. 1992. The Min (multiple intestinal neoplasia) mutation: its effect on gut epithelial cell differentiation and interaction with a modifier system. *J Cell Biol*, 116, 1517-26.

- MOSER, A. R., LUONGO, C., GOULD, K. A., MCNELEY, M. K., SHOEMAKER, A. R. & DOVE, W. F. 1995a. ApcMin: a mouse model for intestinal and mammary tumorigenesis. *Eur J Cancer*, 31A, 1061-4.
- MOSER, A. R., PITOT, H. C. & DOVE, W. F. 1990. A dominant mutation that predisposes to multiple intestinal neoplasia in the mouse. *Science*, 247, 322-4.
- MOSER, A. R., SHOEMAKER, A. R., CONNELLY, C. S., CLIPSON, L., GOULD, K. A., LUONGO, C., DOVE, W. F., SIGGERS, P. H. & GARDNER, R. L. 1995b. Homozygosity for the Min allele of Apc results in disruption of mouse development prior to gastrulation. *Dev Dyn*, 203, 422-33.
- MURPHY, D. 2002. Gene expression studies using microarrays: principles, problems, and prospects. *Adv Physiol Educ*, 26, 256-70.
- MURPHY, L. L. & HUGHES, C. C. 2002. Endothelial cells stimulate T cell NFAT nuclear translocation in the presence of cyclosporin A: involvement of the wnt/glycogen synthase kinase-3 beta pathway. *J Immunol*, 169, 3717-25.
- NAMBIAR, P. R., NAKANISHI, M., GUPTA, R., CHEUNG, E., FIROUZI, A., MA, X. J., FLYNN, C., DONG, M., GUDA, K., LEVINE, J., RAJA, R., ACHENIE, L. & ROSENBERG, D. W. 2004. Genetic signatures of high- and low-risk aberrant crypt foci in a mouse model of sporadic colon cancer. *Cancer Res*, 64, 6394-401.
- NANDAN, M. O. & YANG, V. W. 2010. Genetic and Chemical Models of Colorectal Cancer in Mice. *Curr Colorectal Cancer Rep*, 6, 51-59.
- NEGRE, N., HENNETIN, J., SUN, L. V., LAVROV, S., BELLIS, M., WHITE, K. P. & CAVALLI, G. 2006. Chromosomal distribution of PcG proteins during Drosophila development. *PLoS Biol*, 4, e170.
- NEISE, D., SOHN, D., BUDACH, W. & JANICKE, R. U. 2010. Evidence for a differential modulation of p53-phosphorylating kinases by the cyclin-dependent kinase inhibitor p21WAF1/CIP1. *Cell Cycle*, 9, 3575-83.
- NEVINS, J. R. 2001. The Rb/E2F pathway and cancer. *Hum Mol Genet*, 10, 699-703.
- NISHIHARA, K., SHOMORI, K., FUJIOKA, S., TOKUYASU, N., INABA, A., OSAKI, M., OGAWA, T. & ITO, H. 2008. Minichromosome maintenance protein 7 in colorectal cancer: implication of prognostic significance. *Int J Oncol*, 33, 245-51.
- NISHIHARA, K., SHOMORI, K., TAMURA, T., FUJIOKA, S., OGAWA, T. & ITO, H. 2009. Immunohistochemical expression of geminin in colorectal cancer: Implication of prognostic significance. *Oncol Rep*, 21, 1189-95.
- NORBURY, C. & NURSE, P. 1992. Animal cell cycles and their control. *Annu Rev Biochem*, 61, 441-70.
- NORBURY, C. J. & HICKSON, I. D. 2001. Cellular responses to DNA damage. *Annu Rev Pharmacol Toxicol*, 41, 367-401.
- NORTHOVER, J. M. & MURDAY, V. 1989. Familial colorectal cancer and familial adenomatous polyposis. *Baillieres Clin Gastroenterol*, 3, 593-613.
- NOVAK, A. & DEDHAR, S. 1999. Signaling through beta-catenin and Lef/Tcf. *Cell Mol Life Sci*, 56, 523-37.
- ORTEGA, S., MALUMBRES, M. & BARBACID, M. 2002. Cyclin D-dependent kinases, INK4 inhibitors and cancer. *Biochim Biophys Acta*, 1602, 73-87.
- OSAKI, M., OSHIMURA, M. & ITO, H. 2004. PI3K-Akt pathway: its functions and alterations in human cancer. *Apoptosis*, 9, 667-76.

- OSHIMA, H., OSHIMA, M., KOBAYASHI, M., TSUTSUMI, M. & TAKETO, M. M. 1997. Morphological and molecular processes of polyp formation in Apc(delta716) knockout mice. *Cancer Res*, 57, 1644-9.
- OTAKE, Y., HSIEH, F. & WALLE, T. 2002. Glucuronidation versus oxidation of the flavonoid galangin by human liver microsomes and hepatocytes. *Drug Metab Dispos*, 30, 576-81.
- OYAMA, T., YASUI, Y., SUGIE, S., KOKETSU, M., WATANABE, K. & TANAKA, T. 2009. Dietary tricetin suppresses inflammation-related colon carcinogenesis in male Crj: CD-1 mice. *Cancer Prev Res (Phila Pa)*, 2, 1031-8.
- PALMER, T. H., JR. 1982. Gardner's syndrome: six generations. *Am J Surg*, 143, 405-8.
- PAN, M. H., CHEN, W. J., LIN-SHIAU, S. Y., HO, C. T. & LIN, J. K. 2002. Tangeretin induces cell-cycle G1 arrest through inhibiting cyclin-dependent kinases 2 and 4 activities as well as elevating Cdk inhibitors p21 and p27 in human colorectal carcinoma cells. *Carcinogenesis*, 23, 1677-84.
- PAN, M. H., LAI, C. S., WU, J. C. & HO, C. T. 2011. Molecular mechanisms for chemoprevention of colorectal cancer by natural dietary compounds. *Mol Nutr Food Res*, 55, 32-45.
- PATEL, D., SHUKLA, S. & GUPTA, S. 2007. Apigenin and cancer chemoprevention: progress, potential and promise (review). *Int J Oncol*, 30, 233-45.
- PEDRETTI, S. & RADDATZ, E. 2011. STAT3alpha interacts with nuclear GSK3beta and cytoplasmic RISK pathway and stabilizes rhythm in the anoxic-reoxygenated embryonic heart. *Basic Res Cardiol*, 106, 355-69.
- PERKINS, S., VERSCHOYLE, R. D., HILL, K., PARVEEN, I., THREADGILL, M. D., SHARMA, R. A., WILLIAMS, M. L., STEWARD, W. P. & GESCHER, A. J. 2002. Chemopreventive efficacy and pharmacokinetics of curcumin in the min/+ mouse, a model of familial adenomatous polyposis. *Cancer Epidemiol Biomarkers Prev*, 11, 535-40.
- PERSE, M. & CERAR, A. 2011. Morphological and molecular alterations in 1,2 dimethylhydrazine and azoxymethane induced colon carcinogenesis in rats. *J Biomed Biotechnol*, 2011, 473964.
- PICHOT, C. S., ARVANITIS, C., HARTIG, S. M., JENSEN, S. A., BECHILL, J., MARZOUK, S., YU, J., FROST, J. A. & COREY, S. J. 2010. Cdc42-interacting protein 4 promotes breast cancer cell invasion and formation of invadopodia through activation of N-WASp. *Cancer Res*, 70, 8347-56.
- PILLAIRE, M. J., SELVES, J., GORDIEN, K., GOURRAUD, P. A., GENTIL, C., DANJOUX, M., DO, C., NEGRE, V., BIETH, A., GUIMBAUD, R., TROUCHE, D., PASERO, P., MECHALI, M., HOFFMANN, J. S. & CAZAUX, C. 2010. A 'DNA replication' signature of progression and negative outcome in colorectal cancer. *Oncogene*, 29, 876-87.
- PIMENTEL-NUNES, P., GONCALVES, N., BOAL-CARVALHO, I., AFONSO, L., LOPES, P., RONCON-ALBUQUERQUE, R., JR., SOARES, J. B., CARDOSO, E., HENRIQUE, R., MOREIRA-DIAS, L., DINIS-RIBEIRO, M. & LEITE-MOREIRA, A. F. 2012. Decreased Toll-interacting protein and peroxisome proliferator-activated receptor gamma are associated with increased expression of Toll-like receptors in colon carcinogenesis. *J Clin Pathol*.
- PINE, P. S., BOEDIGHEIMER, M., ROSENZWEIG, B. A., TURPAZ, Y., HE, Y. D., DELENSTARR, G., GANTER, B., JARNAGIN, K., JONES, W. D., REID, L. H. & THOMPSON, K. L. 2008. Use of diagnostic accuracy as a metric for

- evaluating laboratory proficiency with microarray assays using mixed-tissue RNA reference samples. *Pharmacogenomics*, 9, 1753-63.
- PINTO, D., GREGORIEFF, A., BEGTHEL, H. & CLEVERS, H. 2003. Canonical Wnt signals are essential for homeostasis of the intestinal epithelium. *Genes Dev*, 17, 1709-13.
- POTTER, J. D. & STEINMETZ, K. 1996. Vegetables, fruit and phytoestrogens as preventive agents. *IARC Sci Publ*, 61-90.
- POWELL, S. M., ZILZ, N., BEAZER-BARCLAY, Y., BRYAN, T. M., HAMILTON, S. R., THIBODEAU, S. N., VOGELSTEIN, B. & KINZLER, K. W. 1992. APC mutations occur early during colorectal tumorigenesis. *Nature*, 359, 235-7.
- PRENDERGAST, G. C. 1999. Mechanisms of apoptosis by c-Myc. *Oncogene*, 18, 2967-87.
- PRESTON, S. L., LEEDHAM, S. J., OUKRIF, D., DEHEREGODA, M., GOODLAD, R. A., POULSOM, R., ALISON, M. R., WRIGHT, N. A. & NOVELLI, M. 2008. The development of duodenal microadenomas in FAP patients: the human correlate of the Min mouse. *J Pathol*, 214, 294-301.
- RAJAMANICKAM, S., VELMURUGAN, B., KAUR, M., SINGH, R. P. & AGARWAL, R. 2010. Chemoprevention of intestinal tumorigenesis in APCmin/+ mice by silibinin. *Cancer Res*, 70, 2368-78.
- RAM, P. T. & IYENGAR, R. 2001. G protein coupled receptor signaling through the Src and Stat3 pathway: role in proliferation and transformation. *Oncogene*, 20, 1601-6.
- RATTY, A. K. & DAS, N. P. 1988. Effects of flavonoids on nonenzymatic lipid peroxidation: structure-activity relationship. *Biochem Med Metab Biol*, 39, 69-79.
- REYNOLDS, J. V., DONOHOE, C. L. & DOYLE, S. L. 2011. Diet, obesity and cancer. *Ir J Med Sci*, 180, 521-7.
- ROBANUS-MAANDAG, E. C., KOELINK, P. J., BREUKEL, C., SALVATORI, D. C., JAGMOHAN-CHANGUR, S. C., BOSCH, C. A., VERSPAGET, H. W., DEVILEE, P., FODDE, R. & SMITS, R. 2010. A new conditional Apc-mutant mouse model for colorectal cancer. *Carcinogenesis*, 31, 946-52.
- SAITOH, T., MINE, T. & KATOH, M. 2002a. Expression and regulation of WNT8A and WNT8B mRNAs in human tumor cell lines: up-regulation of WNT8B mRNA by beta-estradiol in MCF-7 cells, and down-regulation of WNT8A and WNT8B mRNAs by retinoic acid in NT2 cells. *Int J Oncol*, 20, 999-1003.
- SAITOH, T., MINE, T. & KATOH, M. 2002b. Up-regulation of WNT8B mRNA in human gastric cancer. *Int J Oncol*, 20, 343-8.
- SALE, S., FONG, I. L., DE GIOVANNI, C., LANDUZZI, L., BROWN, K., STEWARD, W. P. & GESCHER, A. J. 2009. APC10.1 cells as a model for assessing the efficacy of potential chemopreventive agents in the Apc(Min) mouse model in vivo. *Eur J Cancer*, 45, 2731-5.
- SANSOM, O. J., REED, K. R., HAYES, A. J., IRELAND, H., BRINKMANN, H., NEWTON, I. P., BATLLE, E., SIMON-ASSMANN, P., CLEVERS, H., NATHKE, I. S., CLARKE, A. R. & WINTON, D. J. 2004. Loss of Apc in vivo immediately perturbs Wnt signaling, differentiation, and migration. *Genes Dev*, 18, 1385-90.
- SANTAMARIA, L., BIANCHI, A., ARNABOLDI, A., RAVETTO, C., BIANCHI, L., PIZZALA, R., ANDREONI, L., SANTAGATI, G. & BERMOND, P. 1988.

- Chemoprevention of indirect and direct chemical carcinogenesis by carotenoids as oxygen radical quenchers. *Ann N Y Acad Sci*, 534, 584-96.
- SATOH, S., DAIGO, Y., FURUKAWA, Y., KATO, T., MIWA, N., NISHIWAKI, T., KAWASOE, T., ISHIGURO, H., FUJITA, M., TOKINO, T., SASAKI, Y., IMAOKA, S., MURATA, M., SHIMANO, T., YAMAOKA, Y. & NAKAMURA, Y. 2000. AXIN1 mutations in hepatocellular carcinomas, and growth suppression in cancer cells by virus-mediated transfer of AXIN1. *Nat Genet*, 24, 245-50.
- SAVILL, J. & FADOK, V. 2000. Corpse clearance defines the meaning of cell death. *Nature*, 407, 784-8.
- SCALBERT, A., ANDRES-LACUEVA, C., ARITA, M., KROON, P., MANACH, C., URPI-SARDA, M. & WISHART, D. 2011. Databases on food phytochemicals and their health-promoting effects. *J Agric Food Chem*, 59, 4331-48.
- SCALBERT, A., MANACH, C., MORAND, C., REMESY, C. & JIMENEZ, L. 2005. Dietary polyphenols and the prevention of diseases. *Crit Rev Food Sci Nutr*, 45, 287-306.
- SCALBERT, A. & WILLIAMSON, G. 2000. Dietary intake and bioavailability of polyphenols. *J Nutr*, 130, 2073S-85S.
- SCHLEGEL, R. A. & WILLIAMSON, P. 2001. Phosphatidylserine, a death knell. *Cell Death Differ*, 8, 551-63.
- SCHMITT, E., BEAUCHEMIN, M. & BERTRAND, R. 2007a. Nuclear colocalization and interaction between bcl-xL and cdk1(cdc2) during G2/M cell-cycle checkpoint. *Oncogene*, 26, 5851-65.
- SCHMITT, E., PAQUET, C., BEAUCHEMIN, M. & BERTRAND, R. 2007b. DNA-damage response network at the crossroads of cell-cycle checkpoints, cellular senescence and apoptosis. *J Zhejiang Univ Sci B*, 8, 377-97.
- SCHWARTZ-ALBIEZ, R., MONTEIRO, R. C., RODRIGUEZ, M., BINDER, C. J. & SHOENFELD, Y. 2009. Natural antibodies, intravenous immunoglobulin and their role in autoimmunity, cancer and inflammation. *Clin Exp Immunol*, 158 Suppl 1, 43-50.
- SCHWARTZ, G. K. 2002. CDK inhibitors: cell cycle arrest versus apoptosis. *Cell Cycle*, 1, 122-3.
- SCHWARZ-ROMOND, T., ASBRAND, C., BAKKERS, J., KUHL, M., SCHAEFFER, H. J., HUELSKEN, J., BEHRENS, J., HAMMERSCHMIDT, M. & BIRCHMEIER, W. 2002. The ankyrin repeat protein Diversin recruits Casein kinase Iepsilon to the beta-catenin degradation complex and acts in both canonical Wnt and Wnt/JNK signaling. *Genes Dev*, 16, 2073-84.
- SHAHI, M. H., AFZAL, M., SINHA, S., EBERHART, C. G., REY, J. A., FAN, X. & CASTRESANA, J. S. 2010. Regulation of sonic hedgehog-GLI1 downstream target genes PTCH1, Cyclin D2, Plakoglobin, PAX6 and NKX2.2 and their epigenetic status in medulloblastoma and astrocytoma. *BMC Cancer*, 10, 614.
- SHELTON, J. R., BURT, S. R. & PETERSON, M. A. 2011. A broad spectrum anticancer nucleoside with selective toxicity against human colon cells in vitro. *Bioorg Med Chem Lett*, 21, 1484-7.
- SHEN, Z. 2011. Genomic instability and cancer: an introduction. *J Mol Cell Biol*, 3, 1-3.
- SHENG, H., SHAO, J., WILLIAMS, C. S., PEREIRA, M. A., TAKETO, M. M., OSHIMA, M., REYNOLDS, A. B., WASHINGTON, M. K., DUBOIS, R. N. &

- BEAUCHAMP, R. D. 1998. Nuclear translocation of beta-catenin in hereditary and carcinogen-induced intestinal adenomas. *Carcinogenesis*, 19, 543-9.
- SHI, L., CAMPBELL, G., JONES, W. D., CAMPAGNE, F., WEN, Z., WALKER, S. J., SU, Z., CHU, T. M., GOODSID, F. M., PUSZTAI, L., SHAUGHNESSY, J. D., JR., OBERTHUER, A., THOMAS, R. S., PAULES, R. S., FIELDEN, M., BARLOGIE, B., CHEN, W., DU, P., FISCHER, M., FURLANELLO, C., GALLAS, B. D., GE, X., MEGHERBI, D. B., SYMMANS, W. F., WANG, M. D., ZHANG, J., BITTER, H., BRORS, B., BUSHEL, P. R., BYLESJO, M., CHEN, M., CHENG, J., CHOU, J., DAVISON, T. S., DELORENZI, M., DENG, Y., DEVANARAYAN, V., DIX, D. J., DOPAZO, J., DORFF, K. C., ELLOUMI, F., FAN, J., FAN, S., FAN, X., FANG, H., GONZALUDO, N., HESS, K. R., HONG, H., HUAN, J., IRIZARRY, R. A., JUDSON, R., JURAEVA, D., LABABIDI, S., LAMBERT, C. G., LI, L., LI, Y., LI, Z., LIN, S. M., LIU, G., LOBENHOFER, E. K., LUO, J., LUO, W., MCCALL, M. N., NIKOLSKY, Y., PENNELLO, G. A., PERKINS, R. G., PHILIP, R., POPOVICI, V., PRICE, N. D., QIAN, F., SCHERER, A., SHI, T., SHI, W., SUNG, J., THIERRY-MIEG, D., THIERRY-MIEG, J., THODIMA, V., TRYGG, J., VISHNUVAJALA, L., WANG, S. J., WU, J., WU, Y., XIE, Q., YOUSEF, W. A., ZHANG, L., ZHANG, X., ZHONG, S., ZHOU, Y., ZHU, S., ARASAPPAN, D., BAO, W., LUCAS, A. B., BERTHOLD, F., BRENNAN, R. J., BUNESS, A., CATALANO, J. G., CHANG, C., CHEN, R., CHENG, Y., CUI, J., et al. 2010. The MicroArray Quality Control (MAQC)-II study of common practices for the development and validation of microarray-based predictive models. *Nat Biotechnol*, 28, 827-38.
- SHI, L., JONES, W. D., JENSEN, R. V., HARRIS, S. C., PERKINS, R. G., GOODSID, F. M., GUO, L., CRONER, L. J., BOYSEN, C., FANG, H., QIAN, F., AMUR, S., BAO, W., BARBACIORU, C. C., BERTHOLET, V., CAO, X. M., CHU, T. M., COLLINS, P. J., FAN, X. H., FRUEH, F. W., FUSCOE, J. C., GUO, X., HAN, J., HERMAN, D., HONG, H., KAWASAKI, E. S., LI, Q. Z., LUO, Y., MA, Y., MEI, N., PETERSON, R. L., PURI, R. K., SHIPPY, R., SU, Z., SUN, Y. A., SUN, H., THORN, B., TURPAZ, Y., WANG, C., WANG, S. J., WARRINGTON, J. A., WILLEY, J. C., WU, J., XIE, Q., ZHANG, L., ZHONG, S., WOLFINGER, R. D. & TONG, W. 2008. The balance of reproducibility, sensitivity, and specificity of lists of differentially expressed genes in microarray studies. *BMC Bioinformatics*, 9 Suppl 9, S10.
- SHI, L., REID, L. H., JONES, W. D., SHIPPY, R., WARRINGTON, J. A., BAKER, S. C., COLLINS, P. J., DE LONGUEVILLE, F., KAWASAKI, E. S., LEE, K. Y., LUO, Y., SUN, Y. A., WILLEY, J. C., SETTERQUIST, R. A., FISCHER, G. M., TONG, W., DRAGAN, Y. P., DIX, D. J., FRUEH, F. W., GOODSID, F. M., HERMAN, D., JENSEN, R. V., JOHNSON, C. D., LOBENHOFER, E. K., PURI, R. K., SCHRIF, U., THIERRY-MIEG, J., WANG, C., WILSON, M., WOLBER, P. K., ZHANG, L., AMUR, S., BAO, W., BARBACIORU, C. C., LUCAS, A. B., BERTHOLET, V., BOYSEN, C., BROMLEY, B., BROWN, D., BRUNNER, A., CANALES, R., CAO, X. M., CEBULA, T. A., CHEN, J. J., CHENG, J., CHU, T. M., CHUDIN, E., CORSON, J., CORTON, J. C., CRONER, L. J., DAVIES, C., DAVISON, T. S., DELENSTARR, G., DENG, X., DORRIS, D., EKLUND, A. C., FAN, X. H., FANG, H., FULMER-SMENTEK, S., FUSCOE, J. C., GALLAGHER, K., GE, W., GUO, L., GUO, X., HAGER, J., HAJE, P. K., HAN, J., HAN, T., HARBOTTLE, H. C.,

- HARRIS, S. C., HATCHWELL, E., HAUSER, C. A., HESTER, S., HONG, H., HURBAN, P., JACKSON, S. A., JI, H., KNIGHT, C. R., KUO, W. P., LECLERC, J. E., LEVY, S., LI, Q. Z., LIU, C., LIU, Y., LOMBARDI, M. J., MA, Y., MAGNUSON, S. R., MAQSODI, B., MCDANIEL, T., MEI, N., MYKLEBOST, O., NING, B., NOVORADOVSKAYA, N., ORR, M. S., OSBORN, T. W., PAPALLO, A., PATTERSON, T. A., PERKINS, R. G., PETERS, E. H., PETERSON, R., et al. 2006. The MicroArray Quality Control (MAQC) project shows inter- and intraplatform reproducibility of gene expression measurements. *Nat Biotechnol*, 24, 1151-61.
- SHI, L., TONG, W., GOODSID, F., FRUEH, F. W., FANG, H., HAN, T., FUSCOE, J. C. & CASCIANO, D. A. 2004. QA/QC: challenges and pitfalls facing the microarray community and regulatory agencies. *Expert Rev Mol Diagn*, 4, 761-77.
- SHIN-KANG, S., RAMSAUER, V. P., LIGHTNER, J., CHAKRABORTY, K., STONE, W., CAMPBELL, S., REDDY, S. A. & KRISHNAN, K. 2011. Tocotrienols inhibit AKT and ERK activation and suppress pancreatic cancer cell proliferation by suppressing the ErbB2 pathway. *Free Radic Biol Med*, 51, 1164-74.
- SHIRODE, A. B. & SYLVESTER, P. W. 2010. Synergistic anticancer effects of combined gamma-tocotrienol and celecoxib treatment are associated with suppression in Akt and NFkappaB signaling. *Biomed Pharmacother*, 64, 327-32.
- SHOHET, J. M., HICKS, M. J., PLON, S. E., BURLINGAME, S. M., STUART, S., CHEN, S. Y., BRENNER, M. K. & NUCHTERN, J. G. 2002. Minichromosome maintenance protein MCM7 is a direct target of the MYCN transcription factor in neuroblastoma. *Cancer Res*, 62, 1123-8.
- SHUKLA, S. & GUPTA, S. 2007. Apigenin-induced cell cycle arrest is mediated by modulation of MAPK, PI3K-Akt, and loss of cyclin D1 associated retinoblastoma dephosphorylation in human prostate cancer cells. *Cell Cycle*, 6, 1102-14.
- SHUKLA, S. & GUPTA, S. 2009. Apigenin suppresses insulin-like growth factor I receptor signaling in human prostate cancer: an in vitro and in vivo study. *Mol Carcinog*, 48, 243-52.
- SHUKLA, S., MISHRA, A., FU, P., MACLENNAN, G. T., RESNICK, M. I. & GUPTA, S. 2005. Up-regulation of insulin-like growth factor binding protein-3 by apigenin leads to growth inhibition and apoptosis of 22Rv1 xenograft in athymic nude mice. *FASEB J*, 19, 2042-4.
- SO, F. V., GUTHRIE, N., CHAMBERS, A. F., MOUSSA, M. & CARROLL, K. K. 1996. Inhibition of human breast cancer cell proliferation and delay of mammary tumorigenesis by flavonoids and citrus juices. *Nutr Cancer*, 26, 167-81.
- STERRENBURG, E., TURK, R., BOER, J. M., VAN OMMEN, G. B. & DEN DUNNEN, J. T. 2002. A common reference for cDNA microarray hybridizations. *Nucleic Acids Res*, 30, e116.
- SU, L. K., KINZLER, K. W., VOGELSTEIN, B., PREISINGER, A. C., MOSER, A. R., LUONGO, C., GOULD, K. A. & DOVE, W. F. 1992. Multiple intestinal neoplasia caused by a mutation in the murine homolog of the APC gene. *Science*, 256, 668-70.

- SUAHEYUN, R., KINOUCI, T., ARIMOCCHI, H., VINITKETKUMNUEN, U. & OHNISHI, Y. 1997. Inhibitory effects of lemon grass (*Cymbopogon citratus* Stapf) on formation of azoxymethane-induced DNA adducts and aberrant crypt foci in the rat colon. *Carcinogenesis*, 18, 949-55.
- SUN, J. & JIN, T. 2008. Both Wnt and mTOR signaling pathways are involved in insulin-stimulated proto-oncogene expression in intestinal cells. *Cell Signal*, 20, 219-29.
- SUN, J., WANG, D. & JIN, T. 2010. Insulin alters the expression of components of the Wnt signaling pathway including TCF-4 in the intestinal cells. *Biochim Biophys Acta*, 1800, 344-51.
- SUN, J. G., LIAO, R. X., QIU, J., JIN, J. Y., WANG, X. X., DUAN, Y. Z., CHEN, F. L., HAO, P., XIE, Q. C., WANG, Z. X., LI, D. Z., CHEN, Z. T. & ZHANG, S. X. 2011. Microarray-based analysis of microRNA expression in breast cancer stem cells. *J Exp Clin Cancer Res*, 29, 174.
- SUTHERLAND, C., LEIGHTON, I. A. & COHEN, P. 1993. Inactivation of glycogen synthase kinase-3 beta by phosphorylation: new kinase connections in insulin and growth-factor signalling. *Biochem J*, 296 ( Pt 1), 15-9.
- SUZUKI, H., TAKATSUKA, S., AKASHI, H., YAMAMOTO, E., NOJIMA, M., MARUYAMA, R., KAI, M., YAMANO, H. O., SASAKI, Y., TOKINO, T., SHINOMURA, Y., IMAI, K. & TOYOTA, M. 2011. Genome-wide Profiling of Chromatin Signatures Reveals Epigenetic Regulation of MicroRNA Genes in Colorectal Cancer. *Cancer Res*.
- SZLISZKA, E., CZUBA, Z. P., BRONIKOWSKA, J., MERTAS, A., PARADYSZ, A. & KROL, W. 2009. Ethanolic Extract of Propolis Augments TRAIL-Induced Apoptotic Death in Prostate Cancer Cells. *Evid Based Complement Alternat Med*.
- SZLISZKA, E., CZUBA, Z. P., JERNAS, K. & KROL, W. 2008. Dietary flavonoids sensitize HeLa cells to tumor necrosis factor-related apoptosis-inducing ligand (TRAIL). *Int J Mol Sci*, 9, 56-64.
- TACHIBANA, K. E., GONZALEZ, M. A. & COLEMAN, N. 2005. Cell-cycle-dependent regulation of DNA replication and its relevance to cancer pathology. *J Pathol*, 205, 123-9.
- TAKAHASHI-YANAGA, F. & SASAGURI, T. 2008. GSK-3beta regulates cyclin D1 expression: a new target for chemotherapy. *Cell Signal*, 20, 581-9.
- TAKAHASHI-YANAGA, F. & SASAGURI, T. 2009. Drug development targeting the glycogen synthase kinase-3beta (GSK-3beta)-mediated signal transduction pathway: inhibitors of the Wnt/beta-catenin signaling pathway as novel anticancer drugs. *J Pharmacol Sci*, 109, 179-83.
- TAKAHASHI, M. & WAKABAYASHI, K. 2004. Gene mutations and altered gene expression in azoxymethane-induced colon carcinogenesis in rodents. *Cancer Sci*, 95, 475-80.
- TAKANAGA, H., OHNISHI, A., YAMADA, S., MATSUO, H., MORIMOTO, S., SHOYAMA, Y., OHTANI, H. & SAWADA, Y. 2000. Polymethoxylated flavones in orange juice are inhibitors of P-glycoprotein but not cytochrome P450 3A4. *J Pharmacol Exp Ther*, 293, 230-6.
- TAKETO, M. M. 2006. Mouse models of gastrointestinal tumors. *Cancer Sci*, 97, 355-61.
- TAKETO, M. M. & EDELMANN, W. 2009. Mouse models of colon cancer. *Gastroenterology*, 136, 780-98.

- TANG, X. L., YANG, X. Y., JUNG, H. J., KIM, S. Y., JUNG, S. Y., CHOI, D. Y., PARK, W. C. & PARK, H. 2009. Asiatic acid induces colon cancer cell growth inhibition and apoptosis through mitochondrial death cascade. *Biol Pharm Bull*, 32, 1399-405.
- THOMPSON, K. L. & PINE, P. S. 2009. Comparison of the diagnostic performance of human whole genome microarrays using mixed-tissue RNA reference samples. *Toxicol Lett*, 186, 58-61.
- THOMPSON, K. L., PINE, P. S., ROSENZWEIG, B. A., TURPAZ, Y. & RETIEF, J. 2007. Characterization of the effect of sample quality on high density oligonucleotide microarray data using progressively degraded rat liver RNA. *BMC Biotechnol*, 7, 57.
- TOMAYKO, M. M. & REYNOLDS, C. P. 1989. Determination of subcutaneous tumor size in athymic (nude) mice. *Cancer Chemother Pharmacol*, 24, 148-54.
- TOMAZELA, D. M., PUPO, M. T., PASSADOR, E. A., DA SILVA, M. F., VIEIRA, P. C., FERNANDES, J. B., FO, E. R., OLIVA, G. & PIRANI, J. R. 2000. Pyrano chalcones and a flavone from *Neoraputia magnifica* and their *Trypanosoma cruzi* glycosomal glyceraldehyde-3-phosphate dehydrogenase-inhibitory activities. *Phytochemistry*, 55, 643-51.
- TRAINER, D. L., KLINE, T., MCCABE, F. L., FAUCETTE, L. F., FEILD, J., CHAIKIN, M., ANZANO, M., RIEMAN, D., HOFFSTEIN, S., LI, D. J. & ET AL. 1988. Biological characterization and oncogene expression in human colorectal carcinoma cell lines. *Int J Cancer*, 41, 287-96.
- TROCHON, V., BLOT, E., CYMBALISTA, F., ENGELMANN, C., TANG, R. P., THOMAIDIS, A., VASSE, M., SORIA, J., LU, H. & SORIA, C. 2000. Apigenin inhibits endothelial-cell proliferation in G(2)/M phase whereas it stimulates smooth-muscle cells by inhibiting P21 and P27 expression. *Int J Cancer*, 85, 691-6.
- TSAI, H. Y., HSI, B. L., HUNG, I. J., YANG, C. P., LIN, J. N., CHEN, J. C., TSAI, S. F. & HUANG, S. F. 2004. Correlation of MYCN amplification with MCM7 protein expression in neuroblastomas: a chromogenic in situ hybridization study in paraffin sections. *Hum Pathol*, 35, 1397-403.
- TSAO, C. C., GEISEN, C. & ABRAHAM, R. T. 2004. Interaction between human MCM7 and Rad17 proteins is required for replication checkpoint signaling. *EMBO J*, 23, 4660-9.
- TURKTEKIN, M., KONAC, E., ONEN, H. I., ALP, E., YILMAZ, A. & MENEVSE, S. 2011. Evaluation of the Effects of the Flavonoid Apigenin on Apoptotic Pathway Gene Expression on the Colon Cancer Cell Line (HT29). *J Med Food*.
- UEKI, K., YAMAMOTO-HONDA, R., KABURAGI, Y., YAMAUCHI, T., TOBE, K., BURGERING, B. M., COFFER, P. J., KOMURO, I., AKANUMA, Y., YAZAKI, Y. & KADOWAKI, T. 1998. Potential role of protein kinase B in insulin-induced glucose transport, glycogen synthesis, and protein synthesis. *J Biol Chem*, 273, 5315-22.
- VAN 'T VEER, L. J., DAI, H., VAN DE VIJVER, M. J., HE, Y. D., HART, A. A., MAO, M., PETERSE, H. L., VAN DER KOOY, K., MARTON, M. J., WITTEVEEN, A. T., SCHREIBER, G. J., KERKHOVEN, R. M., ROBERTS, C., LINSLEY, P. S., BERNARDS, R. & FRIEND, S. H. 2002. Gene expression profiling predicts clinical outcome of breast cancer. *Nature*, 415, 530-6.

- VAN AMERONGEN, R., NAWIJN, M. C., LAMBOOIJ, J. P., PROOST, N., JONKERS, J. & BERNIS, A. 2009. Frat oncoproteins act at the crossroad of canonical and noncanonical Wnt-signaling pathways. *Oncogene*, 29, 93-104.
- VAN DROSS, R., XUE, Y., KNUDSON, A. & PELLING, J. C. 2003. The chemopreventive bioflavonoid apigenin modulates signal transduction pathways in keratinocyte and colon carcinoma cell lines. *J Nutr*, 133, 3800S-3804S.
- VAN ES, J. H., BARKER, N. & CLEVERS, H. 2003. You Wnt some, you lose some: oncogenes in the Wnt signaling pathway. *Curr Opin Genet Dev*, 13, 28-33.
- VELE, R., LARGHERO, P., ARENA, G., SPORN, M. B., ALBINI, A. & TOSETTI, F. 2008. Glycogen synthase kinase 3beta regulates cell death induced by synthetic triterpenoids. *Cancer Res*, 68, 6987-96.
- VERMES, I., HAANEN, C., STEFFENS-NAKKEN, H. & REUTELINGSPERGER, C. 1995. A novel assay for apoptosis. Flow cytometric detection of phosphatidylserine expression on early apoptotic cells using fluorescein labelled Annexin V. *J Immunol Methods*, 184, 39-51.
- VERSCOYLE, R. D., GREAVES, P., CAI, H., BORKHARDT, A., BROGGINI, M., D'INCALCI, M., RICCIO, E., DOPPALAPUDI, R., KAPETANOVIC, I. M., STEWARD, W. P. & GESCHER, A. J. 2006. Preliminary safety evaluation of the putative cancer chemopreventive agent tricetin, a naturally occurring flavone. *Cancer Chemother Pharmacol*, 57, 1-6.
- WALLE, T. 2007. Methoxylated flavones, a superior cancer chemopreventive flavonoid subclass? *Semin Cancer Biol*, 17, 354-62.
- WALLE, T., TA, N., KAWAMORI, T., WEN, X., TSUJI, P. A. & WALLE, U. K. 2007. Cancer chemopreventive properties of orally bioavailable flavonoids--methylated versus unmethylated flavones. *Biochem Pharmacol*, 73, 1288-96.
- WALLE, U. K. & WALLE, T. 2007. Bioavailable flavonoids: cytochrome P450-mediated metabolism of methoxyflavones. *Drug Metab Dispos*, 35, 1985-9.
- WANG, L., CAO, X. X., CHEN, Q., ZHU, T. F., ZHU, H. G. & ZHENG, L. 2009. DIXDC1 targets p21 and cyclin D1 via PI3K pathway activation to promote colon cancer cell proliferation. *Cancer Sci*, 100, 1801-8.
- WANG, Q., ZHOU, Y., JACKSON, L. N., JOHNSON, S. M., CHOW, C. W. & EVERS, B. M. 2011. Nuclear factor of activated T cells (NFAT) signaling regulates PTEN expression and intestinal cell differentiation. *Mol Biol Cell*, 22, 412-20.
- WANG, W., HEIDEMAN, L., CHUNG, C. S., PELLING, J. C., KOEHLER, K. J. & BIRT, D. F. 2000. Cell-cycle arrest at G2/M and growth inhibition by apigenin in human colon carcinoma cell lines. *Mol Carcinog*, 28, 102-10.
- WATSON, A. J. 2006. An overview of apoptosis and the prevention of colorectal cancer. *Crit Rev Oncol Hematol*, 57, 107-21.
- WATTENBERG, L. W. 1983. Inhibition of neoplasia by minor dietary constituents. *Cancer Res*, 43, 2448s-2453s.
- WCRF/AICR 2007. *Food, Nutrition, Physical Activity, and the Prevention of Cancer: A Global Perspective.*, Washington, DC, WCRF/AICR (World Cancer Research Fund/American Institute for Cancer Research).
- WEI, C., LI, J. & BUMGARNER, R. E. 2004. Sample size for detecting differentially expressed genes in microarray experiments. *BMC Genomics*, 5, 87.
- WEI, H., TYE, L., BRESNICK, E. & BIRT, D. F. 1990. Inhibitory effect of apigenin, a plant flavonoid, on epidermal ornithine decarboxylase and skin tumor promotion in mice. *Cancer Res*, 50, 499-502.

- WEN, X. & WALLE, T. 2006a. Methylated flavonoids have greatly improved intestinal absorption and metabolic stability. *Drug Metab Dispos*, 34, 1786-92.
- WEN, X. & WALLE, T. 2006b. Methylation protects dietary flavonoids from rapid hepatic metabolism. *Xenobiotica*, 36, 387-97.
- WHO. 2011. *WHO Global Infobase. 10 Facts about Cancer*. [Online]. Available: <http://www.who.int/mediacentre/factsheets/fs297/en/index.html>.
- WILLIAMSON, P., VAN DEN EIJNDE, S. & SCHLEGEL, R. A. 2001. Phosphatidylserine exposure and phagocytosis of apoptotic cells. *Methods Cell Biol*, 66, 339-64.
- WINKELMANN, I., DIEHL, D., OESTERLE, D., DANIEL, H. & WENZEL, U. 2007. The suppression of aberrant crypt multiplicity in colonic tissue of 1,2-dimethylhydrazine-treated C57BL/6J mice by dietary flavone is associated with an increased expression of Krebs cycle enzymes. *Carcinogenesis*, 28, 1446-54.
- WINTER, D. C., CHOE, E. Y. & LI, R. 1999. Genetic dissection of the budding yeast Arp2/3 complex: a comparison of the in vivo and structural roles of individual subunits. *Proc Natl Acad Sci U S A*, 96, 7288-93.
- WULFKUHLE, J., ESPINA, V., LIOTTA, L. & PETRICOIN, E. 2004. Genomic and proteomic technologies for individualisation and improvement of cancer treatment. *Eur J Cancer*, 40, 2623-32.
- XIE, W., JIN, L., MEI, Y. & WU, M. 2009. E2F1 represses beta-catenin/TCF activity by direct up-regulation of Siah1. *J Cell Mol Med*, 13, 1719-27.
- YAMADA, Y. & MORI, H. 2007. Multistep carcinogenesis of the colon in Apc(Min/+) mouse. *Cancer Sci*, 98, 6-10.
- YAO, H., XU, W., SHI, X. & ZHANG, Z. 2011. Dietary flavonoids as cancer prevention agents. *J Environ Sci Health C Environ Carcinog Ecotoxicol Rev*, 29, 1-31.
- YOST, C., TORRES, M., MILLER, J. R., HUANG, E., KIMELMAN, D. & MOON, R. T. 1996. The axis-inducing activity, stability, and subcellular distribution of beta-catenin is regulated in *Xenopus* embryos by glycogen synthase kinase 3. *Genes Dev*, 10, 1443-54.
- YU, J., MALLON, M. A., ZHANG, W., FREIMUTH, R. R., MARSH, S., WATSON, M. A., GOODFELLOW, P. J. & MCLEOD, H. L. 2006. DNA repair pathway profiling and microsatellite instability in colorectal cancer. *Clin Cancer Res*, 12, 5104-11.
- ZHANG, G. & GHOSH, S. 2002. Negative regulation of toll-like receptor-mediated signaling by Tollip. *J Biol Chem*, 277, 7059-65.
- ZHANG, L., REN, X., ALT, E., BAI, X., HUANG, S., XU, Z., LYNCH, P. M., MOYER, M. P., WEN, X. F. & WU, X. 2010. Chemoprevention of colorectal cancer by targeting APC-deficient cells for apoptosis. *Nature*, 464, 1058-61.
- ZHANG, S. D. & GANT, T. W. 2004. A statistical framework for the design of microarray experiments and effective detection of differential gene expression. *Bioinformatics*, 20, 2821-8.
- ZHANG, S. D. & GANT, T. W. 2005. Effect of pooling samples on the efficiency of comparative studies using microarrays. *Bioinformatics*, 21, 4378-83.
- ZHANG, T., OTEVREL, T., GAO, Z., EHRlich, S. M., FIELDS, J. Z. & BOMAN, B. M. 2001. Evidence that APC regulates survivin expression: a possible mechanism contributing to the stem cell origin of colon cancer. *Cancer Res*, 61, 8664-7.

- ZHONG, Y., KRISANAPUN, C., LEE, S. H., NUALSANIT, T., SAMS, C., PEUNGVICHA, P. & BAEK, S. J. 2010. Molecular targets of apigenin in colorectal cancer cells: involvement of p21, NAG-1 and p53. *Eur J Cancer*, 46, 3365-74.
- ZHOU, J. R., GUGGER, E. T., TANAKA, T., GUO, Y., BLACKBURN, G. L. & CLINTON, S. K. 1999. Soybean phytochemicals inhibit the growth of transplantable human prostate carcinoma and tumor angiogenesis in mice. *J Nutr*, 129, 1628-35.
- ZOU, X. & CALAME, K. 1999. Signaling pathways activated by oncogenic forms of Abl tyrosine kinase. *J Biol Chem*, 274, 18141-4.